An investigation into the structure of a turbulent plane jet.

Bradbury, L. J. S

AN INVESTIGATION INTO THE STRUCTURE OF A TURBULENT PLANE JET

by

L. J. S. Bradbury
(Queen Mary College)

DEGREE OF DOCTOR OF PHILOSOPHY

ABSTRACT.

An experimental investigation into the structure of the plane jet in a moving airstream has been made. The majority of the measurements have been made in a jet exhausting into a slow moving airstream providing an example of a possible self-preserving flow. The experiments showed that the flow does, in fact, become self-preserving at distances downstream from the jet nozzle of thirty jet nozzle widths. The distributions of the turbulent intensities across the jet in the self-preserving region of the flow are shown to be similar to those found in the plane wake. However, the turbulent energy balance for the two flows appears to be quite different. Some measurements of the eddy structure indicate that shear carrying eddies are among the largest eddies in the flow and are also partly responsible for the intermittency phenomenon. The unsteady irrotational flow outside the jet is shown to be adequately described by the theories of Phillips (1955) and Stewart (1956).

Some comments are made on the applicability of the various simple theories of turbulence to the plane jet and the interesting, though not necessarily significant, point emerges that the Prandtl Mixing Length theory gives the best description of the flow structure.

Additional measurements in jets in fast moving airstreams show that the change from a jet to a wake type of turbulence structure takes place at a very slow rate. Several simple theories were developed to account for the spread of a plane jet in a moving airstream but none of them proved wholly adequate.

Apart from the main investigation, some work on the problem of measurements in a turbulent flow is discussed. Aspects of both hot wire anemometer theory and static pressure measurements are re-appraised.

ACKNOWLEDGEMENTS.

I would like to thank Professor A.D. Young, Dr. L.G. Whitehead and Dr. G.J. Hancock for their helpful advice and encouragement during the course of this research. Also, my thanks are due to the workshop staff for their efforts in the manufacture of the apparatus.

LIST OF CONTENTS.

1.0 Introduction.

Many of the fluid flows that are of practical importance are of the turbulent type but, unfortunately, of all aerodynamic problems, turbulence is surely among the most difficult. This is due not only to the non-linearity of the Navier Stokes equations but also to the essential feature of turbulence which is that the velocity and pressure at a point in the fluid contain components which are random functions of time.

The work that has been done on this problem can be divided roughly into three groups. Firstly, there is the analysis of the stability of a laminar flow to small disturbances. This has improved our understanding of the origin of turbulence and of the phenomenon of transition. Furthermore, Malkus (1956) has considered the fully developed turbulent channel flow by an approach similar, in some ways, to that used in the more conventional stability work and he obtained a solution that was not dependent on any empirical constants. However, the analysis was complex and restricted by some important assumptions and it is unlikely that general fluid motion problems can be solved by this approach.

Secondly, there is the approach through the use of statistical analysis. This is suggested by the random nature of the flow. This work has improved our understanding of the physical processes involved in a turbulent flow but it has not as yet given exact quantative solutions to any fluid motion problem.

Finally, there has been the work based upon semi-empirical and phenomenalogical theories which, in the past, has aimed mainly at providing simple methods for calculating the behaviour of general turbulent shear flows. However, in the last decade, a great deal of

effort has gone into checking and improving the physical validity of these theories. This effort has been largely experimental and has concentrated not only on the mean velocities in shear layers but also on the detailed turbulence structure. In consequence, more realistic empirical theories are now possible and some progress in this direction has already been made. Good examples of this are the "law of the wall" and Townsend's large eddy hypothesis.

It seems likely that this last approach to the turbulence problem will be the most rewarding for some time to come and, in his monograph on turbulence, Townsend (1956) has provided a framework into which future work along these lines may be fitted.

It is to be expected that the simplest flows should be these to attract attention initially. In the case of shear layers, these are the self-preserving flows in which the structure of the shear layer is similar at all stations in the free-stream direction and, in consequence, these flows can be specified by a minimum number of parameters. Ideally, one would like detailed information on the development and structure of the whole range of these self-preserving flows. This information would enable the effect of a comparatively few parameters on the flow structure to be observed. It would also provide a test for phenomenalogical theories and might also suggest improvements to them. In addition, it would then be possible to perturb these flows in well defined ways and, by observing the response, deduce further information about the nature of turbulent flows. This last idea resembles the "black box" approach suggested by Clauser (1956) and is typified by the work of Stratford (1959) on the effect of rapid pressure rise on boundary layers.

Comparing the above hope with reality, we find that, in spite of a number of extensive experiments, information on these flows is still far from complete. This is no doubt due to the experimental difficulties involved in turbulence investigations and, in fact, the development of suitable measuring instruments has attracted as much effort as the experiments on turbulent flows. In the case of self-preserving turbulent boundary layers, only Clauser (1954) has investigated the non-zero pressure gradient flows and these experiments did not include turbulence measurements. On the other hand, the zero pressure gradient case has been studied extensively, mainly by Klebanoff (1954) and Townsend (1951). The self-preserving flow in a channel - with and without diverging walls - has also been investigated by Laufer (1951) and Ruetnik and Corrsin (1955). In the case of free turbulent flows, the work of Townsend (1956) and Grant (1958) on the plane wake represents the most extensive study yet undertaken of any self-preserving flow. Jet flows, on the other hand, have not been studied in the same detail although the number of experiments on jets has been considerable. In particular, detailed information on the plane jet as opposed to the axi-symmetric jet is very sparse and this is to be regretted because a comparison with the plane wake structure would be of interest.

In this report, the background of theoretical and experimental work on turbulent free flows and particularly the turbulent plane jet is first reviewed (sections 2 and 3). This review is then followed by an analysis leading to several theories which describe the development of the plane jet in a moving airstream(section 4). These theories make different assumptions about the turbulent flow and they were developed in order to compare with subsequent experimental results.

In sections 5 and 6, a description is given of the plane jet model and instrumentation used in the experiments. The instrumentation included constant current hot wire anemometer equipment and the development of this is fully discussed and includes a description of a simple circuit for measuring the intermittency factor in turbulent flows. The problems of applying the hot wire anemometer are discussed and the basic theory is critically re-assessed. Further, the problem of static pressure measurements in a turbulent flow is also re-considered and the early conclusions of the work of Goldstein and Page (1936) are modified. In sections 7 and 8, the results of experiments on a plane jet exhausting into a comparitively slow moving airstream are described. This flow is an example of a possible self-preserving flow and the results are analysed to provide comprehensive details of the turbulence structure of this flow. A comparison with the results of Townsend (1956) for a plane wake flow is made and, in section 9, the applicability of the various theories of turbulence is discussed. Finally, in sections 10 and 11, results of experiments on a plane jet exhausting into a fast moving airstream are analysed to provide information about the general development of a jet in a moving airstream.

The measurements on the plane jet exhausting into a slow moving airstream show that the flow becomes self-preserving at distances downstream from the jet nozzle larger than thirty jet nozzle widths. In the self-preserving region of the flow, it is found that the distributions of the turbulent intensities across the jet are similar to those found in a plane wake. However, the turbulent energy balance for the plane jet and the plane wake show important differences. Some simple measurements of the eddy structure

seemed to show that shear carrying eddies are among the largest in the flow and are partly responsible for the intermittency phenomenon. The unsteady irrotational flow outside the jet is shown to be adequately described by the theories of Phillips (1935) and Stewart (1956).

In the case of the jet in a fast moving airstream, the flow should develop a structure similar to the plane wake flow. However, the experiments show that the approach to this plane wake type of structure takes place at a very slow rate. None of the simple theories developed in section 4 proved to be adequate to describe the complete development of a plane jet in a moving airstream.

2.0 Review of basic theory.

2.1 The equations of motion and self-preserving flows.

We will be considering only two-dimensional flows. Cartesian co-ordinates will be used with the x-axis and y-axis lying parallel and normal to the free-stream direction respectively. The longitudinal or x-component of mean velocity will be denoted by U and the lateral or y-component by V. The turbulent velocities will be denoted by u, v and w. The full equations of motion for a two-dimensional turbulent shear layer with "boundary layer" assumptions are (Townsend (1956)):-

$$U\frac{\partial U}{\partial x} + V\frac{\partial U}{\partial y} = -\frac{1}{\rho}\frac{dP_1}{dx} + \frac{1}{\rho}\frac{\partial \tau}{\partial y} - \frac{\partial}{\partial x}\left(\overline{u^2} - \overline{v^2}\right) \qquad (2.1.1)$$

$$P_1 = P + \rho\overline{v^2} \qquad (2.1.2)$$

where the shear stress, $\tau = \left(-\rho\ \overline{uv} + \mu\frac{\partial U}{\partial y}\right)$ and P_1 is the static pressure outside the shear layer in the irrotational flow region.

The continuity equation is:-

$$\frac{\partial U}{\partial x} + \frac{\partial V}{\partial y} = 0 \qquad (2.1.3)$$

We will consider initially self-preserving flows in which:-

$$U = U_1 + U_o f(y/\ell)\ ;\ \overline{uv} = U_o^2\, g_{12}(y/\ell)\ ;\ \overline{u^2} = U_o^2\, g_1(y/\delta)\ ;$$

$$\overline{v^2} = U_o^2\, g_2(y/\delta). \qquad (2.1.4)$$

where U_1 is usually taken as the local free-stream velocity and U_o and δ are relevant velocity and length scales respectively of the shear layer. The exact choice of these depends on the type of flow being considered. f, g_{12}, g_1 and g_2 are all functions of y/ℓ only.

Substituting equations (2.1.4) into equation (2.1.1) gives (see Townsend (1956)):-

$$\frac{d}{dx}(U_0U_1)f - \frac{U_0}{\delta}\frac{d}{dx}(U_1\delta)\eta f' + U_0\frac{dU_0}{dx}f^2 - \frac{U_0}{\delta}\frac{d}{dx}(U_0\delta)\,f'\int f d\eta$$

$$+ 2U_0\frac{dU_0}{dx}(g_1 - g_2) - \frac{U_0^2}{\delta}\frac{d\delta}{dx}(g_1' - g_2') + \frac{U_0^2}{\delta}g_{12}' = \frac{\nu U_0}{\delta^2}f'' \qquad (2.1.5)$$

where $\eta = y/\delta$ and dashes denote differentiation with respect to η. To be consistent with the assumption of self-preservation, it is necessary that the coefficients in equation (2.1.5) are in a constant ratio to one another. In the case of laminar flows, this leads to the following conditions:-

(a) $U_0 = U_1 \propto x^m$; $\delta \propto x^{-1/2(m-1)}$ or $U_0 = U_1 \propto \exp(\beta x)$; $\delta \propto \exp(-\beta x/2)$ } Falkner-Skan boundary layer flows.

(b) $U_1 = 0$. $U_0 \propto x^m$; $\delta \propto x$,

with $m = -1/3$ for the laminar plane jet and

with $m = -1/2$ for the laminar plane wall jet.

(c) $U_1 \gg U_0$. $U_0 \propto x^{-1/2}$; $\delta \propto x^{1/2}$ for the laminar plane wake.

In turbulent flows, we obtain:-

$U_0 = U_1 \propto x^{-1}$; $\delta \propto x$.

i.e. the flow between diverging plane walls.

However, if we ignore the viscous term in equation (2.1.5), we also obtain:-

$U_0 \propto U_1 \propto x^m$; $\delta \propto x$.

(a) or

$U_0 \propto U_1 \propto \exp(\beta x)$; $\delta \propto x$.

These can represent a class of self-preserving boundary layer flows.* The neglect of the viscous term requires that the region near the wall is excluded from the self-preserving flow.

(b) $U_1 = 0$. $U_o \propto x^{-1/2}$; $\delta \propto x$. i.e. the turbulent plane jet.

(c) $U_1 = U_o$ = a constant. $\delta \propto x$. i.e. the turbulent mixing layer formed between two parallel streams.

(d) $U_1 \gg U_o$. $U_o \propto x^{-1/2}$; $\delta \propto x^{1/2}$. i.e. the turbulent plane wake.

In the present instant, we are interested only in the turbulent plane jet and wake and we will define U_o as the mean velocity difference between the free-stream and the centre-line of the flow and $\delta = \delta_{0.5}$ as the y-ordinate at which the mean velocity, $U = U_1 + 0.5\, U_o$.

2.2 Theories of turbulence.

From experiments it appears that where a self-preserving flow is possible, there is a tendency for a self-preserving flow to develop. These flows are important because they are the least complicated of the shear flows and the most amenable to theoretical treatment. However, in order to proceed with any theoretical analysis, we must make some assumption relating the turbulent to the mean motion. As yet, there is no case where this has been possible in an exact way and solutions have only been obtained with the use of semi-empirical and phenomenalogical theories. The

*The physical interpretation of these conditions is not necessarily unique. For example, it is possible that solutions could be found representing a free turbulent shear layer with a longitudinal pressure gradient. This comment applies also to the laminar Falkner-Skan conditions which could be interpreted as representing a class of laminar free flows with a longitudinal pressure gradient as an alternative to the more usual boundary layer flows interpretation (Patel and Newman (1961)).

physical significance of these theories has been discussed by a number of authors (see, for example, Batchelor (1950) and Hinze (1959)) but, for completeness, a brief resumé of some of these theories is given below.

The discussion is limited to eddy viscosity theories which assume that:-

$$\tau = -\rho\,\overline{uv} = \varepsilon\,\frac{\partial U}{\partial y} \qquad (2.2.1)$$

and which all make different assumptions for the eddy viscosity coefficient, ε. However, equation (2.2.1) in itself requires that the scale of turbulence is much less than the scale of mean velocity variation (i.e. $(L/U)(\partial U/\partial y) \ll 1.0$, where L is a characteristic length scale of the turbulence).

To provide a simple if naive picture of turbulent mixing processes, it is useful to make the analogy with the molecular theory of gases. We will assume that the turbulent motion consists of small discrete lumps of fluid which have a characteristic path length, L (analogous with the molecular mean free path) and a characteristic velocity, say $\sqrt{\overline{q^2}} = (\overline{u^2} + \overline{v^2} + \overline{w^2})^{1/2}$. If the velocity of the lumps is very high compared with the mean velocity variation, then the turbulent fluctuations will be independent of the local mean velocity gradient and depend more on some overall property of the shear layer. Moreover, the high velocity of the lumps would ensure a homogeneous turbulence structure and, by exact analogy with the simple kinetic theory of gases, we obtain:-

$$\tau \propto \rho L \sqrt{\overline{q^2}}\,\frac{\partial U}{\partial y} = \text{constant} \times \frac{\partial U}{\partial y} \qquad (2.2.2)$$

provided $(\sqrt{\overline{q^2}}/L \gg \partial U/\partial y)$. This theory is referred to as the constant exchange hypothesis since it gives an eddy viscosity coefficient, ε, that is constant across the shear layer. The analogy with the kinetic theory

breaks down when we try to assign values to L and $\sqrt{\overline{q^2}}$ because there is no analogue with the dependence of the molecular mean free path and velocity on temperature. As a result, it has been necessary to determine experimentally the eddy viscosity coeffécients. However, Townsend's large eddy hypothesis is an attempt to overcome this difficulty and, in fact, it does succeed in providing limiting values of the eddy viscosity coefficient. This hypothesis will be discussed later.

As an alternative to the above theory, we can assume that the turbulent velocity fluctuation is identical with the variation of mean velocity over the path length i.e. $\sqrt{\overline{u^2}} = L \frac{\partial U}{\partial y}$. Furthermore, if we assume that the turbulent motion is everywhere similar (i.e. $R_{uv} = \overline{uv}/\sqrt{\overline{u^2}}\sqrt{\overline{v^2}}$, $\overline{u^2}/\overline{v^2}$ etc. are all constants) then:-

$$\tau \propto \rho L^2 \left(\frac{\partial U}{\partial y}\right)^2 \qquad (2.2.3)$$

provided $\sqrt{\overline{u^2}} = L \frac{\partial U}{\partial y}$. This is Prandtl's Mixing Length theory and it requires an additional assumption to determine the path length, L. Batchelor (1950) has discussed this theory from the standpoint of the turbulent energy balance and has shown that, in addition to the assumptions already made, this theory implies that the turbulent energy production ($\overline{uv} \frac{\partial U}{\partial y}$) is equal to the viscous dissipation of turbulent energy.

Other theories that have been fairly extensively employed are von Karman's Similarity hypothesis and G.I. Taylor's Vorticity Transport theory. The former can be regarded as a special case of Prandtl's theory in which $L = (\partial U/\partial y)/(\partial^2 U/\partial y^2)$. The simplest form of G.I. Taylor's theory gives an expression that is identical with Prandtl's theory except that G.I. Taylor's Mixing Length is $\sqrt{2}$ times greater than Prandtl's. This is

of consequence only when the transfer of a passive scalar, such as heat, is considered (see, for example, Hinze(1959)).

The simple theories above cannot possibly represent the actual behaviour of turbulence and all that is hoped for is that one or other of them represents very loosely the relationship between the turbulent and mean motion. Comparison of the various assumptions in the theories with experiments is therefore necessary and will be considered at a later stage.

We will now consider the application of these theories to the self-preserving flows. Referring to equation (2.1.5), it is now possible to express $g_{12} = \overline{uv}/U_o^2$ as a function of the mean velocity profile function, f. According to:-

(a) the constant exchange hypothesis, $g_{12} = -f'/R_T$ where $R_T = U_o\delta/\nu_T$ is an eddy (viscosity) Reynolds number. ν_T equals ε/ρ.

(b) the Prandtl Mixing Length theory, $g_{12} = -(L/\delta)^2 f'^2$ if L is assumed to be constant across any section of the flow.

(c) the von Karman Similarity hypothesis, $g_{12} = -$ constant x f'^4/f''^2.

Thus, to be consistent with the assumption of self-preservation, it is necessary that:-

(a) R_T is a constant for a particular self-preserving flow.

(b) L/δ is a constant for a particular self-preserving flow.

Using the conditions for self-preservation (section 2.1) and any one of the above theories reduces equation (2.1.5) to an ordinary differential equation in f and, in consequence, a solution for f is possible. At present, we are interested only in solutions for the plane jet and plane wake and it is sufficient for present purposes to consider only the form of the velocity profiles obtained from the simpler of these

solutions.* We will compare these profiles on the basis of a reference length $b_{0.5}$ which is the value of the y-ordinate where $(U - U_1) = U_o/2$.

For the constant exchange hypothesis, we have that:-

(a) for the plane jet - $f = \mathrm{sech}^2(0.8814\eta)$

(b) for the plane wake - $f = \exp(-0.6932\eta^2)$

From Prandtl's Mixing Length theory, we have for the plane wake that:-

$$f = \left(1 - \frac{\sqrt{2}-1}{\sqrt{2}}\,\eta^{1.5}\right)^2$$

The Prandtl Mixing Length solution for the plane jet is more complicated (see, for example, Shih-I-Pai (1957)) and f cannot be expressed directly in terms of η. Solutions using von Karman's Similarity hypothesis must also be complicated and this hypothesis is not very convincing for turbulent free flows because it involves a singularity where $f''=0$.† As a result, this theory will not be considered further.

The three simple profiles above are compared with one another in figure (1). It is well known that these profiles are in fair agreement with experimental results and that the mean velocity profiles in a plane jet and a plane wake are very similar although it is generally assumed that the wake profile approaches free-stream conditions more rapidly than the jet profile.

---

*More complete details of these solutions are given by Schlichting (1955).

†I have only seen a reference to a paper by W. Tollmien in which the wake problem was solved using von Karman's Similarity hypothesis. The plane jet problem has not apparently been solved using this hypothesis.

3.0 Comments on existing experimental work.

In the case of the turbulent plane wake, the work of Townsend (1956) and Grant (1958) is the most significant and the structure of this flow has been investigated thoroughly. In the case of jet flows, the situation is less satisfactory. Corrsin and his co-workers have carried out extensive measurements on the axi-symmetric jet but these measurements have almost certainly been affected by the non-linear response of the hot wire anemometers used. Moreover, to enable a direct comparison with Townsend's wake investigations, measurements in a plane jet would be preferred. The most important reports on this flow are those of Forthmann (1936), Miller and Commings(1957), van der Hegge Zijnen (1958a, b & c) and Nakaguchi (1961). Unfortunately, none of these was comparable in detail to Townsend's work.

3.1 The turbulent plane wake.

Far downstream in the wake of a circular cylinder where $U_1 \gg U_o$, it has been shown that self-preservation is possible and that:-

$$U_o \propto x^{-1/2} \; ; \; \delta \propto x^{1/2}.$$

Townsend's measurements show that self-preservation of the turbulence structure occurs only at very large distances from the cylinder i.e.$x/d \geq 500$. The distribution of turbulent intensities across the wake in this region are shown in figure (3)*. Because, in general, the only significant production term in the turbulent energy balance is $\overline{uv}\,\frac{\partial U}{\partial y}$ (see Townsend (1956)), it is to be expected that the $\overline{u^2}$ component of the turbulence is the largest where $\partial U/\partial y$ is significantly non-zero (Corrsin (1957)). On the other hand,

---

*According to Grant (1958), the values of $\overline{v^2}$ and $\overline{w^2}$ measured by Townsend are roughly 25% too large due to the technique used for calibrating the hot wire anemometers. Therefore, although the original values are used in the present work, this possible error should be borne in mind.

at the wake centre and at its edge, $\partial U/\partial y$ is zero and the only source of turbulent energy comes from the advection and diffusion terms in the energy balance. The advection term favours no particular turbulent component but diffusion would tend to diffuse $\overline{v^2}$ more rapidly than $\overline{u^2}$ or $\overline{w^2}$ (Batchelor (1950)). Therefore, one would expect to find that $\overline{v^2}$ is greater than or at least comparable to $\overline{u^2}$ at the wake centre and edge. Furthermore, outside the turbulent fluid, there are irrotational velocity fluctuations induced by the convoluting surface of the turbulent flow and, according to Phillips (1955) and Stewart (1956), the intensities of this irrotational motion are related by:-

$$\overline{v^2} = \overline{u^2} + \overline{w^2}$$

and, further, for large distances from the wake edge:-

$$\overline{v^2}/2 = \overline{u^2} = \overline{w^2} \propto (y - y_o)^{-4}$$

where y_o is the ordinate of the apparent origin of the irrotational velocity fluctuations. Some support for these predictions has been provided by Townsend's measurements.

As to the structure of the turbulent motions, Townsend has postulated what is essentially a double structure for the flow. The largest eddies appear to be "jets" of fluid that originate at the boundary of the strained turbulent fluid with the non-turbulent fluid and which erupt outwards (Grant (1958)). It is these eddies which are responsible for the intermittency phenomenon. The remaining turbulence containing about $80^{o}/_{o}$ of the turbulent energy is assumed to be about one tenth of the scale of the large eddies and to have a homogeneous structure within the wake. Townsend took this model further and proposed that the large eddies were, in the middle period of their life, in energy equilibrium between the energy gained from the

mean motion and the energy lost by work done against the stresses of the smaller scale turbulence. Then he made an assumption for the actual form of these large eddies* and also assumed that the shear stress was carried entirely by the smaller eddies and could be written as a first approximation as:-

$$\tau = -\rho\,\overline{uv} = \varepsilon\,\frac{\partial U}{\partial y}$$

where ε is an eddy viscosity coefficient assumed a constant across the shear layer. The energy equilibrium postulate gave a relationship between the eddy Reynolds number, $R_T = U_0\delta/\nu_T$, and the size and position of the large eddies in relation to the shear layer. The limitations on the large eddy that it must fit into one half of the shear layer and also cause a negligible disturbance at the shear layer centre and edge fixed the value of R_T between 16 and 25 where R_T is based on $\delta = \delta_{0.5}$. The subsequent experiments of Grant (1958) show that the assumed form of the large eddies was incorrect but this does not in itself invalidate the general idea.

From measurements of the rate of spread of the wake, Townsend obtained a value of the eddy Reynolds number in the wake of $R_{T_w} = 14.7$ which is in fair agreement with the lower limit of his theoretical model. This value also agreed with the value obtained directly from a comparison between the measured correlation coefficients and the correlation coefficients obtained from the assumed form for the large eddies.

3.2. The turbulent plane jet.

Since this flow is of central interest in the present work, it is

---

*Townsend assumed that these eddies were long cylindrical eddies with their axes lying in the x-direction but with their planes of rotation inclined at 45° to the x-axis. These eddies do not correspond with the form of the large eddies observed in the later experiments of Grant (1958). However, it is possible that the results of Townsend's analysis are not over sensitive to the assumed form of the large eddies.

appropriate to spend a little time in defining terms. In figure (2) is shown schematically the flow of a plane jet exhausting from a parallel sided nozzle of inner width h into a moving airstream of velocity U_1. It is assumed that the nozzle does not interfere in any way with the flow except to prevent mixing of the jet and the free-stream until the nozzle exit. The jet is assumed to emerge from the nozzle with a uniform velocity, U_J, at ambient pressure. In the immediate vicinity of the nozzle exit, plane mixing layers develop at the junction of the jet with the free-stream on either side of the nozzle. These shear layers will be similar to the self-preserving mixing layer studied by Liepmann and Laufer (1947) and mentioned briefly in section 2.1. Eventually, these two layers will coalesce and the jet will become fully turbulent across its whole width i.e. the potential core disappears at the point of coalescence. In the case when $U_1 = 0$, it is possible for this fully turbulent jet to develop into a self-preserving plane jet flow in which $U_o \propto x^{-1/2}$ and $\delta \propto x$. In the remainder of this section, our attention will be directed solely at this case and the case when $U_1 \neq 0$ will be considered in section 4. For the self-preserving plane jet flow which may subsequently be called the "pure" jet flow, the reference velocity, U_o, can be taken conveniently as the velocity on the jet axis and the length scale, δ, as the y-ordinate at which $U = U_o/2$.

After the mixing layers have coalesced, there will be a region of transitional flow before the turbulent jet becomes self-preserving and, consequently, the self-preserving flow will develop from an apparent origin that is different from the actual origin of the flow at the nozzle exit.*

*The region occupied by the mixing layers is also partly responsible for this shift.

Dimensional analysis gives:-

$$U_o/U_J = \text{function of } (x/h) \qquad (3.2.1a)$$

and $$\delta_{0.5}/h = \text{function of } (x/h) \qquad (3.2.1b)$$

Using these expressions and the conditions for self-preservation, we obtain for the self-preserving region of the flow:-

$$\frac{U_o}{U_J} = \frac{C}{\sqrt{\frac{x}{h} - \frac{x_o}{h}}} \qquad (3.2.2a)$$

$$\frac{\delta_{0.5}}{h} = K\left(\frac{x}{h} - \frac{x_o}{h}\right) \qquad (3.2.2b)$$

where K and C are both constants and x_o/h is a constant and equal to the apparent shift in the origin of the flow.

The momentum integral equation for this flow is:-

$$\rho\int_{-\infty}^{\infty}(U^2 + \overline{u^2} - \overline{v^2})dy = \rho U_J^2 h \text{ , the momentum flux at the nozzle exit.} \qquad (3.2.3)$$

which gives in the self-preserving flow:-

$$U_o^2 \delta_{0.5}\left(I_2 + I_T\right) = U_J^2 h \qquad (3.2.4)$$

where $I_2 = \int_{-\infty}^{\infty} f^2 d\eta$ and $I_T = \int_{-\infty}^{\infty}(g_1 - g_2)d\eta$.

Equation (3.2.4) gives a relationship between the constants k and C in equations (3.2.2a & b). Thus:-

$$C^2 = \frac{1}{K(I_2 + I_T)} \qquad (3.2.5)$$

The value of I_2 can be obtained from the various theoretical curves for the mean velocity profile discussed in section 2 or from experiments. The following table lists the values of I_2 from these sources.

Profile.	I_2
$f = \mathrm{sech}^2(0.8814\eta)$	$(4/3) \times (1/0.8814) = 1.51$
$f = \exp(-0.6932\eta^2)$	$(0.5\pi/0.6932)^{1/2} = 1.51$
$f = \left(1 - \frac{\sqrt{2}-1}{\sqrt{2}}\eta^{1.5}\right)^2$	1.433
Present experiments. (see sections 7,8 & 10)	1.467

The contribution to the momentum integral equation from the turbulent term I_T is small and it is usually ignored. The value of $I_T = 0.046$ was obtained from the present experiments.

Having discussed the simple details of the pure jet flow, we will now consider the results of previous experimenters in this field. Inevitably in the experimental set-ups, there were departures from the ideal model that we have discussed. Firstly, the flows were only quasi-two-dimensional since the jets were obviously of finite span and this may have influenced the results in some cases. Furthermore, the jet flow at the nozzle may not have been uniform and there are also indications to show that the jets emerged at pressures slightly above ambient (see, for example, Miller and Commings (1957)). Notwithstanding these various factors, all the experiments confirmed the prediction that:-

$$U_o \propto x^{-1/2}; \quad \delta \propto x.$$

However, there is some diversity among the various constants of proportionality and the following table lists the essential features and results from the various experiments.

Author	$R_h = U_J h/\nu$	h	Aspect ratio	Max. value of x/h at which measurements were made.	x_o/h	K	C
Forthmann	7.1×10^4	3cms.	20	25	+1.5	0.103	2.3
Van der Hegge Zijnen.	1.3×10^4	0.5cms.	20	40	-0.6	0.096	2.48
	1.3×10^4	1cm	25	40	-1.7	0.099	2.22
Miller & Commings	1.8×10^4	1.3cms	40	40	-1.57	0.096	2.47
Nakaguchi	$0.86\text{-}1.6 \times 10^4$	0.35cms	114	114		0.106	2.3
Reichardt						0.115	

The value of the constant K should not depend on the conditions at the nozzle exit since it is the rate of spread of the jet in the self-preserving region of the flow and, in fact, the various experiments are in moderate agreement over its value. An average of all the data gives $K \approx 0.1$. Using this value and the value of $(I_2 + I_T) = 1.51$ (obtained from the present experiments) in equation (3.2.5), we find that $C = 2.57$. The table shows that the experimental values of C are not in good agreement with this value or, for that matter, with one another. The most likely explanation for this discrepancy is that the jet velocity across the nozzle in the various experiments was not uniform.

An obvious way in which the results in the self-preserving region of the flow can be made independent of the precise nozzle conditions is to regard the nozzle simply as a source of momentum flux, J. Equations (3.2.2a & b) can then be replaced by:-

$$\frac{U_o\sqrt{x-x_o}}{\sqrt{J/\rho}} = C \qquad (3.2.6a)$$

$$\frac{\delta_{0.5}}{x-x_o} = K \qquad (3.2.6b)$$

The constants K and C should now be independent of the nozzle conditions and take values of 0.1 and 2.57 respectively according to the above discussion. Only the shift in the apparent origin of the flow will now depend on the nozzle conditions.

A discussion of the turbulence structure of the plane jet is limited by the fact that,as far as the author is aware, the only experiments in which turbulence measurements were made are those of van der Hegge Zijnen (1958c) and Miller and Commings (1957).

In the experiments of Miller and Commings, static pressure and $\overline{u^2}$ profiles were measured up to x/h = 40 (figure 4). The static pressures were measured with a disc type static probe and the turbulence measurements were made with a constant temperature tungsten hot wire anemometer. These results are interesting because they show that in the outer region of the jet, the $\overline{u^2}$ profiles are apparently self-preserving for $x/h \geq 10$ whereas, even at x/h = 40, the values of $\overline{u^2}/U_o^2$ in the centre region have not become constant although they are clearly not far from becoming so. On the other hand, the static pressure profiles which are effectively regarded as $\overline{v^2}/U_o^2$ profiles, do not exhibit self-preservation anywhere in the jet but it is again clear that they are approaching close to this state at x/h = 40. It also seems that $\overline{u^2}$ and $\overline{v^2}$ are about equal on the jet centre-line.

Van der Hegge Zijnen measured $\overline{u^2}$, $\overline{v^2}$ and $\overline{uv}$ with a constant current tungsten hot wire anemometer and $\overline{u^2}$ and $\overline{v^2}$ again with a heat diffusion technique. The difference between the results from the two measuring techniques and between the measured and calculated shear stress distributions show that the hot wire anemometer is not a very

accurate instrument in this flow where the turbulent intensities relative to the local mean velocity are very high. However, the measured relative magnitudes of the various quantities was probably reasonably accurate and, in addition, van der Hegge Zijnen used an empirical correction which improved the consistency of the results. These results, some of which are shown in figure (5), show that although self-preservation has not been established at x/h=40, the flow is not far from this state. The results also confirm that $\overline{u^2}$ and $\overline{v^2}$ are about equal on the jet centre-line. The numerical differences between the results of van der Hegge Zijnen and Miller and Commings are considerable - figure (5) - and they are presumably due to the instrumentation used. It is not possible to decide which are the most accurate results.

Nakaguchi (1961) also measured some static pressure profiles in a plane jet up to x/h=120 using a conventional static tube. These results (figure (6)) are not in particularly good agreement with those of Miller and Commings but they nevertheless confirm the fact that the flow is closely self-preserving for $x/h \gtrsim 50$.

From measurements of the rate of spread of the jet, it can be shown that the eddy Reynolds number for the pure jet flow is equal to $R_{T_J} = 36.5$* which is over twice the value for the plane wake. According to Townsend, this difference is due to the lateral inflow into the jet (which is absent in the wake) which restricts the lateral growth of the large

---

*This value of the eddy Reynolds number was obtained from a simple integral theory which will be described in section 4.1 and in which the assumed velocity profile is taken from the present experiments. This value of R_{T_J} for the jet should be more representative than the value obtained from the constant exchange hypothesis using $f = \mathrm{sech}^2(0.8814\eta)$ which does not agree particularly well with the experimental velocity profiles.

eddies and causes them to be smaller than those in the wake. According to the energy equilibrium postulate for the large eddies, this leads to a higher value of the eddy Reynolds number (see Townsend (1956) pp.127) which may be related to the value in a wake very roughly by (see Towsend (1956) pp.189):-

$$\frac{R_{TJ}}{R_{Tw}} = \exp\left[-6\left(\frac{\partial U/\partial x}{\partial U/\partial y}\right)_t\right] \qquad (3.2.7)$$

where $\{(\partial U/\partial x)/(\partial U/\partial y)\}_t$ is a typical value in the outer region of the flow of the ratio of the longitudinal strain rate to the lateral strain rate. In the plane jet:-

$$\frac{\partial U/\partial x}{\partial U/\partial y} = \frac{f\frac{dU_o}{dx} - \eta f' \frac{U_o}{\delta_{0.5}}\frac{d\delta_{0.5}}{dx}}{\frac{U_o}{\delta_{0.5}} f'} = \frac{f}{f'}\frac{\delta_{0.5}}{U_o}\frac{dU_o}{dx} - \eta\frac{d\delta_{0.5}}{dx} \qquad (3.2.8)$$

In the outer region of the jet, $f/f' \to 0$ so that:-

$$\frac{\partial U/\partial x}{\partial U/\partial y} \approx -\eta\frac{d\delta_{0.5}}{dx} \qquad (3.2.9)$$

If we take $\eta = 1.5$ as a typical station in the outer region of the flow and $d\delta_{0.5}/dx = 0.1$, we obtain from equations (3.2.7) and (3.2.9) that:-

$$\frac{R_{TJ}}{R_{Tw}} = \exp\left(9\frac{d\delta_{0.5}}{dx}\right) \approx 2.46$$

This agrees (rather too well, in fact) with the observed value of 2.48.

According to Townsend (1956 pp.105), the energy containing eddies are in a state of structural equilibrium in which parameters like R_{uv} are universal constants. Therefore, the larger value of eddy Reynolds number in a plane jet and so lower shear stresses, $\overline{uv}/U_o^2$, should lead also to lower values of the turbulent quantities, $\overline{u^2}/U_o^2$ etc. From the experimental results (figure (5)), this is clearly the case although discrepancies in the data for the plane jet prevent the determination of reliable values of R_{uv}, for example, for comparison with the values found in a wake.

3.3 The turbulent axi-symmetric jet.

Although the present investigation is not directly concerned with the axi-symmetric jet, some of the experimental results on this self-preserving flow are of particular interest. The eddy Reynolds number for this flow is again larger than the value for the plane wake and the Townsend flow model again gives a consistent explanation of this difference. Furthermore, measurements of the intermittency factor in this jet flow (Corrsin and Kistler (1954) reveal that the intermittent region is smaller than in the plane wake, thus supporting Townsend in his conclusion that the large eddies in jets are smaller than those in wakes (Townsend (1956) pp.190). However, it is possible that the smaller intermittent flow region is a characteristic of the axi-symmetric flow and intermittency measurements in a plane jet would be preferable.

Corrsin's measurements (1943) seem to show that self-preservation occurs first in the centre region of the axi-symmetric jet which is opposite to the behaviour of the plane jet. It is also found that $\overline{u^2} > \overline{v^2}$ at the edge of the jet which is in contradiction to Phillips's theory and the results for the plane wake. However, turbulent intensities in a jet are very high at the edge of the flow and, consequently, the accuracy of the hot wire measurements cannot be very good.

Finally, Johannesen (1959) measured static pressure profiles in an axi-symmetric jet up to x/d=100 and found that the pressure coefficient $(-\Delta P_s/\rho U_o^2)$ on the centre-line increased up to a value of 0.048 at x/d=37 and, thereafter, it decreased steadily to a value of 0.013 at x/d=100. This again is not in accord with the results for the plane jet and seems to indicate a very different approach to self-preservation.

4.0 An introduction to the plane jet in a moving airstream.

In this section, we will consider the problem of the plane jet in a moving airstream. Several theories are developed for describing the spread of the jet and the decay of the centre-line velocity. These theories make different assumptions about the relationship between the turbulent shear stresses and the mean velocity profile and the intention is to provide a framework against which subsequent experimental data may be analysed rather than, at this stage, to provide 'working' theories for the plane jet in a moving airstream.

We will consider first the model discussed at the beginning of section 3.2 except that now $U_1 \neq 0$. Dimensional analysis gives for the mean velocity in the jet:-

$$\frac{U}{U_1} = \text{function of } \left(\frac{U_J}{U_1} , \frac{x}{h} , \frac{y}{h} \right) \qquad (4.0.1)$$

and, in particular:-

$$\frac{U_o}{U_1} = \text{function of } \left(\frac{U_J}{U_1} , \frac{x}{h} \right) \qquad (4.0.2a)$$

$$\frac{\delta_{0.5}}{h} = \text{function of } \left(\frac{U_J}{U_1} , \frac{x}{h} \right) \qquad (4.0.2b)$$

In any experimental set-up, the wing must affect the jet flow in the immediate vicinity of the wing trailing edge because of modifications to the local potential flow and also because of the boundary layers on the wing surfaces. However, we can assume that some way downstream these effects will have died out* and in this region the jet nozzle can again

---

*Miller and Commings (1960), for example, carried out measurements in two parallel plane jets whose nozzles were a distance y/h=6 apart. The two jets coalesced forming a single jet whose characteristics for $x/h \geq 20$ were identical with a conventional plane jet in spite of the unusual nozzle exit conditions.

be regarded simply as a source of excess momentum flux, J. Equations (4.0.2a & b) then become:-

$$\frac{U_o}{U_1} = F\left(\frac{J}{\rho U_1^2(x-x_o)}\right) \qquad (4.0.3a)$$

$$\frac{\delta_{0.5}}{J/\rho U_1^2} = G\left(\frac{J}{\rho U_1^2(x-x_o)}\right) \qquad (4.0.3b)$$

where x_o is the apparent shift in the origin of the flow due to the particular nozzle conditions. It is to be noted that as $x \to x_o$, the function F in equation (4.0.2a) must approach the function for a jet exhausting into a stationary atmosphere for which (see equation (3.2.6a):-

$$\frac{U_o\sqrt{x-x_o}}{\sqrt{J/\rho}} = \text{a constant, } C = 2.57$$

Therefore, as $x \to x_o$, we have:-

$$F \longrightarrow C\sqrt{\frac{J}{\rho U_1^2(x-x_o)}} \qquad (4.0.4)$$

Although self-preservation in a jet in a moving airstream is not possible throughout the entire flow field, two types of self-preserving flow can exist in limited regions of the flow. Near the jet exit, where $U_o \gg U_1$, a 'pure' jet flow is possible in which $U_o \propto x^{-1/2}$ and $\delta \propto x$, whereas, far downstream where $U_o \ll U_1$, there will be the possibility of a self-preserving wake type of flow in which $U_o \propto x^{-1/2}$ and $\delta \propto x^{1/2}$. One of the important differences between these two flows is the difference in the eddy Reynolds numbers and, therefore, any theoretical treatment based on this concept must allow for this variation of eddy Reynolds number. It is possible to develop such a theory using Townsend's large eddy hypothesis and details of this theory are given in the following section 4.1.

4.1 Development of a simple theory for the plane jet in a moving airstream.

Since the theory to be developed makes use of integral forms of the momentum and energy equations, some assumption must be made about the mean velocity profiles in a jet. To a good degree of accuracy, the velocity profile in both jets and wakes may be written in the form:-

$$U = U_1 + U_o f(\eta) \tag{4.1.1}$$

where $f(\eta)$ is a universal function. In sections 7, 8 and 10, it will be shown experimentally that this is, in fact, a very good assumption. The momentum integral equation is:-

$$\int_{-\infty}^{\infty} U(U - U_1)dy = \frac{J}{\rho} \tag{4.1.2}$$

where the turbulent terms have been ignored since they are small. Substituting equation (4.1.1) into (4.1.2) gives:-

$$\delta_{0.5}\left(M^2 I_2 + M I_1\right) = \frac{J}{\rho U_1^2} \tag{4.1.3}$$

where $M = U_o/U_1$ and $I_n = \int_{-\infty}^{\infty} f^n d\eta$. Equation (4.1.3) gives a relationship between the jet thickness parameter, $\delta_{0.5}/(J/\rho U_1^2)$, and M. We now require an additional relationship between these variables and the parameter $(x-x_o)/(J/\rho U_1^2)$ - in accordance with equations (4.0.3a & b). We will make use of the energy integral equation and the eddy viscosity concept.* The energy integral equation is :-

$$\frac{1}{2}\rho \frac{d}{dx}\int_{-\infty}^{\infty} U(U^2 - U_1^2)dy = -\int_{-\infty}^{\infty} \tau \frac{\partial U}{\partial y} dy \tag{4.1.4}$$

---

*It will be shown in section 9 that as an empiricism the assumption of an eddy viscosity coefficient constant across the jet is not unreasonable.

Substitution into equation (4.1.4) of the mean velocity profile function - equation (4.1.1) - and an eddy viscosity coefficient assumed constant across the jet gives:-

$$(3M^2I_3 + 6MI_2 + 2I_1)\frac{\delta_{0.5}}{M^3}\frac{dM}{dx} + (M^2I_3 + 3MI_2 + 2I_1)\frac{1}{M^2}\frac{d\delta_{0.5}}{dx} = -\frac{2}{R_T}I' \qquad (4.1.5)$$

where $I' = \int_{-\infty}^{\infty}(f')^2 d\eta$ and $R_T = U_o\delta_{0.5}/\nu_T$ is the eddy Reynolds number.

It is now necessary to specify a form for R_T. If we accept the principle behind Townsend's large eddy hypothesis, we can write:-

$$\frac{R_T}{R_{T_w}} = \exp\left(-\text{constant} \times \left(\frac{\partial U/\partial x}{\partial U/\partial y}\right)_t\right) \qquad (4.1.6)$$

where R_{T_w} is the eddy Reynolds number in the plane wake and $\{(\partial U/\partial x)/\partial U/\partial y)\}$ is a typical value of the strain rate ratio in the outer region of the flow. The use of Townsend's large eddy hypothesis requires that (a) the period of the large eddies is much smaller than the time necessary for an appreciable change in the strain rate ratio and (b) the smaller eddies adjust themselves sufficiently rapidly to ensure that large eddy equilibrium is maintained. Further comments on the applicability of this hypothesis will be made later in section 11. From equation (3.2.8), we have:-

$$\frac{\partial U/\partial x}{\partial U/\partial y} = \frac{f}{f'}\frac{\delta_{0.5}}{M}\frac{dM}{dx} - \eta\frac{d\delta_{0.5}}{dx} \qquad (4.1.7)$$

and, for convenience, we can approximate to equation (4.1.6) by the expression:-

$$\frac{1}{R_T} = \frac{1}{R_{T_w}}\left[1 + \chi\left\{\frac{\delta_{0.5}}{M}\frac{dM}{dx}\left(\frac{f}{f'}\right)_t - \frac{d\delta_{0.5}}{dx}\eta_t\right\}\right] \qquad (4.1.8)$$

where χ is a constant and $(f/f')_t$ and η_t are evaluated at some typical station in the outer region of the flow, say at $\eta = 1.5$.

Using equations (4.1.3) and (4.1.8) in equation (4.1.5) gives after some algebra:-

$$\frac{J/\rho U_1^2}{M^4(M+C)^2}\left(AM^3+BM^2+CM\right)\frac{dM}{dx} = -\frac{2I'}{R_{T_w}} \qquad (4.1.9)$$

where $A = \frac{I_3}{I_2} + \frac{2}{R_{T_w}} \cdot \frac{I'}{I_2}\left(\alpha_1 + 2\alpha_2\right)$

$$B = 2\frac{I_3 I_1}{I_2^2} + 2\frac{I_1 I'}{R_{T_w} I_2^2}\left(\alpha_1+\alpha_2\right)$$

$$C = I_1/I_2$$

and $\alpha_1 = \chi\left(\frac{F}{F'}\right)_t$; $\alpha_2 = \chi\eta_t$.

Equation (4.1.9) may be integrated directly to give:-

$$\log\left(\frac{M+C}{M}\right)\left[\frac{2B-3}{C^3}-\frac{A}{C^2}\right]+\frac{1}{M+C}\left[\frac{A}{C}-\frac{B-1}{C^2}\right]+\frac{1}{M}\left[\frac{2-B}{C^2}\right]-\frac{1}{2CM^2} = \frac{-2I'}{R_{T_w}}\frac{x-x_0}{J/\rho U_1^2} \qquad (4.1.10)$$

The equations (4.1.3) and (4.1.10) give a solution for the spread of the jet and the decay of the centre-line velocity which is in accordance with the dimensional arguments behind equations (4.0.3a & b).

It is to be noted that as $M\to\infty$('pure' jet flow), the equations (4.1.3) and (4.1.10) give:-

$$\frac{\delta_{0.5}}{x-x_0} = \frac{4I'}{R_{T_w} I_2 A} \quad ; \quad \delta_{0.5} U_0^2 I_2 = \frac{J}{\rho} \qquad (4.1.11)$$

i.e. $\delta_{0.5} \propto x$; $U_0 \propto x^{-1/2}$.

and as $M\to 0$(wake flow), they give:-

$$\frac{1}{2M^2C} = \frac{2I'}{R_{T_w}}\frac{x-x_0}{J/\rho U_1^2} \quad ; \quad MI_1 = \frac{J/\rho U_1^2}{\delta_{0.5}} \qquad (4.1.12)$$

i.e. $\delta_{0.5} \propto x^{1/2}$; $U_0 \propto x^{-1/2}$.

A very simple form of the above theory which will be useful for comparative purposes at a later stage can be obtained by assuming that the eddy Reynolds number is constant throughout the flow and equal to the 'pure' jet value. It will, of course, have the wrong asymptotic

behaviour as $M \to 0$ since, as already discussed, the eddy Reynolds number cannot be constant. This theory is easily obtained from equation (4.1.10) by setting $\alpha_1 = \alpha_2 = 0$ and $R_{T_W} = R_{T_J}$. Also of interest for reference purposes is the limiting case of the constant eddy Reynolds number theory when $U_1 = 0$ ('pure' jet flow). The momentum integral (equation (4.1.3)) gives:-

$$\delta_{0.5} U_0^2 I_2 = J/\rho \qquad (4.1.13)$$

whence $$\frac{d\delta_{0.5}}{dx} = -2\frac{\delta_{0.5}}{U_0}\frac{dU_0}{dx} \qquad (4.1.14)$$

The energy integral equation (4.1.5) gives:-

$$3\frac{\delta_{0.5}}{U_0}\frac{dU_0}{dx} + \frac{d\delta_{0.5}}{dx} = -\frac{2}{R_{T_J}}\cdot\frac{I'}{I_3} \qquad (4.1.15)$$

Substitution into equation (4.1.15) of equation (4.1.14) gives:-

$$\frac{\delta_{0.5}}{x - x_0} = \frac{4I'}{R_{T_J} I_3} \qquad (4.1.16)$$

Since both the variable and constant eddy Reynolds number theories must have the same asymptotic behaviour as $U_1 \to 0$, reference to equations (4.1.11) and (4.1.16) show that it is necessary for $R_{T_J} I_3 = R_{T_W} I_2 A$. This can easily be verified as true using equation (4.1.8).

In order to apply the above theories, it is necessary to give values to the integrals I_n (n = 1, 2, 3) and I' and the constants α_1 and α_2. This will be considered later in section 11.

4.2 Existing theories for the turbulent jet in a moving airstream.

The only other theoretical work on the turbulent plane jet in a moving airstream known to the author is that of Abramovich (1958). Discussion of this work has been delayed until now because it is based upon an assumption which has little in common with previously discussed ideas.

The work of Abramovich is based apparently on the notion that the flow spreads as a result of a lateral movement of the jet boundary which is convected downstream with the mean velocity of the flow. Therefore:-

$$\frac{d\delta}{dx} = \frac{V'}{U_M} \qquad (4.2.1)$$

where V' is the velocity of the lateral movement of the jet boundaries and U_M is the mean velocity of the jet. Furthermore, if it is assumed that V' is proportional to the difference in the mean velocity across the shear layer, U_o, we obtain:-

$$\frac{d\delta}{dx} = \Lambda \frac{M}{M+2} \qquad (4.2.2)$$

where Λ is a constant. Using the momentum integral equation (4.1.3) and equation (4.2.2) gives the following solution to the jet problem*:-

$$\frac{2}{C^3}\log\left(\frac{M+C}{M}\right) + \frac{1}{M+C}\left(-\frac{2}{C^2}+\frac{1}{C}\right) - \frac{1}{CM} - \frac{1}{CM^2} = -\Lambda I_2 \frac{x-x_o}{J/\rho U_1^2} \qquad (4.2.3)$$

This equation is similar in form to the solutions obtained in section 4.1.

It is to be noted that for the 'pure' jet flow, equation (4.2.2) gives:-

$$\left(\frac{d\delta_{o\cdot s}}{dx}\right)_{U_1=0} = \Lambda$$

In the notation of the constant eddy Reynolds number theory (equation (4.1.6)), we obtain:-

$$\Lambda = \frac{4I'}{R_{T_J} I_3}$$

Therefore, equation (4.2.3) may be re-written:-

$$\frac{I_3}{2I_2}\left(\frac{2}{C^3}\log\left(\frac{M+C}{M}\right) + \frac{1}{M+C}\left(-\frac{2}{C^2}+\frac{1}{C}\right) - \frac{1}{CM} - \frac{1}{CM^2}\right) = -\frac{2I'}{R_{T_J}}\frac{x-x_o}{J/\rho U_1^2} \qquad (4.2.4)$$

---

*The solution obtained here is quite different from that given in Abramovich's original paper. Abramovich made use of an additional (and redundant) relationship for the centre-line velocity. The common feature of the above work and Abramovich's paper is the use of equation (4.2.2).

As $M \to \infty$, this equation gives the conventional pure jet solution - equation (4.1.16). However, as $M \to 0$ (wake flow), equation (4,2.4) gives:-

$$\frac{1}{2M^2C} = 2\Gamma' \frac{x-x_0}{J/\rho U_1^2} \cdot \frac{I_2}{R_{T_J} I_3} \qquad (4.2.5)$$

This may be compared with the previous wake flow solution – equation (4.1.12). It is clear that the Abramovich wake solution is equivalent to an eddy viscosity solution with an eddy Reynolds number $R_{T_W} = R_{T_J}(I_3/I_2)$. From subsequent experimental results, it will be shown that $I_3/I_2 = 0.82$ whereas, as discussed in section 3, $R_{T_W}/R_{T_J} = 0.4$. Therefore, Abramovich's theory cannot be asymptotically correct as $M \to 0$.

A comparison between the various theories discussed in this section and the experimental results will be given in section 11.

5.0 The plane jet model and its associated equipment.

5.1 The plane jet model.

The apparatus consisted basically of a thin wing spanning horizontally the 4' x 3' closed return tunnel at Queen Mary College with a jet nozzle consisting of a slot 18" x 3/8" extending over the centre 18" of the trailing edge of the wing. The air supply for this jet was provided by a centrifugal fan which supplied air to the jet via a duct within the wing. To approach two-dimensional conditions as closely as possible, two plywood walls were mounted in the tunnel parallel to the airstream, one on either side of the jet.

The basic problems in designing the apparatus were to ensure that the jet had an even spanwise velocity distribution and also that the wing did not appreciably disturb the mainstream either by having a large drag or by modifying the potential flow. These two problems were aggravated to some extent by the fact that the only source of air supply was a low pressure centrifugal fan. In consequence, small high pressure ducting feeding the jet through high loss gauzes could not be used.

In order to obtain some idea of the best internal layout of the full-scale model, a small test model was made (figure 7). This consisted of a sheet of brass bolted to a perspex sheet with duralumin spacers in between forming a duct 6" x 1/4" which contracted to 3" x 1/4" at a right angle corner. Air, supplied from the centrifugal fan, flowed through the 6" duct, negotiated the corner where a variety of corner vanes were tested and then exhausted through the 3" duct to atmosphere.

The perspex plate enabled tufts attached to the duct walls and corner vanes to be observed. A few static holes in the duct walls were also available to check pressure losses. The first tests were carried out with only three corner vanes and a typical velocity distribution across the span of the 3" jet is shown as curve I in figure 8. Clearly this set-up was unsatisfactory because the wakes of the corner vanes produced large variations in the exit velocity distribution. The number of corner vanes was increased to 8 and, as the results in figure 8 curve II show, this improved the distribution. Finally, a 2:1 contraction was added to the jet exit, reducing the jet thickness to 1/8", and, in this way, the velocity distribution given as curve III in figure 8 was obtained. This was regarded as satisfactory and design of the full scale model was then undertaken. Under all conditions, the duct losses were very low and not more than a few inches of water.

The full scale model is shown in diagrams and photographs in figures (9-11). It can be seen that the mid-chord region of the wing consisted of two rectangular sheets of brass screwed to 1" duralumin spacers in between them. These spacers, in addition to keeping the model rigid, also formed the sides of the internal ducting. This rectangular duct within the wing was 13" x 1" expanding to 18" x 1" in negotiating the corner to the jet nozzle. It is to be noted that, unlike the test model, the duct in the full scale model expanded around the corner. This difference resulted from the decision to supply air from one end of the wing only instead of from both ends, as was envisaged in the early stages of the programme. This decision was made on grounds of simplicity.

The corner vanes, of which there were 23, were bent out of brass sheets (18 S.W.G) and had small lugs brazed to them to accommodate 10 b.a. screws which held them to the brass plates (figure 12). The shape, size and density of these corner vanes were arrived at from the results of the test model and also from some data on aircraft ducting (Patterson - 1937)

The nose section of the model was made in three parts, all of them from wood. The centre-section, which was the "working" section of the wing, was made very carefully from mahogany and held by the two metal formers shown as A_1 and A_2 in figure 10. The profile of this nose section was designed by a hodograph method which is fully described in appendix I. The object of this profile was to avoid large adverse pressure gradients at the junction of the nose section with the parallel mid-chord section and, thereby, to avoid transition and a consequent increase in drag. It was gratifying to find that, on test, transition did not occur anywhere on the parallel mid-chord section of the wing. It had been hoped to have static holes in the nose section but this would have involved some difficult machining and, since it was not vital, it was avoided. On either side of the mahogany nose section was a similar nose section but made less carefully out of soft wood.

The trailing edge section over the "working" part of the wing, shown in figure 10, consisted of two shaped mahogany pieces 18" in span and 4" chord. These were mounted on the two metal formers shown as B_1 and B_2 in figure 10. The internal profile of the two pieces provided a contraction from the 1" of the wing duct to 3/8" for the jet exit. The external profile was an arbitrary smooth curve which

simply faired the parallel section down to the jet exit. Sharp trailing edges at the jet exit were obtained by inserting strips of mica into the mahogany which could then be shaped to give a fine edge whereas the mahogany alone could not. These trailing edge pieces were supported only at the ends and, consequently, the jet was entirely free from any obstructing spacers. In retrospect, fine spacers could have been used but, in any event, the variation in the jet slot width was only about $\pm 2^{o/o}$ over the centre 10" of the jet as shown by figure 13.

On either side of the 18" span jet, ordinary soft wood trailing edge pieces were mounted.

On the completed model, the holes for countersunk screws and gaps between the various wooden pieces and the brass plates were filled with Araldite and the whole model carefully rubbed down and polished.

The model was supported in the tunnel by 8 adjustable brass legs, four above and four below the model (see figure 9). These enabled the model to be aligned accurately in both the streamwise and spanwise directions. On either side of the jet, 3/8" thick plywood false walls were mounted parallel to the mainstream. They extended from floor to ceiling and to as far back as 30" from the jet exit. Static holes in these walls enabled them to be aligned accurately with the airstream.

Air was supplied to the wing duct from a 7 h.p. centrifugal fan outside the tunnel via a contracting duct (figures 15). This duct was designed according to the method of Whitehead, Wu and Waters (1951) and tests indicated that the velocity distribution at its exit was very even.

A number of tests were carried out to check the two-dimensionality of the flow and in all cases the spanwise variations were not excessive. At the jet exit, the variation in total head across the span was not greater than $1^{o/o}$. Further downstream at x = 19", the spanwise distribution of total head on the jet centre-line began to develop the "saddleback" charateristic shown in figure (14) and noted also by van der Hegge Zijnen (1958a) in his experiments. However, over the centre 10" of the span, the total head variation was still not greater than $4^{o/o}$.

5.2 <u>The traversing gear</u>.

The traversing gear consisted of two basic units,namely the vertical traversing mechanism and the longitudinal traversing mechanism (these can be seen in figure (16)).

The carriage for carrying the measuring instruments was screwed up and down by a 1/4" diameter B.S.F. screwed rod (26 t.p.i.). This screw was driven by a Bowden cable from outside the tunnel by a 12 volt D.C. motor with a mechanical counter attached to it for recording the number of motor revolutions. Ten revolutions of the motor were equivalent to one turn of the screw.

The longitudinal traversing mechanism which was similar in construction to the vertical traversing mechanism was mounted on the tunnel ceiling and again driven from outside by an electric motor. The vertical traversing mechanism was suspended from the longitudinal traversing gear on a movable carriage. The lower end of the vertical traversing mechanism ran on ball races in a rail on the floor of the tunnel and which constrained the gear from moving sideways (see figure (16).

Both pitot, static tubes and hot wire anemometers could be fitted to the measuring instruments carriage. By means of simple adjusting screws, incidence of the measuring instruments could be varied over the limited range of $\pm 3^{o}$. Also, the design allowed the instruments to be rotated about their axes in steps of 90^{o}. This feature was incorporated to enable sloping hot wire anemometers to be rotated easily through 180^{o}- a maneouvre necessary for the measurement of the turbulent shear stress and the $\sqrt{\overline{v^2}}$ and $\sqrt{\overline{w^2}}$ turbulent intensities.

6.0 Instrumentation.

In the experiments, pitot and static tubes were generally used for mean flow measurements whereas a hot wire anemometer was used for turbulence measurements. Notwithstanding the considerable amount of work that has been dome on the use of these instruments in turbulent flows, many problems still remain and only with the greatest care can reasonably accurate results be obtained. In consequence, a rather full account will be given of both the theoretical and practical work the author undertook on the subject. Furthermore, since a large part of the research programme was taken up in the construction and development of the hot wire anemometer equipment, this will be fully described also.

6.1 The theory of the hot wire anemometer.

There are a number of different techniques for operating a hot wire anemometer. The most common are:-

(i) The constant current technique for both mean flow and turbulence measurements.

(ii) The constant current technique for turbulence measurements only. The mean resistance is then kept constant for different mean velocities.

(iii) The constant resistance technique for both turbulence and mean flow measurements.

In the first two methods, the wire, which is usually one arm of a Wheatstone bridge, is operated in series with a large resistance so that in the presence of fluctuating velocities the current remains almost constant even though the resistance varies. However, in method (i) the current is kept constant even for different values of mean velocity and a calibration consists of measuring the variation of wire resistance

as a function of mean velocity. In method (ii), the mean resistance of the wire is kept constant for different values of the mean velocity by adjusting the supply voltage to the Wheatstone bridge. A calibration consists of measuring the variation of mean current through the wire as a function of mean velocity. Finally, in method (iii), the resistance is kept constant for both mean velocity variations and turbulence by means of a feedback amplifier that adjusts the Wheatstone bridge supply voltage to maintain the constant resistance condition. A calibration is identical to that required for method (ii).

The constant resistance method (iii) is almost certainly the most satisfactory provided the basic problem of developing a suitable feedback amplifier has been overcome. The advantages of this method are (a) the mean flow calibration can be applied directly to fluctuating velocities (b) that since the temperature of the wire remains sensibly constant, thermal inertia effects are generally negligible, and (c) errors due to the non-linear response of the hot wire anemometer are smaller using this method than either of the other two techniques. Of these other two techniques, method (ii) is generally regarded as superior because it has greater sensitivity and mean flow calibrations are more readily obtained. The disadvantage is that knowledge of the heat transfer law for the wire is required. Both constant current methods require compensation for thermal inertia effects. However, the apparatus is less complicated than that required for constant resistance operation and, also, measurements involving more than wire can more easily be carried out.

On the grounds that some constant current equipment was already available and also due to its greater simplicity, it was decided to employ the constant current technique and, in particular, method (ii).

In the past, it has been usual to assume that the steady state heat transfer law for a hot wire normal to an airstream could be written:-

$$Nu = A' + B'(R_d)^{1/2} \qquad (6.1.1)$$

where Nu and R_d are the Nusselt and Reynolds numbers respectively and A' and B' are constants. However, as a result of some careful experiments, Collis and Williams (1959) proposed a new heat transfer law:-

$$Nu\left(\frac{T_m}{T_\infty}\right)^{-0.17} = A'' + B''(R_d)^n \qquad (6.1.2)$$

where the constants A", B" and n take the following values.

	n	A"	B"
$0.02 \leqslant R_d \leqslant 44$	0.45	0.24	0.56
$44 \leqslant R_d \leqslant 140$	0.51	0	0.48

T_∞ is the absolute ambient temperature and T_m is the mean of the ambient and wire temperatures. The fluid properties in Nu and R_d were evaluated at this mean temperature. The effect of yawing the wire may be accounted for by multiplying the second term on the right hand side of equation (6.1.2) by a function $S(\psi)$ where ψ is the angle between the wire and the direction of the airstream. If only the component of velocity normal to the wire was effective in the heat transfer processes, $S(\psi)$ would be equal to $(\sin\psi)^n$. However, according to some experiments of C.A.G. Webster (1962):-

$$S(\psi) = \sin^n\psi(1 + a^2\cot^2\psi)^{n/2} \qquad (6.1.3)$$

where "a" is a constant which was found to be 0.2 for the range of

wire lengths normally used for turbulence measurements.

In order to apply equations (6.1.2) and (6.1.3) to the measurement of turbulence, it is necessary to make a number of assumptions. The most fundamental of these is that the steady state heat transfer law applies instantaneously even when the flow is unsteady. This will be valid if the characteristic time for the establishment of steady flow past the wire is much less than the characteristic time for the velocity fluctuations. If we crudely assume that d/q and L/q are the respective characteristic times then it is simply necessary that:-

$$d/L \ll 1.0$$

where d is the wire diameter and L and q are the characteristic length and velocity scales of the turbulence respectively. This inequality is always fulfilled in normal applications of hot wire anemometers.

Equation (6.1.2) may be written in terms of practical parameters in the form (see Collis and Williams (1959)):-

$$\frac{iR_H}{T_H - T_\infty} = A\left[1 + \Omega(T_H - T_\infty)\right] + B\left[1 + \Pi(T_H - T_\infty)\right] U^n S(\psi) \qquad (6.1.4)$$

where i is the current through the wire, T_H and R_H are the absolute operating temperature of the wire and the wire resistance at this temperature respectively. A and B are constants for a given wire, fluid and ambient temperature. Ω and Π are also constant for a given ambient temperature and take values of 0.00164 and 0.00025 respectively at 293^{o}A according to Collis and Williams. The parameters Ω and Π are only weakly dependent on the ambient temperature and can be regarded as absolute constants over the range of ambient temperatures normally encountered.

For the general relationship between the wire resistance, R, and its absolute temperature, T, we will assume that:-

$$R = R_o\left(1 + \alpha(T-T_o) + \beta(T-T_o)^2\right) \qquad (6.1.5)$$

Where T_o is 273^oA and R_o is the wire resistance at this temperature.

α and β are temperature coefficients of resistivity for the wire.

Since, in general, $\beta \ll \alpha$ we may re-write equation (6.1.5) as:-

$$T_H - T_\infty = \frac{R_H - R_\infty}{\alpha R_o}\left[1 - \frac{\beta}{\alpha}\,\frac{R_H + R_\infty - 2R_o}{\alpha R_o}\right] \qquad (6.1.6)$$

and substituting this equation in equation (6.1.4), we obtain:-

$$\frac{I^2 R_H}{R_H - R_\infty}\left(\frac{\alpha R_o}{1 - \frac{\beta}{\alpha}\cdot\frac{R_H + R_\infty - 2R_o}{\alpha R_o}}\right) = A\left[1 + \frac{\Omega}{\alpha R_o}(R_H - R_\infty)\left(1 - \frac{\beta}{\alpha}\,\frac{R_H + R_\infty - 2R_o}{\alpha R_o}\right)\right]$$

$$+ B\left[1 + \frac{\Pi}{\alpha R_o}(R_H - R_\infty)\left(1 - \frac{\beta}{\alpha}\,\frac{R_H + R_\infty - 2R_o}{\alpha R_o}\right)\right] U^n S(\psi) \qquad (6.1.7)$$

Equation (6.1.7) is non-linear and consequently the response of the hot wire to a turbulent flow is extremely complex and, in an exact way, detailed knowledge of the structure of the particular flow would be necessary before this response could be determined. However. linearization of the equation is possible if only first derivatives are used in the Taylor expansion:-

Taylor expansion:-

$$R_H + \delta R_H = R_H + \frac{\partial R_H}{\partial U}\delta U + \frac{\partial R_H}{\partial \psi}\delta\psi + \frac{\partial R_H}{\partial i}\delta i + \frac{\partial^2 R_H}{\partial U^2}\frac{(\delta U)^2}{2} + \frac{\partial^2 R_H}{\partial \psi^2}\frac{(\delta\psi)^2}{2} + \frac{\partial^2 R_H}{\partial i^2}\frac{(\delta i)^2}{2} + \ldots.$$

This will be possible only for small turbulence levels when, also:-

$$\delta U = \sqrt{(U+u)^2 + v^2} - U \approx U\left(\frac{u}{U} + \frac{1}{2}\,\frac{u^2+v^2}{U^2}\right) \approx u$$

and $$\delta\psi = \tan^{-1}\frac{v}{U+u} \approx \frac{v}{U} \qquad (6.1.8)$$

This linearization is algebraically complex and only the end result

will be quoted here. We find that for constant current operation:-

$$\frac{-i^2}{i^2-i_o^2}\ \frac{R_\infty}{R_H(R_H-R_\infty)}\ (1+\phi)\,\delta R_H = n\frac{\delta U}{U} + \frac{\partial S}{\partial \psi}\cdot\frac{\delta \psi}{S}$$

or, using equations (6.1.3) and (6.1.8):-

$$\frac{-i}{i^2-i_o^2}\ \frac{R_\infty}{R_H(R_H-R_\infty)}\ (1+\phi)\,e = n\frac{u}{U} + n\cot\psi\left[1-\frac{a^2}{\sin^2\psi\,(1+a^2\cot^2\psi)}\right]\frac{v}{U} \qquad (6.1.9)$$

where the values of i, R_H, U and ψ are now mean values and where $e = i\,\delta R_H$ is the change in voltage across the wire due to the turbulent velocities u and v. i_o is the current at U=0 obtained from equation (6.1.7). Also:-

$$\phi = \frac{R_H}{R_\infty}\ \frac{R_H-R_\infty}{R_o}\left[\frac{i_o^2}{i^2}\cdot\frac{\Omega}{\alpha}\ \frac{1}{1+\frac{\Omega}{\alpha R_o}(R_H-R_\infty)} + \frac{i^2-i_o^2}{i^2}\ \frac{\Pi}{\alpha}\ \frac{1}{1+\frac{\Pi}{\alpha R_o}(R_H-R_\infty)} - \frac{\beta}{\alpha^2}\right]$$

Equation (6.1.9) is similar in form to the expression obtained by Ruetnik (1955) using King's law and differs from the more usual expressions (see, for example, Newman and Leary (1950)) by the inclusion of the $(1+\phi)$ term. This term can be important and, if it is ignored, errors may result of about $20^{o}/_{o}$ to $30^{o}/_{o}$ in the values of $\overline{u^2}$, say. As pointed out by Ruetnik, the β/α^2 term in the expression for ϕ is positive for Tungsten and negative for Platinum taking the respective values of +0.026 and -0.045.

The application of equation (6.1.9) to practical measurements follows conventional procedure. Equation (6.1.9) may be written:-

$$\hat{\beta}\,e = n\frac{u}{U} + n\cot\psi\,F(\psi)\,\frac{v}{U} \qquad (6.1.10)$$

where $\hat{\beta} = \frac{-i}{i^2-i_o^2}\ \frac{R_\infty}{R_H(R_H-R_\infty)}\ (1+\phi)$ and $F(\psi) = 1-\frac{a^2}{\sin^2\psi\,(1+a^2\cot^2\psi)}$

The wire is operated at a constant value of R_H/R_∞. i_o^2 is obtained from the mean flow calibration of i^2 against $U^{0.45}$. In practice, the

mean square of the voltage signal, e , from the wire is measured so that if we square equation (6.1.10) and take the mean value, we obtain the relationship between this voltage measurement and the turbulent intensity. For the measurement of $\overline{u^2}$, a wire with $\psi = 90^0$ is used. In this case:-

$$\hat{\beta}^2 \overline{e^2} = n^2 \frac{\overline{u^2}}{U^2}$$

For the measurement of $\overline{uv}$ and $\overline{v^2}$, a single sloping wire may be used if two measurements are made with the wire first in one position and then rotated through 180^0. In this case, we have for the two measurements:-

$$\text{(i)} \quad \hat{\beta}^2 \overline{e_1^2} = n^2 \frac{\overline{u^2}}{U^2} + n^2 \cot^2\psi \, F^2(\psi) \frac{\overline{v^2}}{U^2} + 2n^2 \cot\psi \, F(\psi) \frac{\overline{uv}}{U^2}$$

$$\text{(ii)} \quad \hat{\beta}^2 \overline{e_2^2} = n^2 \frac{\overline{u^2}}{U^2} + n^2 \cot^2\psi \, F^2(\psi) \frac{\overline{v^2}}{U^2} - 2n^2 \cot\psi \, F(\psi) \frac{\overline{uv}}{U^2}$$

The difference between these two measurements gives:-

$$\hat{\beta}^2 \left(\overline{e_1^2} - \overline{e_2^2} \right) = 4n^2 \cot\psi \, F(\psi) \frac{\overline{uv}}{U^2}$$

from which $\overline{uv}$ can be obtained.

Half the sum gives:-

$$\hat{\beta}^2 \left(\frac{\overline{e_1^2} + \overline{e_2^2}}{2} \right) = n^2 \frac{\overline{u^2}}{U^2} + n^2 \cot^2\psi \, F^2(\psi) \frac{\overline{v^2}}{U^2}$$

If $\overline{u^2}$ has already been measured, $\overline{v^2}$ can be obtained. This single sloping wire technique for $\overline{v^2}$ is convenient but not very accurate. The use of a two wire X-probe is more accurate but it was not used because of the difficulty of making them.

Compensation for thermal inertia effects follows conventional practice and, in the present experiments, the square wave method of compensation was used.

It is relevant to mention briefly the effect of high level turbulence. In this case, the non-linear response of the hot wire

becomes important and the accuracy of both mean velocity and turbulence measurements is affected. Hinze (1959) made an attempt to assess this error in the case of the measurement of $\overline{u^2}$. He obtained the following relationship between the actual value of $\overline{u^2}$ and the measured value using linear relationships similar to those derived above:-

$$\left(\frac{\overline{u^2}}{U^2}\right)_{linear} = \left(\frac{\overline{u^2}}{U^2}\right)_{actual} \times \left[1 + \hat{\alpha}\left(\frac{\overline{u^2}}{U^2}\right)_{actual}\right]$$

where $\hat{\alpha}$ has a value between about 2.0 and 3.5 depending on the nature of the turbulence. According to this expression, if errors in $\overline{u^2}$ due to non-linearity are to be less than $10^{o/o}$, $\overline{u^2}/U^2$ should be no greater than 0.04. What precise effect high level turbulence has on measurements of shear stress and lateral intensities is unkhown.

6.2 <u>The hot wire anemometer equipment</u>.

The main aim in the development of the hot wire equipment was to ensure that the apparatus was reliable and of high accuracy. As previously mentioned, the equipment was of the constant current type and consisted of the following units:-

(i) Hot wire probes.

(ii) Bridge circuit.

(iii) D.C. supply for the bridge.

(iv) Amplifier.

(v) Square wave generator.

(vi) Oscillator.

(vii) Variable high and low pass filter.

(viii) Differentiating circuit.

(ix) Intermittency meter.

(x) Thermo-junction.

A block diagram and photograph of the equipment is shown in figures (17) and (18).

(i) The hot wire probes.

The probes (figure (19)) consisted of 24 s.w.g. copper wire threaded down fine twin bore quartz tube which was in turn fixed into a brass holder with Araldite. It subsequently became necessary to coat the quartz tubing with Araldite to prevent vibrations of this quartz tube.

(ii) The bridge circuit.

The bridge circuit (figure (20)) was of fairly conventional design and constructed throughout with precision resistors. The 1Ω resistors in series with the hot wire enabled the current through each wire to be determined by measuring the voltage drop across these resistors. For balancing the bridge, an internal galvanometer could be used but for obtaining a very fine balance, a Sefram light spot galvanometer could be plugged in. This latter instrument which was of shock proof design was also used to measure the voltage drop across the 1Ω series resistors and was valuable in making accurate measurements both reliable and easy. In its dual role as a galvanometer and voltmeter, it had a variety of ranges that could be selected by a switch on the front panel. These were:-

0.5 ; 1.5 ; 6 ; 15 ; 30 ; 60 millivolts.

5 ; 15 ; 30 microamperes.

The meter scale length was 30 cm.

A Tinsley potentiometer was also available if extra accuracy was needed.

(iii) D.C. supply for the bridge.

This was provided by three transistor stabilised power packs giving a total of 45 volts. Ripple was less than 3 mv.

(iv) The amplifier.

An amplifier and its associated power supplies was already available. However, the amplifier was completely rebuilt and modified.

The circuit diagram is shown in figures (21a) and (21b). The first stage was constructed throughout with high stability carbon resistors and to ensure low hum and good self-balancing properties, the circuit modifications suggested by D. R. Birt (1960) were incorporated. A noticeable improvement of these properties was obtained.

The compensation stage had provision for a range of time constants of 0-1 milliseconds. An analysis of the performance of R.C. compensation networks is given in appendix II.

The push-pull output stage signal could be fed directly into the circuit shown in figure (22) which consisted of a transformer (manufactured especially for these operating conditions) with the thermo-junction as load. Provision was made to monitor the input and output signals to the transformer. A dummy load could be switched in as the load to the transformer so that the signal level could be adjusted to prevent overloading the thermo-junction when it was subsequently switched in.

The variable high and low pass filter unit could be interposed if necessary between the amplifier output stage and the thermo-junction circuit.

Figure (23) shows the frequency response of the amplifier in a variety of operating conditions. It appears that the 2nd stage

attenuator, which simply altered the a.c. anode load, affected the frequency response and this was almost certainly due to stray capacitance across the d.c. anode loads. Thus, the amplifier was used wherever possible with the 2nd stage attenuator in positions 2-6 under which conditions the gain was constant from 5c/s to 10kc/s to within $5^{o/o}$.

(v) The square wave generator.

The square wave generator (figure (24)) was very similar to the one used by Newman and Leary (1950) and had a frequency range from 400 c/s to 1kc/s.

(vi) The differentiating circuit.

Some turbulence measurements were carried out which necessitated the measurement of the mean square of the time derivative of the u-component of the turbulence, $\overline{(\partial u/\partial t)^2}$. The simple differentiating circuit shown with its performance in figure (25) was constructed for this purpose. An analysis of the differentiating circuit performance is given in appendix II.

(vii) The intermittency meter.

The circuit for this instrument is shown in figure (26). The object of this instrument was to measure the percentage of time for which turbulence was present in the flow. If the hot wire signal was differentiated (or passed through the high pass filter), there were well defined "bursts" of turbulence near the edge of the jet(figure (28)). This intermittent high frequency signal was amplified by V1 and the output from the anode load transformer was then rectified and smoothed. This signal was then applied to the grid of a Schmitt trigger circuit (V2).

When there was no signal above a certain threshold value applied to this circuit, the valve V2a was conducting and V2b was cut-off. However, when the applied voltage to V2a exceeded a certain threshold value, the circuit'flipped' into a state in which V2b was conducting and V2a was not. Thus, when fed with the intermittent hot wire signal, pulses of turbulence resulted in constant amplitude pulses of the same duration from the Schmitt trigger circuit. Finally, to obtain a steady meter reading of the percentage time that turbulence was present, the trigger circuit output was attenuated by 15:1, heavily smoothed (RC = 4secs) and then fed into a d.c. coupled cathode follower (V3). The "time average" was obtained using a 1 volt d.c. meter connected across the cathode load.

A difficulty with this instrument was to select a sufficiently large smoothing condenser to provide a d.c. signal that would fire the Schmitt trigger circuit during a turbulent "burst" and yet was not so large that the trigger circuit did not cut-off until some time after the end of the turbulent "burst". The effect of these two extremes is shown schematically in figure (27). The effect of having too large a capacitor was limited to some extent by the use of a Zener diode which prevented the rectified signal from exceeding 12 volts.

The technique for setting up the instrument was to first adjust the two potentioneters (I and II in figure (26)) so that full scale deflection of the meter was obtained with the trigger circuit in the "on" and "off" states. The "d.c. level control" was then adjusted so that the d.c. level on the grid of valve V2a was about 10 volts below that necessary for triggering. The intermittent signal was then applied and it's amplitude gradually increased until the trigger circuit began to fire. It was then

a process of observing simultaneously the output from the trigger circuit and either the rectified or differentiated turbulence signal and adjusting the level of the input signal and the d.c. level control until the Schmitt trigger output coincided as near as possible with a turbulent "burst". For values of the intermittency factor, γ, less than 0.7, this correspondence could be obtained fairly readily but for values greater than this, the C.R.O. traces became too confused to judge. However, the overall accuracy of the intermittency factor is probably about ± 0.1. In figure (28) are shown traces of the filtered turbulence signal along with outputs from the rectifier circuit and the Schmitt trigger circuit.

(x) The thermo-junction.

The thermo-junctions gave outputs of about 6 millivolts for an r.m.s. input voltage of about 0.5 volts (coil resistance $\approx 100\Omega$). Ideally the output voltage (v_o) should be proportional to the mean square of the input voltage (v_i). However, in practice, this proportionality was not obtained and only for mean input voltages of less than 0.3 volts was this even approximately the case and, in consequence, it was necessary to restrict input voltages to values less than 0.3 volts. As a matter of interest, the best fit was obtained with $v_o \propto v_i^{1.9}$ which has been previously noted by Bradshaw (1961).

6.3 The practical application of the hot wire anemometer.

For the sake of brevity, published reports do not generally go into details concerning experimental techniques. However, the present author experienced difficulty in developing the hot wire anemometer so that reasonably accurate measurements could be obtained and, since the accuracy and consistency of hot wire results depends so much on the

experimental technique, a brief account of the development and use of the hot wire anemometer would seem to be of value.

Both tungsten and platinum wires were used and the usual techniques described by Bradshaw (1961) were used for mounting the wires on the probes. In common with general experience, it took several months before this task could be readily undertaken. However, a useful point that came out of this "apprenticeship" was a technique for soldering the wire to the probe.* It was found that a flux (in addition to the flux in the core of the solder) was vital and that if both probe and wire were tinned, the wire could be readily soldered to the probe by holding it against the probe tip and applying the soldering iron to the probe prong a little way from the proposed wire-probe junction. The heat conducted along the probe was sufficient to melt the solder and fine junctions could be obtained in this way.

A rough check on the heat transfer law of the wire was made to ensure that no gross errors existed in the experimental set-up. In figure (31) is shown a few sample calibrations compared with the heat transfer law of Collis and Williams (1959). The agreement is satisfactory considering the uncertainties about the precise diameter and temperature coefficient of resistance of the wire used.

The conventional square wave method of compensation was used and typical output traces of an uncompensated and compensated wire respectively are shown in figure (29). The frequency of the square wave was about 600 c/s which is much higher than that normally used. However, adequate compensation was apparently achieved.

---

* This technique was suggested by M. Gaster in a private communication.

In the case of measurements with sloping wires, it was necessary to know the angle of the wire to the mainstream. This angle was obtained by the crude expedient of putting the probe in a photographic enlarger and measuring the angle between the wire and the probe axis on the projected image with a protractor. A typical example of such an image is shown in figure (30) and it appeared quite feasible to measure the angle to an accuracy of better than 1^{o}*. The alignment of the probe axis with the free-stream was a comparatively easy task and rotating a wire through 180^{0} when exposed to the free-stream did not produce a change in the current through the wire†.

Three main problems were encountered in actually carrying out measurements. These were (a) a rise in the ambient temperature of the tunnel after it had been running for some time (b) mechanical vibrations of the probe and (c) dust accumulation on the wire which radically affected the calibration of the wire . The first of these was simply overcome by running the tunnel for at least one hour before taking any measurements. After this time, the tunnel temperature remained practically constant.

The mechanical vibrations occurred at two frequencies of about 7 kc/s and 400 c/s. The former was traced to the quartz rod used in the construction of the probes and the latter came from the brass stem of the probe. Both were overcome by coating the whole probe in a thin layer of Araldite.

---

*This figure was arrived at by comparing the angles measured by about half a dozen people - with no collusion!

† In the vicinity of the edge of the jet, differences were obtained due to the inclination of the flow in this region.

The dust problem was more difficult to overcome. Much of the problem arose initially from the considerable amount of dust and dirt in the tunnel itself and some time was spent in thoroughly cleaning it out. The tunnel corner vanes were covered in grease in the hope that this would collect additional dust particles. As the jet was introducing air into the tunnel, it was necessary to filter the air passing through the centrifugal fan. Consequently, a simple filter comprising a wooden framework 6' x 2' x 2' covered in chicken wire and several layers of tissue paper was mounted on the fan intake. Although these steps made things better, they did not eliminate the problem entirely and, in most cases, a wire was used only for one traverse across the jet - which would take about one to two hours - before it was discarded. Although the frequent replacement of wires was time consuming, it had the advantage that it proved the ability to obtain consistent results with a large number of different wires. In fact, during the course of the investigation, just over fifty wires were used.

The procedure for taking turbulence measurements was comparatively complicated and it was some time before a routine was developed which could be easily adhered to. Prior to each traverse, the amplifier gain was carefully measured. The cold resistance of wire was then measured - the lead resistance having been allowed for - and a mean flow calibration obtained at a value of the overheating ratio R_w/R_∞ of about 1.5. The time constants for the wire were also measured. Then, at each measuring station the bridge was balanced and the mean current through the wire recorded. From this current, the appropriate time constant was obtained from a calibration graph and the amplifier compensation network adjusted

accordingly. With the galvanometer across the bridge switched out of circuit to avoid attenuation of the turbulence signal, the amplifier attenuators were adjusted until the output signal across the dummy lead - used in place of the thermo-junction - was less than 1 volt peak to peak. The thermo-junction was then switched in and the output from this device recorded. At the end of a traverse, a check was made on the cold resistance of the wire and the amplifier gain. The wire was also re-calibrated to check that it had not undergone a radical change.

A final assessment of the accuracy of the turbulence measurements is difficult but certainly the repeatability of the measurements is good - see sections 7 and 8. The absolute accuracy, however, cannot be determined with certainty but, reference to measured and calculated values of the turbulent shear stress(see section 8.5 and 10.2) show that the error in $\overline{uv}$ is probably not worse than $\pm 15^{o/o}$. The measurement of $\overline{v^2}$ and $\overline{w^2}$ will be subject to a somewhat greater error because of the use in the present experiments of the less accurate single sloping wire technique. These figures for the possible error are somewhat larger than these usually suggested (see, for example, Cooper and Tulin (1955) where $\pm 5^{o/o}$ for $\overline{uv}$ is quoted) but from reference to a large number of published papers the author came to the conclusion that these latter estimates were in a general way optimistic because, even in the most carefully conducted experiments, errors arose which were not explicable - see, for example, the shear stress measurements of Laufer (1951). Such events show that hot wire anemometry is still not free of uncertainties.

As a first exercise in the application of the hot wire anemometer, the turbulence level in the Queen Mary College closed return tunnel was measured. The results of this early test are shown in figure (32).

The results were worked out using both the conventional King's law analysis and the improved analysis given in section 6.1 and, from figure (32), we see that the turbulent intensities $\sqrt{\overline{u^2}}/U$ calculated from the latter method are roughly $15^{o/o}$ larger than those obtained from the King's law analysis. A difference of this magnitude can generally be expected but the precise difference depends upon the exact operating conditions of the wire.

6.4 The application of pitot and static tubes.

The mean velocities and static pressures were measured generally with separate pitot and static tubes. These were made from 0.05" diameter hyperdermic tubing. The static tube used only two static holes placed diametrically opposite one another and it was used always with these two holes in the horizontal (or XZ) plane. Both the pitot and static tubes were checked against a standard N.P.L. pitot-static tube and were found to be satisfactory. The pitot pressures were measured on a sloping manometer whereas the static pressures were measured on one of two micro-manometers. These latter instruments relied on the change of capacitance produced between a diaphragm and a fixed pick-up when the diaphragm deflected under the applied pressure. The output from the instruments was fed onto a pen recorder with a paper width of 10". Full scale deflection was obtained for a pressure of about 0.1" and 1.0" of water respectively when applied to the two micro-manometers. Both the sloping manometer and micro-manometers were calibrated against a Betz manometer.

Although no corrections were applied to the pitot and static tube readings for the effect of turbulence on these instruments, some consideration was given to the problem and an account of this work is given below. The initial semi—theoretical arguments have been largely superseded by the work of Toomre (1960) who approached the problem in a slightly more rigorous fashion. However, his main conclusions are essentially the same as those reached here.

In the case of the pitot tube, Goldstein (1936) suggested that the pitot pressure in a turbulent flow is:-

$$P_p = P + \frac{1}{2}\rho U^2 + \frac{1}{2}\rho(\overline{u^2} + \overline{v^2} + \overline{w^2}) \qquad (6.4.1)$$

where P_p and P are the measured pitot pressure and true static pressure respectively. U is the true mean velocity and $\overline{u^2}$, $\overline{v^2}$ and $\overline{w^2}$ are the mean squares of the turbulent velocities. This correction is probably satisfactory except where the turbulence level is sufficiently high to introduce incidence effects. It might then be better to write:-

$$P_p = P + \frac{1}{2}\rho U^2 + \frac{1}{2}\rho(\overline{u^2} + k_v\overline{v^2} + k_w\overline{w^2}) \qquad (6.4.2)$$

where k_v and k_w are functions of the average incidences $\tan^{-1}(\sqrt{\overline{v^2}}/U)$ and $\tan^{-1}(\sqrt{\overline{w^2}}/U)$ respectively, say. However, neither of these functions can be specified.

In the case of the static tube, it would seem reasonable for circular cross-section tubes to write:-

$$P_S = P + \frac{1}{2}\rho n(\overline{v^2} + \overline{w^2}) \qquad (6.4.3)$$

where P_S is the measured static pressure and 'n' is a factor to be determined.

If the scale of the turbulence is small compared to the static tube diameter then the instantaneous values of the turbulent velocities around the circumference of the tube will be different and uncorrelated. In these circumstances, we may use the second equation of motion (2.1.2) and take the average of the pressures around the tube circumference. We obtain:-

$$P_S = P + \frac{1}{2}\rho(\overline{v^2} + \overline{w^2}) \qquad (6.4.4)$$

This result was obtained by Toomre (1960) and gives a value of n = +1.0 in equation (6.4.3) which is twice the original value proposed by Goldstein (1936).

If the scale of the turbulent motions is large compared to the static tube diameter, the tube may be regarded, qualitatively at least,

as being subjected to an oscillating cross flow which would give rise to a negative value of n in equation (6.4.3) because the mean pressure coefficient for flow around a circular cylinder is always negative. In these circumstances, we may write:-

$$P_S = P + \frac{1}{2} \rho \left(\overline{v^2} + \overline{w^2} \right) C_{P_{mean}}. \qquad (6.4.5)$$

where $C_{P_{mean}}$ is a mean pressure coefficient - replacing 'n' in equation (6.4.3) - which we could as a first estimate interpret as the mean pressure coefficient for steady flow around a circular cylinder. In inviscid flow, $C_{P_{mean}} = -1.0$ whereas $C_{P_{mean}} = -0.56$ in viscid flow at sub-critical Reynolds numbers. It is interesting to note that this last value of $C_{P_{mean}}$ is very close to the value of -0.61 obtained by Fage (1936) from experiments on yawed static tubes if we assume that for the yawed tube;

$$P_S = P + \frac{1}{2} \rho \left(U \sin\theta \right)^2 C_{P_{mean}} \qquad (6.4.6)$$

where θ is the angle between the static tube and the free-stream. However, Teomre (1960) argues that in the unsteady flow of turbulence the inviscid flow value of $C_{P_{mean}}$ is probably more appropriate.

In a more general way, the mean pressure coefficient may be expressed as:-

$$C_{P_{mean}} = \text{function of} \left(\frac{L}{d} , \frac{qd}{\nu} , \frac{\omega d}{q} \right) \qquad (6.4.7)$$

where L, ω and q are some relevant length, frequency and velocity scales respectively of the turbulence. d is the static tube diameter. It seems likely that the effect on $C_{P_{mean}}$ of the last two parameters in equation (6.4.7) will be slight over the range of values of these parameters normally encountered and, therefore, $C_{P_{mean}}$ will depend almost entirely on the ratio L/d. The foregoing arguments suggest that for

$L/d \ll 1.0$, $C_{P_{mean}} = +1.0$ whereas for $L/d \gg 1.0$, $C_{P_{mean}} = -1.0$. In practice, we would expect both small and large eddy effects to be present because the turbulence consists of a whole spectrum of eddy sizes.

The only data with which to check the above ideas is the experimental work of Fage (1936) who carried out some measurements of static pressure in a 5" diameter pipe flow and a 2" deep channel flow with a static tube 0.086" in diameter which had 12 static holes distributed evenly around the circumference of the tube. For these two flows, the static pressure can be computed if the distributions of $\overline{v^2}$ and $\overline{w^2}$ are known. For pipe flow,

$$r\frac{\partial}{\partial r}\left(\frac{P}{\rho} + \overline{v^2}\right) = \overline{w^2} - \overline{v^2} \qquad (6.4.8)$$

and for two-dimensional channel flow,

$$\frac{\partial}{\partial y}\left(\frac{P}{\rho} + \overline{v^2}\right) = 0 \qquad (6.4.9)$$

Fage obtained the $\overline{v^2}$ and $\overline{w^2}$ distributions from measurements with his ultra-microscope on the assumption that the r.m.s. values of the turbulent velocities were one third of the maximum values. Thus, by comparing the computed and measured distributions of static pressure, Fage obtained for both flows a value of $C_{P_{mean}} = +0.5$. This result is surprising because the energy containing eddies in these flows must surely have been larger than the static tube diameter and, consequently, a negative value of $C_{P_{mean}}$ would be expected. It was therefore decided to re-examine Fage's results in the light of the more recent pipe and channel flow measurements of Laufer (1951 and 1955). In figure (33) is shown a comparison between the results of Fage

and Laufer for the distributions of $\overline{v^2}$ and $\overline{w^2}$ in both pipe and channel flows. The differences between the two sets of results are considerable. The most likely explanation is that Fage's assumption relating the r.m.s. values of the turbulent velocities to the maximum values is inaccurate. It is also possible that there may be some Reynolds number effects. However, since the Reynolds numbers of Laufer's experiments are within the range of values of Fage's static pressure measurements, Laufer's results are applicable.* We can now re-calculate $C_{P_{mean}}$ using Laufer's results for the turbulent intensities and Fage's results for the static pressure measurements. For channel flow, equation (6.4.9) gives,

$$\frac{P-P_c}{\rho U_\tau^2} + \frac{\overline{v^2}-\overline{v_c^2}}{U_\tau^2} = 0 \qquad (6.4.10)$$

and from equation (6.4.5), we have:-

$$\frac{P_s-P_{s_c}}{\rho U_\tau^2} = \frac{P-P_c}{\rho U_\tau^2} + \frac{1}{2}\frac{(\overline{v^2}+\overline{w^2})-(\overline{v^2}+\overline{w^2})_c}{U_\tau^2} C_{P_{mean}} \qquad (6.4.11)$$

where the suffic 'c' refers to values on the centre-line of the channel. U_τ is the skin friction velocity, $\sqrt{\tau_o/\rho}$. Values of the various terms in the equations (6.4.10) and (6.4.11) are given in the table below and in graphical form in figure (34).

y/h	$(P_S-P_{S_c})/\rho U_\tau^2$	$(P-P_c)/\rho U_\tau^2$	$\frac{(\overline{v^2}+\overline{w^2})-(\overline{v^2}+\overline{w^2})_c}{\rho U_\tau^2}$	$C_{P_{mean}}$
0.4	-0.15	-0.198	0.58	+0.17
0.6	-0.26	-0.43	1.04	+0.33
0.8	-0.39	-0.575	1.39	+0.27

The average value of $C_{P_{mean}}$ is roughly +0.26. Although this is still

*Fage's turbulence measurements were made at Reynolds numbers below those of his static pressure measurements (see figures (33) & (34)).

positive, it is now half the original value found by Fage.

In order to repeat the above process for the circular pipe, we replace equation (6.4.10) by the expression:-

$$\frac{P-P_c}{\rho U_\tau^2} + \frac{\overline{v^2}-\overline{v_c^2}}{U_\tau^2} = \int_0^{r/a} \frac{\overline{w^2}-\overline{v^2}}{U_\tau^2} \cdot \frac{1}{r/a}\, d\left(\frac{r}{a}\right) \qquad (6.4.12)$$

The results for the pipe flow are summarized in the table below and also in figure (34).

r/a	$(P_S-P_{S_c})/\rho U_\tau^2$	$(P-P_c)/\rho U_\tau^2$	$\frac{(\overline{v^2}+\overline{w^2})-(\overline{v^2}+\overline{w^2})_c}{\rho U_\tau^2}$	$C_{P_{mean}}$
0.4	-0.15	-0.061	0.535	-0.332
0.5	-0.23	-0.097	0.815	-0.326
0.6	-0.29	-0.135	1.09	-0.284
0.7	-0.33	-0.143	1.35	-0.277
0.8	-0.21	-0.139	1.62	-0.087

The average value of $C_{P_{mean}}$ is -0.26.

Before discussing the possible significance of these new values of $C_{P_{mean}}$, some additional measurements of Fage in a turbulent wake will first be analysed. The measurements were made in the wake of a 0.375" diameter cylinder at a station 30 diameters downstream. In addition to the mean velocity and static pressure profiles, the $\overline{u^2}$, $\overline{v^2}$ and $\overline{w^2}$ components of the turbulence were measured on the wake centre-line using a hot-spot technique developed by Townend (see Fage (1936)) and the ultra-microscope of Fage. The results of these

*The ultra-microscope measurements were actually made in the wake of a triangular prism. It is possible that the turbulent intensities at x/d = 30 are not the same in this flow as these in the wake of a circular cylinder.

measurements on the wake centre-line are summarized in the following tables.

TURBULENT INTENSITIES ON THE WAKE CENTRE-LINE AT x/d=30.

	$\overline{u^2}/U_o^2$	$\overline{v^2}/U_o^2$	$\overline{w^2}/U_o^2$
Hot spot technique.	0.302	0.302	0.24
Ultra-microscope.	0.29	0.152	0.203

STATIC PRESSURE MEASUREMENTS ON THE WAKE CENTRE-LINE AT x/d=30.

	$\Delta P_S/\rho U_o^2$
Tube A. 0.086"dia. - 12 holes around the circumference.	-0.266
Tube C. 0.043"dia. - 4 holes around the circumference.	-0.308
Tube D. 0.043"dia. - 4 holes along a generator. 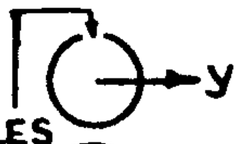 STATIC HOLES	-0.342
Tube D. 0.043"dia. - 4 holes along a generater. 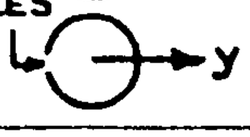	-0.308

In these tables, U_o is the difference in mean velocity across the wake and ΔP_S is the difference in measured static pressure between the wake centre-line and the free-stream. Significant features about the results are that the turbulent intensities obtained from the two measuring techniques are in fair agreement with one another with the exception of the $\overline{v^2}$ component. Also, a larger static pressure drop across the wake was measured with the smaller tube C compared to that obtained with tube A. This indicates that large eddy effects were present. The results with tube D are also interesting because they show that the static pressure difference measured with this tube depended on whether the holes were in the XZ or XY plane. This effect must be due to a difference in the $\overline{v^2}$ and $\overline{w^2}$ intensities on the centre-line. If large eddy effects were predominant, the results with

tube D suggest that $\overline{v^2} \gg \overline{w^2}$ and vice-versa if the small eddy effects were the more important.

Equation (2.1.2) gives:-

$$\frac{\Delta P}{\rho U_o^2} = -\frac{\overline{v^2}}{U_o^2} \qquad (6.4.13)$$

where ΔP is the true static pressure difference across the wake. Thus, the measurement of $\overline{v^2}/U_o^2$ gives the true static pressure drop and this may be compared with the measured values to obtain values of $C_{P_{mean}}$. Using the ultra-microscope value of $\overline{v^2}/U_o^2$, we obtain from the four static tube measurements an average value of $C_{P_{mean}} = -0.87$. This indicates a large eddy effect and, therefore, the tube D results suggest that $\overline{v^2} \gg \overline{w^2}$. However, the ultra-microscope measurements indicate that $\overline{v^2} \ll \overline{w^2}$. This inconsistency suggests that the ultra-microscope measurements are not applicable. Using the hot-spot results, we obtain for tube A, $C_{P_{mean}} = +0.13$. For tube C, $C_{P_{mean}} = 0$. The hot spot results give $\overline{v^2} \gg \overline{w^2}$ which indicates on comparison with the tube D results that large eddy effects are the more important for the 0.043" diameter static tubes. Although these hot spot results are not completely consistent, they will be used because they are certainly more consistent and acceptable than the ultra-microscope results.

As is no doubt obvious, the re-analysis of the early work of Fage is full of uncertainties. For example, the process of 'mixing' the results of two experimenters in the re-analysis of the pipe and channel flow results is open to question and, consequently, the results of this re-analysis should be viewed with some caution. Nevertheless,

we will carry this work to the limit by tabulating the various values of $C_{P_{mean}}$ and the appropriate values of the ratio L_y/d where $L_y = \int_0^\infty R_y dy$ is the lateral integral scale of the turbulence and d is the static tube diameter. The values of L_y/d are only approximate and have been estimated by reference to experimental results from a number of published reports.

Flow.	Static tube diameter.	$C_{P_{mean}}$	L_y/d
Channel flow.	0.086"	+0.26	2.3 - 3.5
Wake flow.	0.086"	-0.26	2.3
Wake flow.	0.043"	0	4.6
Pipe flow.	0.086"	-0.26	5.8

The surprising feature of these results is that a measure of correlation exists between the values of $C_{P_{mean}}$ and the ratios L_y/d. Roughly speaking, it would seem that for $L_y/d \leq 4$, $C_{P_{mean}}$ takes positive values whereas for $L_y/d \geq 4$, $C_{P_{mean}}$ becomes negative. It is surprising to find that the length scale of the eddies must apparently be so much larger than the static tube diameter before large eddy effects become predominant and it may be that the nose effect of the static tube discussed by Toomre (1960) is responsible. Obviously, more work is required on this problem but the above re-analysis shows that doubts raised about the conclusiveness of Goldstein and Fage's early work appear not unfounded.

The effects of turbulence on the present measurements in the plane jet will now be considered. The effect of turbulence on the mean velocity measurements with a pitot tube can be ignored because in almost all cases $\frac{1}{2}\rho U^2 \gg \frac{1}{2}\rho \overline{q}^2$ and the correction would be too small to have

a significant effect on the results even if its correct value and sign could be determined. The turbulence effect on the measurements of the static pressure coefficient, $\Delta P_s/\rho U_o^2$, is,however, significant. In addition to the turbulence effect, an allowance must also be made for the inclination of the flow at the edge of the jet due to entrainment. Outside the jet,

$$P_{S_1} = P_1 + \frac{1}{2}\rho V_1^2 C_P \qquad (6.4.14a)$$

where P_{S_1} and P_1 are the measured and true static pressures outside the jet respectively. The last term on the right hand side represents a contribution to the static tube error from the flow inclination. V_1 is the inflow velocity at the edge of the jet and C_p is a pressure coefficient which will be assumed approximately equal to -1.0.

Inside the jet,

$$P_S = P + \frac{1}{2}\rho(n_v\overline{v^2} + n_w\overline{w^2}) + \frac{1}{2}\rho V^2 C_p \qquad (6.4.14b)$$

The coefficients n_v and n_w are introduced because, in the present case, a static tube with only two holes lying in the XZ-plane was used and the response of this tube to v- and w-fluctuations will be different. The last term on the right hand side again is due to flow inclination. Now, the second equation of motion (2.1.2) gives:-

$$\frac{\Delta P}{\rho U_o^2} = -\frac{\overline{v^2}}{U_o^2} \qquad (\Delta P = P - P_1) \qquad (6.4.15)$$

whereas, equations (6.4.14a & b) give,

$$\frac{\Delta P_S}{\rho U_o^2} = -\frac{\overline{v^2}}{U_o^2} + \frac{1}{2}\left(n_v\frac{\overline{v^2}}{U_o^2} + n_w\frac{\overline{w^2}}{U_o^2}\right) + \frac{1}{2}\frac{V^2 - V_1^2}{U_o^2}C_p \qquad (6.4.16)$$

From previous considerations of the range of possible values of n_v and n_w, it is clear that $\Delta P_S/\rho U_o^2$ can be significantly different from $\Delta P/\rho U_o^2$.

On the other hand, if the flow is self-preserving so that $\overline{v^2}/U_o^2$, $\overline{w^2}/U_o^2$ and $(V^2-V_1^2)/U_o^2$ are functions of $y/\delta_{0.5}$ only, then the measured distributions of the static pressure coefficient, $\Delta P_s/\rho U_o^2$, will also be functions of $y/\delta_{0.5}$ only provided n_v and n_w do not alter during the development of the flow.* Thus, static pressure measurements provide a simple means of checking how a flow approaches self-preservation even though the measured and actual static pressures may be quite different.

Finally, in figure (48), the measured distributions of $\Delta P_s/\rho U_o^2$ across the jet are compared to the measured $\overline{v^2}/U_o^2$ distribution. After an allowance has been made for the flow inclination effect, it appears that, in the centre region of the flow, small eddy effects predominate whereas large eddy effects predominate in the outer region. Uncertainty about the precise response of the static tube prevents separate values being assigned to n_v and n_w in equation (6.4.15). However, by setting $n_v = n_w = C_{P_{mean}}$, it is found that on the centre line of the jet $C_{P_{mean}} \simeq +0.1$ whereas it is about -0.5 over most of the outer region. These values lie within the limits prescribed by earlier semi-theoretical arguments although it is difficult to understand why the sign of $C_{P_{mean}}$ should vary across the flow. The values of L_y/d ranged from 5 to 12 in the present experiments so that we would expect negative values of $C_{P_{mean}}$ throughout. However, as discussed in section 6.3, it is quite possible that the $\overline{v^2}$ measurements may be in error by as much as $25^{o/o}$, say, and this could account possibly for the apparent variation of $C_{P_{mean}}$.

---

*It is possible that n_v and n_w might vary if the ratio of the static tube diameter to the flow width altered appreciably during the development of the flow.

7.0 Presentation and discussion of results for the plane jet with $U_1/U_J = 0.07$

The first objective of the present experiments was to study the structure of the self-preserving pure jet flow for which $U_o/U_1 \gg 1.0$, $\delta \propto x$, and $U_o \propto x^{-1/2}$. There are considerable experimental advantages in carrying out these measurements on a jet emerging into a slow moving airstream, as compared to the stationary surrounding fluid case, because, although turbulence quantities like $\overline{u^2}/U_o^2$ will be unaltered, the turbulent intensities relative to the local mean velocities will be reduced. Thus, errors due to the non-linear response of the measuring instruments will be reduced and recording the output from these instruments will be made easier. Initial measurements were made, therefore, with a value of $U_1/U_J = 0.07$.* However, it was soon apparent that the turbulent intensities at the edge of the jet were still too high to allow reliable and easy measurements. Consequently, most of the turbulence measurements were made with $U_1/U_J = 0.162$. Nevertheless, the comparatively few measurements at $U_1/U_J = 0.07$ are of importance in establishing that the subsequent measurements with $U_1/U_J = 0.162$ at values of $U_o/U_1 = O(1)$ were representative of a self-preserving pure jet flow.

7.1. Self-preservation and Reynolds number similarity in a plane jet with $U_1/U_J = 0.07$

The measurements involved:-

(a) mean velocity and static pressure traverses across the jet at four longitudinal stations in the fully turbulent part of the jet flow.

---

* This value of U_1/U_J was obtained with the tunnel motor switches off. The jet induced a small free-stream velocity through the tunnel sufficient to give $U_1/U_J = 0.07$.

(b) several longitudinal traverses in which the mean velocity and static pressure on the centre-line of the jet were measured.

(c) several lateral and longitudinal traverses with hotwire anemometers measuring the $\overline{u^2}$ intensity.

The majority of measurements were made with a jet exit velocity of 170 ft/sec and a Reynolds number of $R_h = U_J h/\nu = 3.3 \times 10^4$. This Reynolds number was thought to be sufficiently high to avoid any Reynolds number effects but, in any case, this point was subsequently checked experimentally.

The mean velocity profiles, shown in non-dimensional form in figure (35), are geometrically similar and it is to be noted that there is comparatively little scatter in the results at the edge of the jet in contrast to previous work (see, for example, Forthmann (1936). This is certainly due to the lower turbulent intensities encountered in the present experiments. The rate of spread of the jet and the decay of the centre-line velocity obtained from the results of both the lateral traverses across the jet and the longitudinal traverses along the jet centre-line are shown in figure (36). Up to the limit of the measurements at x/h=70, the condition for self-preservation that $U_o/U \gg 1.0$ is approximately fulfilled and it appears indeed that $\delta \propto x$ and $U_o \propto x^{-1/2}$. It is, however, well known that apparent self-preservation of the mean velocity profiles is no guarantee that the turbulence structure is self-preserving. The static pressure measurements, which are related to the turbulent intensities as discussed in section 6.4, give some guide to this last point. In figure (37) is shown the variation of static pressure coefficient, $\Delta P_s/\rho U_o^2$, across the jet at the four measuring stations. Although there is considerable scatter in the results,

it appears that the profiles for $x/h \geq 30$ are roughly similar.* In addition, the static pressure coefficients on the centre-line of the jet, shown in figure (38), become apparently constant at about -0.05 for $x/h \geq 30$. The conclusion from this is that the jet flow including the turbulence structure is closely self-preserving for $x/h \geq 30$.

The turbulence measurements made with U_1/U_J=0.07 were among the first turbulence measurements made by the author and before discussing the results, some comment is necessary on the history of this early work. The first measurements were made with a single 0.00015" diameter tungsten wire which was used to measure the distribution of $\overline{u^2}$ across the jet at three longitudinal stations. In order to check the repeatability of the measurements, two further traverses were made at one of these longitudinal stations, namely x/h =66, with another 0.00015"diameter tungsten wire and also a 0.0001"diameter platinum wire. At this stage in the programme, the hot wire results were worked out using the conventional King's law analysis (see, for example, Newman and Leary (1950)) and it was disturbing to find that the agreement between the respective traverses was not very good. It was largely as a result of this that led the author to the re-examination of the hot wire anemometer theory given in section 6.1. This new analysis reduced the discrepancies in the results but it did not eliminate them. In figure (39) are shown the $\overline{u^2}/U_o^2$ profiles obtained with the single tungsten wire at three stations in the jet. These results can be compared with the results from the other two traverses shown in figure (40).

---

*This scatter is a result mainly of drift in both the calibrations and zeros of the micro-manometers. In later experiments, frequent checks were made to avoid this source of error and the scatter was greatly reduced.

It can be seen that whereas the latter two traverses are in fair agreement with on another, the agreement between the first results and these latter traverses is not very good. It is a matter of regret that the reason for this discrepancy was not resolved but it was found as a result of some further traverses that the repeatability of measurements with different platinum wires was very good and, consequently, all subsequent measurements were made with platinum wires. It should be mentioned that additional concern was felt at this time because of the comparitively poor agreement with the turbulence measurements of Miller and Commings (1957) in a plane jet. It was only after several months of checking a wide variety of possibilities that the author felt confident to proceed further with turbulence measurements.*

Returning to the discussion of the turbulence measurements, a longitudinal traverse with a hot wire anemometer was made along the centre-line of the jet. The results of this traverse, shown in figure (41), are in poor agreement with the results of Miller and Commings - see figure (5). At the time, it was thought that this might conceivably be a Reynolds number effect and the traverse was repeated at a lower value of Reynolds number equal to 1.8×10^4. As can be seen from figure (41), no significant Reynolds number effect can be observed for $x/h \geqslant 20$. Thus, over this limited Reynolds number range, the principle of Reynolds number similarity has been confirmed. In addition, these traverses indicate that the value of $\overline{u^2}/U_e^2$ on the jet centre-line

---

*This checking involved ensuring that the resistance-temperature relationship of the wire was linear and also that the measured heat transfer coefficients agreed with the results of Collis and Williams (1959). The possibility of errors due to therme-electric effects and inadequate de-plating of the wire was also considered.

becomes constant at roughly 0.04 for $x/h \geqslant 30$. This confirms the previous conclusion based on the static pressure measurements that the jet flow is closely self-preserving for $x/h \geqslant 30$.

7.2 Further discussion of the results for U_1/U_J=0.07 and a comparison with previous work.

In order to obtain more information about the jet flow, some calculations were undertaken. In the first place, a check was made on the constancy of the jet momentum flux. The momentum integral equation for the region of the jet flow where the mean velocity profiles are geometrically similar can be written:-

$$\frac{\delta_{0.5}}{h}\left[\left(\frac{U_0}{U_1}\right)^2 I_2 + \left(\frac{U_0}{U_1}\right) I_1\right] \quad = \text{momentum coefficient, } J/\rho U_1^2 h \qquad (7.2.1)$$

where $I_n = \int_{-\infty}^{\infty} f^n d\eta$. The small turbulent terms have been ignored. From the measured velocity profiles, it was found that I_1= 2.025 and I_2= 1.467. Thus, the momentum coefficient, C_J, could be calculated at each of the four measuring stations. These results are given in tabular form below.

x/h	$\delta_{0.5}/h$	U_0/U_1	$(U_0/U_1)^2$	C_J
66.1	5.23	4.25	18.1	184.5
50.8	4.15	4.91	24.1	188.5
30.6	2.59	6.46	41.9	193.7
15.5	1.28	9.21	85	186
			Average value of C_J =	188.3

The agreement between the results at the various stations is satisfactory.

From figure (36), it can be seen that the mean velocity on the centre-line of the jet may be represented by:-

$$\left(\frac{U_1}{U_o}\right)^2 = C\left(\frac{x}{h} - \frac{x_o}{h}\right) \text{ where } C=0.00863 \text{ and } x_o/h=2.0. \qquad (7.2.2)$$

Using equations (7.2.1) and (7.2.2) and the average value of C_J give:-

$$\frac{\delta_{0.5}}{h} = \left(\frac{U_1}{U_o}\right)^2 \frac{C_J}{I_2} \frac{1}{\left(1+\frac{U_o}{U_1}\frac{I_1}{I_2}\right)} = \frac{0.111\left(\frac{x}{h}-2\right)}{1+0.0406\sqrt{\frac{x}{h}-2}} \qquad (7.2.3)$$

This expression shows that $\delta_{0.5}$ is not exactly proportional to 'x' although the departure from this linear relationship is clearly small. Equation (7.2.3) can be used to accurately calculate both $\delta_{0.5}$ and $d\delta_{0.5}/dx$ at any longitudinal station in the jet.* In turn, this is useful in the following calculation of the shear stress distribution across the jet.

The momentum equation may be written (see Townsend (1956)):-

$$\frac{U_1}{U_o}\left[\frac{\delta}{U_o}\frac{dU_o}{dx} f - \frac{d\delta}{dx}\eta f'\right] + \frac{\delta}{U_o}\frac{dU_o}{dx} f^2 - \frac{1}{U_o}\frac{d}{dx}(\delta U_o) f' \int_o^\eta f\,d\eta$$

$$+ 2\frac{\delta}{U_o}\frac{dU_o}{dx}(g_1-g_2) - \frac{d\delta}{dx}\eta(g_1'-g_2') + g_{12}' = 0 \qquad (7.2.4)$$

This may be integrated to give:-

$$\frac{U_1}{U_o}\left[\frac{\delta}{U_o}\frac{dU_o}{dx} + \frac{d\delta}{dx}\right]\int_o^\eta f\,d\eta - \frac{U_1}{U_o}\frac{d\delta}{dx}\eta f + \left(2\frac{\delta}{U_o}\frac{dU_o}{dx} + \frac{d\delta}{dx}\right)\int_o^\eta f^2 d\eta$$

$$-\left(\frac{\delta}{U_o}\frac{dU_o}{dx} + \frac{d\delta}{dx}\right) f\int_o^\eta f\,d\eta + \left(2\frac{\delta}{U_o}\frac{dU_o}{dx} + \frac{d\delta}{dx}\right)\int_o^\eta (g_1-g_2)\,d\eta - \frac{d\delta}{dx}\eta(g_1-g_2) + g_{12} = 0 \qquad (7.2.5)$$

The terms containing the functions g_1 and g_2 are small and can be ignored.† Thus, from equations (7.2.2) and (7.2.3) and the measured mean velocity profile function, f , the distribution of $g_{12} = \overline{uv}/U_o^2$ across

---

*Equation (7.2.3) is shown in figure (36) for comparison with the experimental results.

†This was checked by using the measured values of the functions g_1 and g_2.

the jet can be calculated. In figure (42) are shown the results of such calculations at two longitudinal stations in the jet. The profiles are apparently identical.

Owing to the small but finite value of U_1 in the present experiments, a direct comparison with previous experimenters' results with $U_1=0$ of the rate of spread of the jet is not possible. However, the shear stress profiles can be compared. It is easy to show from equation (7.2.5) that if $U_1=0$ then:-

$$g_{12} = -\frac{1}{2}\frac{d\delta}{dx} f\int_0^\eta f\,d\eta \qquad (7.2.6)$$

Using the value of $d\delta_{0.5}/dx=0.1$ obtained in section 3.2, the shear stress distribution has been calculated using equation (7.2.6) and this distribution is compared with the previous calculations for $U_1/U_J=0.07$ in figure (42). The shear stresses for $U_1/U_J=0.07$ are $9^{o/o}$ larger than those obtained with $U_1=0$ and $d\delta_{0.5}/dx=0.1$ but, considering all things, this is nevertheless quite good agreement.

The inflow into jets is of interest and, consequently, calculations of the lateral mean velocity profile have been made. Now:-

$$V = -\int_0^\eta \frac{\partial U}{\partial x}\,dy = -\delta\frac{dU_0}{dx}\int_0^\eta f\,d\eta + U_0\frac{d\delta}{dx}\int_0^\eta \eta f'\,d\eta$$

$$\text{so that}\quad \frac{V}{U_0} = -\frac{\delta}{U_0}\frac{dU_0}{dx}\int_0^\eta f\,d\eta + \frac{d\delta}{dx}\left(\eta f - \int_0^\eta \eta f\,d\eta\right) \qquad (7.2.7)$$

Equation (7.2.7) has been used to calculate lateral mean velocity profiles for the jet both with $U_1/U_J=0.07$ and also with $U_1=0$ and $d\delta_{0.5}/dx=0.1$. As shown in figure (43), the results for the respective cases are again in quite good agreement although small departures from true self-preservation can be detected in the profiles for $U_1/U_J=0.07$.

We will now reconsider the static pressure and turbulence measurements in relation to previous work. A comparison between previous and present experimental results for both the static pressure and $\overline{u^2}$ measurements can be made by reference to figures (5), (6), (38) and (41). It is disturbing to find that the agreement between each set of data is comparatively poor. The differences that exist in magnitude between the various results could be due to the different types of instrumentation used.However, even the trends in the results are slightly different. The present results show that self-preservation is established for $x/h \geq 30$ whereas the results of other experimenters show that self-preservation does not occur until $x/h \geq 50$. The causes of these differences cannot now be decided but it is worth noting that the experimental set-ups in every case differed from one another in aspect ratio, the type of end plates used and the nozzle conditions. However, the various checks that were carried out on the present measurements encourage a belief in their results ; in any case studies of the turbulence structure of the self-preserving jet have been largely restricted to values of $x/h \geq 50$ and in this region the results can safely be taken to be representative of a truly self-preserving jet.

One further comment about the present work is necessary. Because U_1 is finite we may consider the jet to be swept along by the free-stream. Therefore, when comparing the results of the present investigation with previous work with $U_1=0$, it must be noted that at a given value of x/h, the fluid particles that left the jet exit arrive at this station more rapidly with finite values of U_1 than with $U_1=0$. In order to obtain some idea of this effect, the time - which we will subsequently refer to as the "existence" time - for a particle travelling with the jet centre-line

velocity to reach a particular longitudinal station was calculated for both $U_1=0$ and $U_1\neq0$. In general, we may write for the existence time, t_e, that:-

$$t_e = \int_0^x \frac{dx}{U_\infty + U_1} \qquad (7.2.8)$$

Now, if we assume that $\frac{U_\infty\sqrt{x/h}}{\sqrt{U_J(U_J-U_1)}} = C$ where C is a constant with a value of 2.57,* we obtain:-

$$\frac{U_J t_e}{h} = \frac{2}{U_1/U_J}\left[\frac{1}{2}\frac{x}{h} - \hat{K}\sqrt{\frac{x}{h}} + \hat{K}^2 \log\left(1+\frac{\sqrt{x/h}}{\hat{K}}\right)\right] \qquad (7.2.9)$$

where $\hat{K} = C\sqrt{\frac{U_J}{U_1}\left(\frac{U_J}{U_1}-1\right)}$

For $U_1=0$, equation (7.2.9) gives:-

$$\frac{U_J t_e}{h} = \frac{2}{3C}\left(\frac{x}{h}\right)^{3/2} \approx 0.26\left(\frac{x}{h}\right)^{3/2} \qquad (7.2.10)$$

For $U_1/U_J=0.07$:-

$$\frac{U_J t_e}{h} = 28.4\left[\frac{1}{2}\frac{x}{h} - 35.2\sqrt{\frac{x}{h}} + 1240\log\left(1+\frac{\sqrt{x/h}}{35.2}\right)\right]$$

From these last two relationships it was found that on this existence time basis the flow at $x/h=70$ with $U_1=0.07$ would be equivalent to the flow at $x/h=65$ with $U_1=0$. Thus, there is no serious stretching of the x-co-ordinate to be considered.

---

* This equation is a re-arrangement of the asymptotic relationship for U_∞/U_1 as $U_1 \to 0$ given in section 4.0 as equation (4.0.4). It will be shown later in section 11.0 that this equation is in moderate agreement with experimental results for values of $U_\infty/U_1 \geq 0.8$.

8.0 Presentation and discussion of results for a plane jet with U_1/U_J=0.162.

As a result of the high turbulence levels encountered at the edge of the jet with U_1/U_J=0.07, a further and far more comprehensive series of measurements with U_1/U_J=0.162 were undertaken. These experiments were carried out with a jet velocity of 150 f.p.s. and a Reynolds number, $R_h = U_J h/\nu = 2.9 \times 10^4$. These experiments involved the following series of measurements:-

(a) Mean velocity and static pressure traverses at a number of longitudinal stations. In addition, several longitudinal traverses were made along the jet centre-line.

(b) Both lateral and longitudinal traverses with hot wire anemometers measuring the $\overline{u^2}$ component of the turbulence.

(c) Traverses at several longitudinal stations measuring the intermittency factor.

(d) At two longitudinal stations, traverses measuring $\overline{uv}$, $\overline{v^2}$ and $\overline{w^2}$.

(e) At one longitudinal station, a traverse measuring the viscous dissipation of turbulent energy.

(f) At one longitudinal station, a limited number of correlation and spectra measurements.

(g) At one longitudinal station, measurements of $\overline{u^2}$, $\overline{v^2}$ and $\overline{w^2}$ in the irrotational region of the flow.

8.1 The flow in the immediate vicinity of the jet nozzle.

Because the flow in the immediate vicinity of the jet nozzle was not strictly relevant to the flow in the fully turbulent region of the jet, little attention was paid to this region of the flow. However, a few mean velocity traverses were made with a hot wire anemometer in this

region and the resulting profiles are shown in figure (44). It is of some interest to compare these results with the semi-empirical analysis of Abramovich (1958) for this region of the flow. Abramovich defined the boundaries of the mixing layer by the ordinates at which the mean velocity in the mixing layer is equal to the jet exit velocity on the one hand and the free-stream velocity on the other. These ordinates he called y_1 and y_2 respectively and he obtained the following results:-

$$(a) \qquad \frac{d(y_1+y_2)}{dx} = 0.22\,\frac{U_J - U_1}{U_J + U_1}$$

$$(b) \qquad y_2/y_1 = \frac{0.584 - 0.134(U_1/U_J)}{0.416 - 0.134(U_1/U_J)}$$

In the present case, U_1/U_J=0.162 and we obtain from these two relationships:-

$$y_1/x = 0.069 \; ; \; y_2/x = 0.089$$

These boundaries are compared with the experimental results in figure (44). In view of the fact that Abramovich's theory takes no account of the boundary layers on either the internal or external surfaces of the jet nozzle, the agreement is quite good.

8.2 Self-preservation of the mean velocity profiles.

Mean velocity profiles measured in the fully turbulent region of the jet are shown in figure (45) in non-dimensional form. The profiles are all geometrically similar and in good agreement with the result obtained with U_1/U_J=0.07. For reference purposes, values of the mean velocity profile function , $f(y/\delta_{0.5})$, are tabulated in table I along with the values of the various integrals of the mean velocity function used in the theories of the plane jet developed in section 4. Alternatively,

a good fit to the velocity profile is:-

$$f = \exp\left[-0.6749\eta^2(1 + 0.0269\eta^4)\right]$$

The form of this expression was suggested by an expression used by Townsend (1956) for the mean velocity profile in a plane wake*.

Figure (46) shows the spread of the jet and the decay of the centre-line velocity. This shows that the condition for self-preservation that $U_e \gg U_1$ is now only roughly fulfilled and only by comparison with the previous results for U_1/U_J=0.07 and U_1=0 can we be sure that the turbulence structure is essentially the same as that in a truly self-preserving jet flow.

The momentum integral check on the constancy of the excess momentum flux, outline in section 7.2, was repeated for the present results which are given in tabular form below.

x/h	$\delta_{0.5}/h$	U_e/U_1	$(U_e/U_1)^2$	C_J
68.5	4.22	1.628	2.65	30.32
58.5	3.7	1.77	3.14	30.25
48.5	3.21	1.98	3.92	31.26
38.7	2.66	2.27	5.15	32.31
28.8	2.07	2.64	6.95	32.09
23.8	1.81	2.86	8.16	32.06
18.9	1.475	3.29	10.8	33
13.9	1.09	3.75	14.1	30.78
8.9	0.79	4.52	20.5	31.12
			Average value of C_J =	31.47

The agreement between the various values of C_J is satisfactory.

---

*The expression of Townsend(1956 pp.161)did not use $\delta_{0.5}$ as the reference length. However, in terms of $\delta_{0.5}$, his expression is:-

$$f = \exp\left[-0.6619\eta^2(1 + 0.0565\eta^4)\right]$$

The lateral mean velocity profiles across the jet have again been calculated - section 7.2 - and a comparison of the V/U_o and V/U profiles in the present case with the corresponding profiles in a plane jet with $U_1=0$ is given in figures (47a) and (47b). It is clear from this comparison that the lateral mean velocity profiles, V/U_o, for the jet with $U_1/U_J=0.162$ differ from those in a jet with $U_1=0$ and, moreover, a departure from true self-preservation is apparent. It is also noteworthy that the inflow angle - $\tan^{-1}(V/U)$ - at the edge of the jet with $U_1/U_J=0.162$ is much less than in a jet with $U_1=0$. This reduction of the inflow angle is of importance in so far as it will lead to more accurate measurements in this region of the flow especially in the case of the measurement of shear stress where accurate alignment of the hot wire probe axis with the direction of the mean flow is important.

8.3 Self-preservation of the turbulence structure.

The distributions of the static pressure coefficient across the jet at the various longitudinal stations are shown in figure (48). The profiles are essentially similar for $x/h \geqslant 30$ and this shows that beyond this station the turbulence structure is at least close to a state of self-preservation. The distribution of the static pressure coefficient on the jet centre-line shown in figure (50) naturally confirms this and may be compared with the results obtained with $U_1/U_J=0.07$ - figure(38). This comparison shows that the two sets of results are practically identical and supports the idea that the measurements with $U_1/U_J=0.162$ are representative of a truly self-preserving plane jet.

Confirmation of the above conclusion was obtained from the measurements of the $\overline{u^2}$ component of the turbulence. The lateral distributions of $\overline{u^2}$ across the jet are shown in figure (49) and the $\overline{u^2}/U_o^2$ distribution along the jet centre-line is given in figure (51). It is noteworthy that where traverses were repeated, the agreement between the respective results is very good. Comparison with the corresponding results with U_1/U_J=0.07 leads again to the conclusion that the results for the two velocity ratios are essentially identical.

The existence time for the flow with U_1/U_J=0.162 was calculated from equation (7.2.9) and it was found that on this basis the flow at x/h=70 with U_1/U_J=0.162 would be equivalent to the flow at x/h=60 with U_1=0. Thus, again, there is no serious stretching of the x-co-ordinate to be considered.

It is instructive at this stage to compare the approach to self-preservation of the plane jet with the plane wake. Townsend showed that self-preservation of the turbulence structure of a plane wake did not occur until the distance downstream of the circular cylinder was greater than 500 diameters although the main features of the self-preserving flow were established at roughly 200 diamters downstream. In the case of the plane jet, the present work indicates that the flow is closely self-preserving for $x/h \geqslant 50$ and possibly even for $x/h \geqslant 30$. A simple though not necessarily precise means of comparing the results for the two flows is on the existence time basis. For a plane wake, Townsend (1956) obtained:-

$$\frac{U_1 t_e}{d} = 1.1\ (x/d)$$

For the plane jet (U_1=0), we have (section 7.2):-

$$\frac{U_J t_e}{h} = 0.26\ (x/h)^{3/2}$$

Thus, for equal existence times:-

$$(x/h)^{3/2}_{jet} = 4.25\ (x/d)_{wake}.$$

Using the results for the plane wake suggests that the structure of the plane jet will be approximately self-preserving for $x/h \geq 90$ and closely self-preserving for $x/h \geq 160$. These values are significantly larger than the values obtained from the present experiments. A likely cause for this difference is that the wake flow close to the circular cylinder contains a considerable excess of turbulent energy over the self-preserving wake and this excess of energy will take a long time to decay. The conditions at the nozzle of the plane jet, by contrast, are such that the turbulent energy is much less than that contained in the self-preserving jet and the approach to self-preservation is characterised by a production of turbulent energy up to, rather than by a process of decaying down to, the equilibrium self-preservimgvalue. Now, although the production and dissipation times for the turbulent energy are roughly similar (see Townsend (1956) pp.96 and also section 8.8), the difference between the turbulent energy close to the cylinder in the wake flow and far downstream in the self-preserving region of the flow is much greater than the difference in a plane jet between the conditions close to the jet nozzle and far downstream and this may well account

for the somewhat different approaches to self-preservation of the wake and the jet. In this context, it would be interesting to study the approach to self-preservation of a wake flow behind a streamline body which did not generate the same excess of turbulent energy as the comparatively bluff circular cylinder.

8.4 The intermittency factor.

It is well known that at the edge of a turbulent flow, the turbulence becomes intermittent (see figure 28a) and if we define an intermittency factor as the fraction of time for which the flow is turbulent, we find that this factor varies from unity in the flow centre to zero at the flow edge. If we are interested in properties connected solely with the turbulent flow, it is necessary to make an allowance for this intermittency factor. For example, quantities like the turbulent energy and the turbulent shear stress are small or zero in the irrotational flow that occurs between the turbulent 'bursts' and, therefore, it would be necessary to divide these quantities as measured by the intermittency factor to obtain the average values within the turbulent fluid. In the present case, the intermittency factor was measured at several longitudinal stations and, as can be seen from figure (53), the results are in fair agreement with the measurements of Corrsin and Kistler (1954) in an axi-symmetric jet and, consequently, with Townsend's assertion that the large eddies in jets are smaller than those in wakes. A point of interest is whether the essentially irrotational flow that exists between the turbulent 'bursts' has a mean velocity equal to the free-stream velocity or whether it is accelerated by pressure forces to have a mean velocity

equal to that of the turbulent fluid. Direct measurements by Townsend in a wake flow indicate that the irrotational flow has essentially the same mean velocity as the turbulent flow. On the other hand, some observations by Klebanoff (1954) in a flat plate boundary layer of the output signals from a hot wire anemometer seem to support the opposite view. The present writer had hoped to undertake some direct measurements on this matter but equipment could not be developed in time. However, observations of traces from the hot wire output did not reveal any obvious correlation between a turbulent 'burst' and a rise in the 'mean' velocity of the sort observed by Klebanoff. It may be that on this point there is some difference between the free turbulent flows and the boundary layer flows.

According to Townsend, the eddies which are responsible for intermittency contain only 10 - 20$^{o/o}$ of the total turbulent energy and are similar in scale to the half width of the flow in the case of jets and wakes. The remaining turbulence is assumed to be an order of magnitude smaller and contain most of the turbulent energy. In order to obtain more information on this point, the output from the intermittency meter was fed into a frequency meter which gave the average frequency of those eddies responsible for intermittency. This was an extremely crude experiment and the frequencies obtained may be as much as 50$^{o/o}$ in error. In order that the significance of these measurements may be visualised in a simple way, let us consider first an imaginary case in which the boundary of the turbulent flow is in the form of a sine wave travelling with the average mean velocity of the flow, U_M(figure (52a)). The use of this average mean velocity is

suggested by auto-correlation measurements (Davies et al (1963)) which show that the convection speed of the large eddies is roughly equal to this average mean velocity. Now, in the imaginary flow, the outputs from the intermittency meter at different positions in the intermittent region would be similar to those shown in figure (52b). The frequency meter would give a constant value of frequency in the intermittent region, say 'n', and zero frequency in the fully turbulent flow or non-turbulent flow (figure (32c)). This frequency may be used to define an eddy wavelength, U_M/n. If these large eddies are to be consistent with self-preservation, their wavelength should be a constant proportion of the jet width so that the distribution of the parameter $n\delta_{0.5}/U_M$ across the jet should be independent of the longitudinal station. The results of the present measurements are shown in figure (54) and they show that,although the accuracy of the measurements is very poor, the results are not obviously in contradiction with self-preservation of the large eddies. Further, since the turbulence is made up of a whole spectrum of eddies, the frequency distribution is not 'square'. Nevertheless, we may take the maximum value of the parameter, $n\delta_{0.5}/U_M$, to give an idea of the average frequency and wavelength of the eddies responsible for intermittency. On this basis, we can assume that $n\delta_{0.5}/U_M = 0.3 \pm 0.1$. We will use this value at a later stage when discussing some spectrum measurements.

8.5 The distribution of the turbulent shear stress and intensities across a self-preserving plane jet.

As a result of the preceding work, subsequent measurements of the turbulence structure were restricted to two stations in the

self-preserving region of the flow at x/h=50 and x/h=70. Measurements of the shear stresses at these two stations are compared in figure (55) with the shear stresses calculated from the momentum equation - see section 7.2. The agreement between the measured and calculated results is quite reasonable and provides a welcome check on the accuracy of the hot wire measurements. The shear stresses in the present case are about $10^{o/o}$ larger than those encountered in the jet with U_1/U_J=0.07. This comparatively small difference will be discussed later in section 9.3.

The measured distributions of the $\overline{v^2}$ and $\overline{w^2}$ components of the turbulent motion are shown in figure (56). Although an increase in scatter among the results would be expected as a result of the use of the single sloping wire technique, the difference between the results for the two $\overline{w^2}$ traverses suggests that in one case or the other something was amiss. However, the use of the average values from the two traverses should give the distribution of $\overline{w^2}$ to within about $25^{o/o}$ of the actual distribution.

The results of the whole series of turbulent intensity measurements have been summarised into figures (57) and (58) which show the distributions of the three components of the turbulent motion $\overline{u^2}/U_o^2$, $\overline{v^2}/U_o^2$ and $\overline{w^2}/U_o^2$ and the turbulent energy, $\overline{q^2}/U_o^2 = (\overline{u^2}+\overline{v^2}+\overline{w^2})/U_o^2$* respectively across the jet in the self-preserving region of the flow. By comparison with figure (3), it is clear that the distributions of these various quantities across the plane jet and plane wake are very similar although they are different in magnitude. This similarity with the wake flow is better illustrated by reference to figures (59) and (60) which show the distributions of the ratios $\overline{v^2}/u^2$ and $\overline{w^2}/u^2$ and $\overline{uv}/u^2$ respectively across

*The values of these quantities are tabulated in table I.

both the plane jet and plane wake. The results for the two flows are in moderate agreement with one another and they show that over the main portion of the flow there is a measure of similarity in the turbulence structure although it is at best only a very rough similarity.

Finally, the results of measurements of the shear stress correlation coefficient, R_{uv}, in a turbulent plane wall jet by Eskinazi and Kruka (1962) and also in a turbulent axi-symmetric jet by Gibson (1963) are compared with the present results in figure (61). The agreement is again quite good and supports the idea of a tendency towards a universally similar structure for all turbulent jet and wake shear flows.*

8.6 The turbulent energy balance.

The turbulent energy equation may be written in the approximate form (see Townsend (1956)):-

$$\underbrace{\frac{U}{2}\frac{\partial \overline{q^2}}{\partial x} + \frac{V}{2}\frac{\partial \overline{q^2}}{\partial y}}_{\text{Advection}} + \underbrace{\overline{uv}\frac{\partial U}{\partial y}}_{\substack{\text{Production}\\ \text{from shear}\\ \text{stress.}}} + \underbrace{(\overline{u^2} - \overline{v^2})\frac{\partial U}{\partial x}}_{\substack{\text{Production}\\ \text{from normal}\\ \text{stresses.}}} + \underbrace{\frac{\partial}{\partial y}\left(\frac{\overline{q^2 v}}{2} + \overline{pv}\right)}_{\text{Diffusion}} + \underbrace{\varepsilon}_{\text{Dissipation.}} = 0.$$

where $\varepsilon = \nu\overline{\left(\frac{\partial u_i}{\partial x_j}\right)^2}$.

If the distributions of the advection, production and dissipation terms are known, the distribution of the diffusion term can readily be obtained by difference. The advection and production terms can be obtained from the turbulent intensity measurements already described and it remains to obtain the distribution of the dissipation term. The turbulent eddies which are responsible for the viscous dissipation

---

*This similarity probably extends to the outer region of boundary layers. For example, for the flat plate boundary layer, Klebanoff (1954) obtained R_{uv}=0.5. The parameter, $\overline{uv}/\overline{q^2}$, in the flat plate boundary layer and in channel flow has a value of about 0.15. In the present experiments, $\overline{uv}/\overline{q^2} \simeq 0.$

are those in the high frequency range and it is well known that there is a tendency to isotropy in this region of the spectrum. If this isotropy exists, then it is possible to write for the viscous dissipation term:-

$$\epsilon = 15\nu\overline{\left(\frac{\partial u}{\partial x}\right)^2}$$

Furthermore, if the dissipating eddies are assumed to be swept along with the local mean velocity then $\partial/\partial x = (1/U)(\partial/\partial t)$ and $\epsilon = (15\,\nu/U^2)\overline{(\partial u/\partial t)^2}$. The quantities in this last expression can, in principal, be readily measured and it is a very convenient way to obtain the dissipation term. However, in the present experiments, it was found that the frequencies of the dissipating eddies extended up to about 15kc/s and it is certain that wire length effects and possibly inadequate compensation led to values of the viscous dissipation term that were much too small. Nevertheless, the energy balance has been obtained by suitably scaling the measured values of viscous dissipation to ensure in the final energy balance that:-

$$\int_0^\infty \frac{\partial}{\partial y}\left(\tfrac{1}{2}\overline{q^2 v} + \overline{pv}\right) dy = 0$$

i.e. the net diffusion across the flow is zero.

This energy balance is shown in figure (63). It was necessary to multiply the measured distribution of the viscous dissipation by a factor of two in order to obtain a sensible energy balance.

The main features of the energy balance are:-

(a) The distribution of the viscous dissipation term is very similar to that obtained in a wake flow (see Townsend (1956) pp.167) and shows that, over the central region of the flow, this term is roughly constant. By making an allowance for the intermittency factor, the region of

approximately constant viscous dissipation is extended further.

(b) The viscous dissipation and production terms are the most significant in the energy balance. This may be illustrated by comparing the integral values of the various terms in the energy balance over the jet width given in the following table.

Production.	$\frac{\delta_{0.5}^2}{U_0^3}\int_0^\infty \overline{uv}\frac{\partial U}{\partial y}dy$	-0.0169
Dissipation.	$\frac{\delta_{0.5}^2}{U_0^3}\int_0^\infty \varepsilon\, dy$	+0.0207
Advection.	$\frac{\delta_{0.5}^2}{U_0^3}\int_0^\infty \left(\frac{U}{2}\frac{\partial \overline{q^2}}{\partial x}+\frac{V}{2}\frac{\partial \overline{q^2}}{\partial y}\right)dy$	-0.0038
Diffusion.	$\frac{\delta_{0.5}^2}{U_0^3}\int_0^\infty \frac{\partial}{\partial y}\left(\frac{1}{2}\overline{q^2v}+\overline{pv}\right)dy$	0

(c) ulike the wake flow, it appears that the diffusion of turbulent energy $(\frac{1}{2}\,\overline{q^2v}+\overline{pv})$ is at least roughly correlated with the local mean intensity gradient (see Townsend (1956) pp.168).

The micro-scale of the turbulence $\lambda=\sqrt{\overline{u^2}/\left(\frac{\partial u}{\partial x}\right)^2}$ can be calculated from the viscous dissipation term and, as showmin figure (62), the distribution of this lengthscale across the jet is again very similar to that obtained in a wake flow.

Finally, it is interesting to check the validity of the local isotropy assumption in the present measurements. According to Corrsin (1957) it is necessary that two conditions should be fulfilled. These are:-

(a) $\dfrac{(\varepsilon/\nu)^{\frac{1}{2}}}{(\partial U/\partial y)} \gg 1\cdot 0$ and (b) $\dfrac{(\varepsilon/\nu)^{\frac{1}{4}}}{\frac{1}{\sqrt{v^2}}\frac{\partial U}{\partial y}} \gg 1\cdot 0$

The first condition is simply a requirement that the rate of strain due to the dissipating eddies is much larger than that due to the mean velocity gradient and the other condition is a requirement that the wavenumbers of the dissipating eddies are much larger than those

at which energy is fed into the turbulence. The results of this check are given in the following table where also a comparison is made with some results of previous investigators.

	$\frac{(\varepsilon/\nu)^{1/2}}{\partial U/\partial y}$	$\frac{(\varepsilon/\nu^3)^{1/4}}{\frac{1}{\sqrt{2}}\times\frac{\partial U}{\partial y}}$
Present measurements - plane jet.	24	125
Uberoi - Distortion of homogeneous turbulence.	0.5	-
Klebanoff - Boundary layer on a flat plate.	10	45

Thus, the use of the simplified expression for the viscous dissipation term would seem to be well justified in the present experiments.

8.7 The eddy structure.

In order to provide some additional insight into the flow structure, a limited number of spectra and correlation measurements were made. This work was limited in its objectives and the results are far from comprehensive. The measurements were carried out in the jet at $y/\delta_{0.5}$=0.5 and x/h=51 and they consisted of measurements of the $R_{11}(0,r,0)$ correlation coefficient and the $\overline{u^2}$ and $\overline{uv}$ spectra.

The correlation coefficient measurements of $R_{11}(0,r,0)$ - written subsequently as R_y - were obtained with one hot wire fixed at $y/\delta_{0.5}$=0.5 and the other wire traversed outwards towards the edge of the jet. In order to obtain some idea of the length scales appropriate to the various frequencies, these correlation measurements were obtained by passing the various signals through the filter unit and measuring the outputs for different settings of the high pass filter. The resulting correlation coefficients are shown in figure (64). The significance of the results will be discussed later in relation to the spectra measurements and, for the moment, we will simply compare the integral scale $L_y = \int_0^\infty R_y dy$ with

the values found in other free turbulent flows. Since the mean velocity profiles in all these flows are roughly similar, we are justified in using $\delta_{0.5}$ as a reference length throughout. In addition to a comparison of values of L_y, the following table also compares values of the integral scale $L_x = \int_0^\infty R_x dx$ where values are available.

FLOW.	AUTHOR.	$L_y/\delta_{0.5}$	$L_x/\delta_{0.5}$	L_x/L_y
Isotropic turbulence.	Theoretical result.	-	-	2.0
Plane jet.	Present measurements.	0.38	-	-
Plane wake.	Townsend (1956)	0.6	0.83	1.37
Plane wake.	Grant (1958)	0.5	0.83	1.66
Mixing layer.	Liepmann & Laufer(1947)	0.26	-	-
Mixing layer.	Laurence(1956)	-	-	2.5–3.0
Circular jet.	Corrsin (1943)	0.23	-	-
Circular jet.	Corrsin & Uberoi (1949)	0.17	0.92	5.4
Circular jet.	Gibson (1963)	-	0.95	-

Although the data is not very complete, it seems that the longitudinal integral scale L_x is very roughly constant for all the flows considered but the lateral scale L_y is smaller in jets than it is in wakes. This is consistent with the idea that the comparatively large lateral mean velocities found in jets but not in wakes inhibit the growth of the eddies in the lateral direction.

The spectrum measurements were obtained by passing the hot wire anemometer signals through the filter unit and measuring the mean square output voltages for a range of settings of the high pass filter. If $\overline{u^2}F(k)$ and $\overline{uv}G(k)$ represent the contributions to $\overline{u^2}$ and $\overline{uv}$ respectively from wavenumbers between k and k+dk, then the outputs from the filter

unit gave $\int_{k'}^{\infty} F(k)dk$ and $\int_{k'}^{\infty} G(k)dk$ respectively where k' is the setting of the high pass filter. These latter quantities are plotted in figure (65). These results show that the eddies responsible for the major part of the shear stress are also responsible for the major part of the turbulent energy and these eddies are contained in the wavenumber range from zero to about 0.5 cm^{-1}. This wavenumber range is equivalent to a range of values of the parameter $n\delta_{0.5}/U_M$ from zero to about 0.34. In section 8.4 it was shown that the average frequency of eddies responsible for intermittency was given by $n\delta_{0.5}/U_M \approx 0.3$ and this suggests that those eddies which are responsible for intermittency may also be responsible for the major part of the shear stress. It is appreciated that the average frequency of the eddies responsible for intermittency obtained from the intermittency meter does not necessarily correspond to the eddy frequencies of the spectra measurements. However, even if this average frequency is too large by a factor of two, this would not seriously affect the conclusion that the shear carrying eddies and the eddies causing intermittency are essentially the same. Also of interest is the fact that the shear stress spectrum approaches zero more rapidly than the u^2 spectrum. This shows that there is a range of eddies which do not contribute anything to the shear stress and this is a necessary condition for the existence of local isotropy and shows that the turbulence structure is at least not obviously inconsistent with the local isotropy hypothesis.

It is well known that the longitudinal correlation coefficient coefficient R_x and the one-dimensional spectrum function F(k) are

Fourier transforms of one another.

i.e.

$$R_x = \int_0^\infty F(k)\cos kx\, dk \qquad (8.7.1)$$

$$F(k) = 2/\pi \int_0^\infty R_x \cos kx\, dx \qquad (8.7.2)$$

From these relationships, it is easily shown that:-

$$\text{(a) } \epsilon = 15\nu \int_0^\infty k^2 F(k)dk \text{ for isotropic turbulence.} \qquad (8.7.3)$$

$$\text{(b) } L_x = \frac{\pi}{2} F(0) \qquad (8.7.4)$$

Equation (8.7.3) shows that the contribution to the viscous dissipation is heavily weighted in favour of eddies with a high frequency - a result which is well known. The one-dimensional spectrum function F(k) was obtained by graphically differentiating the curve of $\int_{k'}^\infty F(k)dk$ with respect to the wavenumber, k'. The distributions of F(k) and $k^2F(k)$ obtained in this way are shown in figure (66). The value of F(0) was obtained from equation (8.7.4) by assuming that $L_x = 2L_y$. It was not possible to obtain reliable data for wavenumbers less than about 0.3 cm^{-1} (which corresponds to a frequency of about 100 c/s) because of the limitations in the filter unit in the low frequency range. In addition, at wavenumbers equal to or greater than the reciprocal of the hot wire length, finite hot wire length effects become important and lead to values of the spectrum function F(k) which are much too small. Notwithstanding these difficulties, the figure (66) shows that the eddies responsible for the major part of the turbulent energy are reasonably well separated in wavenumber number space from those eddies responsible for the major part of the viscous dissipation. This separation,

in fact, appears to be sufficient to permit the existence of an inertial subrange (see Batchelor (1956) or Hinze(1959)) because when $\log_{10}F(k)$ is plotted against $\log_{10}k$ (figure (67)), a region is found in which $F(k) \propto k^{-5/3}$. The conditions necessary for the existence of an inertial subrange are that there should be a region of the spectrum in wavenumber space which contributes very little either to the turbulent energy or the viscous dissipation. This requires a very high Reynolds number and Corrsin has suggested that $R_\lambda = \sqrt{u^2}\,\lambda/\nu$ should not be less than 500. In the present experiments, the value of R_λ was about 350 which seems to be large enough to permit the existence of a limited inertial subrange. The Universal Equilibrium theory (see, for example, Hinze (1959)) shows that in the inertial subrange, the spectrum function is given by:-

$$\overline{u^2}F(k) = \frac{18}{55} A\varepsilon^{2/3}k^{-5/3}$$

where A is a universal constant. The present results give A = 1.54 which is in very good agreement with the value of 1.6 obtained by Gibson (1963) in a circular jet and the value of 1.44 obtained by Grant et al (1962) in a tidal channel.*

Finally, we will consider the results of the filtered correlation measurements - figure (64). From the spectrum measurements, it appears that half the shear stress in the present case is carried by eddies in the wavenumber range from 0 to 0.3 cm^{-1} (corresponding to a frequency range from 0 to 100 c/s) and over 70% by eddies in the wavenumber range from 0 to 0.6 cm^{-1}. According to the correlation measurements, however,

*Considering all things, this agreement is better than one might reasonably expect and, to some extent, must be fortuitous.

there is no sudden reduction in the extent of the R_y correlation nor of the integral scale, L_y, of the turbulence when the high pass filter is set at these respective wavenumbers in the correlation measurements. Moreover, the integral scale is reduced by only 30% when the high pass filter is set at a wavenumber of 0.3 cm^{-1} so that the earlier conclusion that the eddies responsible for a major part of the shear stress are among the largest eddies in the flow is re-affirmed. As before in the discussion of the intermittency meter results, it must be admitted that the interpretation put upon the present results is not free from objections. Nevertheless, there is clearly some ground for a critical re-examination of this problem of the eddy structure.

8.8 The characteristic times.

The characteristic times for the development of the flow and the turbulent motions give some guide to the validity of theories of turbulence and also, in a more general way, some idea of the flow structure (see Townsend (1956) pp.96). Townsend introduced the following characteristic times:-

(a) The time for appreciable development of the flow;

$$t_D = \frac{\delta}{U_M \, d\delta/dx}$$

where U_M is the average mean velocity over the flow cross-section. It can be shown that t_D is a simple multiple of the existence time introduced in section 7.2.

(b) The time for substantial rate of strain by the mean flow;

$$t_S = 1/(\partial U/\partial y)_{max.}$$

(c) The time scale representative of energy transfer;

$$t_p = \int_{-\infty}^{\infty} \overline{q^2} \, dy \Big/ 2 \int_{-\infty}^{\infty} \overline{uv} \, \frac{\partial U}{\partial y} \, dy$$

which may be thought of as the time necessary to produce the turbulent energy.

(d) The time scale representative of viscous dissipation;

$$t_V = \int_{-\infty}^{\infty} \overline{q^2}\, dy \Big/ 2\int_{-\infty}^{\infty} \varepsilon\, dy$$

(e) The time for a substantial rate of strain by the energy containing eddies;

$$t_E = L_x / \sqrt{\overline{q^2}}$$

The values of these characteristic times for the various free flows are given in the following table

	t_S/t_D	t_P/t_D	t_V/t_D	t_E/t_D
Plane jet (Present experiments).	0.073	0.3	0.26	0.16
Planewake (Townsend).	0.17	0.24	0.19	-
Mixing layer (Liepmann & Laufer).	0.08	0.45	-	-
Circular jet (Corrsin).	0.07	0.24	-	0.105

In isotropic turbulence, it is found that (Townsend (1956)):-

$$\varepsilon \approx \frac{3}{2}\frac{\left(\overline{u^2}\right)^{3/2}}{L_x} = \frac{1}{2\sqrt{3}}\frac{\left(\overline{q^2}\right)^{3/2}}{L_x}$$

Now, Townsend found that this relationship was also roughly correct in the plane wake and concluded that it was probably valid in other shear flows as well. If this is so, then t_V and t_E are simply related by:-

$$t_\varepsilon = \frac{t_V}{\sqrt{3}}^{*}$$

Referring to the above table, we see that the results for the plane jet are in good agreement with this last expression.

The time for appreciable development of the flow, t_D, is related

---

* Townsend (1956) pp.97 quotes $t_\varepsilon = \frac{2t_V}{3\sqrt{3}}$ which is apparently an error.

to the existence time, t_e, for the plane jet by:-

$$t_e = 0.333\ t_D$$

and, therefore, it is apparent that the production and dissipation times are comparable to the existence time. This feature, which has previously been commented upon by Townsend (1950) in connection with the wake flow, leads one to expect that the flow at any station is strongly dependent on upstream conditions. This is a strong objection to any simple gradient transport theory which postulates some sort of local equilibrium. However, as we will discuss in section 9.3, it may be possible to make an allowance for the upstream history of the flow in the gradient transport theories by making use of additional postulates of the kind embodied in Townsend's large eddy hypothesis.

8.9 The unsteady irrotational motion.

The convoluting edge of the turbulent flow induces unsteady but irrotational velocity fluctuations in the free-stream. According to Phillips (1955) and Stewart (1959), the components of this unsteady motion are related to one another such that:-

$$\overline{v^2} = \overline{u^2} + \overline{w^2} \qquad (8.9.1)$$

Furthermore, at large distances from the edge of the turbulent flow, it is found that:-

$$\overline{v^2}/2 = \overline{u^2} = \overline{w^2} \propto (y - y_o)^{-4} \qquad (8.9.2)$$

where y_o is the apparent origin of these irrotational fluctuations. Measurements of the $\overline{u^2}$ intensity obtained from the present experiments confirm the validity of equation (8.9.2) for this term, as shown by figure (68)*. This data is well represented for $y/\delta_{0.5} \geq 2.3$ by the

*A special traverse was made at x/h=49 with the sole purpose of measuring the turbulence in the irrotational region of the flow. However, results from other traverses are also used in this work.

expression:-

$$\frac{\overline{u^2}}{U_o^2} = 0.0016 \left(\frac{y - y_o}{\delta_{0.5}}\right)^{-4} \quad \text{where } y/\delta_{0.5} = 1.33 \pm 0.03 \qquad (8.9.3)$$

It is to be noted that the apparent origin of the fluctuations, $y_o/\delta_{0.5}$, lies well within the region where turbulent flow exists - the intermittency factor is approximately 0.8 at $y/\delta_{0.5} = 1.33$. It is also to be noted that equation (8.9.2) appears to be valid even quite close to the edge of the turbulent flow. This was found to be true also in the case of wake flow - see Phillips (1955).

The $\overline{v^2}$ and $\overline{w^2}$ intensities in the irrotational flow region were obtained with a single sloping wire which measured the quantity $u^2 + \alpha(\overline{v^2}$ or $\overline{w^2})$ where α is a constant for any given hot wire - see section 6.1. In order to determine the ratios $\overline{v^2}/\overline{u^2}$ and $\overline{w^2}/\overline{u^2}$, we will assume that:-

$$\frac{\overline{u^2}}{U_o^2} = k_u \left(\frac{y - y_o}{\delta_{0.5}}\right)^{-4}$$

and

$$\frac{\overline{v^2}}{U_o^2} = k_v \left(\frac{y - y_o}{\delta_{0.5}}\right)^{-4}$$

From the measurements with the single sloping wire, we obtain:-

$$\frac{\overline{u^2}}{U_o^2} + \frac{\overline{v^2}}{U_o^2} = (k_u + \alpha k_v)\left(\frac{y - y_o}{\delta_{0.5}}\right)^{-4}$$

From these experimental results, graphs of $(\overline{u^2}/U_o^2 + \alpha \overline{v^2}/U_o^2)^{-4}$ against $(y - y_o)/\delta_{0.5}$ can be plotted from which $(k_u + \alpha k_v)$ can be obtained. The results of these experiments are given in the following table.

x/h	α	$(k_u + \alpha k_v)$	$(k_u + \alpha k_w)$	k_w/k_u	k_v/k_u
48.5	0.593	0.00355	0.00275	1.21	2.06
70	0.41	0.00355	0.00225	1.02	3.00
51	0.84	0.00345	0.0026	0.75	1.38
Average values.				1.0	2.5

Considering the inherent lack of accuracy of the single sloping wire technique, these results can be regarded as providing a most satisfactory confirmation of equation (8.9.2).

9.0 Additional comments on the self-preserving plane jet including applicability of the various theories of turbulence.

Both the constant exchange hypothesis and the mixing length theories postulate a gradient transport mechanism but this is not the only type of transport mechanism that is possible in turbulent shear flows. Townsend (1956) and Batchelor (1950) have considered a model flow in which the transport process may be represented as the sum of a gradient transport mechanism and a bulk transport mechanism. This model is in keeping with Townsend's suggestion that the turbulent eddies may be divided roughly into two groups, namely the large eddies which will be responsible for the bulk transport and the energy containing eddies which are much smaller and will be responsible for the gradient transport mechanism. For this model, we may write:-

$$\overline{\theta v} = \bar{\theta}\bar{V} + K\frac{\partial\bar{\theta}}{\partial y}$$

where $\bar{\theta}$ is the average value of the transported property, $\bar{V}$ is the average value of the bulk transport velocity and K is a gradient diffusion coefficient. On a qualitative basis, Townsend was able to explain many of the observed features of a turbulent shear flow but difficulties arise when quantatative use of this model is attempted because, in the first place, the relative importance of the bulk and gradient transport mechanisms depends on the nature of the property transported and there is also, of course, the problem of attaching values to the bulk transport velocity and the gradient diffusion coefficient. This lack of precision in the above model makes a detailed comparison with experimental data difficult and,in the present case,we

will restrict ourselves to the more straightforward comparison with the gradient transport theories discussed in section 2.2, namely the constant exchange hypothesis and the Prandtl Mixing Length theory.

9.1 The constant exchange hypothesis.

It was shown in section 2.2 that, for the constant exchange hypothesis to have any physical validity, it is required that the turbulence structure be reasonably homogeneous across the jet and also that $\sqrt{\overline{q^2}}/L \gg \partial U/\partial y$. Now, although the fine structure of the turbulence is apparently closely homogeneous across the width of the flow, reference to the distribution of the turbulent energy - figure (58) - shows that homogeneity of the energy containing eddies cannot be regarded as a particularly good assumption although, at the same time, it is not wholly unreasonable and it has been argued that the "stirring" action of the large eddies will tend to ensure a roughly homogeneous turbulence structure. However, the discovery that $(\sqrt{\overline{q^2}}/L)/(\partial U/\partial y) = O(1)$ is sufficient to show that the constant exchange hypothesis cannot have real physical validity. Notwithstanding this last objection, this hypothesis remains a useful empiricism and if we calculate the distribution of eddy viscosity across a plane jet including an allowance for the intermittency factor, we find that the eddy viscosity coefficient is roughly constant over an appreciable region of the flow - figure (69)*.

---

* Figure (69) shows the distribution of the reciprocal of the eddy Reynolds number $1/R_T = \nu_t/U_o\delta = g_{12}(\eta)/f'(\eta)$ and also $1/\gamma R_T$. The calculations were made for $U_1=0$ and $d\delta_{0.5}/dx=0.1$ for simplicity.

9.2 Prandtl's Mixing Length theory.

In the case of Prandtl's Mixing Length theory, it is necessary that $\sqrt{\overline{u^2}}/L \approx \partial U/\partial y$ and that the turbulent velocity fluctuations should be similar throughout the flow i.e. parameters like $\overline{v^2}/\overline{u^2}$ etc. and R_{uv} should be constants.

If we calculate the distribution of the mixing length across the jet by assuming that (a) $L/\delta = (\sqrt{\overline{u^2}}/\delta)/(\partial U/\partial y) = \sqrt{g_1(\eta)}/f'(\eta)$ and (b) $L/\delta = (\sqrt{\tau/\rho}/\delta)/(\partial U/\partial y) = \sqrt{g_{12}(\eta)}/f'(\eta)$, we obtain the results shown in figure (70). With the obvious exception of the central region of the flow, both distributions show that the mixing length is roughly constant over the main portion of the jet and, moreover, it is interesting that the former relationship gives a value of $L/\delta_{0.5}=0.35$ which is in close agreement with the measured value of $L_y/\delta_{0.5}=0.38$. The numerical difference between the two calculated distributions of the mixing length is not important since it arises from the fact that $R_{uv} \neq 1.0$ and $\overline{u^2} \neq \overline{v^2}$.

The validity of the flow similarity assumption can be tested by reference to figures (59), (60) and (61) which show the distributions across the jet of $\overline{v^2}/\overline{u^2}$, $\overline{w^2}/\overline{u^2}$, $\overline{uv}/\overline{u^2}$, and R_{uv} respectively. With the exception of the region near the flow centre, it appears that the assumption of similarity may not be wholly unreasonable although, at the same time, it is obviously not a very precise assumption either.

Finally, it has been shown by Batchelor (1950) that the Prandtl Mixing Length theory requires an energy balance between the production and viscous dissipation of turbulent energy. Reference to the energy balance - figure (63) - shows that, over a region of the flow, the

production and viscous dissipation terms are indeed predominant although the diffusion and advection terms are by no means negligible.

9.3 Further comments on the theories of turbulence.

On balance, it seems that of the two simple gradient transport theories discussed, the Prandtl Mixing Length theory gives a slightly better description of the flow. However, this result does not necessarily have any far reaching significance since it is restricted to the plane jet flow. For example, in the plane wake, the energy balance between turbulent energy production and viscous dissipation of turbulent energy implied in the Mixing Length theory is not found. In any case, the structure of the flow does not obviously conform to any really well defined pattern as witnessed by the comparative ease with which the experimental results were shown to exhibit features associated with quite different assumptions about the flow. On the one hand, in connection with the constant exchange hypothesis, it was shown that the assumptions of a roughly constant value of turbulent energy across the jet and also that $\tau \propto (\partial U/\partial y)$ were not unreasonable. On the other hand, it was then shown that $\sqrt{u^2} \propto L\frac{\partial U}{\partial y}$ and $\tau \propto (\partial U/\partial y)^2$ were also reasonable assumptions! This duplicity of interpretation is not uncommon in work on turbulence and it arises, to some extent, because the turbulence comprises a whole spectrum of eddies with their own length and time scales and which are subjected to different physical controlling factors. This diversity of eddy scales ensures that no single simple mechanism can be expected to describe the whole of the turbulence structure. Hence, where there is apparently a measure of support from the experimental work for two different assumptions, it may well be that both assumptions

apply but to different regions of the spectrum. In fact, it is clear that to be able to make any progress on the turbulence problem, it is necessary to split the spectrum into groups of eddies (even though this in itself is artificial) with more or less distinct scales of length and time and to then construct theories or mechanisms to account for the behaviour of each eddy group and also its interaction, if any, with other eddy groups. This is, of course, precisely the approach used in the theories of the dissipating range of eddies and also used by Townsend in his large eddy hypothesis. However, unlike the former example, the development of the Townsend flow model was strongly dependent on experimental work and, consequently, it is of interest to re-consider the flow structure in the light of the more recent experiments of Grant (1958) and some of the present results.

According to Grant, the most obvious large scale motions in a wake are "a series of more or less regularly spaced 'jets' of turbulent fluid preceding outwards from the central plane of the wake." Motions similar to those described by Grant can often be seen in jets of steam and in smoke from chimneys and these jet-like motions are clearly responsible for intermittency. According to Townsend, these large scale motions are an order of magnitude larger than the bulk of the shear and energy carrying eddies. However, there is a strong suggestion in the present results that the large eddies responsible for intermittency might also be responsible for a large part of the shear stress.* Additional evidence in favour of this idea is the fact that the integral

---

*Recent experiments by Bradshaw et al (1963) also point to this conclusion.

scale, L_y, was reduced by only $30^{o/o}$ when the high pass filter was set to about a wavenumber of 0.3 cm^{-1} which removed eddies responsible for about half the total shear stress. Also, the straightforward observation that wavenumbers up to 0.3 cm^{-1} in the present case correspond to an eddy wavelength range (where this wavelength = U/n) up to about $6\delta_{0.5}$ supports the conclusion that the shear carrying eddies are among the largest in the flow. Although this conclsuion appears contrary to Townsend's flow model, there is a good deal of evidence showing that mechanisms at least similar to those postulated by Townsend are at work in turbulent shear flows. It may be therefore that his flow model is adequate if some allowance for the contribution from the large eddies to the overall shear stress can be made. Grant's experiments also show that the form of the large eddies used by Townsend requires modification. However, more experimental work is required on this problem before any of the above modifications can even be contemplated with confidence.

The discovery that the Prandtl Mixing Length description of the flow structure is not altogether unreasonable is interesting because the jet-like eddy motions described by Grant would give rise to a distribution of the $\sqrt{\overline{u^2}}$ intensity similar to that postulated by the Prandtl theory provided the lateral velocity with which the mixing jets grew was large enough to prevent appreciable diffusion of the fluid within the mixing jets during the course of their development. If this last condition is fulfilled and these eddies are also responsible for a large part of the shear stress, we can expect that a high instantaneous value of the shear stress would be accompanied by a higher than average

value of the v-component of the turbulent motion. This suggest that a test of these ideas would be provided by measurements of the quantity $\overline{u^2}v/\overline{uv}\sqrt{\overline{v^2}}$ which should be much greater than 1.0 if the above ideas are correct.

It is interesting now to discuss Townsend's hypothesis from a somewhat different standpoint. It has been shown that the mean velocity profiles in a plane jet and a plane wake are practically identical. Therefore at some longitudinal station in either a plane wake or a plane jet in a moving airstream the flow structure will depend on the following dimensionless groups:-

$$\frac{y}{\delta_{0.5}}\,,\ \frac{U_0}{U_1}\,,\ \frac{d\delta_{0.5}}{dx}\,,\ \frac{\delta_{0.5}}{U_0}\frac{dU_0}{dx}\,,\ \delta_{0.5}\frac{d\delta_{0.5}^2}{dx^2}\,,\ \frac{\delta_{0.5}^2}{U_0}\frac{d^2U_0}{dx}\,,\ \text{etc.}$$

In a self-preserving flow, these parameters, with the exception of $y/\delta_{0.5}$, must all be constants since it is a condition of self-preservation that the flow structure depends only on $y/\delta_{0.5}$. For example, it is easily shown that in a self-preserving plane jet:-

$$U_0/U_1 = \infty$$

$$d\delta_{0.5}/dx = K, \text{ a constant.}$$

$$\delta_{0.5}^{n-1}\frac{d^n\delta_{0.5}}{dx} = 0 \quad \text{for} \quad n \geq 2$$

$$\frac{\delta_{0.5}^n}{U_0}\frac{d^nU_0}{dx^n} = (-K)^n\frac{(2n-1)!}{2^n}$$

By contrast, in a self-preseriving plane wake, all these parameters tend to zero. It would appear from the present experiments that the distributions of the various turbulent intensities and shear stress across a plane jet and a plane wake are very similar so that we are tempted to write:-

$$\overline{u^2} = U_0^2\, g_1\left(\frac{y}{\delta_{0.5}}\right) F\left(\frac{U_1}{U_0}\,,\ \frac{d\delta_{0.5}}{dx}\,,\ \frac{\delta_{0.5}}{U_0}\frac{dU_0}{dx}\,,\ \ldots\right)$$

$$\overline{v^2} = U_0^2\, g_2\left(\frac{y}{\delta_{0.5}}\right) F\left(\frac{U_1}{U_0}\,,\ \frac{d\delta_{0.5}}{dx}\,,\ \frac{\delta_{0.5}}{U_0}\frac{dU_0}{dx}\,,\ \ldots\right)$$

$$\overline{w^2} = U_0^2\, g_3\left(\frac{y}{\delta_{0.5}}\right) F\left(\frac{U_1}{U_0}\,,\ \frac{d\delta_{0.5}}{dx}\,,\ \frac{\delta_{0.5}}{U_0}\frac{dU_0}{dx}\,,\ \ldots\right)$$

$$\overline{uv} = U_o^2 g_{12}\left(\frac{y}{\delta_{0.5}}\right) F\left(\frac{U_o}{U_1}, \frac{d\delta_{0.5}}{dx}, \frac{\delta_{0.5}}{U_o}\frac{dU_o}{dx}, \ldots\right) \qquad (9.3.1)$$

where the functions g_1, g_2, g_3 and F are universal. In relation to the earlier discussion of the theories of turbulence, we may view the form of the 'g-functions' as being controlled by the type of transport mechanism in the turbulent flow whereas the function F can be thought of as representing the effects of the flow history on the length and time scales of the eddies responsible for the transport processes. We will define the limiting values of the function F so that for a self-preserving plane jet, F=1 and for the self-preserving plane wake, $F \approx 2.5$ (see section 3.2). The problem now arises of determining the function F. The large eddy hypothesis of Townsend provides a possible form for this function and, from section 3.2, we see that this form is:-

$$F = \exp\left[-6\left\{\left(\frac{\partial U/\partial x}{\partial U/\partial y}\right)_{t_J} - \left(\frac{\partial U/\partial x}{\partial U/\partial y}\right)_t\right\}\right]$$

$$= \exp\left[-6\left\{\left[\left(\frac{\delta_{0.5}}{U_o}\frac{dU_o}{dx}\right)_J - \left(\frac{\delta_{0.5}}{U_o}\frac{dU_o}{dx}\right)\right]\left(\frac{f}{f'}\right)_t - \left[\left(\frac{d\delta_{0.5}}{dx}\right)_J - \left(\frac{d\delta_{0.5}}{dx}\right)\right]\eta_t\right\}\right] \qquad (9.3.2)$$

where $(f/f')_t$ and η_t are evaluated at some typical station in the outer region of the jet, say η=1.5. The suffix J refers to "pure" jet conditions when U_1=0. This hypothesis shows no dependency on the parameters U_1/U_o, $\delta_{0.5}^{n-1}\frac{d^n\delta_{0.5}}{dx^n}$ and $\frac{\delta_{0.5}^n}{U_o}\frac{d^nU_o}{dx^n}$ for $n \geq 2$. In the following table, the ratios of the shear stresses with U_1/U_J=0.162 to the shear stresses with $U_1 \approx 0$ have been calculated at a number of longitudinal stations in the jet using experimental values of $\left\{(\partial U/\partial x)/(\partial U/\partial y)\right\}_t$ and equation (9.3.2). These values are compared with the observed values.

$\{(\partial U/\partial x)/\partial U/\partial y)\}_t$=-0.167 for U_1=0, $d\delta_{0.5}/dx$=0.1			
x/h	$\{(\partial U/\partial x)/(\partial U/\partial y)\}_t$ U_1/U_J=0.162	F Equation (9.3.2)	F Observed(approx.)
20	-0.095	1.5	1.1
40	-0.078	1.7	1.1
60	-0.069	1.8	1.1

It is quite clear from the discrepancies between the calculated and observed values of the function F that a straightforward application of Townsend's hypothesis is not valid. This matter will be discussed further in section 11.

Finally, it is worth noting that another concept that has attracted attention in recent years is the idea that the rate of change of volume flow within a flow is a parameter of importance in defining the flow structure (see, for example, Head (1958)). On this basis, we may define an 'inflow' velocity, V_∞, such that:-

$$V_\infty = \frac{d}{dx}\int_0^\infty U\,dy = I_1\frac{d(U_o\delta_{0.5})}{dx}$$

and we find that the non-dimensional parameter, V_∞/U_o, which is a suitable parameter for defining the rate of change of volume flow within a flow becomes:-

$$\frac{V_\infty}{U_o} = I_1\left[\frac{\delta_{0.5}}{U_o}\frac{dU_o}{dx} + \frac{d\delta_{0.5}}{dx}\right]$$

Thus, again, we find that the parameters U_o/U_1, $\delta_{0.5}^{n-1}\frac{d^n\delta_{0.5}}{dx^n}$ and $\frac{\delta_{0.5}^n}{U_o}\frac{d^nU_o}{dx^n}$ for $n \geq 2$ play no part in this hypothesis. Unlike Townsend's hypothesis, no concrete form for the function F using the parameter V_∞/U_o can be given and it would be necessary to test this idea experimentally unless further assumptions can be made.

10.0 Presentation and discussion of results for a plane jet with U_1/U_J=0.58.

As the jet spreads downstream or, alternatively, as the ratio of free-stream to jet velocity increases, the values of U_o/U_1 cease to be much larger than 1.0 and a self-preserving pure jet flow is no longer possible. On the other hand, as $U_o/U_1 \rightarrow 0$, the flow can develop a structure similar to that of a plane wake. Therefore, we may regard the plane jet in a moving airstream as an interesting example of a perturbed self-preserving flow whose structure should gradually approach that of a self-preserving plane wake as we move far downstream. In an attempt to observe this change of structure, some additional measurements were made with U_1/U_J=0.58. These tests included the following measurements:-

(a) mean velocity traverses at a number of longitudinal stations in the jet using a pitot and static tube.

(b) both lateral and longitudinal traverses with a hot wire anemometer measuring the $\overline{u^2}$ component of the turbulence.

(c) at a number of longitudinal stations, the intermittency factor was measured.

(d) at two longitudinal stations, the distributions of $\overline{uv}$, $\overline{v^2}$ and $\overline{w^2}$ were measured.

10.1 The mean velocity measurements.

As shown in figure (71), the mean velocity profiles are again geometrically similar and identical with those obtained at the lower values of U_1/U_J. The spread of the jet and the decay of the centre-line velocity are shown in figure (72). U_o/U_1 is now much less than 1.0 so that we would expect the flow to show some similarity with the plane wake flow structure.

The following table summarises the results of the mean velocity traverses and includes the usual check on the constancy of the momentum flux.

x/h	$\delta_{0.5}/h$	U_o/U_1	$(U_o/U_1)^2$	C_J
70.1	1.77	0.206	0.0424	0.847
60.7	1.68	0.217	0.0471	0.857
51.3	1.58	0.225	0.0507	0.837
45.9	1.50	0.244	0.0595	0.87
40.5	1.43	0.251	0.063	0.858
33.75	1.29	0.263	0.0688	0.815
25.65	1.11	0.294	0.0863	0.814
13.5	0.776	0.408	0.167	0.831
Average value of C_J				= 0.841

As in previous cases, calculations have been made to determine the shear stress and lateral mean velocity profiles in the jet at a number of longitudinal stations. These calculations showed that the shear stress distribution was independent of the longitudinal station for $20 \leqslant x/h \leqslant 70$ and took the form shown in figure (76). The shear stresses are about $40^{o/o}$ larger than these for a jet in a near stationary airstream and this seems to show an approach to the wake flow structure. However, it is surprising that these shear stress profiles do not show any dependency on the distance from the jet exit for $x/h \geqslant 20$.

The lateral mean velocity profiles (figure (73)) show that the inflow into the jet is now much less than that encountered in a jet in a near stationary airstream (c.f.figure (43) for U_1/U_J=0.07).

According to Townsend's large eddy hypothesis, we may write (see equation(3.2.7)):-

$$\frac{R_{T1}}{R_{T2}} \approx \frac{(\overline{uv})_2}{(uv)_1} \approx \exp\left[-\left\{\left(\frac{\partial U/\partial x}{\partial U/\partial y}\right)_{t_1} - \left(\frac{\partial U/\partial x}{\partial U/\partial y}\right)_{t_2}\right\}\right] \qquad (10.1.1)$$

Where the suffices 1 and 2 refer to different longitudinal stations in the jet where the respective strain rate ratios are different. In the following table, the ratios of the shear stresses with U_1/U_J=0.58 to the shear stresses with $U_1 \approx 0$ have been calculated at a number of stations in the jet using equation (10.1.1). The position in the jet at which 'typical' values of the strain rate ratio have been calculated is η=1.5.

$\{(\partial U/\partial x)/(\partial U/\partial y)\}_t = -0.167$ for U_1=0 and $d\delta_{0.5}/dx$=0.1			
x/h	$\{(\partial U/\partial x)/(\partial U/\partial y)\}_t$ U_1/U_J=0.58	$\overline{uv}/(\overline{uv})_{U_1=0}$ Equation (10.1.1)	$\overline{uv}/(\overline{uv})_{U_1=0}$ Observed.
20	-0.023	2.38	1.4
40	-0.018	2.42	1.4
60	-0.016	2.47	1.4

According to the large eddy hypothesis, the strain rate ratios for U_1/U_J=0.58 are so low that the flow should be practically identical to the plane wake flow. However, the measurements show that the shear stresses, $\overline{uv}/U_e^2$, are still much less than in a wake and it seems, therefore, that the approach to a wake flow structure takes place very slowly and a direct application of Townsend's large eddy hypothesis is clearly invalid. Possible reasons for this failure will be discussed in section 11.

10.2 The turbulence structure.

Because of the high free-stream velocity, the effects on the flow structure of the precise jet nozzle conditions will be felt further downstream in the present case than with $U_1 \approx 0$. In figure (74) are shown the distributions of $\Delta P_s/\rho U_o^2$ and $\overline{u^2}/U_o^2$ * along the jet centre-line and these results suggest that independence of the nozzle conditions is obtained only for $x/h \geq 40$.

The measured distributions of $\overline{u^2}/U_o^2$ and the shear stress across the jet for $x/h \geq 40$ are shown in figures (75) and (76) respectively. The agreement between the measured and calculated shear stress distributions is again quite good.

The $\overline{v^2}$ and $\overline{w^2}$ profiles were also measured and in figure (77) are shown the final distributions of these quantities and $\overline{u^2}/U_o^2$ also obtained for $x/h \geq 40$. The important feature of these results is the obvious similarity with both the previous results for $U_1/U_J = 0.162$ and the plane wake flow. This is convincing evidence in favour of the idea of a universally similar structure for plane jets and wakes.

Intermittency measurements were also made and, as shown in figure (78), the distributions of the intermittency factor across the jet are similar to those obtained with $U_1/U_J = 0.162$. No approach to the more extensive distribution of intermittency for a wake can be observed. The frequency parameter of the eddies responsible for intermittency (figure (79)) has a value of $n\delta_{0.5}/U_M \approx 0.4$ which is, to the accuracy of these frequency measurements, identical to the previous value obtained with $U_1/U_J = 0.162$.

---

*The fact that the values of $\Delta P_s/\rho U_o^2$ are a good deal larger than $\overline{u^2}/U_o^2$ should not be interpreted as showing that $\overline{v^2}$ is also much larger than $\overline{u^2}$, as will subsequently be shown. The reason for the large values of $\Delta P_s/\rho U_o^2$ is unknown but it may be due to misalignment of the probe with the flow since it is possible to show that errors in $\Delta P_s/\rho U_o^2$ due to misalignment grow without limit as $U_o \to 0$

10.3 The energy balance.

Although the viscous dissipation term in the turbulent energy balance was not measured in the present case, we may nevertheless obtain the energy balance if we assume that the shape of the viscous dissipation curve across the jet is similar to that obtained with U_1/U_J=0.162* and scaling its actual value to ensure that:-

$$\int_0^\infty \frac{\partial}{\partial y}\left(\tfrac{1}{2}q^2\overline{v} + \overline{pv}\right) dy = 0$$

This energy balance, shown in figure (80), is not very different from that obtained with U_1/U_J=0.162 although the contributions from the diffusion and advection terms are slightly larger. The energy balance is still very different from the wake flow energy balance (see Townsend (1956)pp.167) and this shows that the flow with U_1/U_J=0.58 has still more in common with the pure jet flow than it has with the wake flow even though $U_o/U_1 \approx 0.2$-0.3.†

---

*The distribution of viscous dissipation across the jet with U_1/U_J=0.162 was nearly identical in shape to that obtained by Townsend in a wake. This similarity almost certainly extends to the'intermediate' flow of a jet in a moving airstream.

†A similar conclusion has recently been reached by Maczynski(1962) in the case of an axi-symmetric jet in a moving airstream.

11.0 A comparison between experimental and theoretical results for the spreading of a plane jet in a moving airstream.

A basic assumption in any of the theories of turbulent jets is that at some distance downstream of the jet nozzle, the exact nozzle conditions are unimportant and the jet nozzle can be thought of simply as a source of excess momentum flux, J. Then, as shown in section 4.0:-

$$\frac{\delta_{0.5}}{J/\rho U_1^2} = \text{function of } \frac{x-x_o}{J/\rho U_1^2} \text{ only} \qquad (11.0.1a)$$

and

$$U_o/U_1 = \text{function of } \frac{x-x_o}{J/\rho U_1^2} \text{ only} \qquad (11.01bb)$$

where x_o is the apparent shift in the origin of the flow due to the particular nozzle conditions. In order to compare experimental results with equations (11.0.1a and b) in a satisfactory way, it would be necessary to carry out measurements several hundred jet widths downstream of the jet nozzle so that independence of the precise nozzle conditions could be assured and, also, so that an extensive region of overlap of values of U_1/U_o and $\delta_{0.5}/(J/\rho U^2)$ could be obtained for different values of U_1/U_J. Unfortunately, the present experimental work was limited to a value of x/h=70* and, as we have discussed earlier, independence of the jet nozzle conditions was probably only properly obtained in the relatively restricted range from x/h=30-70 for $U_1/U_J \approx 0$ and x/h= 40-70 for $U_1/U_J \approx 0.6$*. Notwithstanding this drawback, it would appear that the present results can be fitted quite well into the form of equations(11.0.1a and b) as shown in figures (81) and (82) which show results of mean velocity traverses for values of U_1/U_J= 0.16, 0.31, 0.5 and 0.6 plotted in the form suggested above.

---

*Unfortunately, the importance of being able to make measurements at really large distances from the jet nozzle was not fully appreciated when the apparatus was designed.

The apparent origin of the flow, x_o/h, was obtained simply by shifting the experimental data along the $(x-x_o)/(J/\rho U_1^2)$ axis until a reasonably smooth curve was obtained from all the data.

We are now in a position to compare the simple theories developed in section 4.0 with the experimental results for the development of a plane jet. It is however necessary to assign values to the constants involved in the various theories. The values of the integrals $I_n = \int_{-\infty}^{\infty} f^n d\eta$ for n=1, 2 and 3 and $I' = \int_{-\infty}^{\infty} (f')^2 d\eta$ were obtained from the measured mean velocity profiles and the values are given in table I. The eddy Reynolds number of the self-preserving jet in a stationary atmosphere can be obtained from the expression - see section 4.1 :-

$$\frac{\delta_{0.5}}{x} = \frac{4I'}{I_3} \frac{1}{R_T} \qquad (11.0.2)$$

From the results of previous investigators, it was found that $\delta_{0.5}/x \simeq 0.1$. However, in the present experiments with $U_1/U_J = 0.07$, it was found that the shear stress distribution was consistent with a rate of spread of the jet with $U_1 = 0$ of $\delta_{0.5}/x = 0.109$ and this value is used in the calculations to ensure agreement of the experimental and theoretical results for small values of U_1/U_J. From equation (11.0.2), we obtain:-

$$R_{T_J} = 33.4$$

With this last constant, the development of the plane jet can be calculated by both the constant eddy Reynolds number theory and Abramovich's theory. For the variable eddy Reynolds number theory, it was assumed that:-

$$\frac{R_{T_w}}{R_T} = 1 + \chi\left[\left(\frac{\delta_{0.5}}{M}\frac{dM}{dx}\right)\left(\frac{f}{f'}\right)_t - \frac{d\delta_{0.5}}{dx}\eta_t\right] \qquad (11.0.3)$$

where the constants η_t, $(f/f')_t$ and χ need to be determined.

Now, according to Townsend's measurements in a plane wake, $R_{T_w} = 14.7$. We will consider the case of a jet when $U_1=0$ when it can be shown also that $\frac{\delta_{0.5}}{M}\frac{dM}{dx} = -\frac{1}{2}\frac{d\delta_{0.5}}{dx} = -\frac{0.109}{2}$. The constants $(f/f')_t$ and η_t are evaluated at some typical station in the outer region of the jet, say, $\eta=1.5$ when it is found that $(f/f')_t=-0.345$ and, of course, $\eta_t=1.5$. With these values the constant χ is determined to be 3.87.

The development of the plane jet according to the various theories is compared with the experimental results in figures (81) and (82). Also shown in these figures are the asymptotic forms of the functions in equations (11.0.1a & b) for $U_1 \to 0$, namely:-

$$\frac{\delta_{0.5}}{J/\rho U_1^2} = 0.109\,\frac{x-x_0}{J/\rho U_1^2} \qquad (11.0.4a)$$

$$\left(\frac{U_1}{U_0}\right)^2 = 0.16\,\frac{x-x_0}{J/\rho U_1^2} \qquad (11.0.4b)$$

As we might expect from previous discussions, the variable eddy Reynolds number theory does not agree at all well with the experimental results and quite clearly the assumptions involved in the theory are invalid. The most satisfactory agreement obtained is with the theory of Abramovich but, as discussed in section 4.2, this theory has the wrong asymptotic behaviour as $U_0/U_1 \to 0$. It is therefore clear that a satisfactory theory of the plane jet in a moving airstream is still not available. However, it would appear from figure (81) that, for values of $(x-x_0)/(J/\rho U_1^2) \leq 10$, the decay of the jet centre-line velocity can be predicted to an accuracy of about $10^{o/o}$ using the asymptotic relationship for $U_1 \to 0$ given above as equation (11.0.4b). The jet width can be predicted to a similar accuracy by substituting the equation (11.0.4b) into the momentum integral equation from which we obtain:-

$$\frac{\delta_{0.5}}{J/\rho U_1^2} = \frac{1}{\left(\frac{U_0}{U_1}\right)^2 I_2 + \left(\frac{U_0}{U_1}\right) I_1} = 0.109\,\frac{x-x_0}{J/\rho U_1^2}\,\frac{1}{1+0.551\sqrt{\frac{x-x_0}{J/\rho U_1^2}}} \qquad (11.0.5)$$

It has not been possible to decide the reason for the failure of the variable eddy Reynolds number theory with certainty. However, two explanations seem possible. It was mentioned in section 4.1 that the variable eddy Reynolds number theory required that (a) the period of the large eddies was much smaller than the time necessary for an appreciable change in the strain rate ratio and (b) that the small eddies adjusted sufficiently rapidly to ensure that large eddy equilibrium was maintained. The period of the large eddy according to Townsend is of the order of $3/(\partial U/\partial y)_{may} = 3t_s$ where t_s is the time for a substantial rate of strain by the mean flow and it is known - section 8.8.- that this is of a similar order to the time for appreciable development of the flow. It is likely therefore that the large eddies at any given station are dependent on the strain rate ratio some way upstream rather than on the local value. By similar time scale arguments, it is also likely that the energy equilibrium between the large and smaller eddies is never set up in a flow with a continually changing strain rate ratio in the way postulated in Townsend's theory. Although both of these factors would tend to account for the failure of the theory, they may not be solely responsible. There has been some suggestion that the large eddy hypothesis itself may not be correct and, although some mechanism similar to that postulated by Townsend is clearly at work, it is apparent, for example, that the separation of large eddies from shear carrying eddies in the large eddy hypothesis is not very satisfactory. In principle, it might be possible to make some allowance in a theory for the above factors but it would be introducing too may variable and indeterminate parameters at this stage to make it a worthwhile exercise. Further experiments on the structure of the shear carrying eddies are required before further theoretical models can be proposed with any confidence.

12.0 Conclusions.

In the Introduction, the importance of self-preserving flows was discussed and a considerable part of the present work was concerned with investigating the structure of just one of these, namely the self-preserving plane jet. A comparison between the distributions of the turbulent intensities and the turbulent shear stress in a plane jet and a plane wake showed that these distributions were very similar for the two flows and this finding provides some support for the idea of a universally similar structure for all turbulent free flow. The major differences between the two flows, which were partly anticipated by Townsend, were that the large eddies in the plane jet were somewhat smaller than those found in the plane wake and, also, the turbulent energy balance for the plane jet showed a greater contribution from the production and dissipation terms than in the plane wake case. The structure of the small scale turbulence responsible for the viscous dissipation appeared to be constant over the central portion of the jet width and all the indications were that it was closely isotropic. In fact, some evidence was found suggesting the existence of an inertial subrange. As far as the shear carrying eddies were concerned, it appeared that these were among the largest eddies in the flow and responsible, in part at least, for the intermittency phenomenon. This conclusion is contrary to Townsend's large eddy hypothesis and is a matter that deserves additional attention. It was also found that the assumption of a nearly uniform level of turbulent energy across the jet was not a particularly good assumption since it proved possible to represent the distribution of the $\sqrt{\overline{u^2}}$ intensity quite well by the Prandtl Mixing Length hypothesis thus showing a strong correlation between the turbulent energy level and the mean velocity gradient. Finally, the investigation of the

irrotational velocity fluctuations outside the jet bore out the conclusions of the theories of Phillips (1955) and Stewart (1956) and the anomolies between these theories and the experimental work of Corrsin (1943) on a circular jet can now be regarded as definitely due to the instrumentation only.

The remaining work in this thesis was concerned with the plane jet exhausting into a moving airstream whose velocity was not small compared to the jet velocity. The structure of this flow was expected to show some sort of approach to a wake flow structure and although some very slight evidence of this was found, the change to a wake flow structure clearly takes place at a very slow rate. The idea, for instance, that Townsend's large eddy hypothesis could be used for predicting the development of the jet proved inadequate and it is suggested that this may be due to the considerable time scales involved in establishing the equilibrium postulated in the large eddy hypothesis and also, possibly, to some inadequacy in the large eddy hypothesis itself.

Scope for future work exists both in the self-preserving plane jet problem and also in the problem of the plane jet in a moving airsteaam. In the former case, further work is required on the large eddy structure of the flow and some interesting experiments could be conducted on the intermittency phenomenon. In this context, a fuller investigation of the output signals from an intermittency meter would be of interest. Also, of course, more detailed correlation measurements are required. In the case of a jet in a moving airstream it is important that future work be carried out on a model in which measurements at distances at least several hundred jet widths downstream of the jet nozzle could be made. This is necessary to ensure independence of the flow of the exact

nozzle conditions and also to permit the approach to a plane wake type of structure to be studied more satisfactorily. This change of flow structure is a problem of great interest because it enables the effect of a minimum number of parameters on the turbulence structure to be studied and real progress in understanding the controlling factors in a turbulent flow might well result.

SYMBOLS.

Only symbols that are used frequently are defined below. Other symbols used only once or twice should be adequately defined in the text.

x, y	Cartesian co-ordinates for two-dimensional flows with the x and y-axes in the direction of and normal to the free-stream respectively
U, V	x and y-components of the mean velocity respectively.
u, v	x and y-components of the turbulent velocity respectively.
w	Component of the turbulent velocity normal to the xy plane.
U_1	Free-stream velocity.
U_J	Velocity of jet at nozzle.
U_o	Reference velocity of shear layer. In free turbulent flows, it is the difference in the mean velocity between the centre of the flow and the free-stream.
M	U_o/U_1.
U_M	Average mean velocity across the jet $\approx U_1 + 0.5U_o$.
P	True static pressure (mean value).
p	Unsteady component of the static pressure.
P_1	Free-stream static pressure.
P_S	Static pressure measured with a static tube,
P_P	Total head measured with a pitot tube.
ΔP_S	Difference in measured static pressure between a point in the free turbulent flow and the free-stream i.e. $P_S - P_{S_1}$
ρ	Fluid density.
μ	Fluid viscosity.
ν	Fluid kinematic viscosity.
h	(a) Plane jet nozzle width. (b) Two-dimensional channel width - section 6.4.

d	(a) In plane wake flow, it is the cylinder diameter.
	(b) In axi-symmetric jet flow, it is the jet nozzle diameter
	(c) In section 6.4, it is the static tube diameter,
	(d) In section 6.1, it is the hot wire anemometer diameter.
a	Radius of pipe in section 6.4.
J	Excess momentum flux per unit span for the plane jet.
C_J	Jet momentum coefficient, $J/\rho U_1^2$.
R_h	Jet Reynolds number = $U_J h/\nu$.
R_d	Hot wire anemometer Reynolds number = Ud/ν .
R_λ	Micro-scale Reynolds number = $\sqrt{\overline{u^2}}\lambda/\nu$.
δ	Reference length for the width of the shear layer.
$\delta_{0.5}$	y-ordinate in shear flows at which $U = U_1 + 0.5\ U_o$.
η	y/δ or $y/\delta_{0.5}$.
τ	Shear stress.
ε	(a) Eddy viscosity or
	(b) Viscous dissipation term in the turbulent energy balance in section 8.6.
ν_T	Kinematic eddy viscosity, ε/ρ
R_T	Eddy Reynolds number = $U_o\delta/\nu_T$.
R_{T_J}	Eddy Reynolds number in a self-preserving plane jet.
R_{T_W}	Eddy Reynolds number in a self-preserving plane wkae.
$f(\eta)$	Mean velocity profile function = $(U - U_1)/U_o$.
$g_n(\eta)$	n = 1, 2 and 3 are $\overline{u^2}/U_o^2$, $\overline{v^2}/U_o^2$ and $\overline{w^2}/U_o^2$ respectively.
$g_{12}(\eta)$	$\overline{uv}/U_o^2$
$\overline{q^2}$	Total turbulent energy = $(\overline{u^2} + \overline{v^2} + \overline{w^2})$
q	A characteristic turbulent velocity not requiring precise definition
I_n	$\int_{-\infty}^{\infty} f^n d\eta$; n = 1, 2, 3.

I' $\int_{-\infty}^{\infty}(f')^2 d\eta$.

n (a) Frequency of turbulence.

(b) Factor in correction to static tube reading due to turbulence - section 6.4.

(c) A constant in the heat transfer law of Collis and Williams (1959) - section 6.1.

k Wavenumber = $2\pi n/U$.

R_x Longitudinal correlation coefficient = $R_{11}(r,0,0)$.

R_y Lateral correlation coefficient = $R_{11}(0,r,0)$.

R_{uv} Shear stress correlation coefficient = $\overline{uv}/\sqrt{u^2}\sqrt{v^2}$.

L (a) The Mixing Length in Prandtl's theory of turbulence.

(b) A characteristic length scale of the turbulence not requiring precise definition.

L_x Longitudinal integral scale = $\int_0^{\infty} R_x dx$.

L_y Lateral integral scale = $\int_0^{\infty} R_y dy$.

λ Micro-scale of turbulence.

$F(k)$ $d(\overline{u^2})/\overline{u^2}$ where $d(\overline{u^2})$ is the contribution to $\overline{u^2}$ from wavenumbers between k and k+dk.

$G(k)$ $d(\overline{uv})/\overline{uv}$ where $d(\overline{uv})$ is the contribution to $\overline{uv}$ from wavenumbers between k and k+dk.

γ Intermittency factor.

α,β Temperature coefficients of resistance.

T_∞ Ambient temperature (absolute).

T_0 273°A.

T_H Absolute temperature of the hot wire anemometer.

T_m $(T_H + T_\infty)/2$.

R_∞ Resistance of hot wire anemometer at T_∞ °.

R_H Resistance of the hot wire anemometer at T_H^o.

R_o Resistance of hot wire anemometer at T_o^o.

Nu Nusself number for the hot wire anemometer.

ψ Angle between the hot wire anemometer and the free-stream direction.

i Current through the wire.

i_o Current through the wire with $U_1=0$ according to equation (6.1.7)

$C_{P_{mean}}$ Pressure coefficient in the static tube correction.

REFERENCES.

ABRAMOVICH, G.N. 1958. The turbulent jet in a moving fluid. R.A.E. Translation 778.

BATCHELOR, G.K. 1950. Note on free turbulent flows with special reference to the two-dimensional wake. J.Aero.Sci. 17

BATCHELOR, G.K. 1956. The Theory of Homogeneous Turbulence. Cambridge University Press.

BIRT, D.R. 1960. Self-balancing push-pull circuits.Wireless World, May 1960.

BRADSHAW, P. 1961. An introduction to turbulence measurements with hot wire anemometers. Part 1. NPL Aero. Rep. 427.

BRADSHAW, P. & GEE, M.T. 1962. Turbulent wall jets with and without an external stream. A.R.C. R.&M. 3252.

BRADSHAW, P., FERRISS, D.H., & JOHNSON, R.F. 1963. Turbulence in the noise producing region of a circular jet. NPL Aero. Rep.1054.

CLAUSER, F.H. 1954. Turbulent boundary layers in adverse pressure gradients. J. Aero. Sci. 21.

CLAUSER, F.H. 1956. The turbulent boundary layer. Advances in Appl. Mech. Vol.IV.

COLLIS, D.C. & WILLIAMS, M.J. 1959. Two-dimensional convection from heated wires at low Reynolds numbers. J.Fluid.Mech. Vol.6.Pt.3

COOPER, R.D. & TULIN, M.P. 1955. Turbulence measurements with the hot wire anemometer. NATO Agardograph 12.

CORRSIN, S. 1943. Investigation of the flow in an axially symmetric heated jet. NACA Wartime Rep. W-94.

CORRSIN, S. 1957. Some current problems in turbulent shear flows. Naval Hydrodynamics, Chapt.XV, Publication 515, Nat.Acad.Sci. - Nat. Res.Council.

CORRSIN, S. & KISTLER, A.L. 1954. The free-stream boundaries of turbulent flow. NACA TN 3133.

CORRSIN, S. & UBEROI, M.S. 1951. Spectra and diffusion in a round turbulent jet. NACA Rep. 1040.

DAVIES, P.O.A.L., FISHER, M.J. & BARRAT, M.J. 1963. The characteristics of the turbulence in the mixing region of a round jet. J.Fluid Mech. Vol.15 Pt.3.

ESKINAZI, S. & ERUKA, V. 1962. Turbulence measurements in a two-dimensional rectangular wall jet with longitudinal free-stream. Syracuse University Research Institute Rep. No. ME937 - 6205P.

FAGE, A. 1936. On the static pressure in fully developed turbulent flow. Proc. Roy. Soc. Ser.A. Vol.155.

FORTHMANN, E. 1936. Turbulent jet expansions. NACA TM 789.

GIBSON, M.M. 1963. Spectra of turbulence in a round jet. J.Fluid Mech.Vol.15 Pt.2.

GOLDSTEIN, S. 1936. A note on the measurement of total head and static pressure in a turbulent stream. Proc.Roy.Soc.Ser.A. Vol.155.

GRANT, H.L. 1958. The large eddies of turbulent motion. J.Fluid Mech. Vol.4 Pt.2.

GRANT, H.L., STEWART, R.W. & MOILLIET, A. 1962. Turbulence spectra from a tidal channel. J.Fluid Mech. Vol.12.

HEAD, M.R. 1958. Entrainment in the turbulent boundary layer. ARC FM 2727.

HINZE, J.O. 1959. Turbulence. McGraw Hill Book Co. Inc.

JOHANNESEN, N.H. 1959. Further results on the mixing of free axially symmetrical jets at Mach number 1.4. ARC FM 2817.

KLEBANOFF, P.S. 1954. Characteristics of turbulence in a boundary layer with zero pressure gradient. NACA TN 3178.

LAUFER, J. 1951. Investigation of turbulent flow in a two-dimensional channel. NACA Rep. 1053.

LAUFER, J. 1955. The structure of turbulence in fully developed pipe flow. NACA Rep. 1174.

LAURENCE, J.C. 1956. Intensity, Scale and spectra of turbulence in mixing region of a free subsonic jet. NACA Rep. 1292.

MACZYNSKI, J.F.C. 1962. A round jet in an ambient co-axial stream. J.Fluid Mech. Vol.13 Pt.4.

MALKUS, W.V.R. 1956. Outline of a theory of turbulent shear flow. Vol.1 Pt.5.

MILLER, D.R. & COMINGS, E.W. 1957. Static pressure distribution in the free turbulent jet. J.Fluid Mech. Vol.3.

MILLER, D.R. & COMINGS, E.W. 1960. Force-momentum fields in a dual jet flow. J.Fluid Mech. Vol.7.

NAKAGUCHI, H. 1961. Jet along a curved wall. Engineering Faculty, Tokyo University. T.Morijan Memorial Seminar for Aerodynamics Res. Memo.4.

NEWMAN, B.G. & LEARY, B.G. 1950. The measurement of the Reynolds stresses in a circular pipe as a means of testing a hot wire anemometer. Dept. of Supply, Aero Res. Lab., Rep.A72.

PATEL, R.P. & NEWMAN, B.G. 1961. Self-preserving, two-dimensional turbulent jets and wall jets in a moving airstream. Mech.Eng.Res.Lab. Aerodynamics Section Rep. No. Ae.5 (McGill University).

PATTERSON, G.N. 1937. Note on the design of corners in duct systems. R & M 1773.

PHILLIPS, O. 1955. The irrotational motion outside a free turbulent boundary. Proc.Camb.Phil.Soc.51.

RUETNIK, J.R. 1955. The effect of the temperature dependence of King's constant A on the hot wire sensitivity coefficient. J.Ae.Sci.Vol.22.

RUETNIK, J.R. & CORRSIN, S. 1955.Equilibrium turbulent flow in a slightly divergent channel. 50 Jahre Grenzschichtforschung.

SCHLICHTING, H. 1955. Boundary Layer Theory. Pergammon Press.

SHIH-I-PAI. 1955. Viscous flow theory II - Turbulent flow. D.Van Nostrand Co.

STEWART, R.W. 1956. Irrotational motion associated with free turbulent flows. J.Fluid Mech. Vol.5.

STRATFORD, B.S. 1959. The prediction of separation of the turbulent boundary layer. J.Fluid Mech. Vol.5.

TAYLOR, G.I. 1936. The spectrum of turbulence. Proc.Roy.Soc.A164.

TOWNSEND, A.A. 1950. The eddy viscosity in turbulent shear flow. Phil. Mag.41.

TOWNSEND, A.A. 1956. The Structure of Turbulent Shear Flow. Cambridge University Press.

TOOMRE, A. 1960. Effect of turbulence on static pressure measurement. ARC FM 2972.

VAN DER HEGGE ZIJNEN, B.G. 1958a. Measurements of the velocity distribution in a plane turbulent jet of air. App.Sci.Res. Vol.A-7.

VAN DER HEGGE ZIJNEN, B.G. 1958b. Measurements of the distribution of heat and matter in a plane turbulent jet of air. App.Sci.Res.Vol.A-7.

VAN DER HEGGE ZIJNEN, B.G. 1958c. Turbulence measurements in a two-dimensional jet. App.Sci.Res.Vol.A-7.

VAN DER HEGGE ZIJNEN, B.G. 1951. On the construction of hot wire anemometers for the investigation of turbulence. App.Sci.Res.Vol.A-2.

TOWNSEND, A.A. 1951. The structure of the turbulent boundary layer. Proc. Camb. Phil. Soc. 47.

WHITEHEAD, L.G., WU, L.Y. & WATERS, M.H.L. 1951. Contracting ducts of finite length. Aero.Quarterly Vol.2.

WEBSTER, C.A.G. 1963. A note on the sensitivity to yaw of a hot wire anemometer. J.Fluid Mech. Vol.13 Pt.2.

APPENDIX I.

Design of a nose profile for a parallel sided aerofoil by a hodograph method.

The flow in which we are interested is similar to that shown in figure (83a). The free-stream velocity is taken to be unity. In the hodograph plane, this flow can be represented by a doublet at a point (1,0) and a semi-circular streamline with a diameter of (1+k), as shown in figure (83b). In the region CD of figure (83a), the flow on the aerofoil surface has to decelerate from a velocity of (1+k) at C to 1.0 at D and, clearly, for a small adverse pressure gradient in this region, k should be as small as possible.

If the doublet at the point (1,0) in the hodograph plane has a strength of +1.0 then another doublet of strength $-(1+k)^2/(1-k)^2$ must be placed at the point $\left(\frac{1+k}{1-k},0\right)$ in order to obtain the semi-circular streamline of diameter (1+k) shown in figure (83b). Now, the complex potential, w, of this doublet pair is :-

$$w = \phi + i\psi = \frac{-1}{q-1} + \frac{(1+k)/(1-k)}{q - \frac{1+k}{1-k}} \qquad (AI.1)$$

where $q = U - iV$. Now,

$$q = \frac{dw}{dz} \qquad (AI.2)$$

where $z = x + iy$. In principal, equations (AI.1) and (AI.2) could be explicitly solved to give q as a function of z only. However, the numerical technique of Whitehead, Wu and Waters (1951) is used to obtain the profile shape because of its simplicity. From equation (AI.2), it is easy to show that co-ordinates of a point along a given streamline are given by:-

$$x = \int \frac{U}{U^2+V^2}\, d\phi \;;\; Y = \int \frac{V}{U^2+V^2}\, d\phi \qquad (AI.3)$$

On AB in figure (83b), q is real only so that we see from equation (AI.1) that $\psi=0$ everywhere on the nose profile. Therefore, on the nose profile:-

$$q^2 + q\left[\frac{-4k - 2(1-k)\phi}{(1-k)^2\phi}\right] + \left[\frac{\phi(1-k^2) + 2k(1+k)}{(1-k)^2\phi}\right] = 0 \qquad \text{(AI.4)}$$

Thus,

$$q = \frac{-\beta \pm \sqrt{\beta^2 - 4\gamma}}{2} \qquad \text{(AI.5)}$$

where $\beta = \dfrac{-2(1-k)\phi - 4k}{(1-k)^2\phi}$; $\gamma = \dfrac{\phi(1-k^2) + 2k(1+k)}{(1-k)^2\phi}$

Now, from equation (AI.1), we have,

(a) for q=0 at B that $\phi = -2k/(1-k)$

(b) for q=1+k at C that $\phi = -2/k$,

so that we may use equation (AI.5) to calculate values of q for a range of values of ϕ between these two limits and then by numerical integration using equations (AI.3), the co-ordinates of the nose profile may be obtained.

For k=0.05 the profile shown in figure (83c) was obtained and this was used on the jet model. Smaller values of k would have led to inordinately long nose sections and the advantage of a smaller adverse pressure gradient would have to be weighed against the disadvantage of a very long nose section.

APPENDIX II

The performance of the compensation network and the differentiating circuit.

(a) The compensation network.

We will consider the circuit shown as the compensation stage in figure (21b). The amplitude gain of this stage is:-

$$A = A' \frac{1 + g_m R_k}{\sqrt{(1+g_m R_k)^2 - 4\omega^2 C^2 R_k^2}} \sqrt{1 + 4\omega^2 C^2 R_k^2} \qquad \text{(A II.1)}$$

where g_m is the mutual conductance of the valves, R_k is the cathode load resistance, C is the coupling capacitance across the cathodes of the two valves and ω is the signal frequency (rads/sec). A' is the uncompensated gain of the stage and is given by:-

$$A' = \frac{g_m R_L}{1 + g_m R_k}$$

where R_L is the anode load resistance. If $(1 + g_m R_k)^2 \gg 4\omega^2 C^2 R_k^2$, equation (A II.1) can be written:-

$$A = A' \sqrt{1 + 4\omega^2 C^2 R_k^2} \qquad \text{(A II.2)}$$

The amplitude output from a hot wire anemometer is of the form:-

$$\text{Output signal} \propto \frac{1}{\sqrt{1 + M^2\omega^2}}$$

where M is the wire time constant. From equation (A II.2), we see that correct compensation for the wire is obtained when $M = 2CR_k$. In the present experiments, correct compensation was required up to about 10 kc/s with time constants of about 0.25–0.5 milli-seconds. With the EF86 valves used in the compensation stage, $(1 + g_m R_k)^2 \approx 2.25 \times 10^4$ and $M^2\omega^2 \approx 0.025\text{–}0.1 \times 10^4$, so that amplitude compensation could be accurately maintained.

Finally, it is to be noted that this RC compensation is only amplitude compensation since phase shifts are introduced by the circuit

given by:-

$$\psi = \tan^{-1} \frac{2\omega C R_k . g_m R_k}{4\omega^2 C^2 R_k^2 + 1 + g_m R_k} \approx \tan^{-1} \frac{M\omega . g_m R_k}{4\omega^2 C^2 R_k^2 + 1 + g_m R_k}$$

whereas the wire causes phase shifts given by:-

$$\psi = \tan^{-1}(M\omega)$$

It can be seen that only if $g_m R_k \gg (1 + M^2\omega^2)$ will the network give correct phase shift compensation. As an example, with $g_m R_k = 150$, the phase shifts will be correct only if $M^2\omega^2 = 0(10)$ say. For M=0.25 milli-seconds (which is a typical value for a 0.0001" dia. wire), correct compensation will be obtained only for a frequency of less than 2000 6/s.

(b) The differentiating circuit.

For the circuit shown in figure (25), the relationship between output and input signals is:-

$$\frac{V_o}{V_i} = j\omega C \frac{g_m R_L}{1 + j\omega C_k R_k + g_m R_k} \cdot \frac{1 + j\omega C_k R_k}{1 + j\omega CR} \qquad \text{(AIII.4)}$$

where V_o and V_i are the output and input signals respectively. Now, the operation on V_i of j is easily shown to be equivalent to differentiating V_i. Thus, in the circuit of figure (25), if $C_k R_k = CR$ and $\omega C_k \ll g_m$, then:-

$$V_o \approx j\omega C \frac{g_m R_L}{1 + g_m R_k} V_i = \frac{g_m R_L}{1 + g_m R_k} C \frac{dV_i}{dt}. \qquad \text{(AIII.5)}$$

which is the required type of relationship.

TABLE I.

η	$\overline{u^2}/U_\bullet^2$	$\overline{v^2}/U_\bullet^2$	$\overline{w^2}/U_\bullet^2$	$\overline{q^2}/U_\bullet^2$	$f(\eta)$
0	0.0437	0.0582	0.0327	0.135	1.0
0.1	0.045	0.0581	0.033	0.136	0.990
0.2	0.0482	0.0578	0.0345	0.141	0.968
0.3	0.0518	0.0573	0.039	0.148	0.931
0.4	0.0555	0.0563	0.0435	0.155	0.885
0.5	0.059	0.055	0.046	0.160	0.829
0.6	0.0616	0.0527	0.0467	0.161	0.766
0.7	0.0638	0.05	0.0455	0.159	0.703
0.8	0.0641	0.0465	0.044	0.155	0.637
0.9	0.062	0.043	0.0405	0.1455	0.569
1.0	0.0583	0.039	0.037	0.134	0.5
1.1	0.0537	0.034	0.0325	0.120	0.43
1.2	0.0477	0.029	0.028	0.105	0.362
1.3	0.0407	0.025	0.0245	0.09	0.296
1.4	0.034	0.02	0.205	0.0745	0.234
1.5	0.026	0.016	0.016	0.058	0.176
1.6	0.0195	0.013	0.0123	0.0448	0.128
1.7	0.014	0.0105	0.0091	0.0336	0.0898
1.8	0.0098	0.008	0.0066	0.0245	0.0605
1.9	0.007	0.0065	0.005	0.0185	0.039
2.0	0.005	0.0055	0.00375	0.01425	0.022

$I_1 = 2.025 \quad I_2 = 1.467 \quad I_3 = 1.197 \quad I' = 1.0914$

$$\int_0^\infty (\overline{q^2}/U_\bullet^2)\, d\eta = 0.213$$

FIG. 1

COMPARISON OF VARIOUS THEORETICAL CURVES FOR THE MEAN VELOCITY PROFILES IN TURBULENT FREE FLOWS.

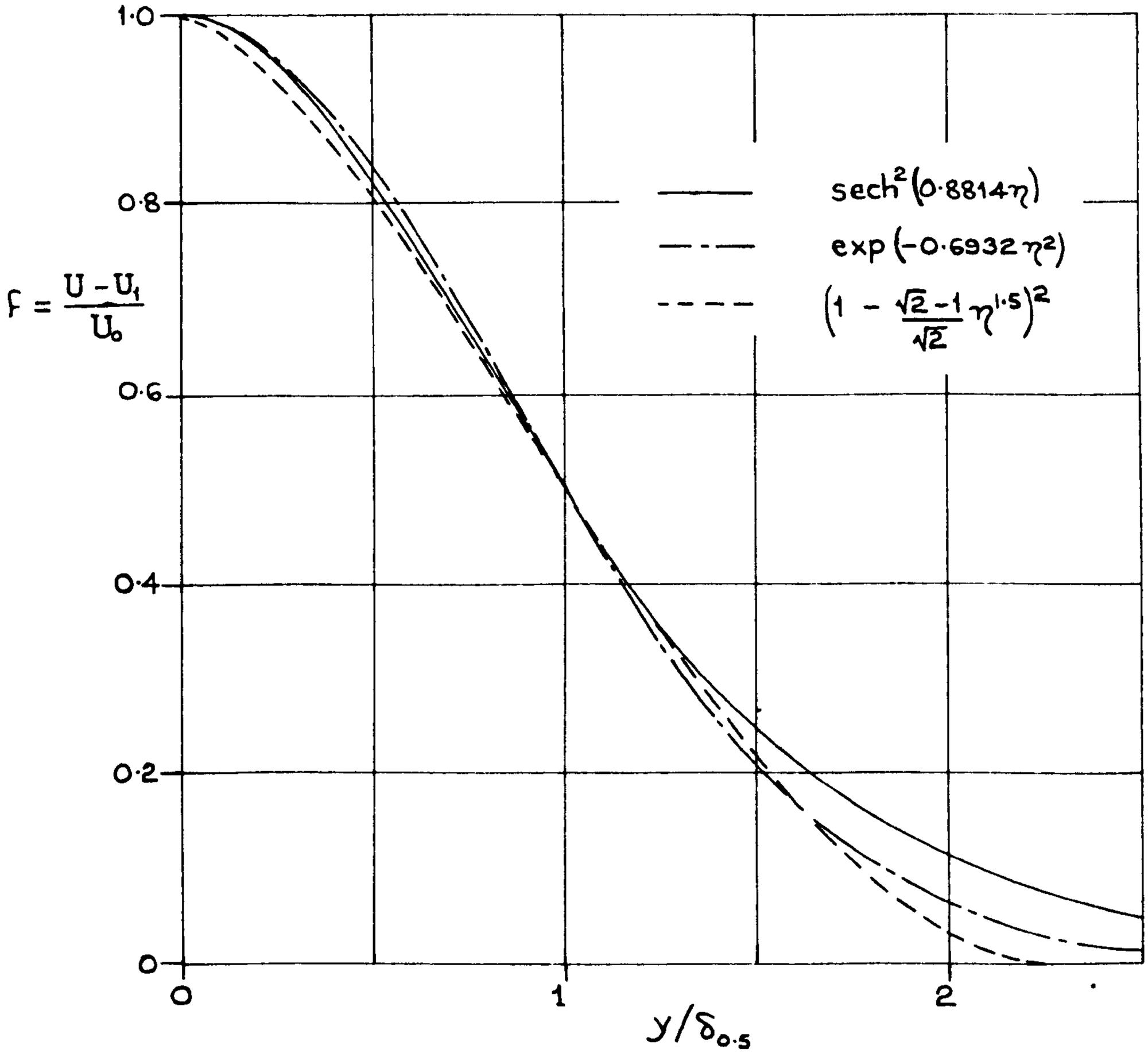

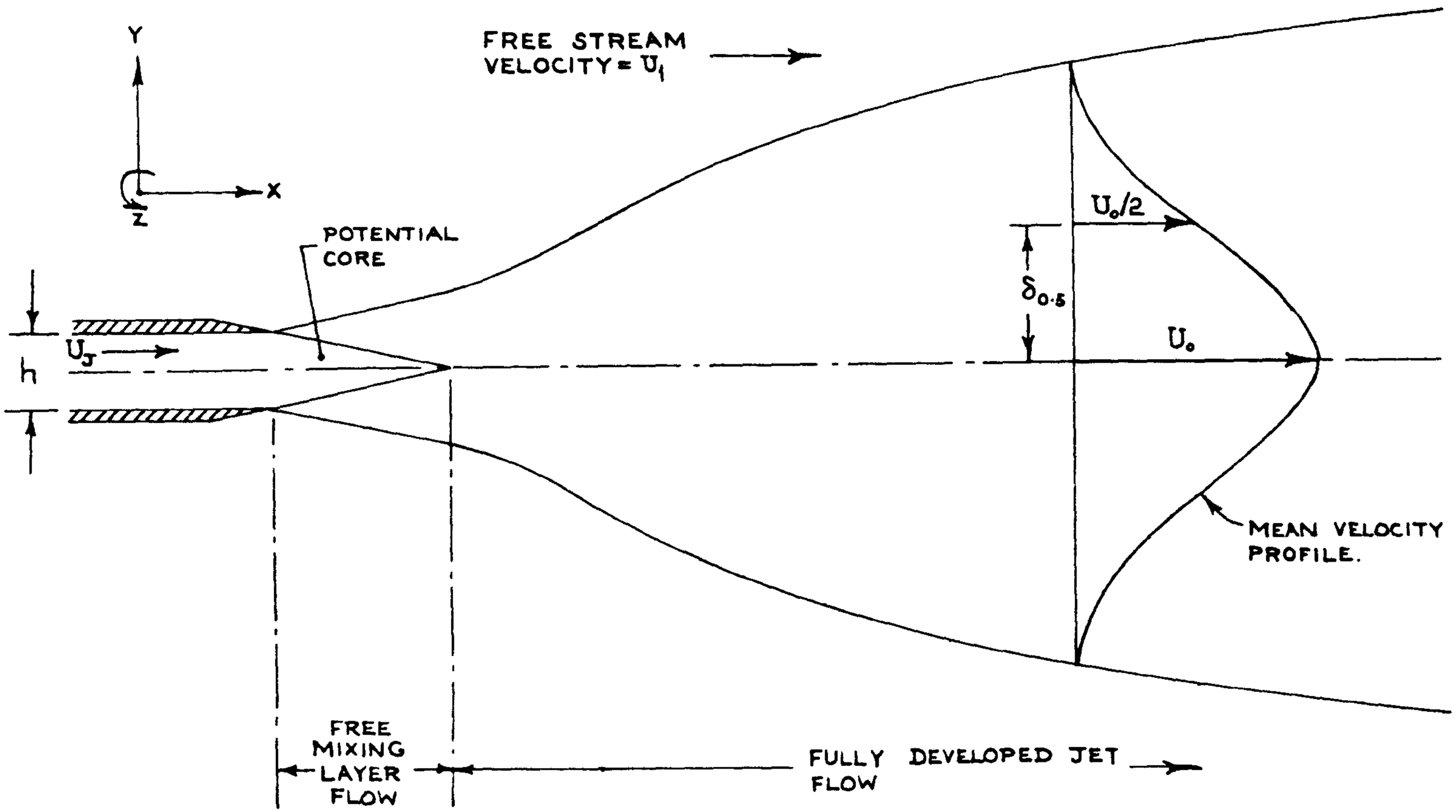

SCHEMATIC DIAGRAM OF FLOW IN A PLANE JET.

FIG. 2

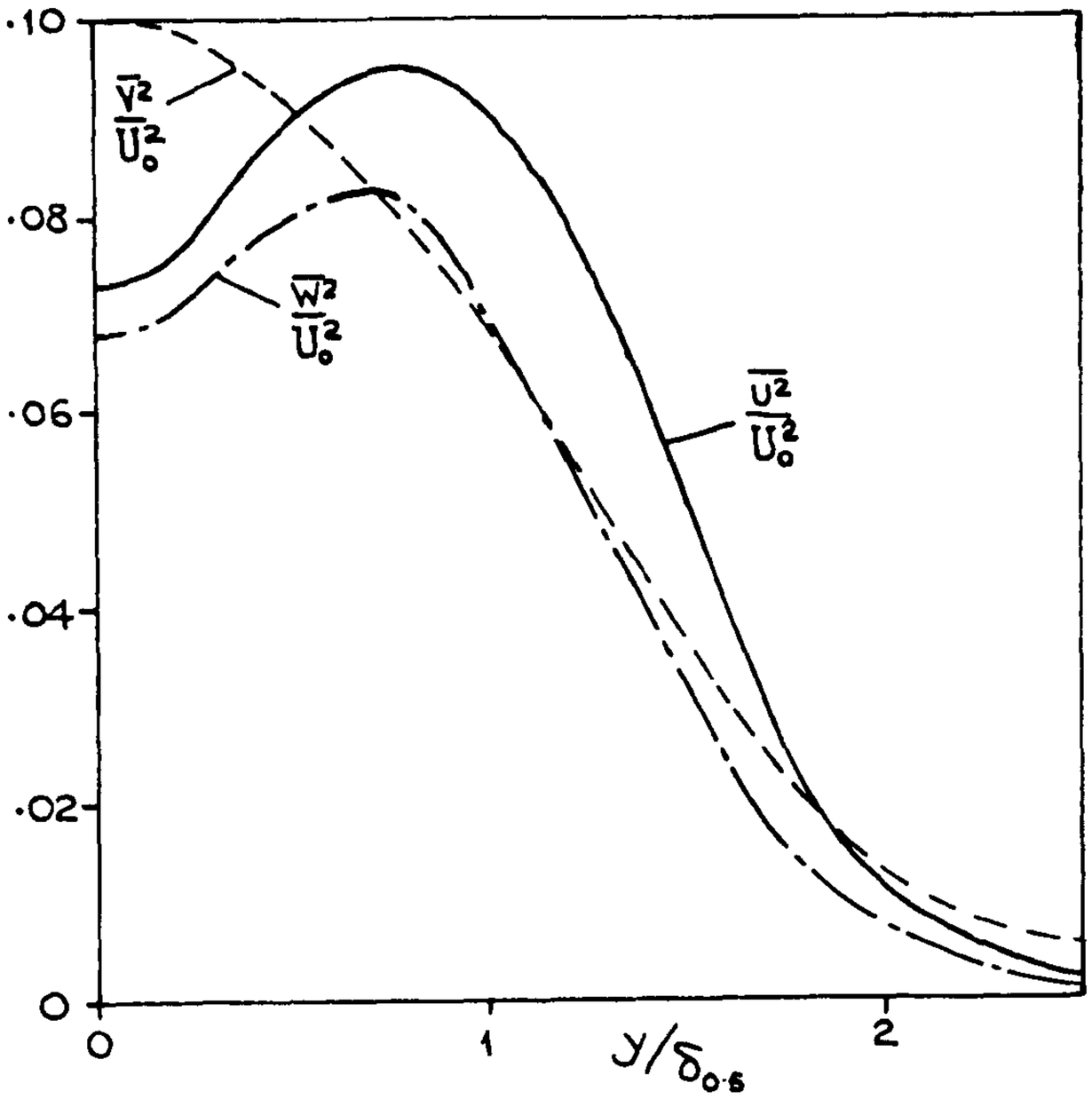

DISTRIBUTION OF TURBULENT INTENSITIES IN A PLANE WAKE (TOWNSEND - 1956)

FIGURE 3

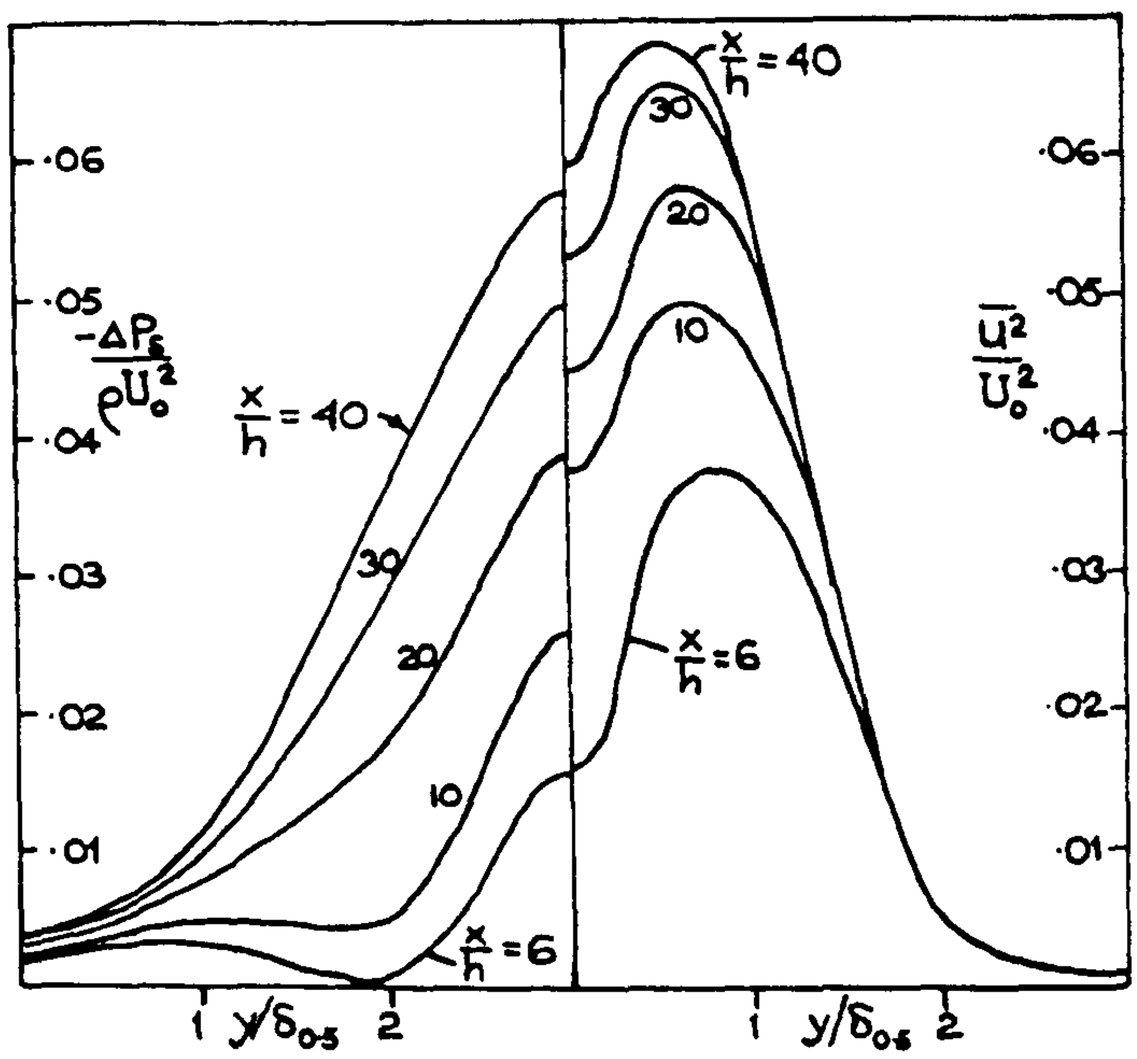

DISTRIBUTION OF $\overline{U^2}$ INTENSITY AND STATIC PRESSURE IN A PLANE JET. (MILLER & COMMINGS - 1957)

FIGURE 4

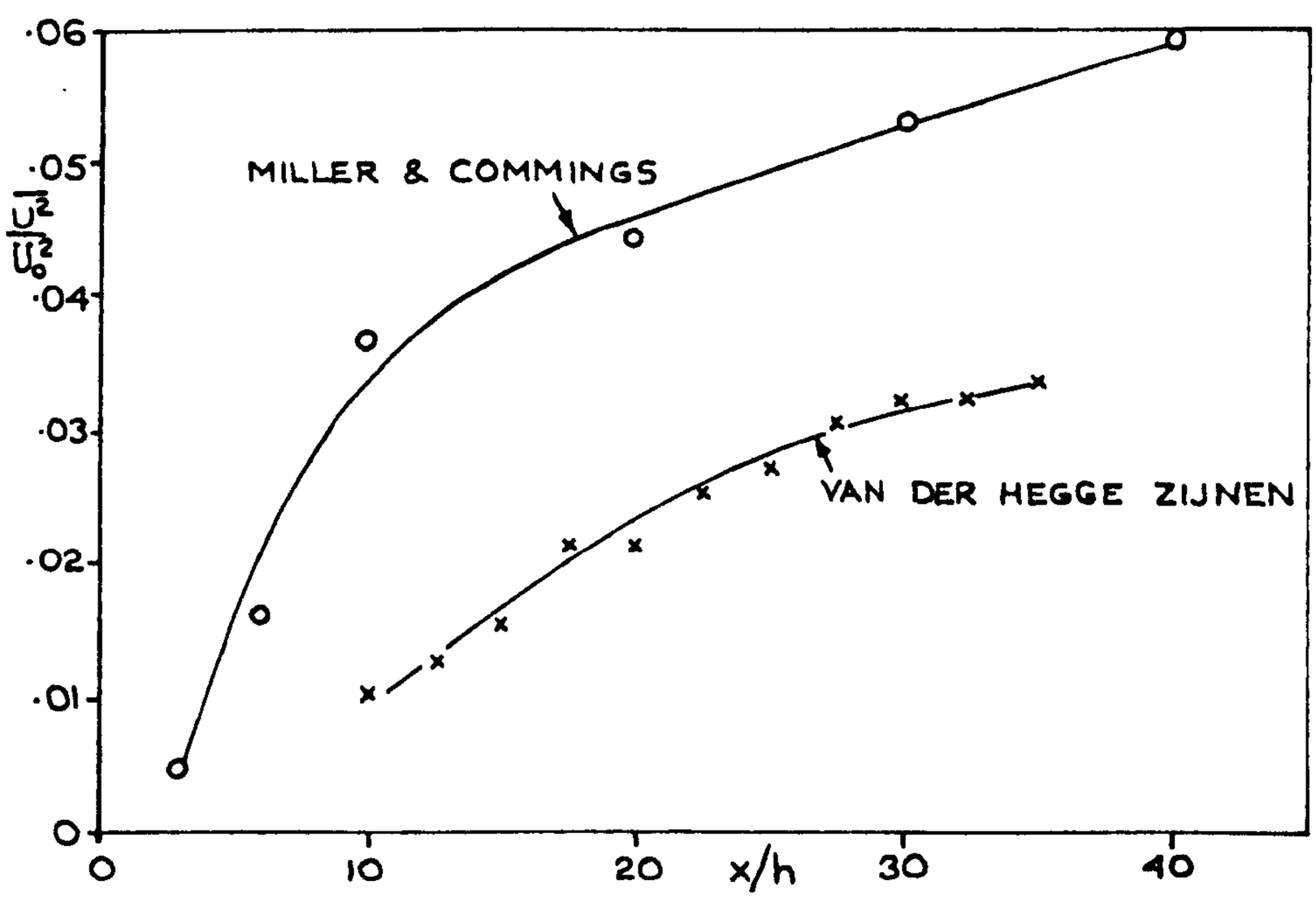

VARIATION OF THE $\overline{u^2}$ INTENSITY ALONG THE CENTRE-LINE OF A PLANE JET.

FIGURE 5

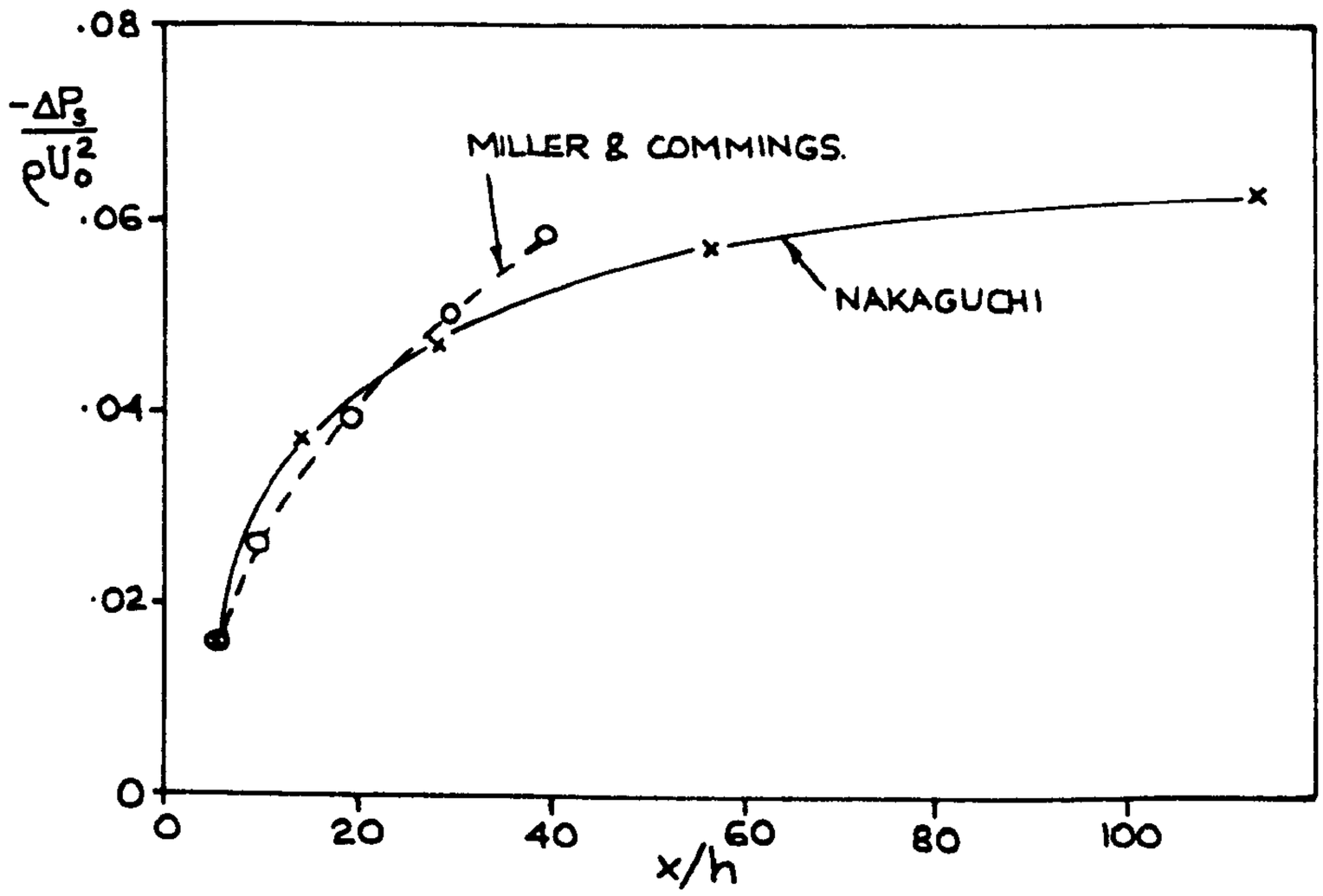

VARIATION OF THE STATIC PRESSURE ALONG THE CENTRE-LINE OF A PLANE JET.

FIGURE 6

THE TEST MODEL.

FIGURE 8 .

TYPICAL SPANWISE DISTRIBUTIONS OF JET EXIT VELOCITY ON THE TEST MODEL.

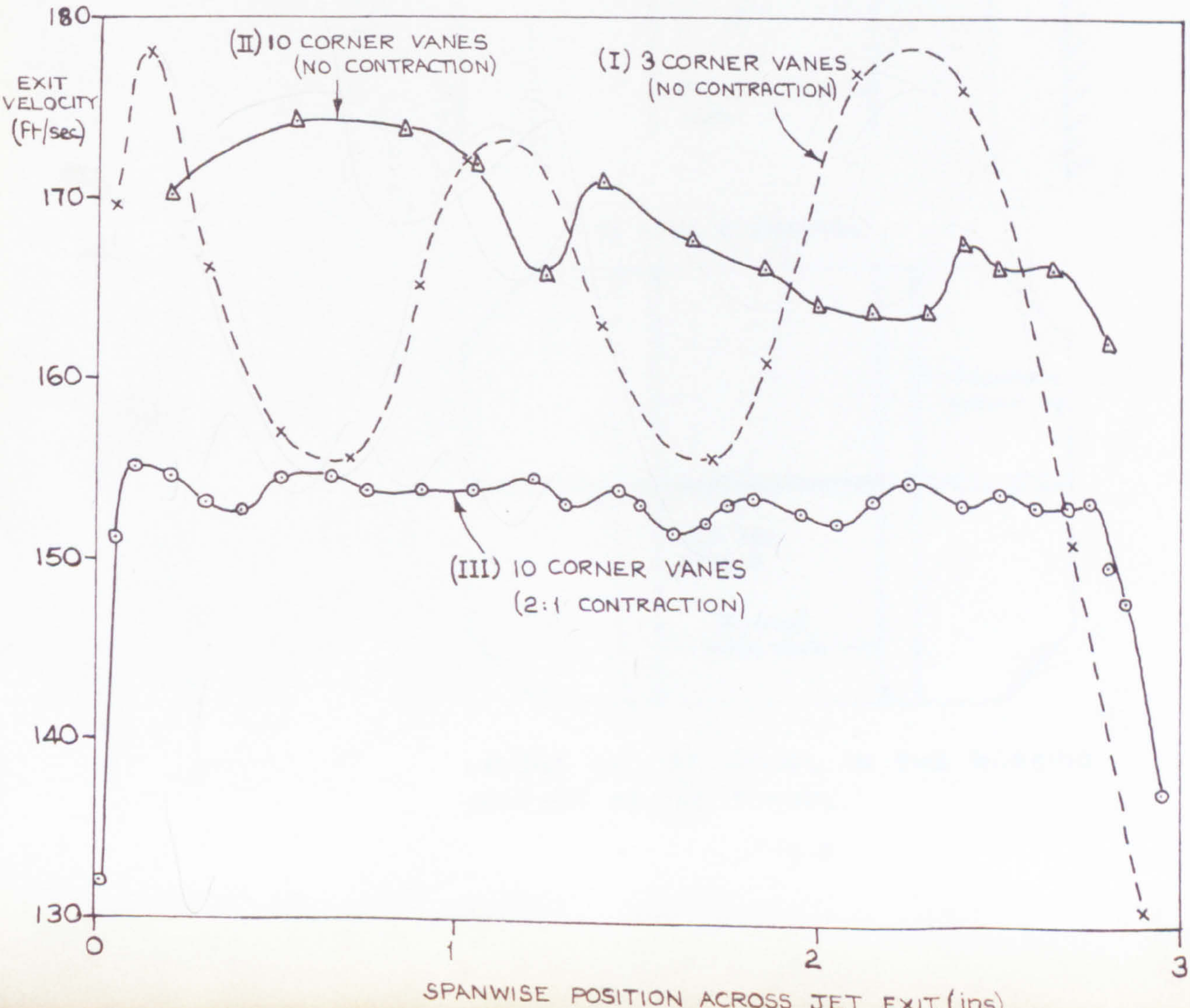

(a) PLAN VIEW WITH TUNNEL CEILING REMOVED.

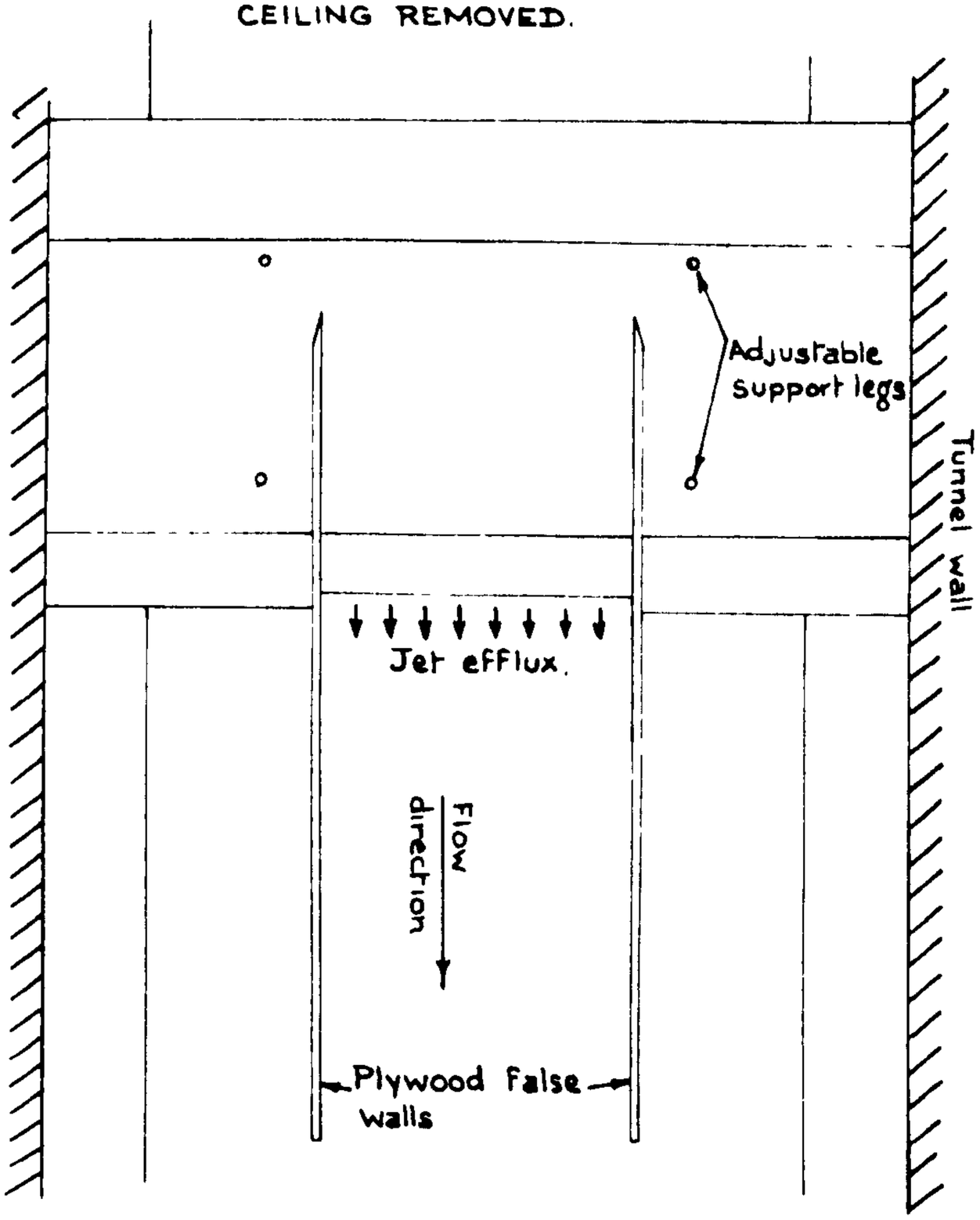

(b) END ELEVATION.

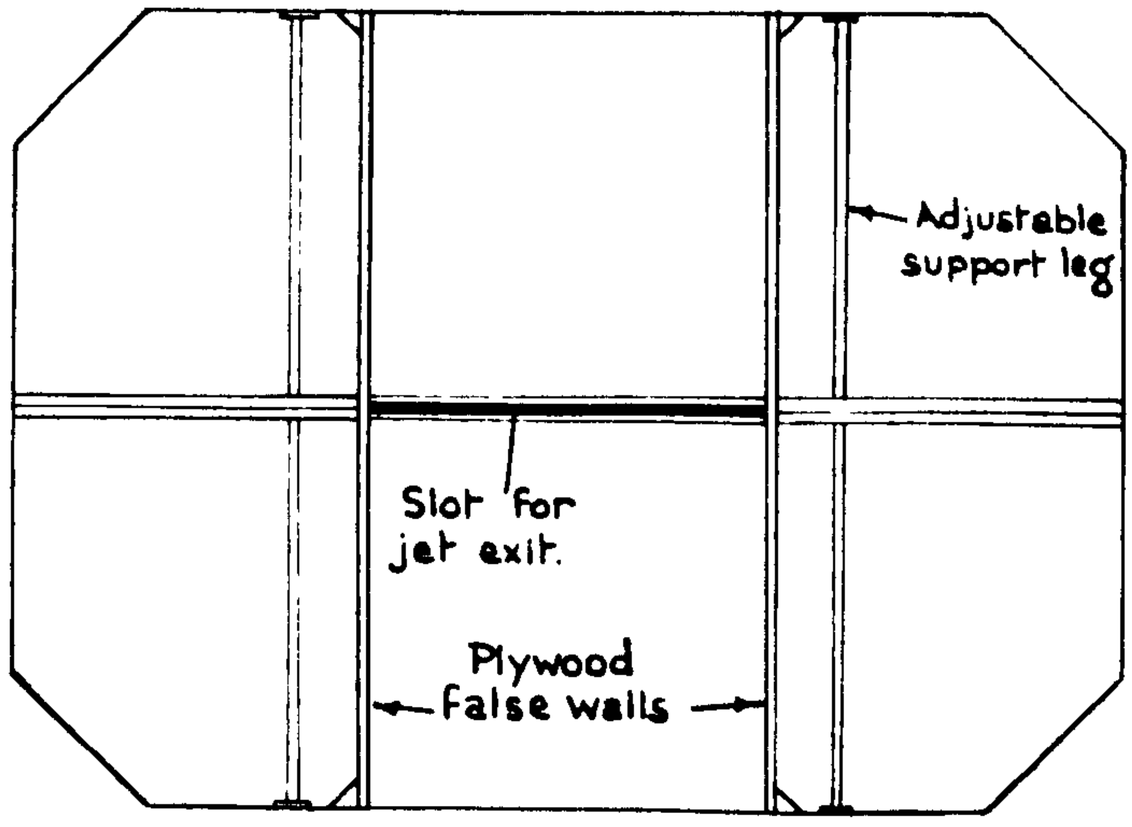

LAYOUT OF JET MODEL IN THE WORKING SECTION OF THE TUNNEL.

FIG. 9

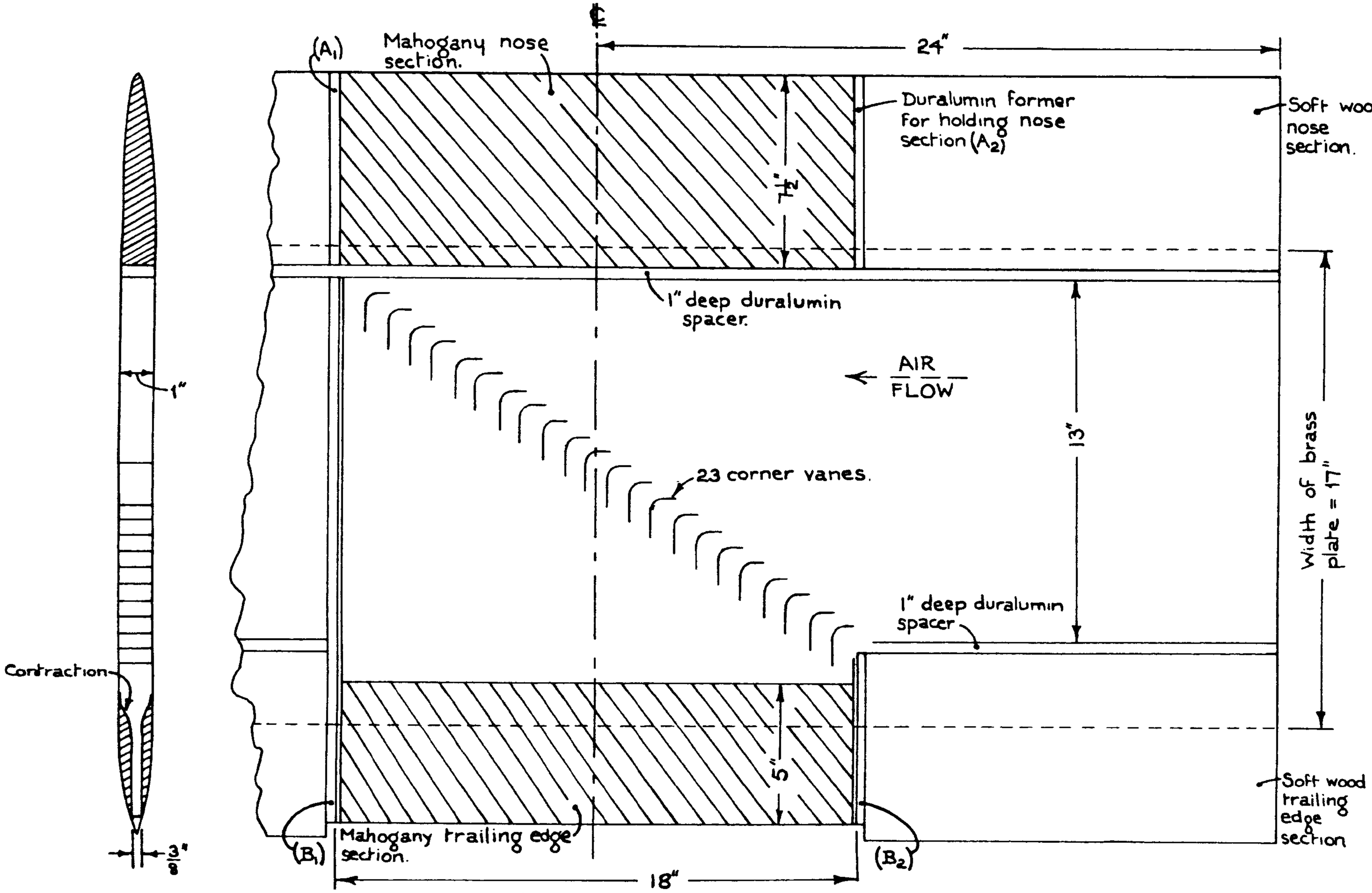

(a) SECTION THRO' CENTRE-LINE.

(b) PLAN VIEW WITH TOP BRASS PLATE REMOVED.

FIG. 10 DETAILS OF JET MODEL.

FIGURE 11.
PHOTOGRAPH OF JET MODEL (TOP PLATE REMOVED).

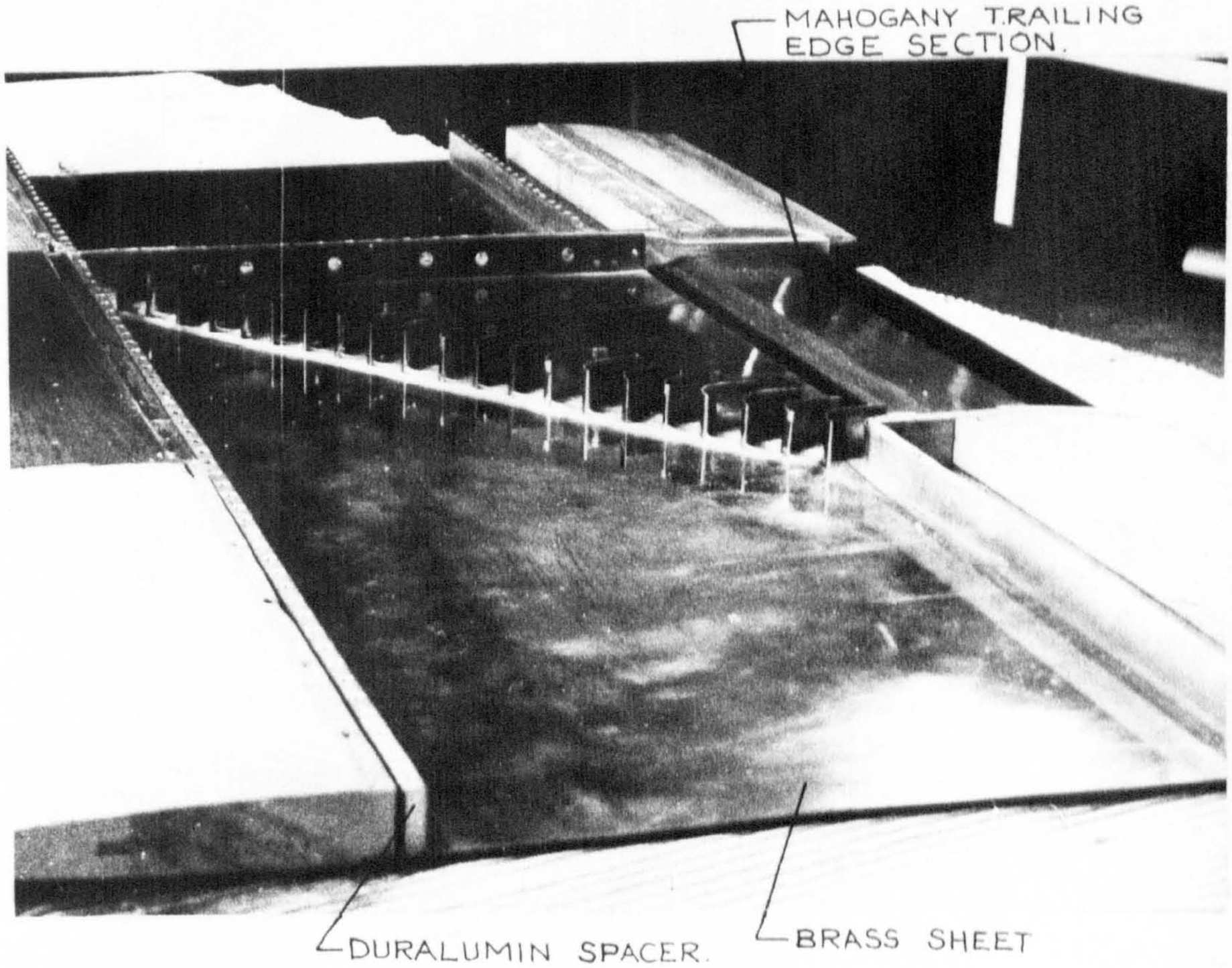

FIGURE 12
CORNER VANES.

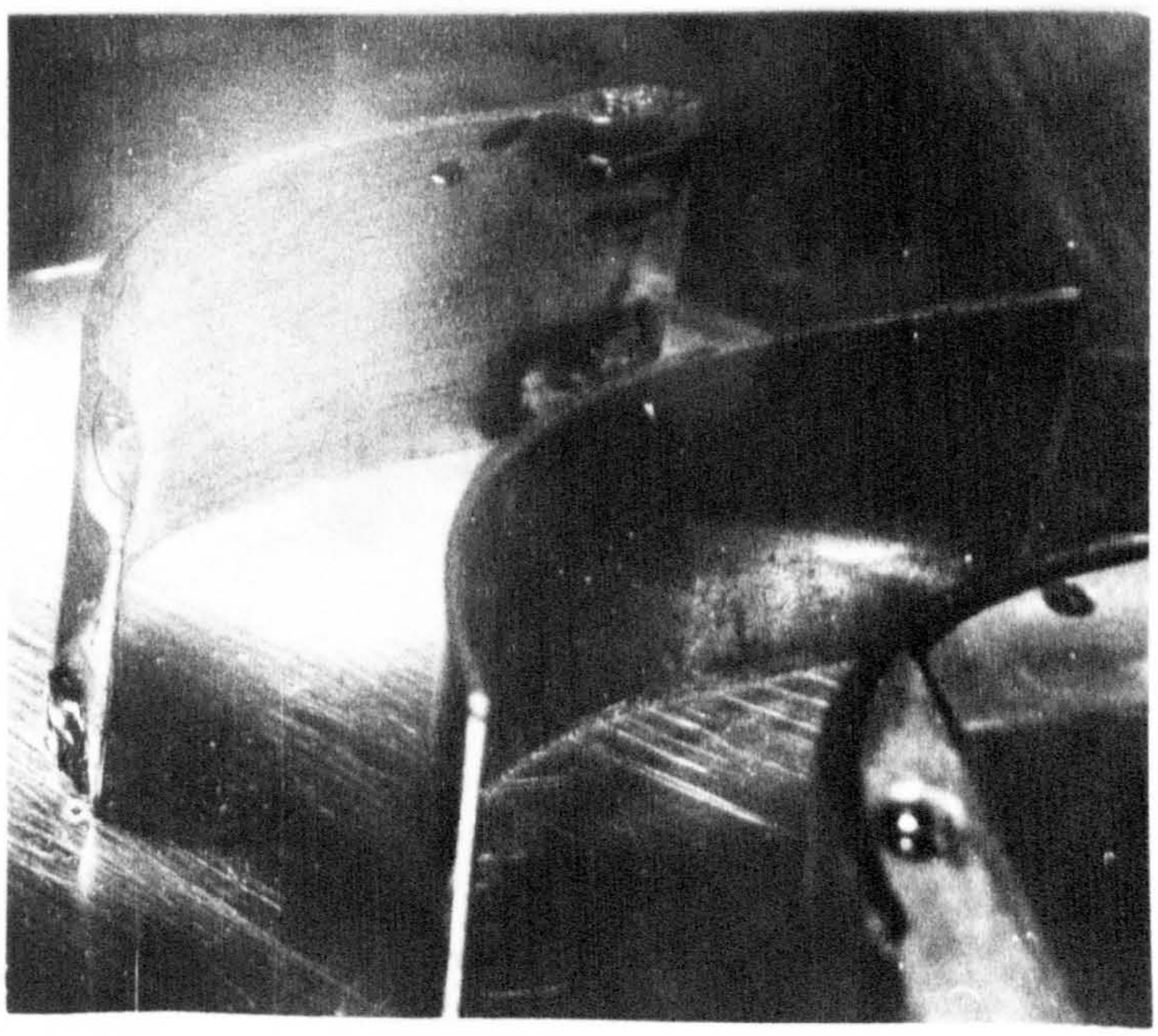

FIG. 13

SPANWISE DISTRIBUTION OF JET WIDTH

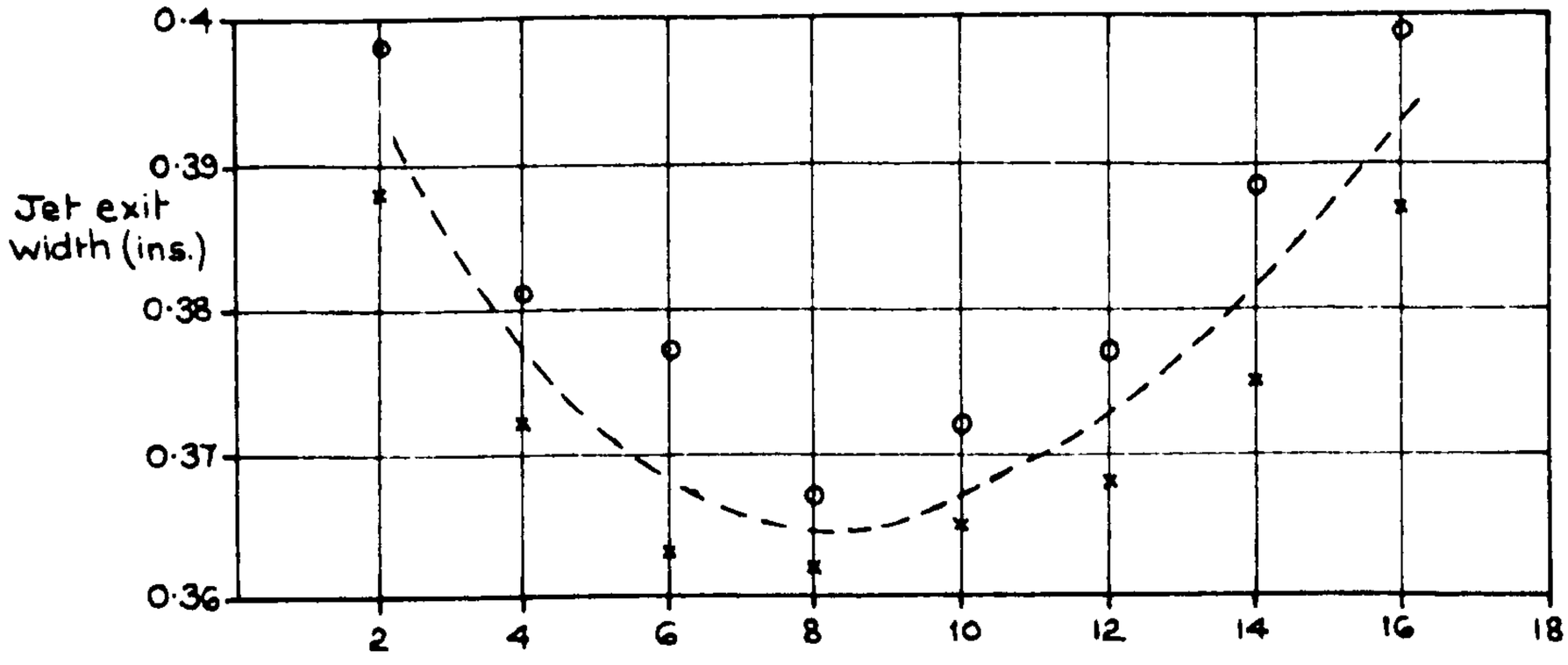

o	Measured with a height gauge.
x	Measured with feeler gauges.

Average thickness over the centre 10" = 0·37
Variation in thickness " " " " ≈ ±2·0%

FIG. 14

SPANWISE DISTRIBUTION OF JET TOTAL HEAD.

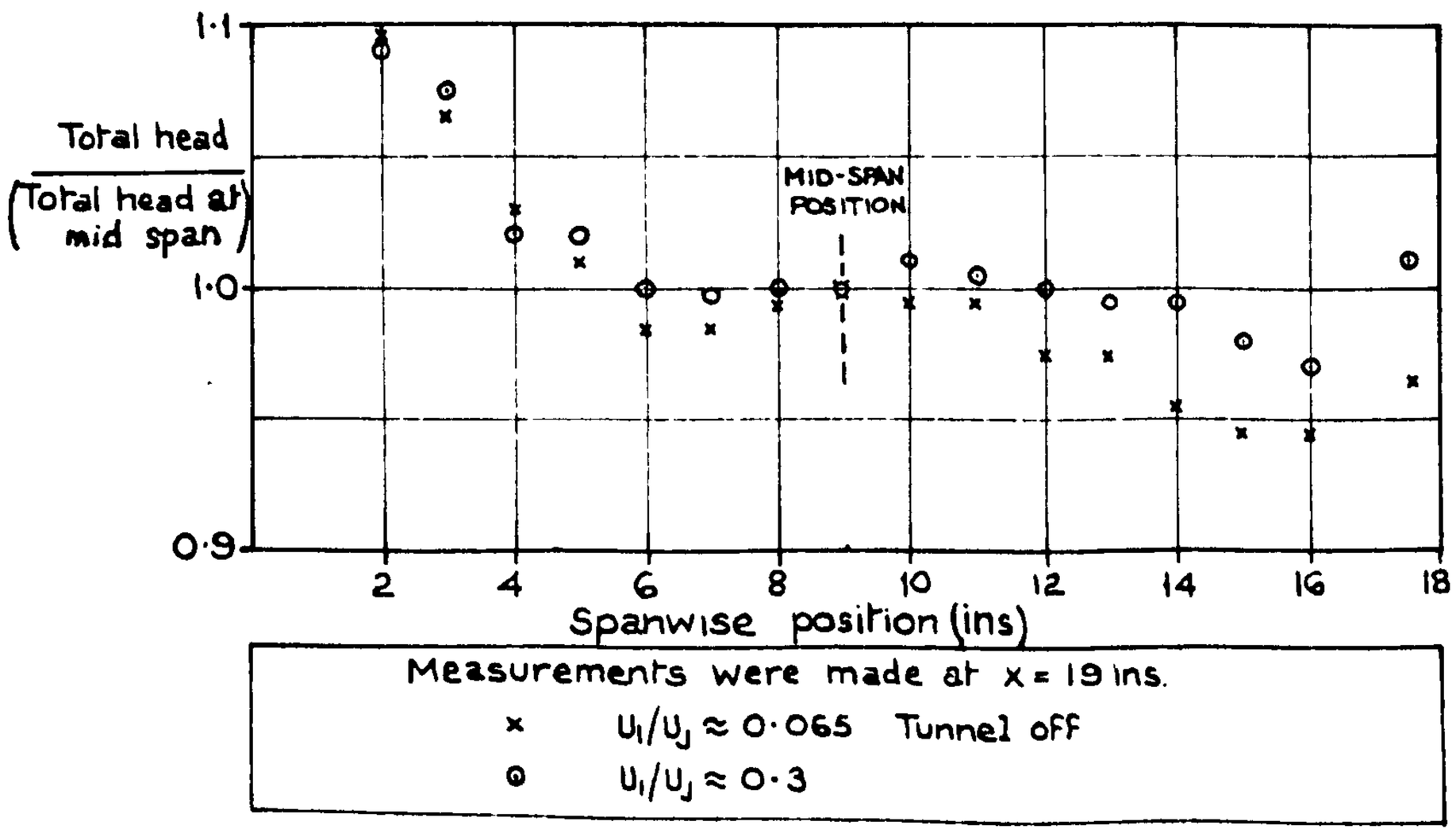

Measurements were made at x = 19 ins.

x	$U_1/U_j \approx 0·065$ Tunnel off
o	$U_1/U_j \approx 0·3$

FIG. 15

CENTRIFUGAL FAN & EXTERNAL DUCTING FOR JET MODEL.

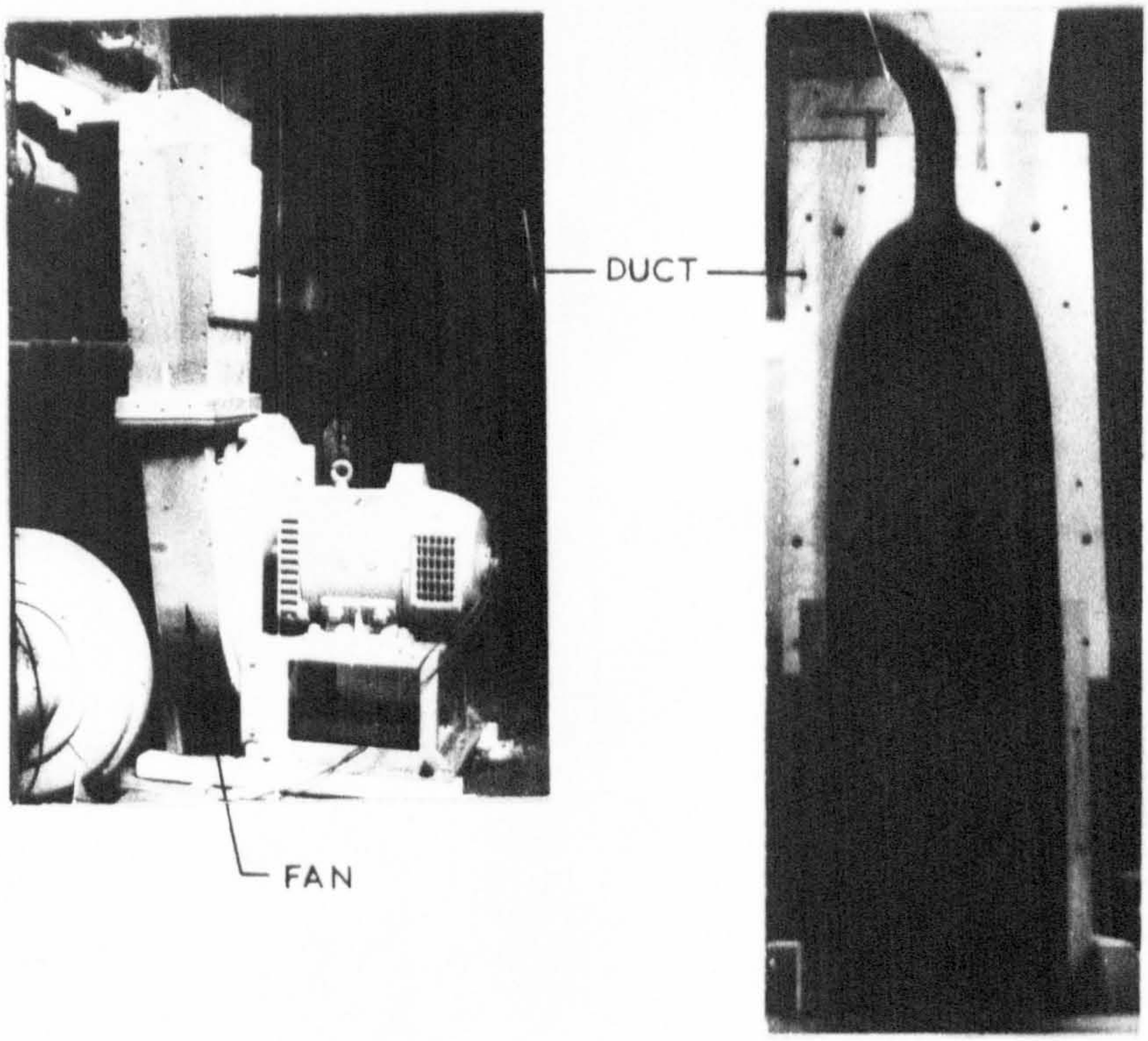

FIG. 16

DETAILS OF MODEL IN THE TUNNEL WORKING SECTION.

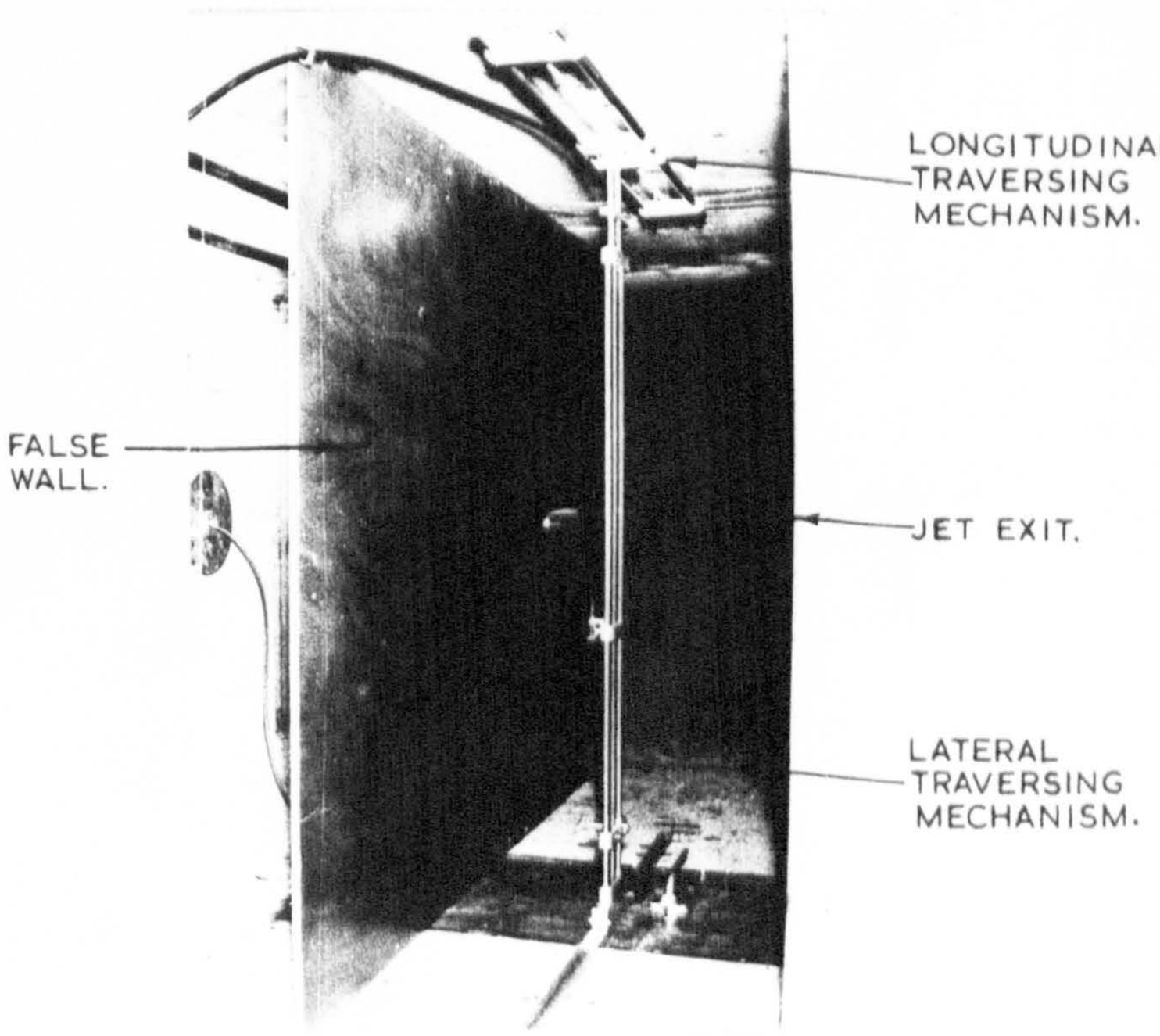

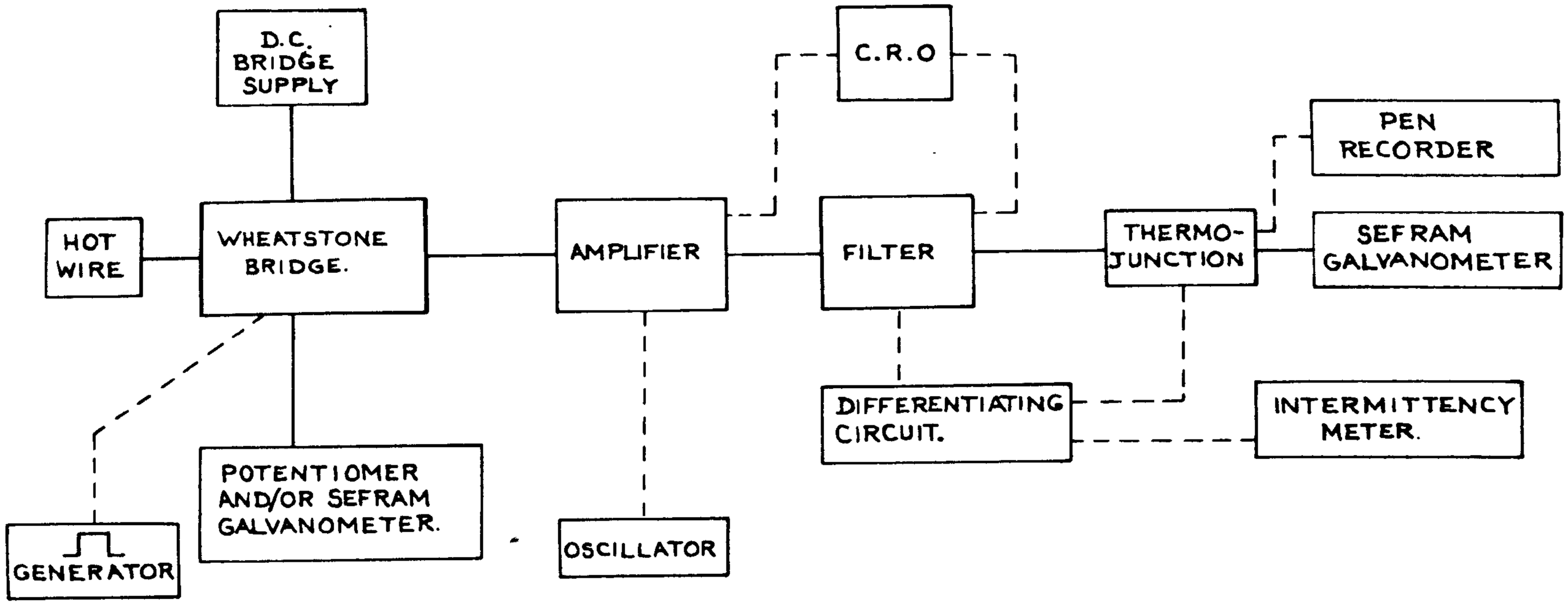

BLOCK DIAGRAM OF HOT WIRE ANEMOMETER EQUIPMENT.

FIG. 17

FIGURE 18

THE HOT WIRE ANEMOMETER EQUIPMENT.

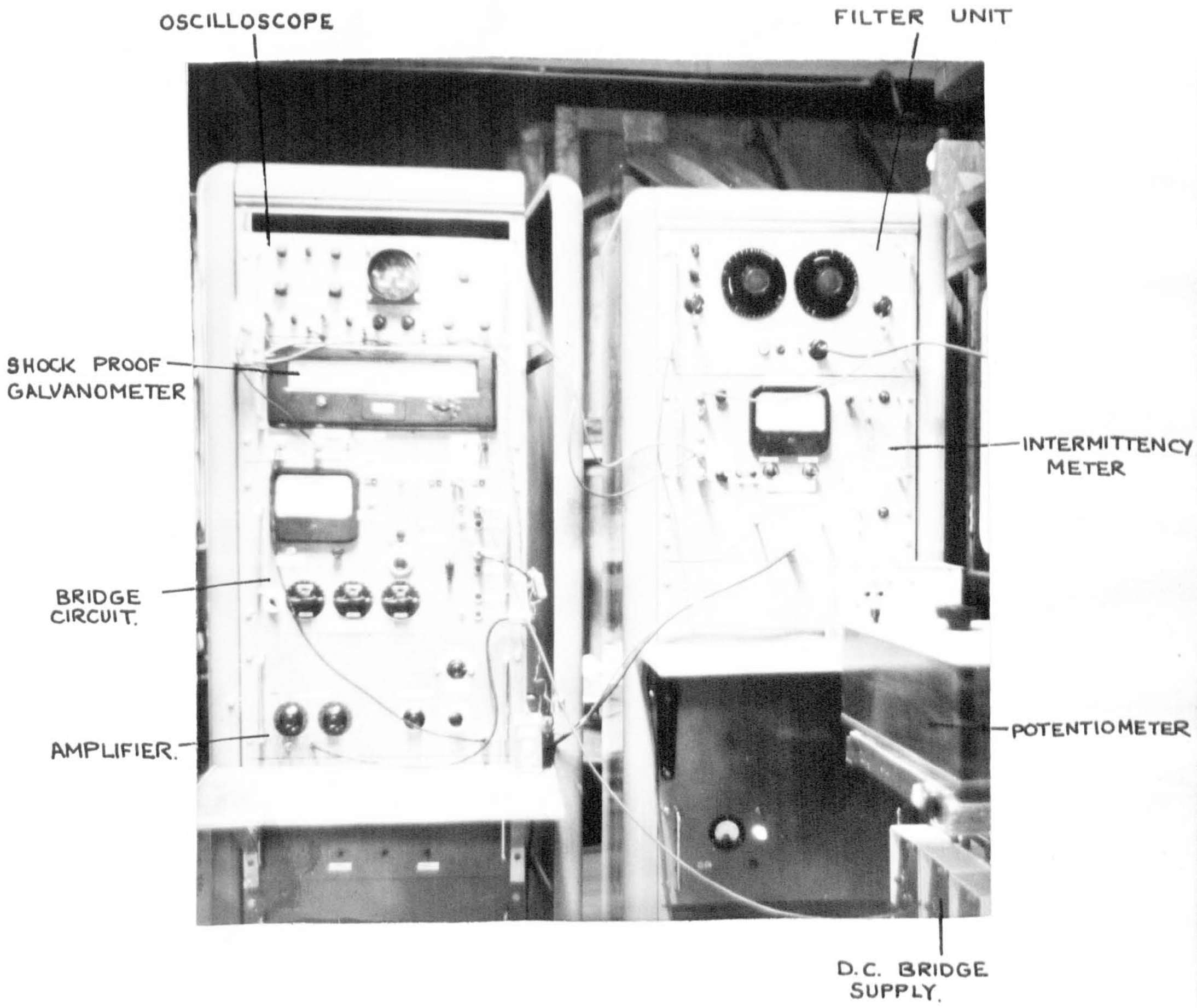

FIGURE 19.
HOT WIRE ANEMOMETER PROBE.
(TWICE FULL SIZE)

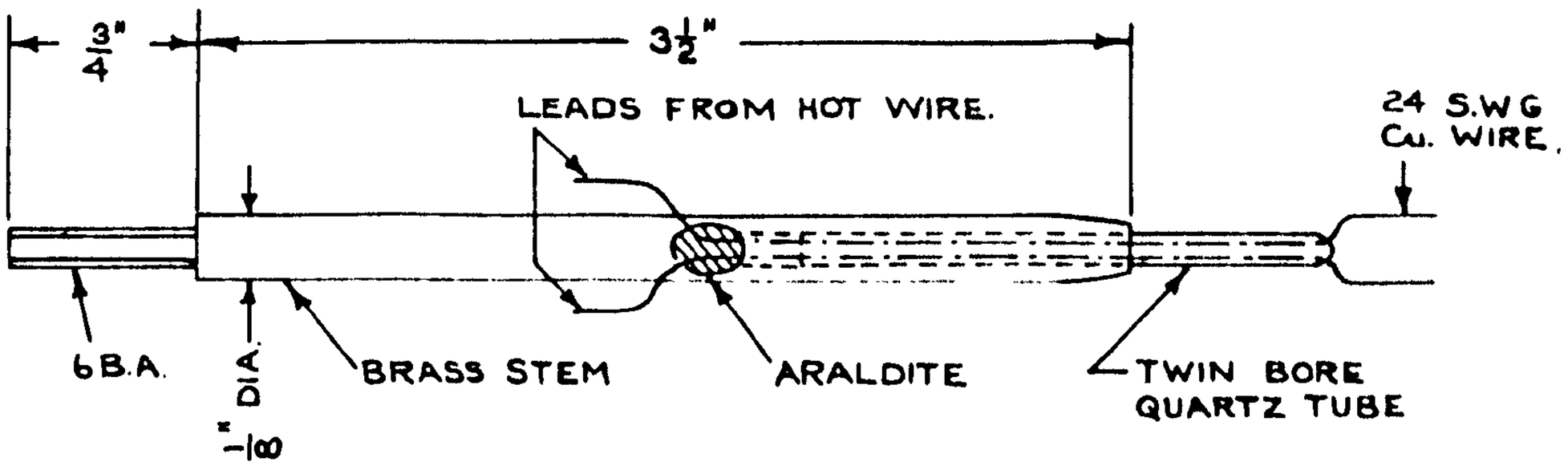

FIGURE 20
THE BRIDGE CIRCUIT.

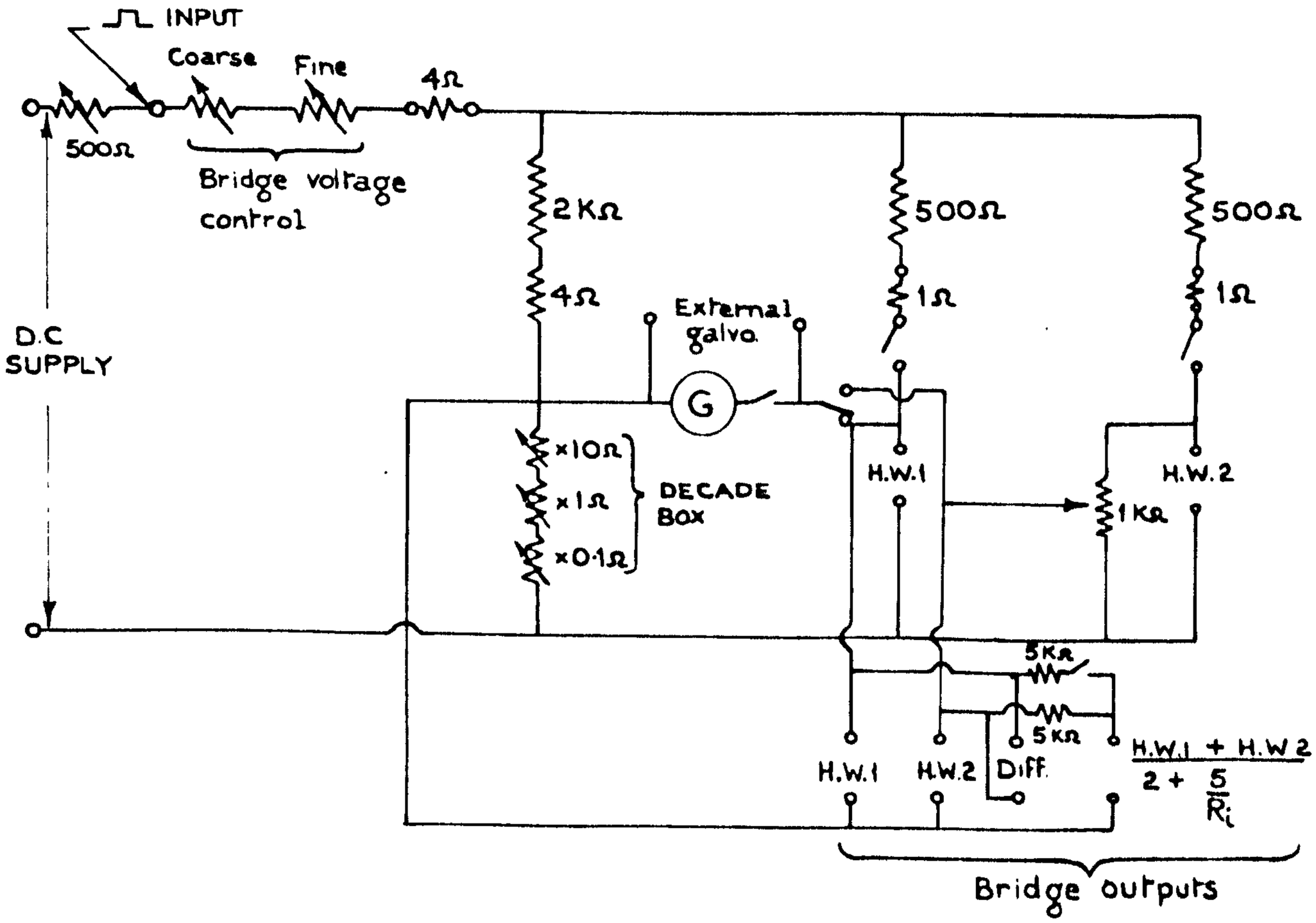

Diff. = H.W.1 − H.W.2
R_i = INPUT RESISTANCE TO AMPLIFIER.

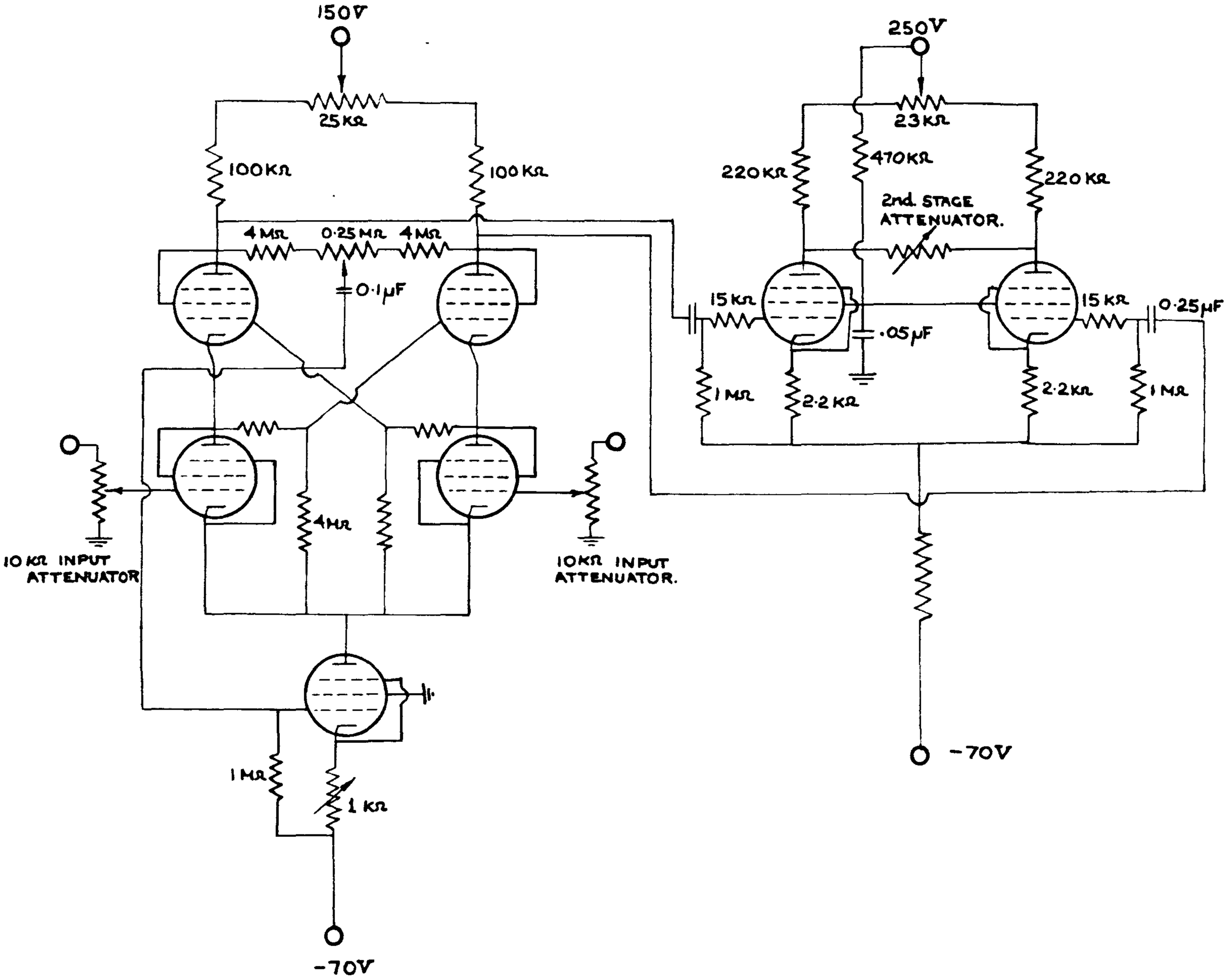

FIG. 21 (A)

THE AMPLIFIER

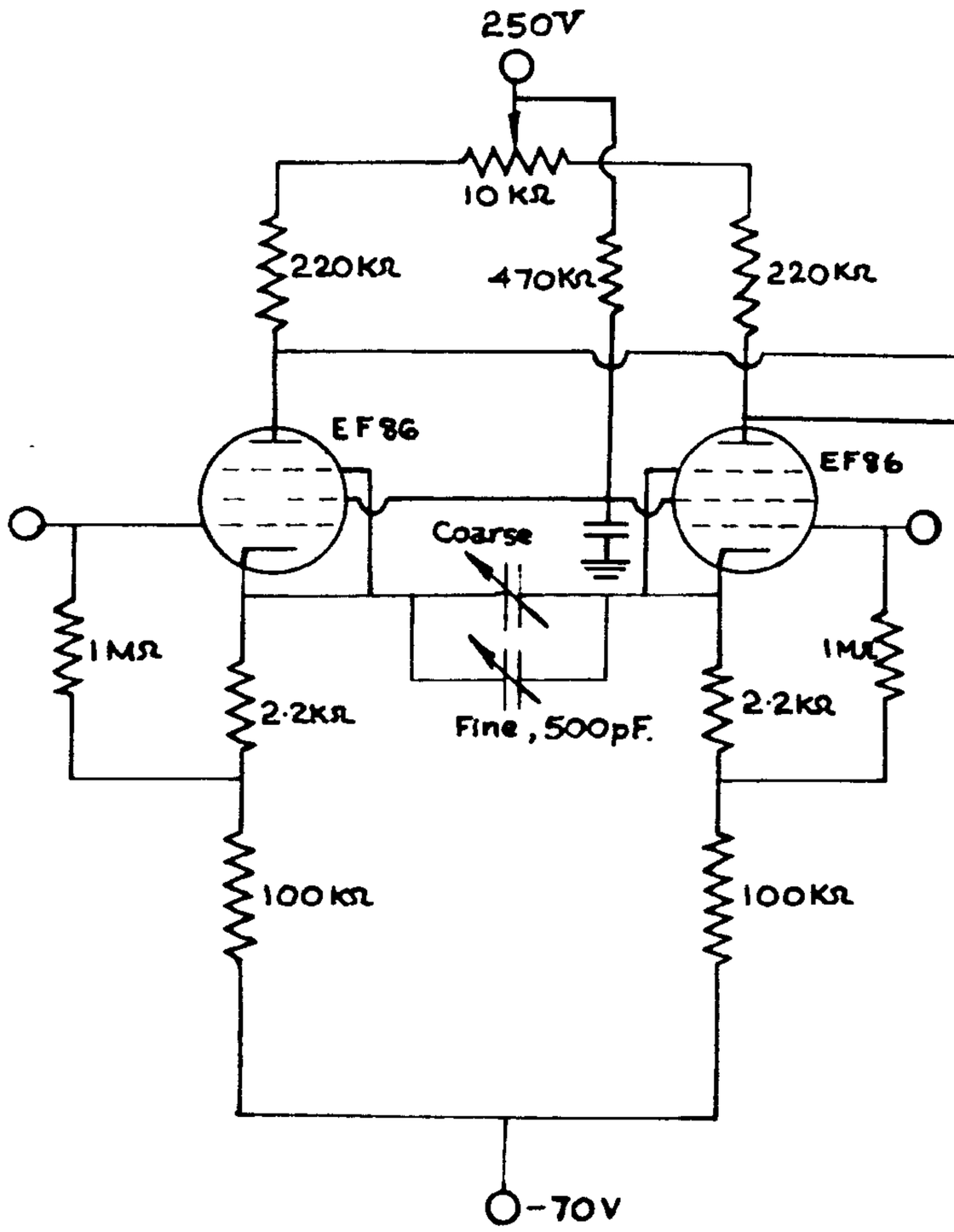

COMPENSATION STAGE.

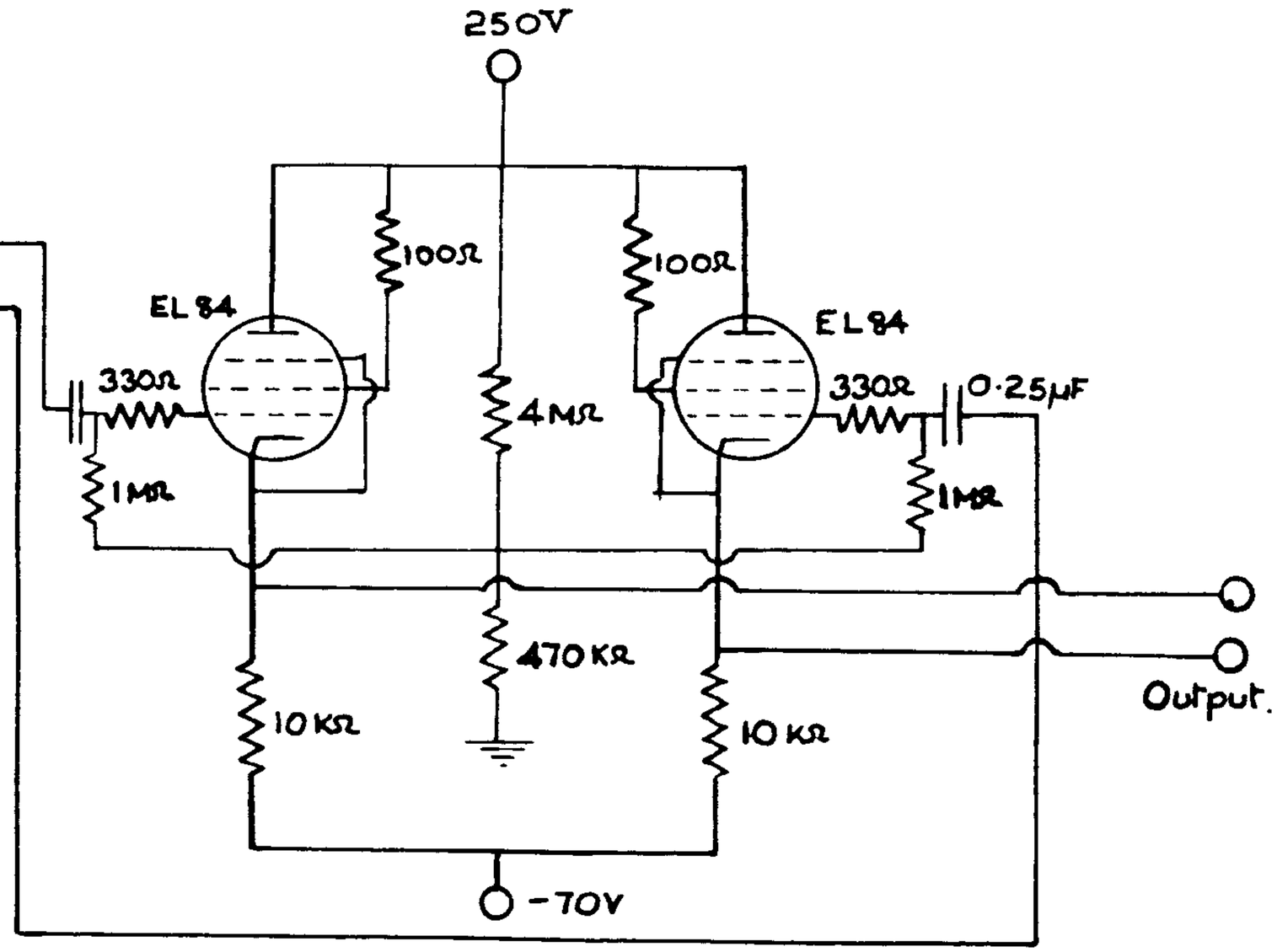

OUTPUT STAGE.

FIG. 21(B)

THE AMPLIFIER

FIG. 22

THE THERMO-JUNCTION CIRCUIT.

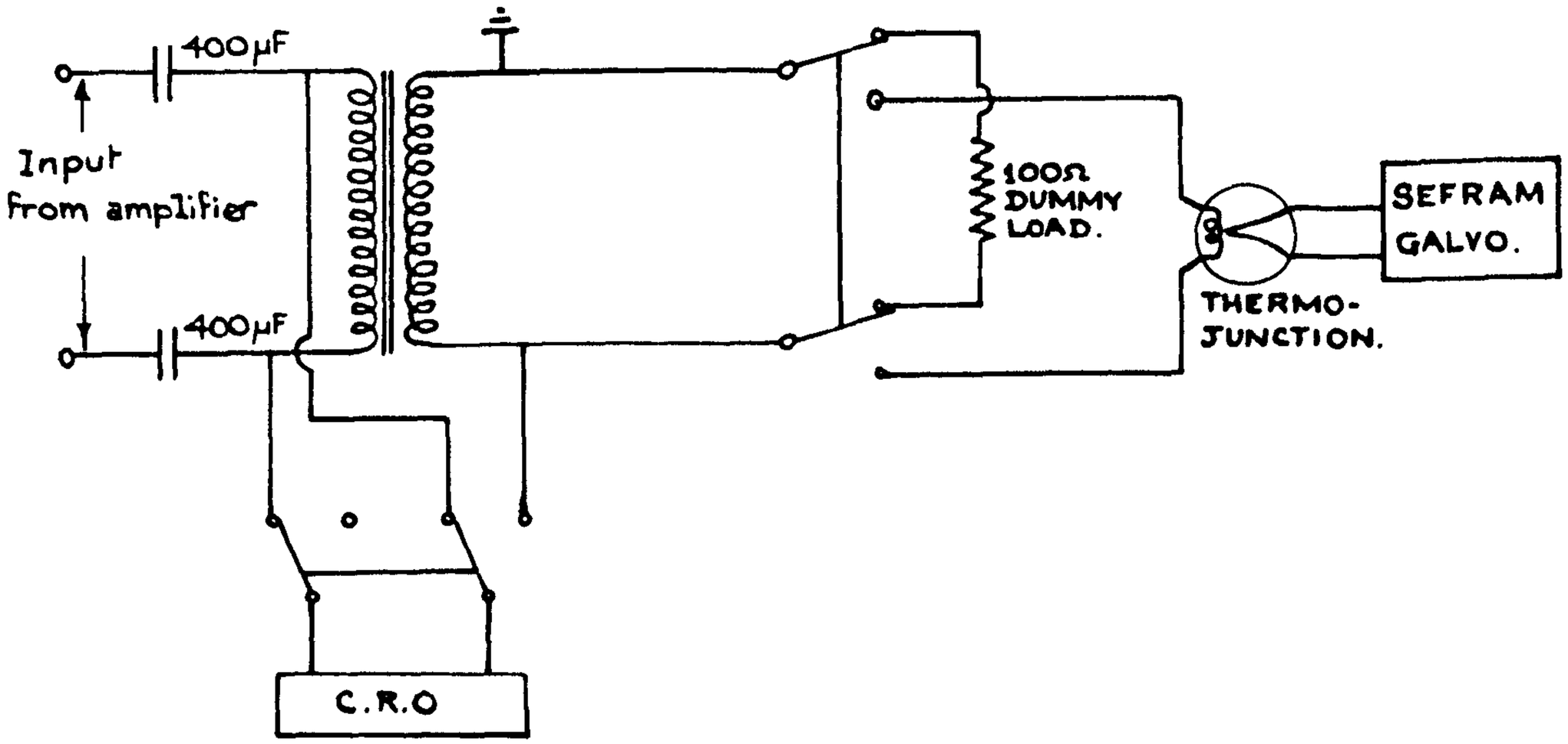

FIG. 23

AMPLIFIER FREQUENCY RESPONSE.

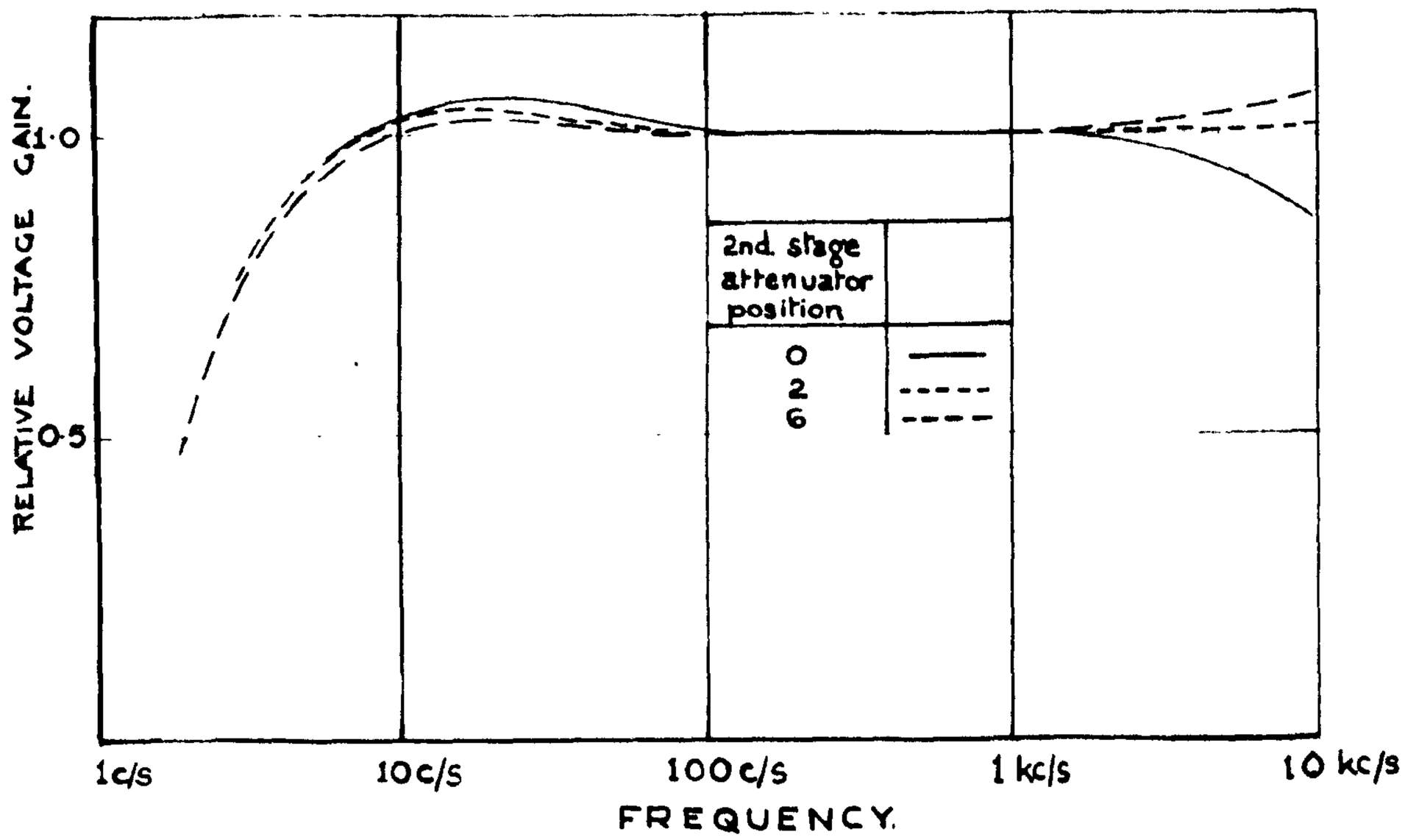

FIG. 24

SQUARE WAVE GENERATOR.

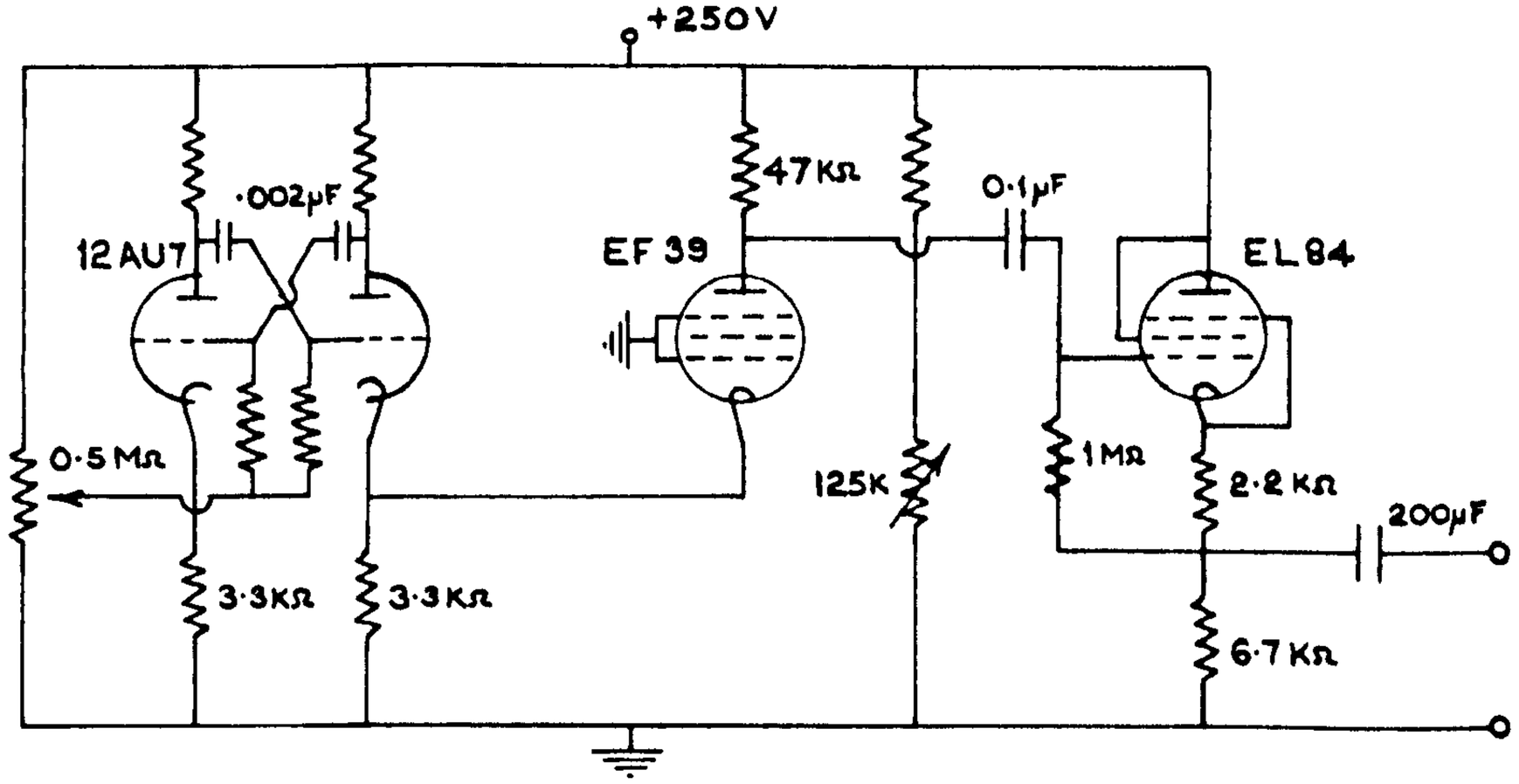

FIGURE 25

DIFFERENTIATING CIRCUIT AND IT'S PERFORMANCE

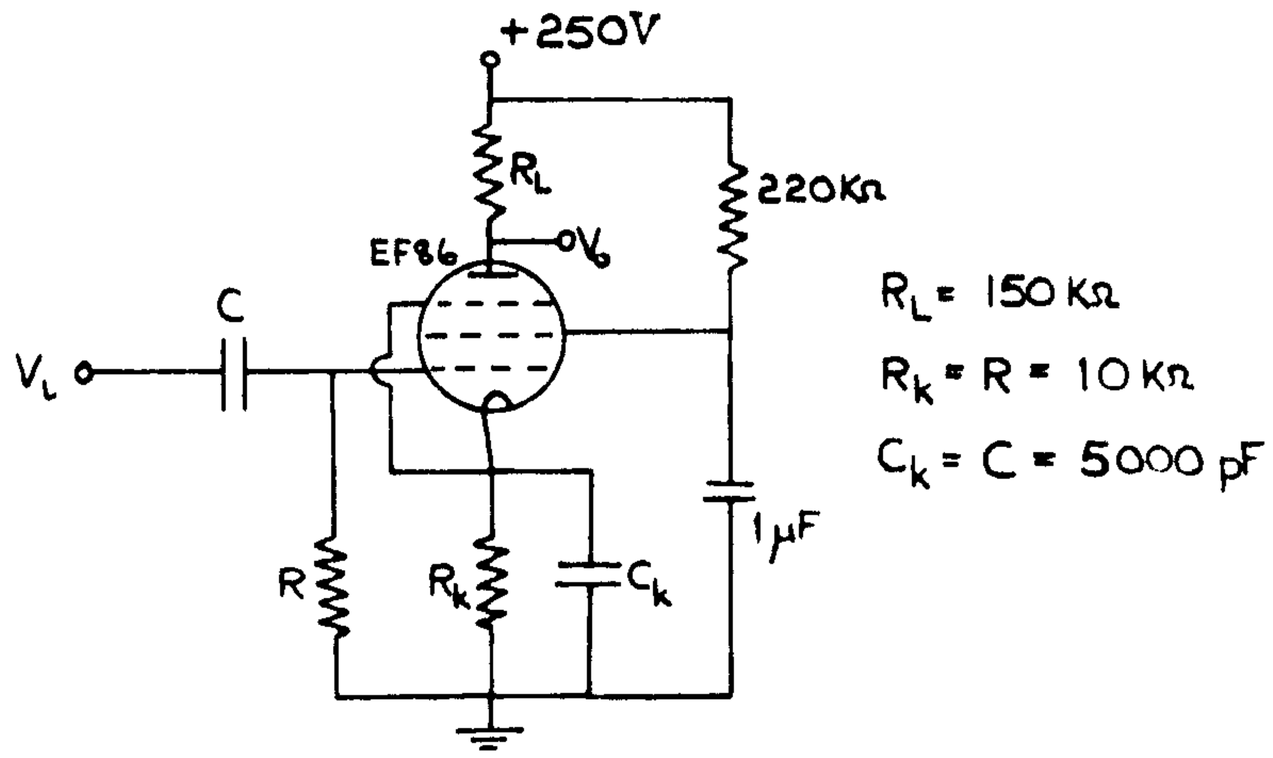

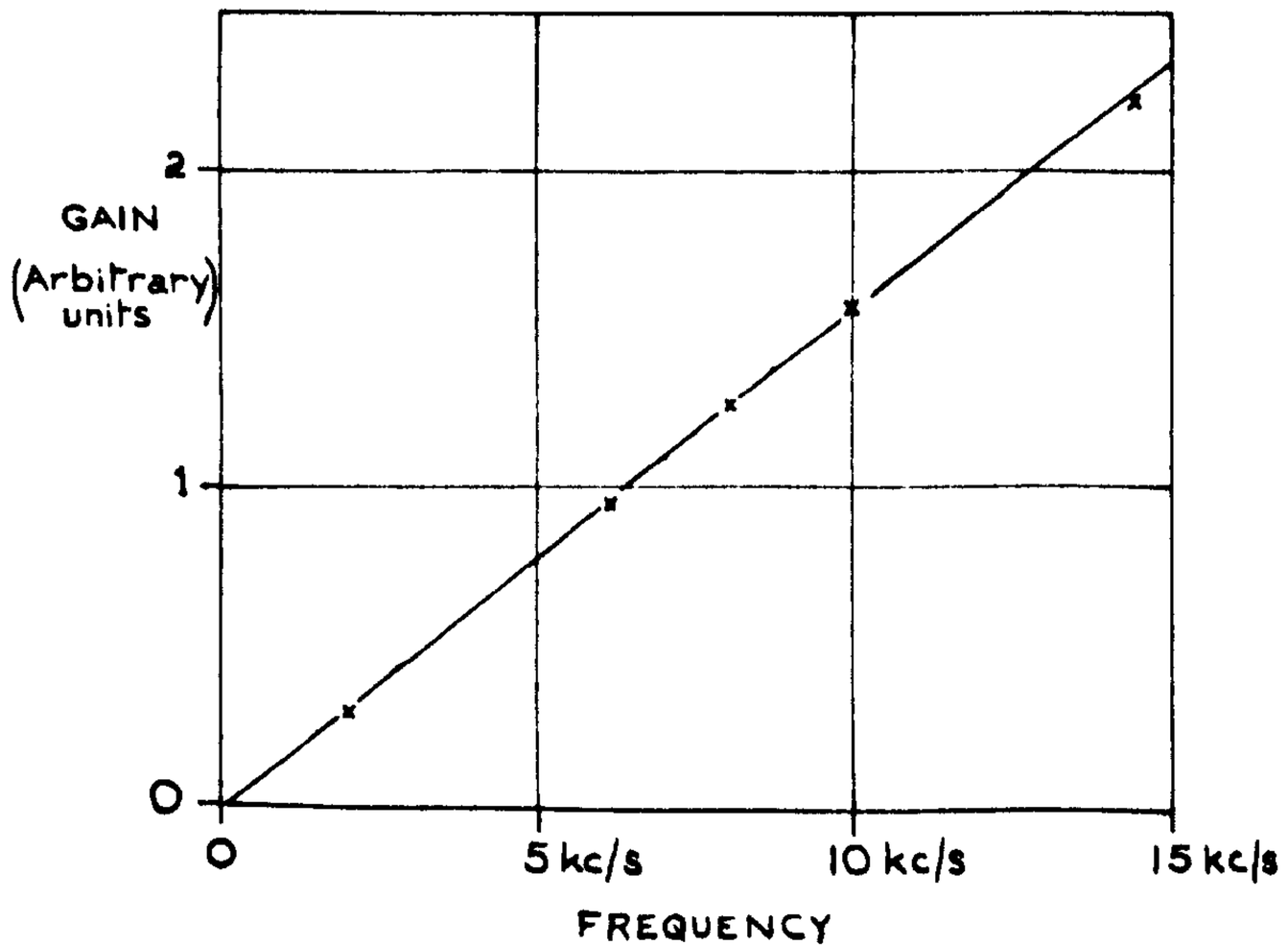

FIG. 26

THE INTERMITTENCY METER

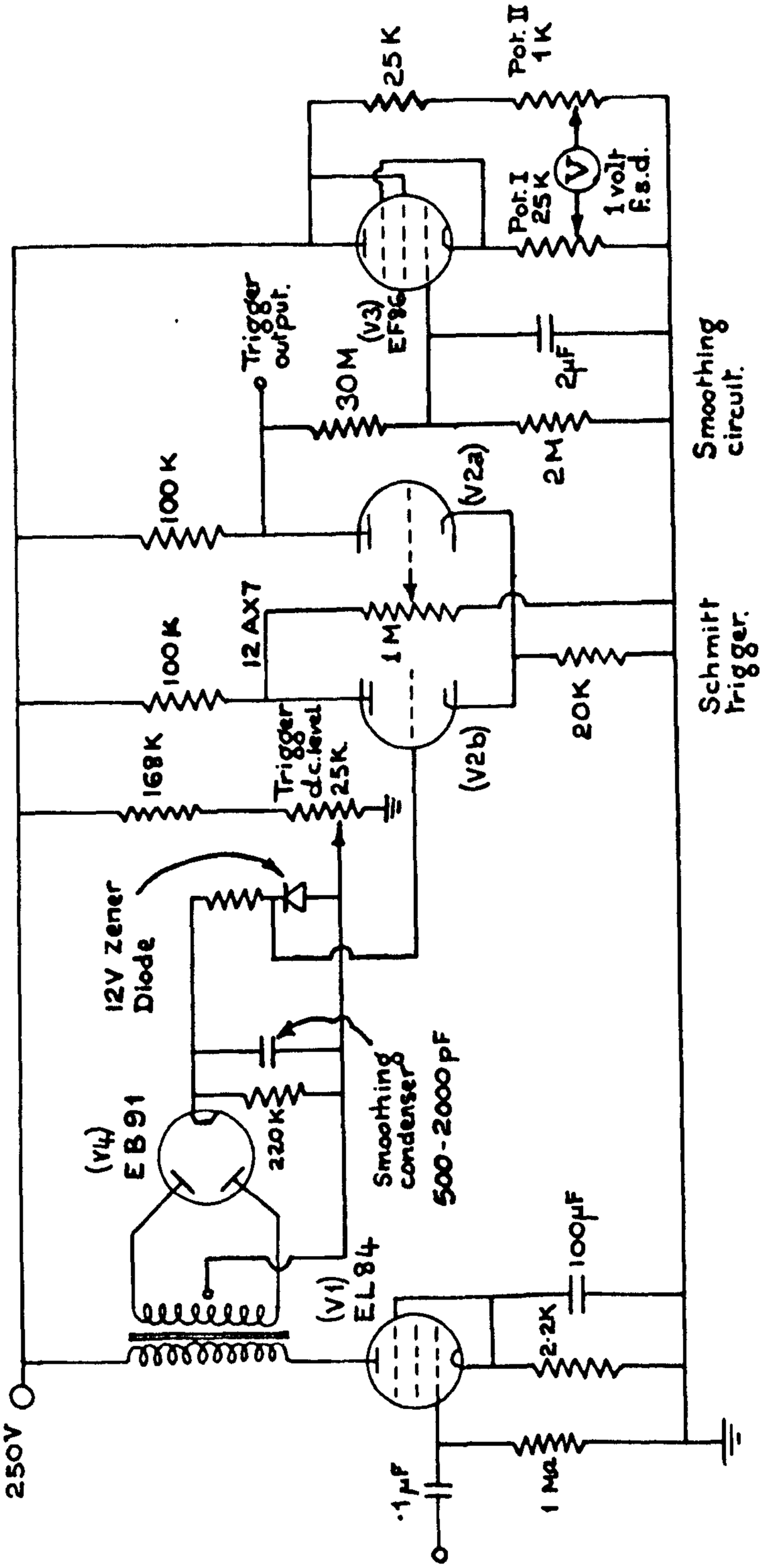

FIGURE 27

THE EFFECT OF INCORRECT RC SETTING ON THE INTERMITTENCY METER.

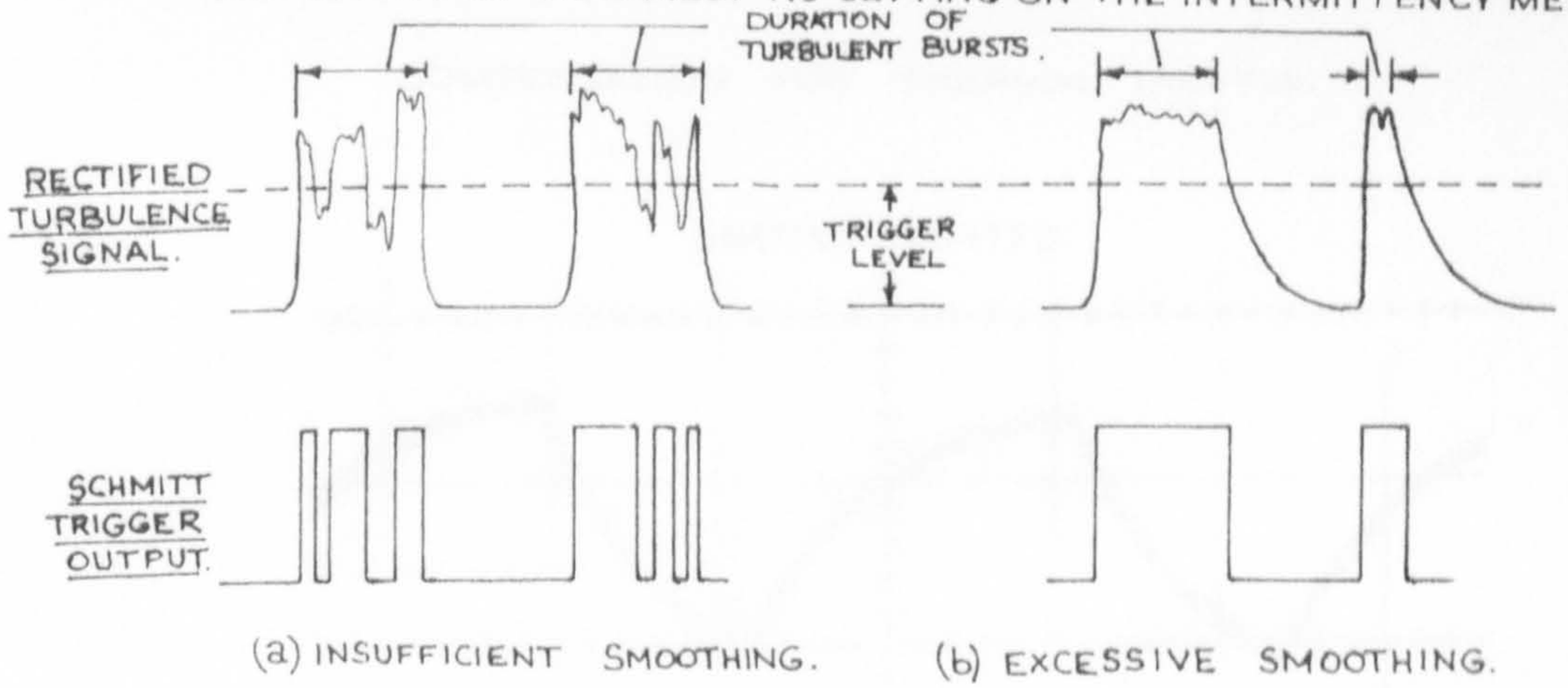

(a) INSUFFICIENT SMOOTHING. (b) EXCESSIVE SMOOTHING.

FIGURE 28

EXAMPLES OF SIGNALS FROM THE INTERMITTENCY METER.

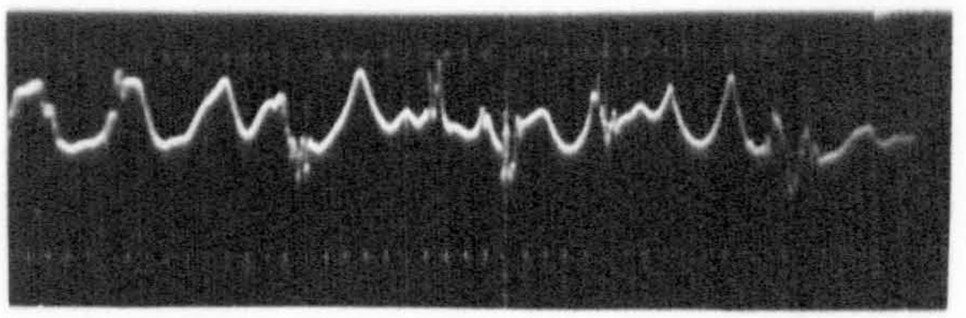

UNFILTERED SIGNAL AT THE JET EDGE.

(a)

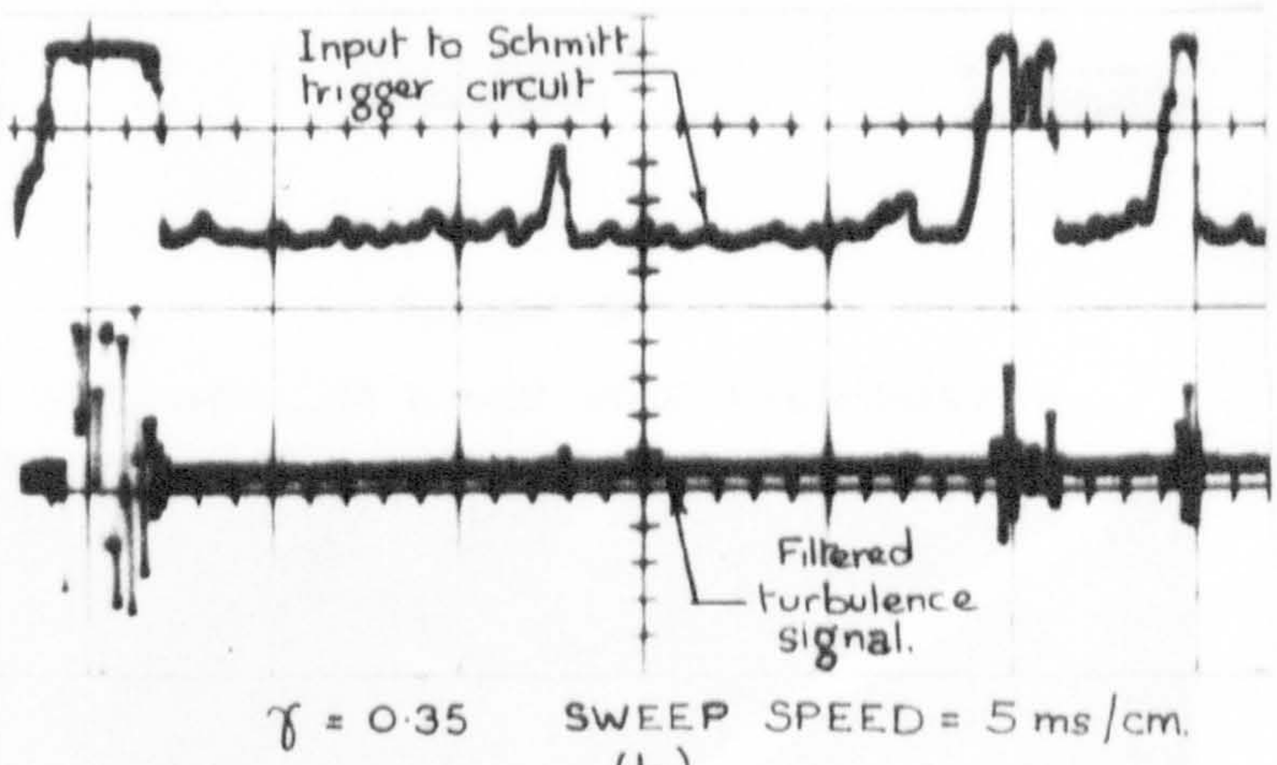

γ = 0·35 SWEEP SPEED = 5 ms/cm.

(b)

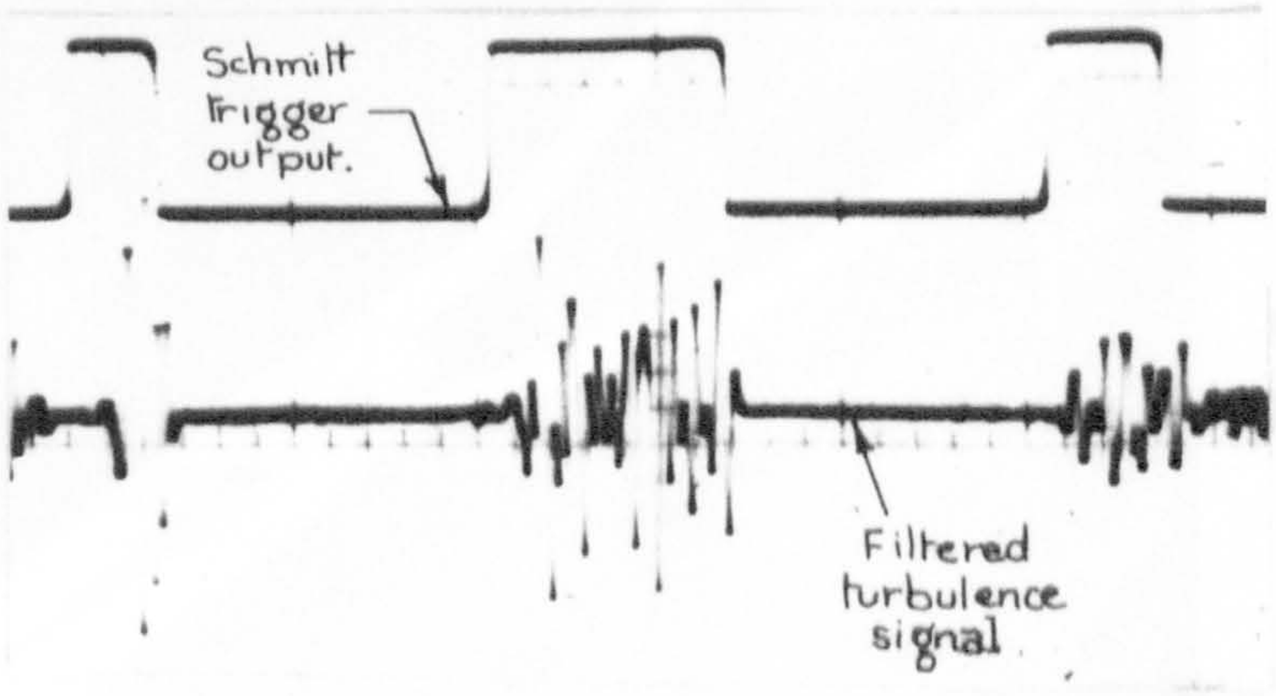

γ = 0·35 SWEEP SPEED = 5 ms/cm.

(c)

FIGURE 29

COMPENSATION FOR THERMAL INERTIA.

UNCOMPENSATED.

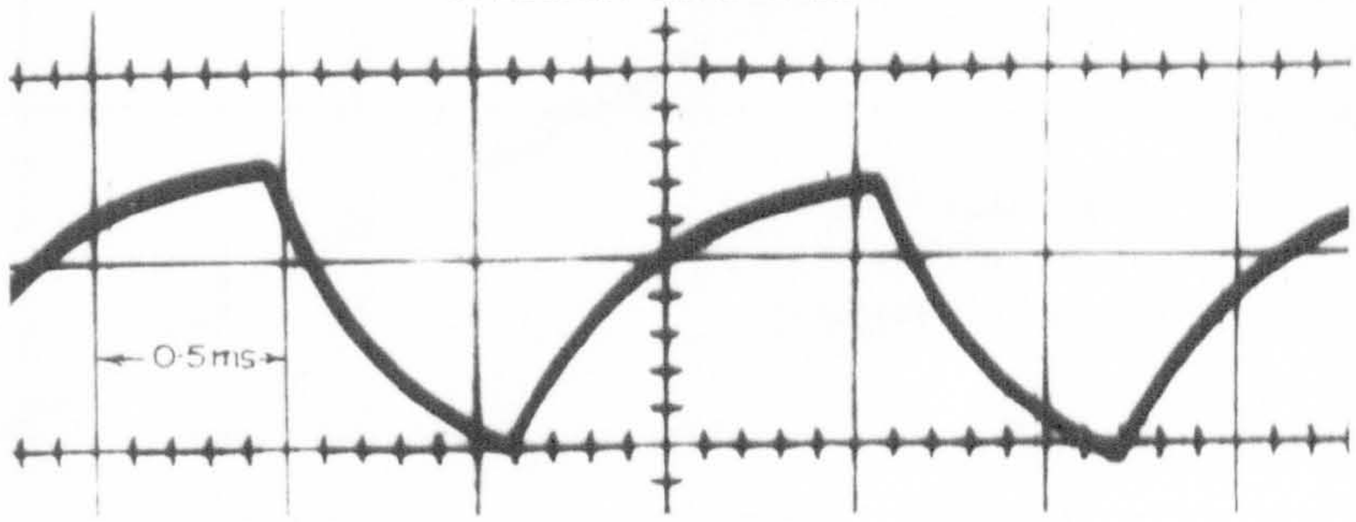

COMPENSATED.

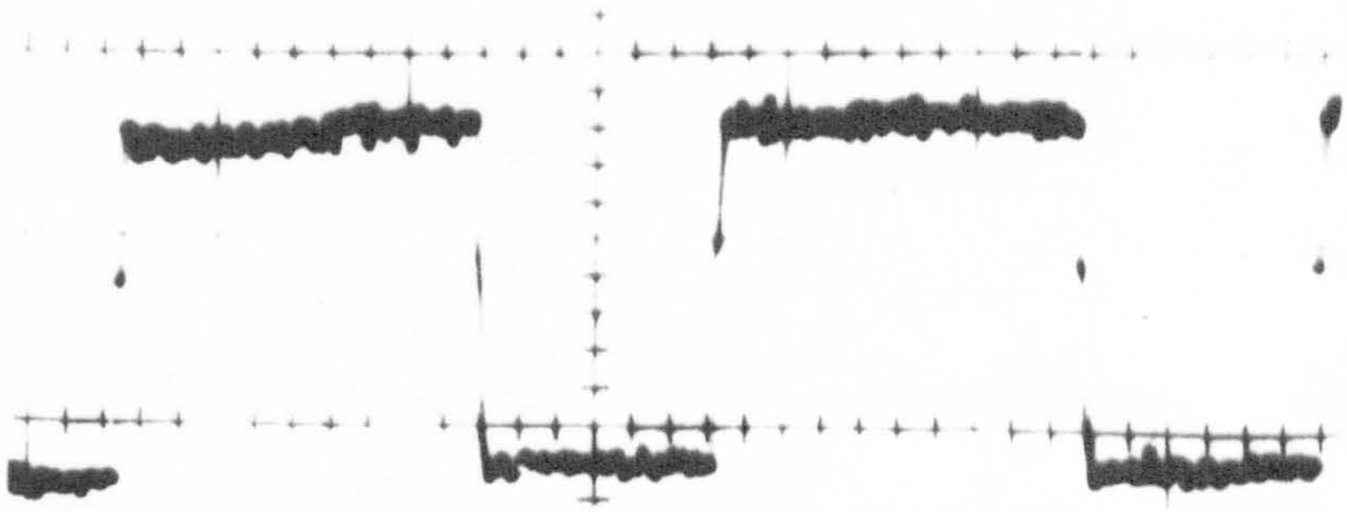

FIGURE 30

SHADOW PHOTOGRAPH OF A HOT WIRE ANEMOMETER.

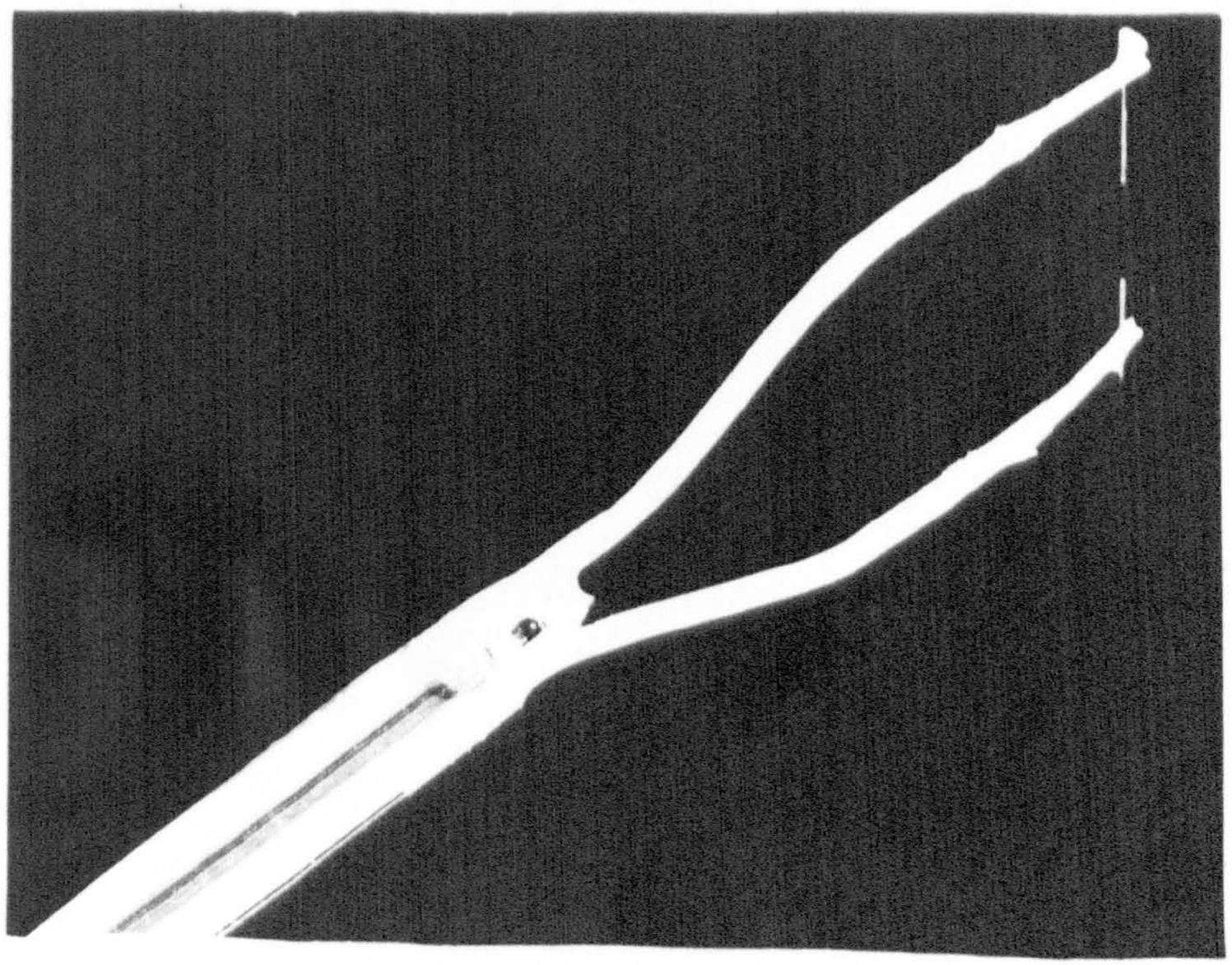

FIGURE 31.

HEAT TRANSFER LAW FOR THE HOT WIRE ANEMOMETER.

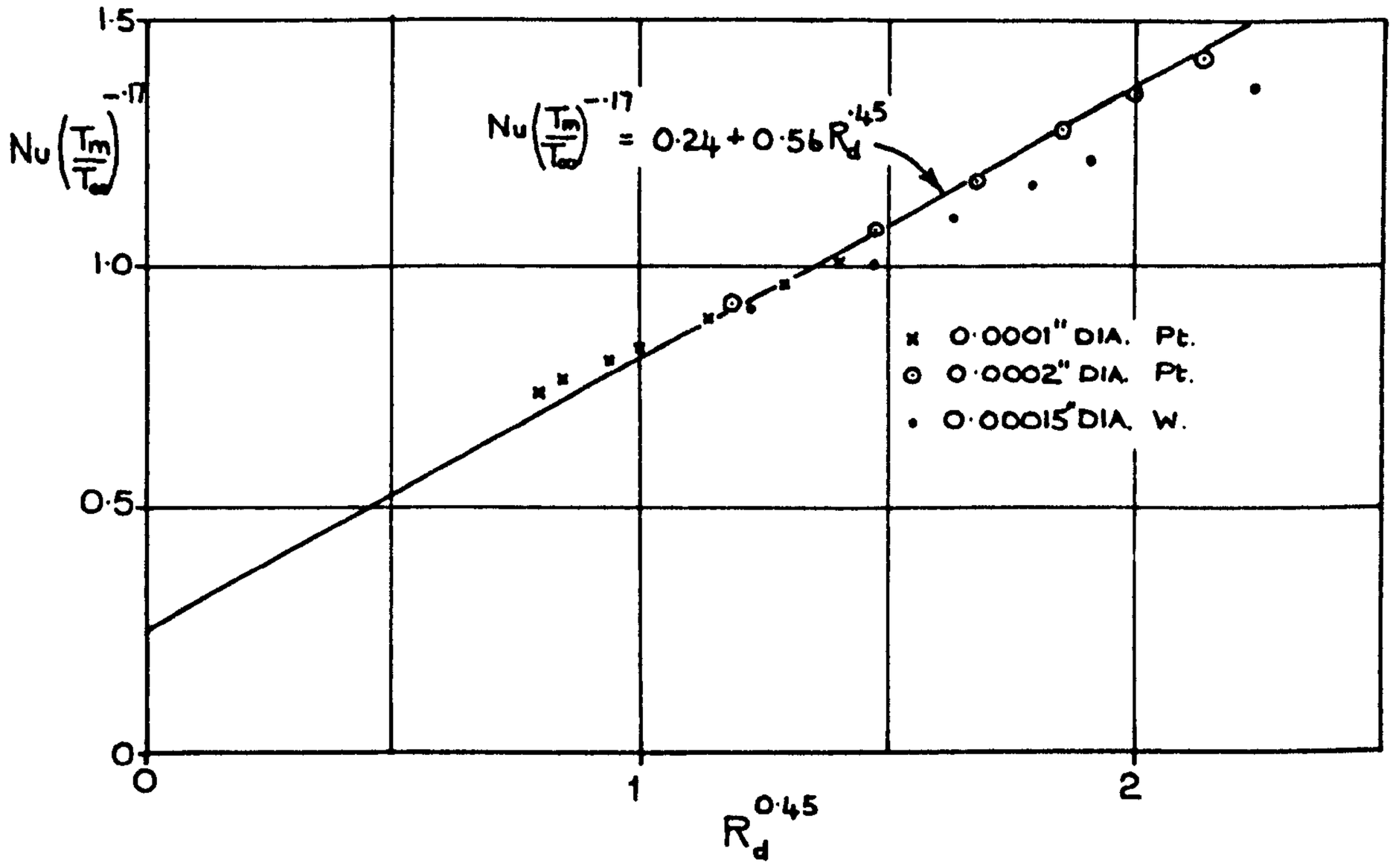

FIGURE 32.

INTENSITY OF WIND TUNNEL TURBULENCE.

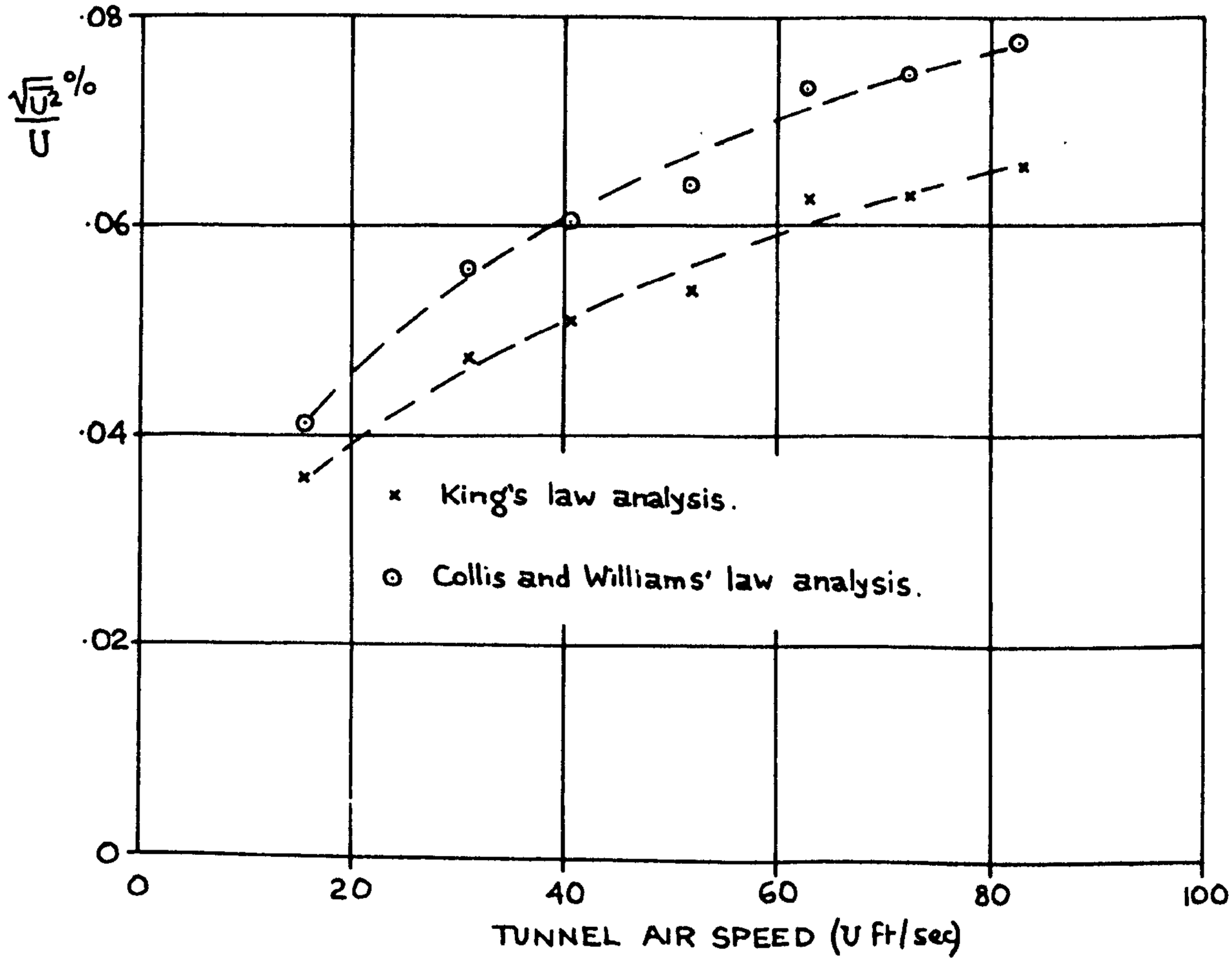

FIGURE 33

DISTRIBUTION OF $\sqrt{\overline{v^2}}/U_\tau$ AND $\sqrt{\overline{w^2}}/U_\tau$ IN PIPE AND CHANNEL FLOW.

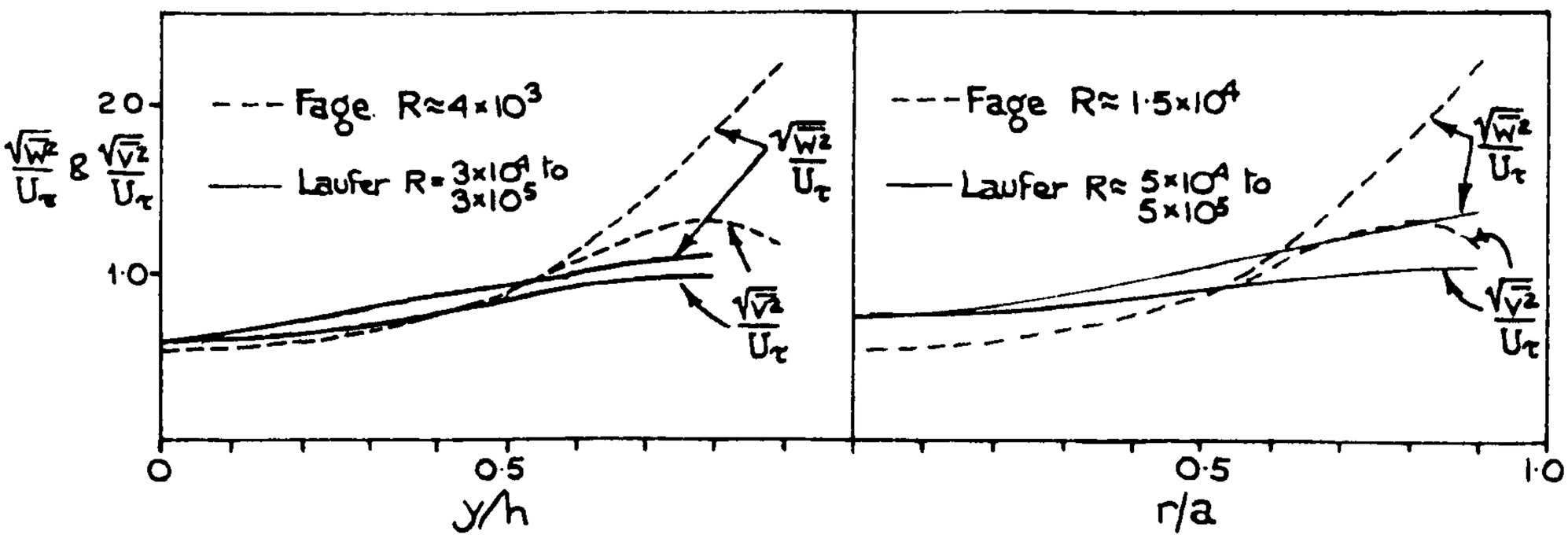

FIGURE 34

COMPARISON OF MEASURED AND COMPUTED STATIC PRESSURE DISTRIBUTIONS IN PIPE AND CHANNEL FLOW

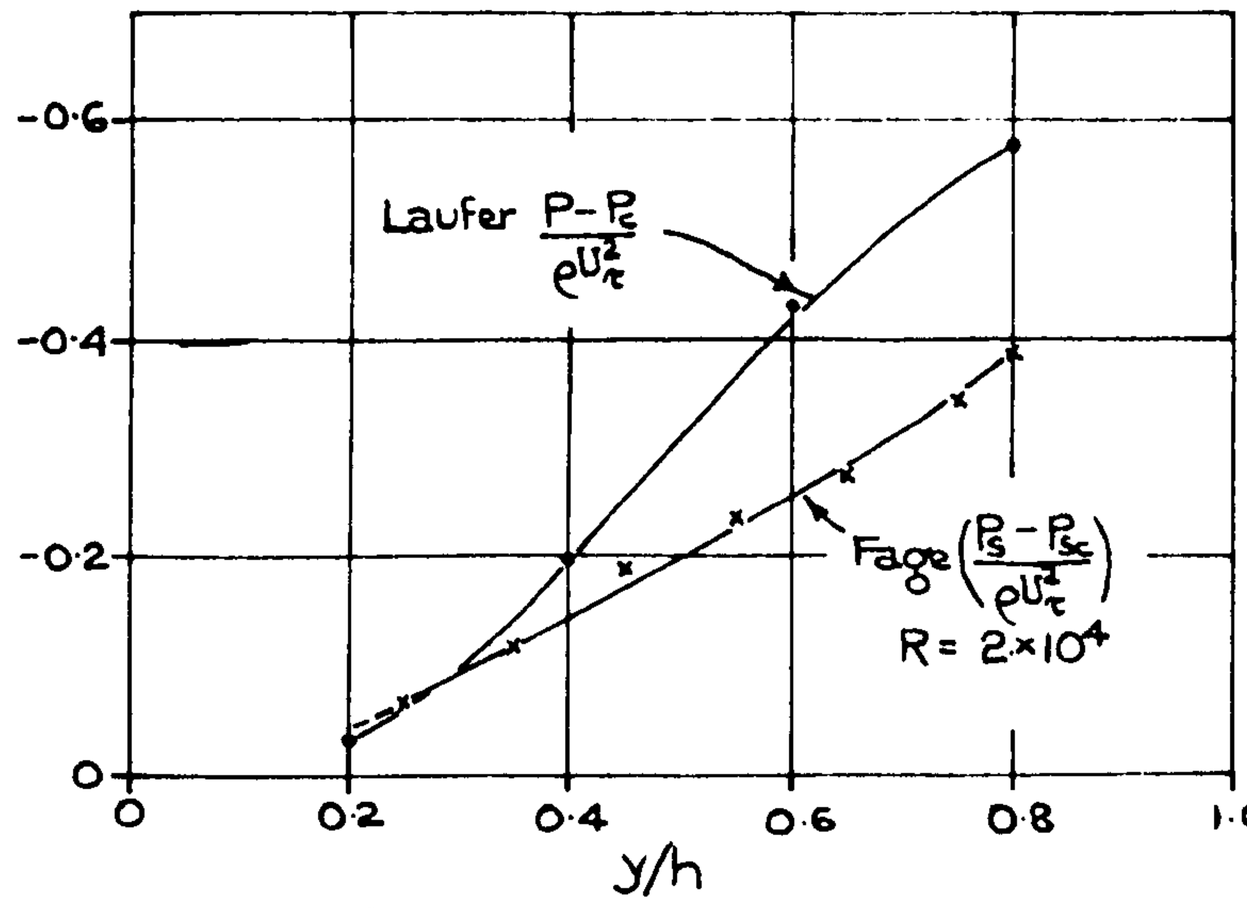

(a) CHANNEL FLOW

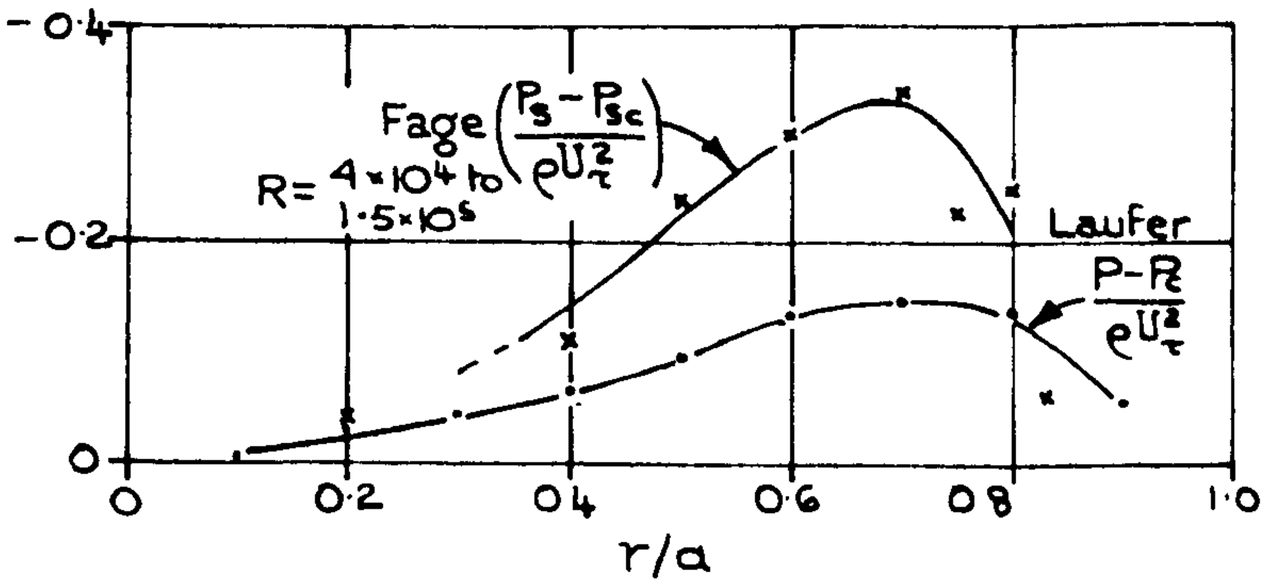

(b) CIRCULAR PIPE FLOW.

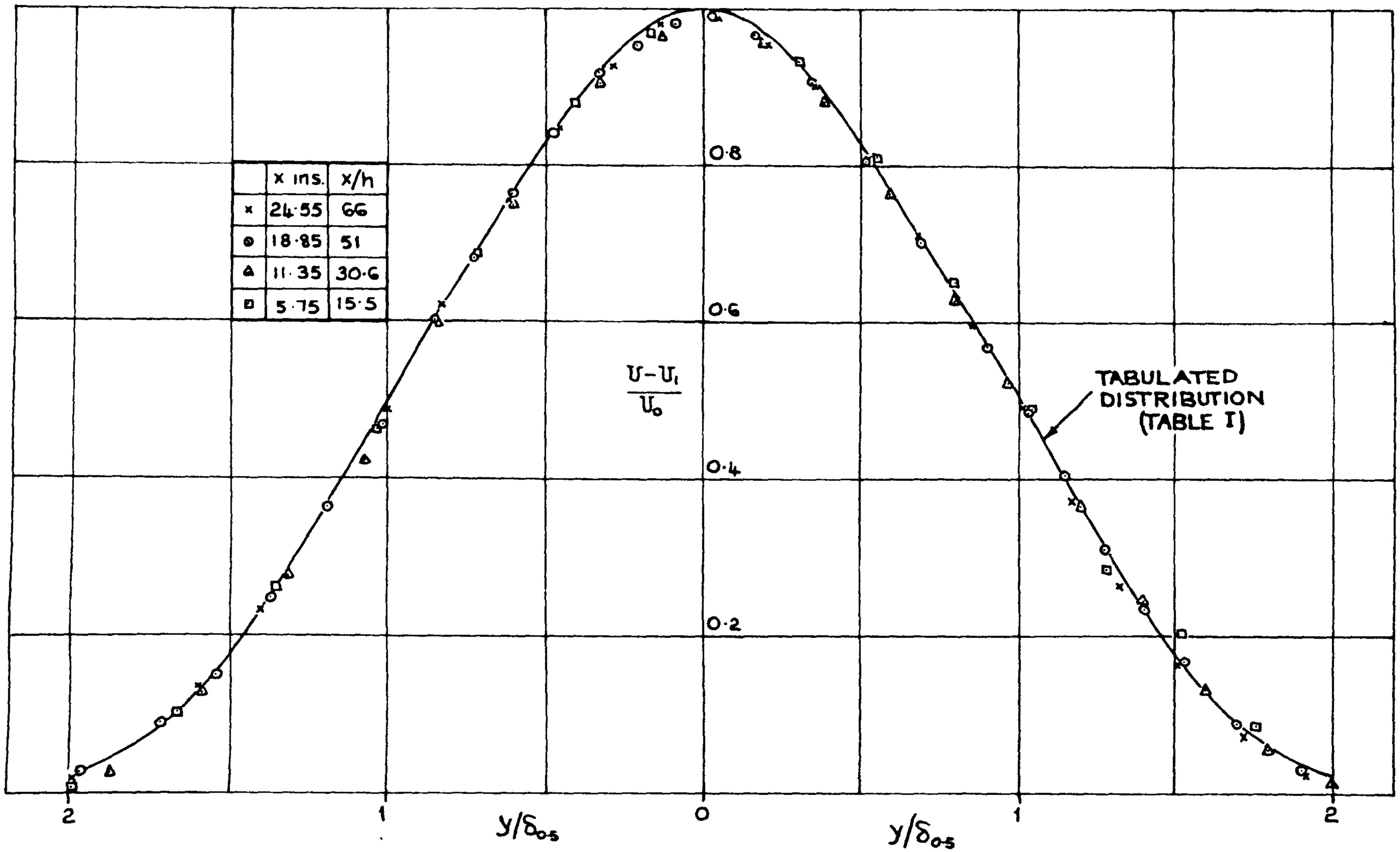

MEAN VELOCITY PROFILES IN A PLANE JET WITH $U_1/U_j = 0.07$
(MEASURED WITH A PITOT AND STATIC TUBE)

FIG. 35

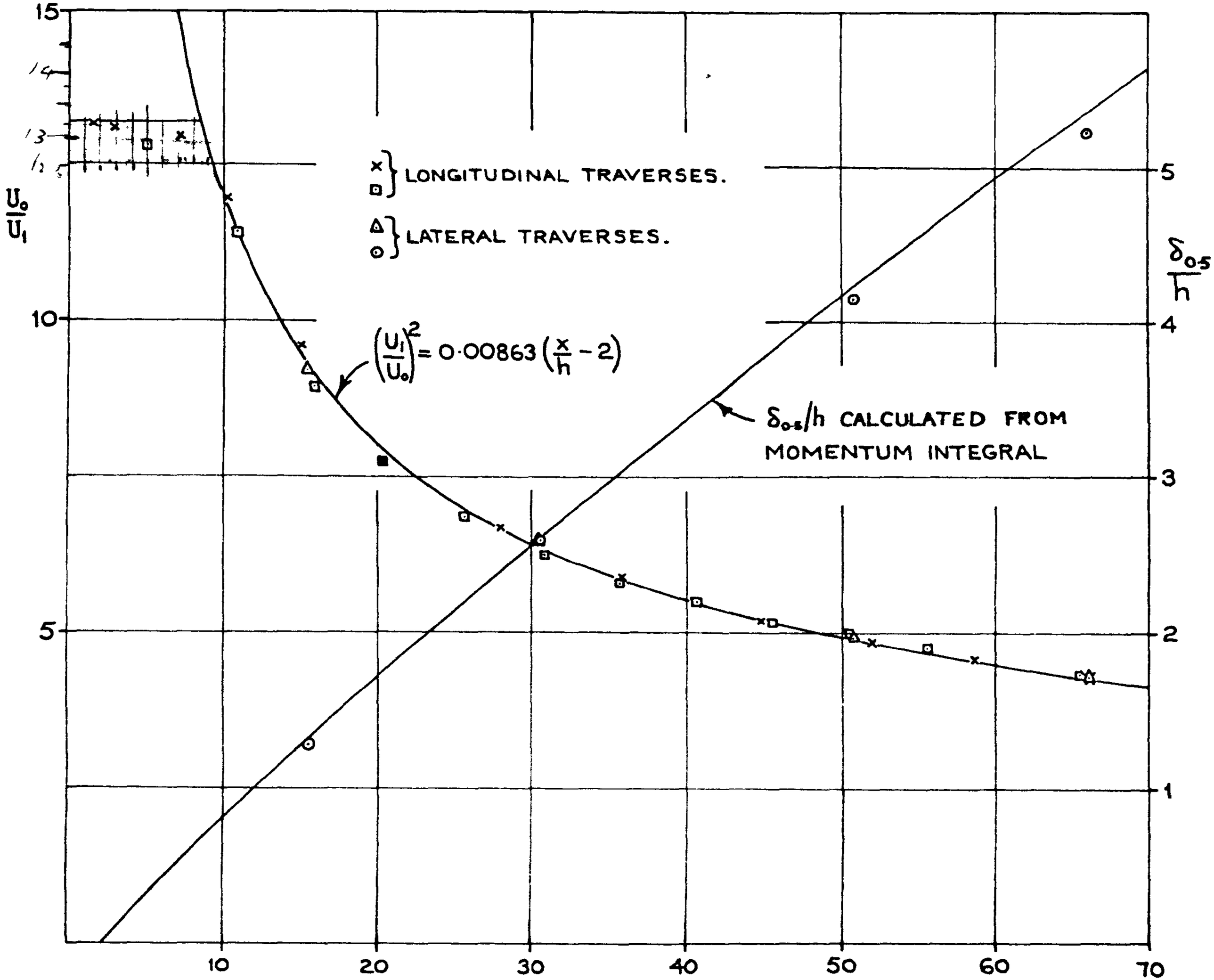

VARIATION OF JET WIDTH AND CENTRE-LINE VELOCITY IN A PLANE JET.
$U_1/U_J = 0.07$
FIG. 36

FIGURE 37

STATIC PRESSURES PROFILES IN A PLANE JET.

$U_1/U_J = 0.07$

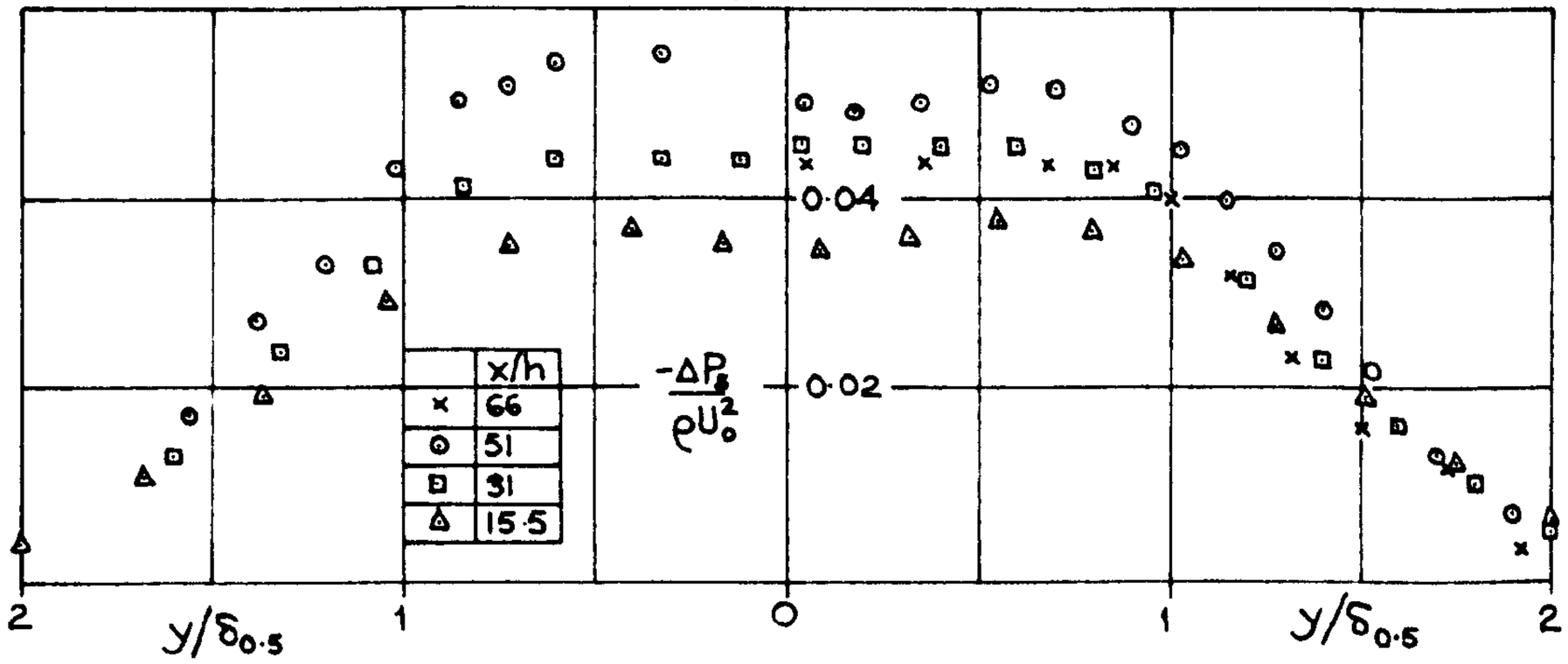

FIGURE 38

STATIC PRESSURE ON THE CENTRE-LINE OF A PLANE JET

$U_1/U_J = 0.07$

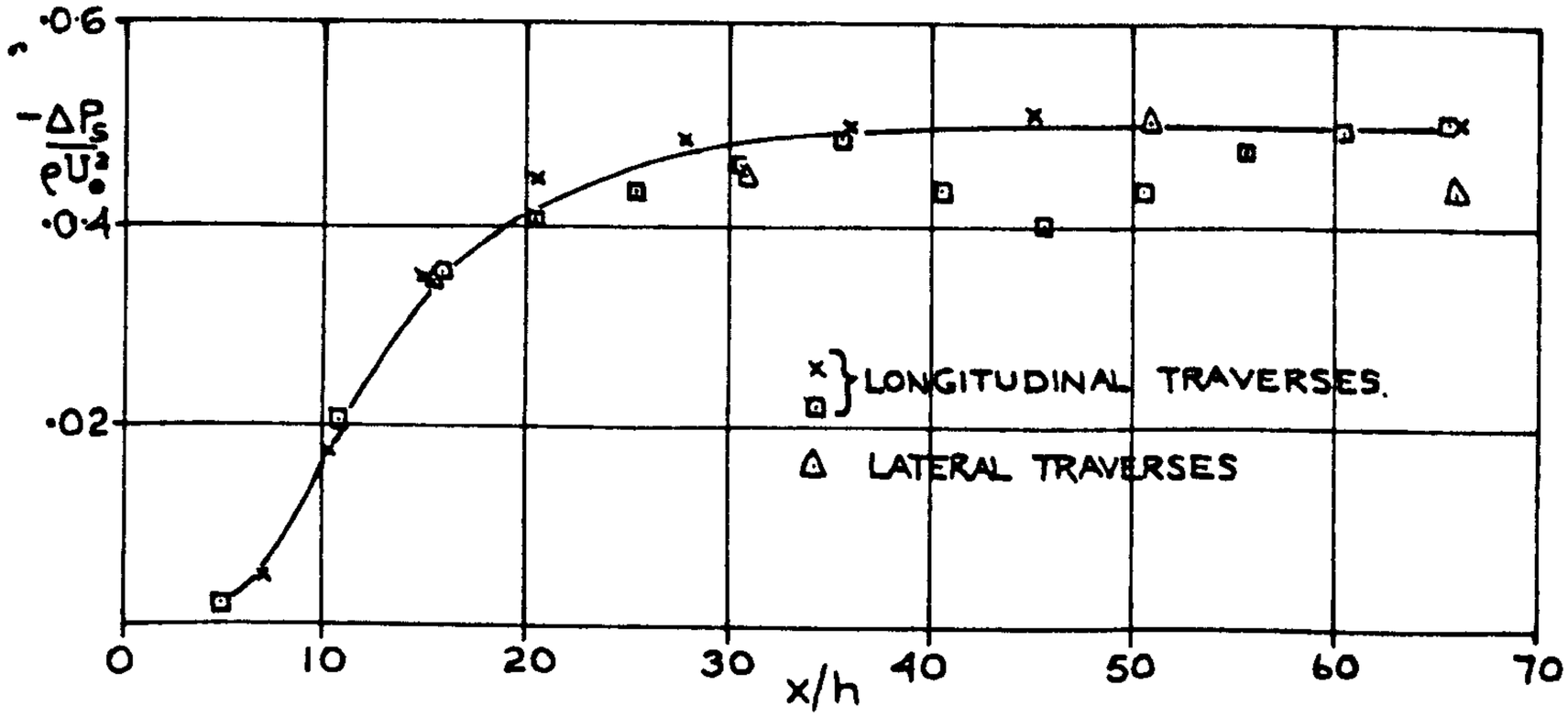

FIG. 42

CALCULATED SHEAR STRESS DISTRIBUTION IN A PLANE JET.

$U_1/U_J = 0.07$

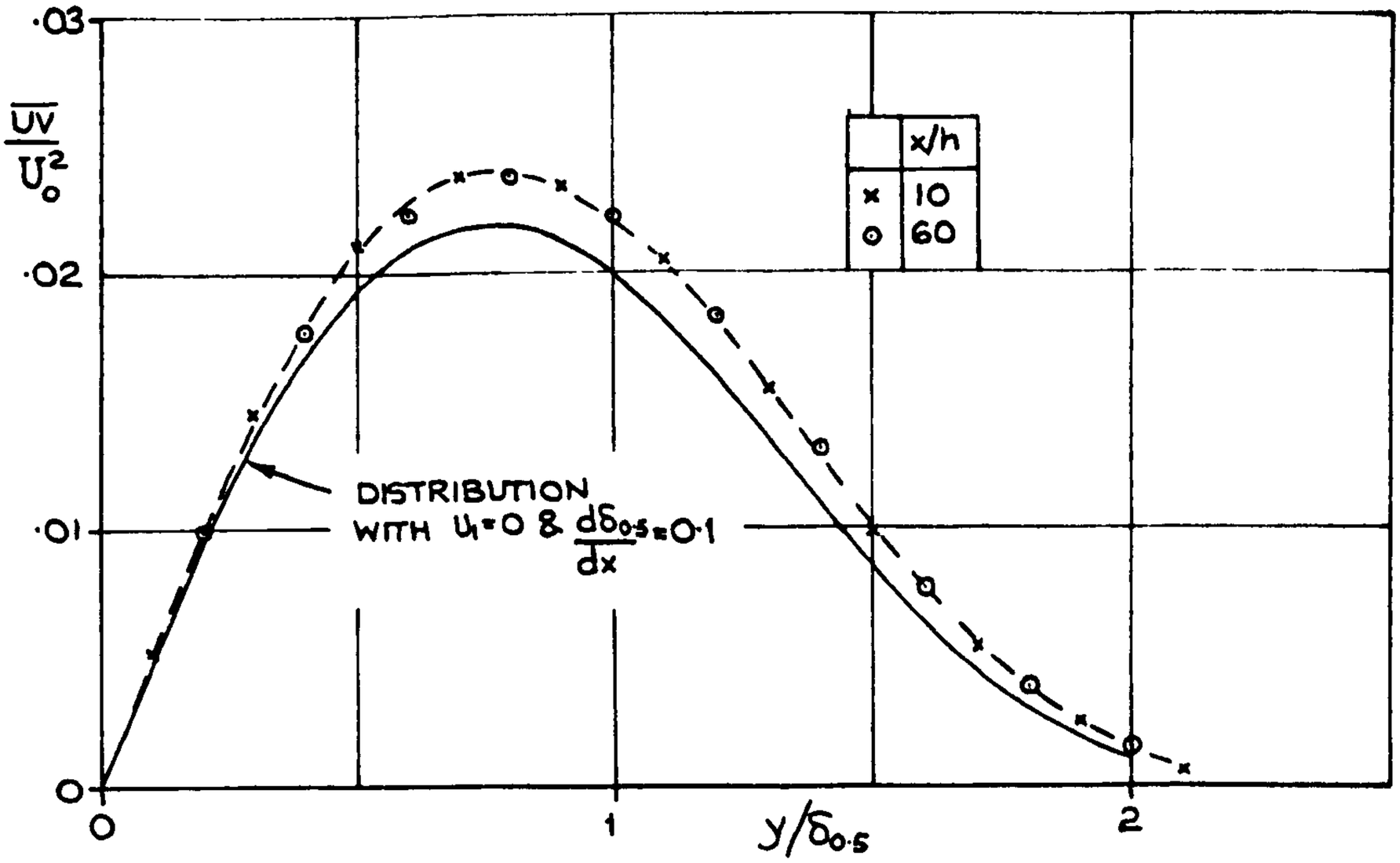

FIG. 43

LATERAL MEAN VELOCITY DISTRIBUTION IN A PLANE JET.

$U_1/U_J = 0.07$

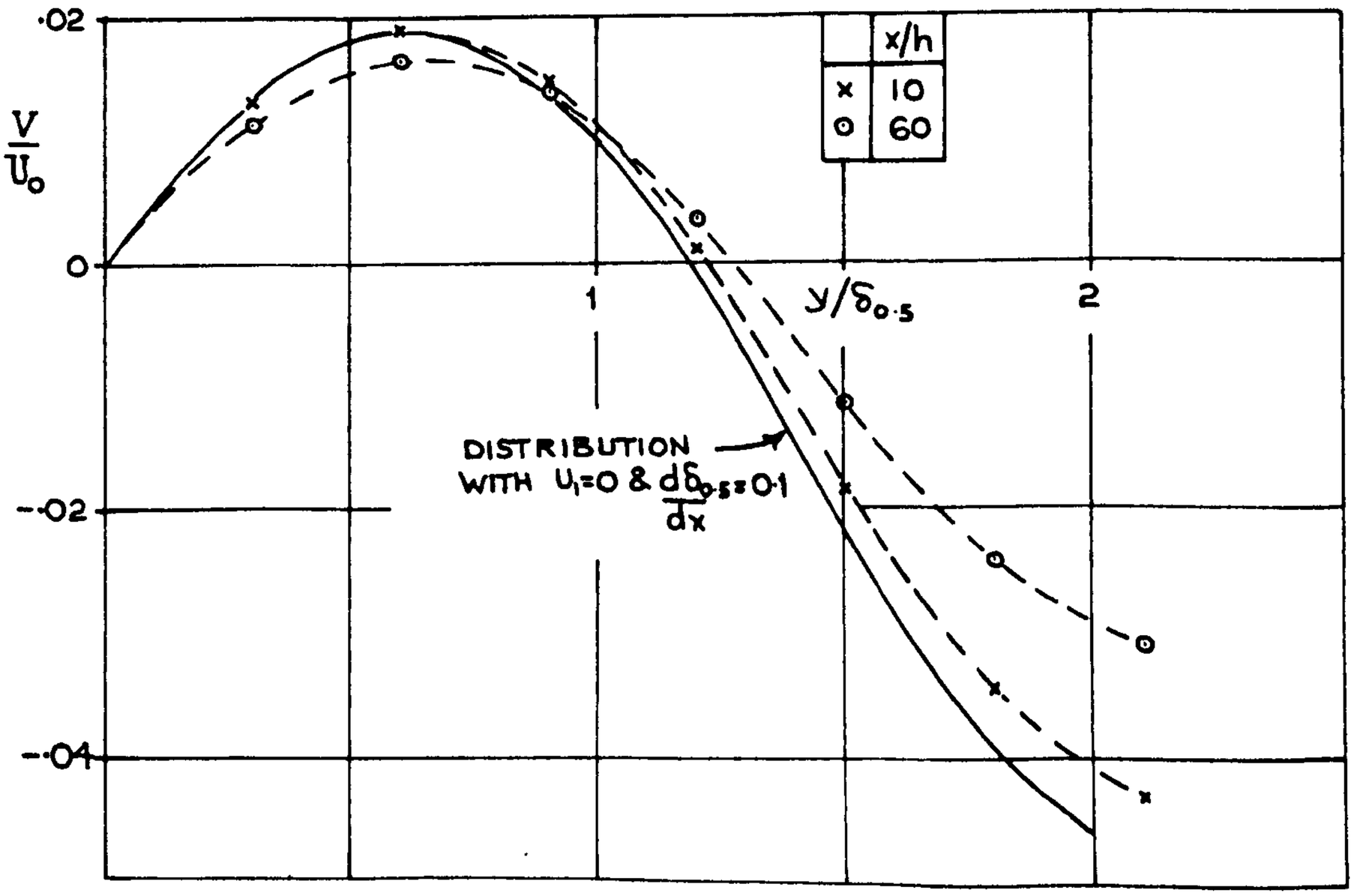

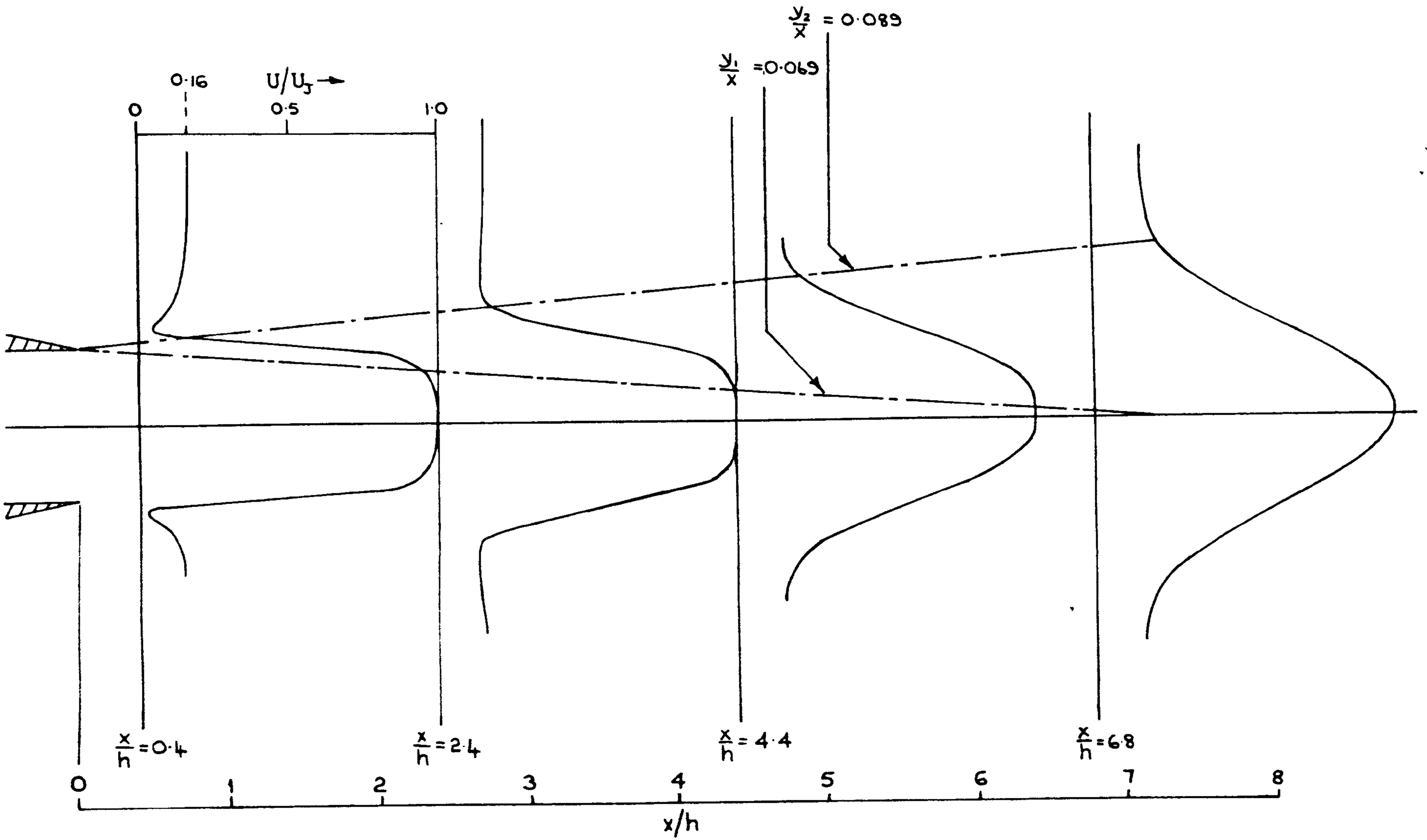

FIGURE 44 . SPREAD OF THE JET IN THE POTENTIAL CORE REGION. $U_1/U_J = 0.162$.

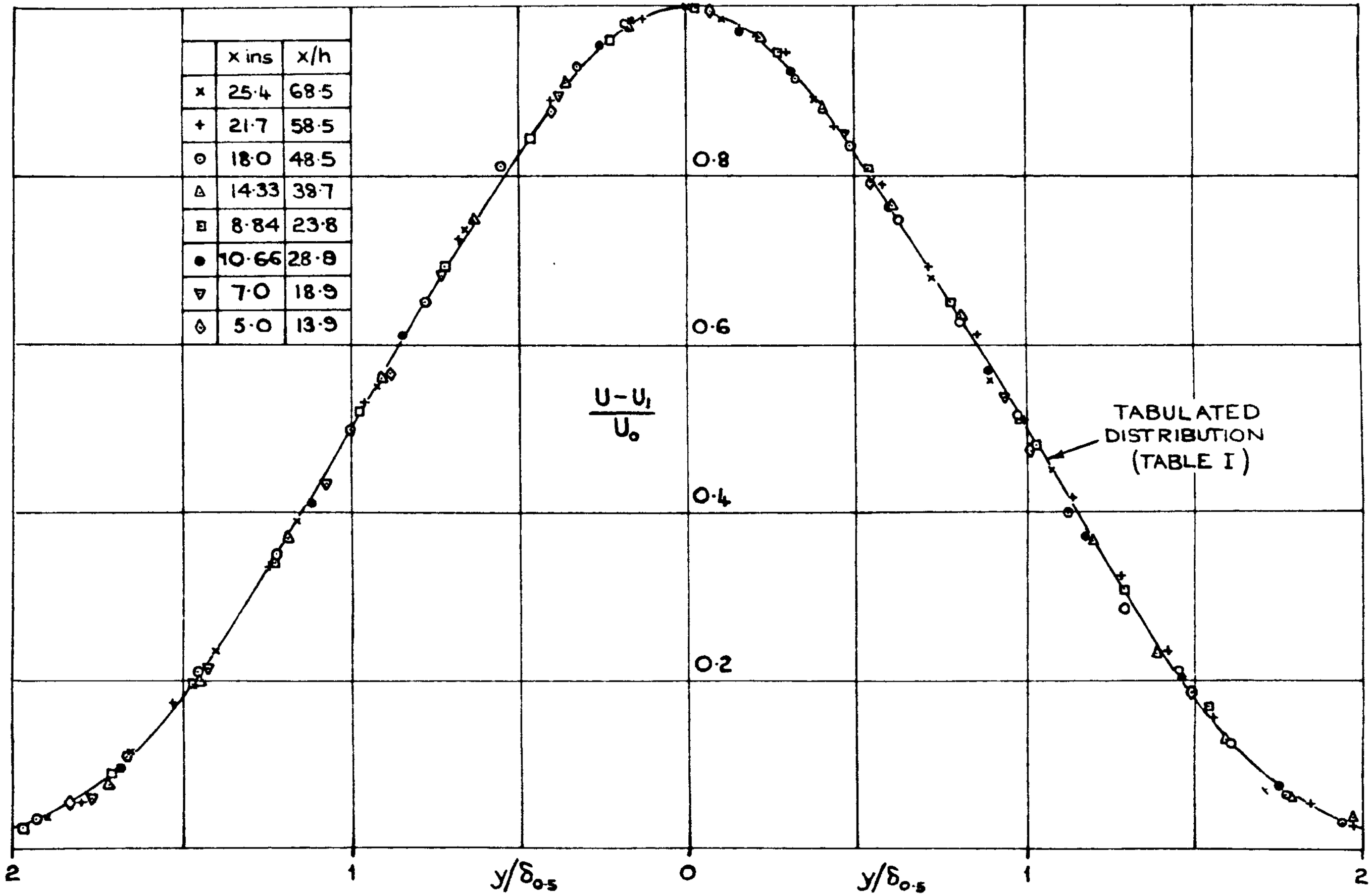

MEAN VELOCITY PROFILES IN A PLANE JET WITH $U_1/U_J = 0{\cdot}162$
(MEASURED WITH A PITOT AND STATIC TUBE)
FIG. 45

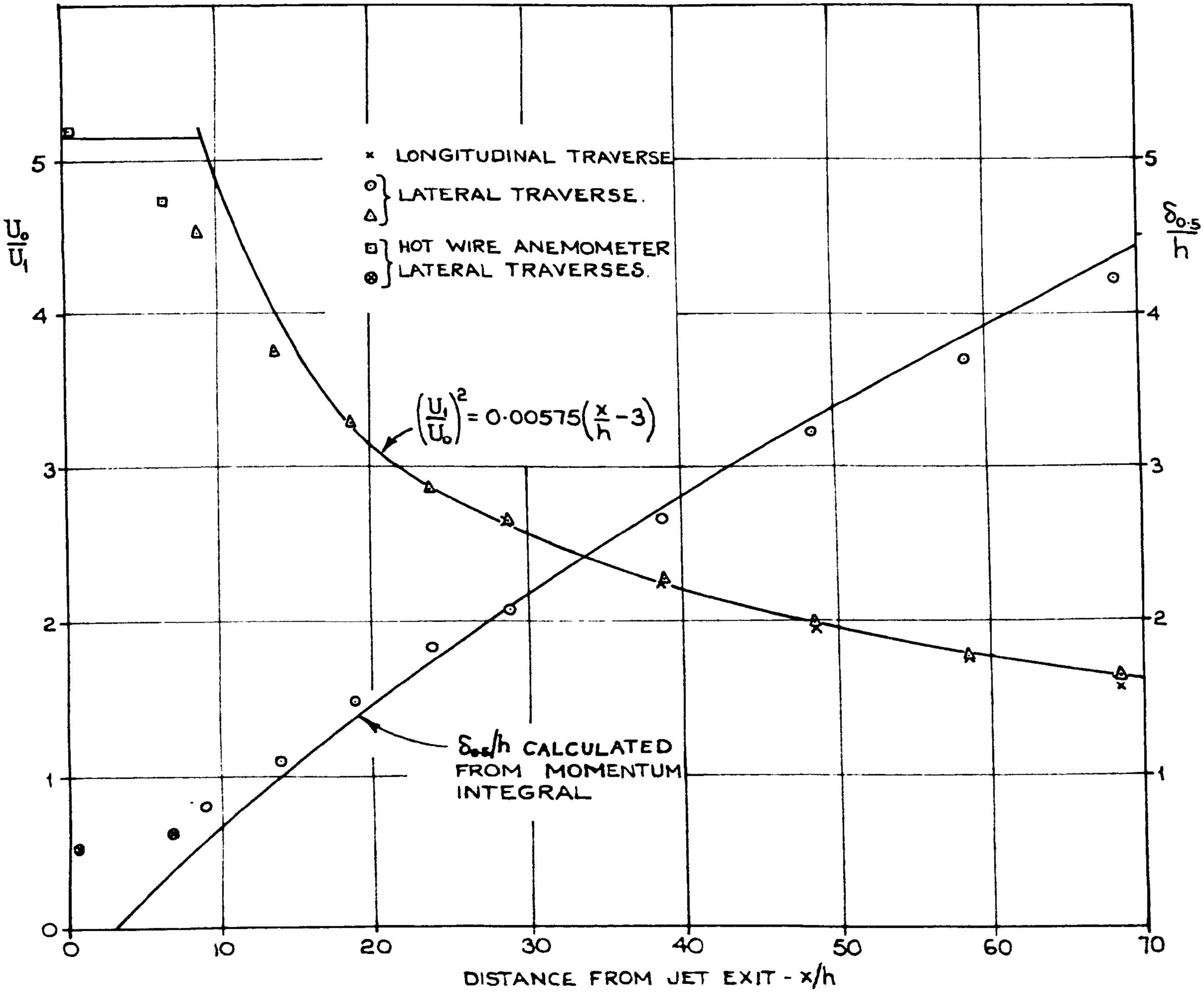

VARIATION OF JET WIDTH AND CENTRE-LINE VELOCITY IN A PLANE JET.

$U_1/U_J = 0.162$

FIG. 46

FIGURE 47.

LATERAL MEAN VELOCITY PROFILES IN A PLANE JET.

$U_1/U_j = 0.162$

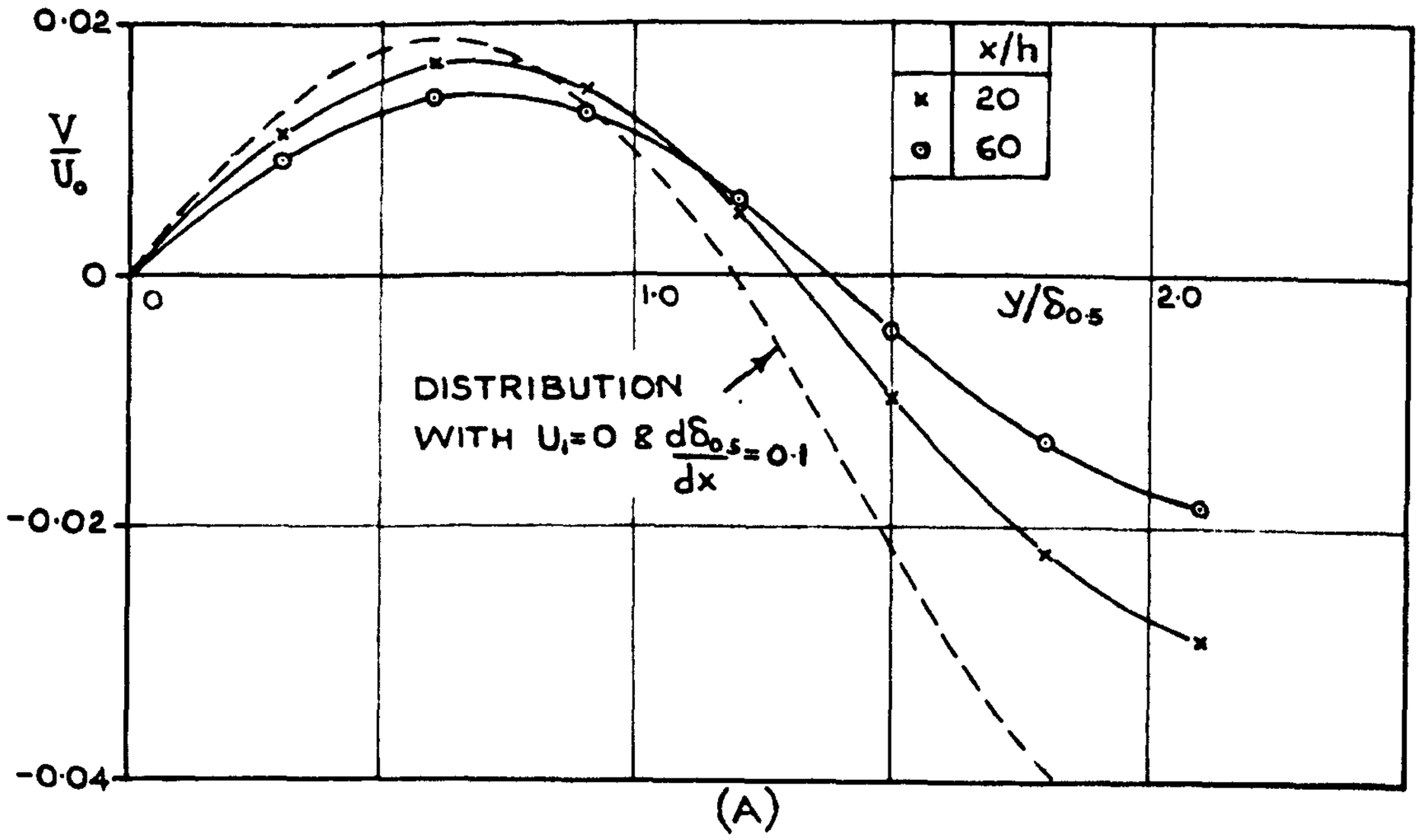

(A)

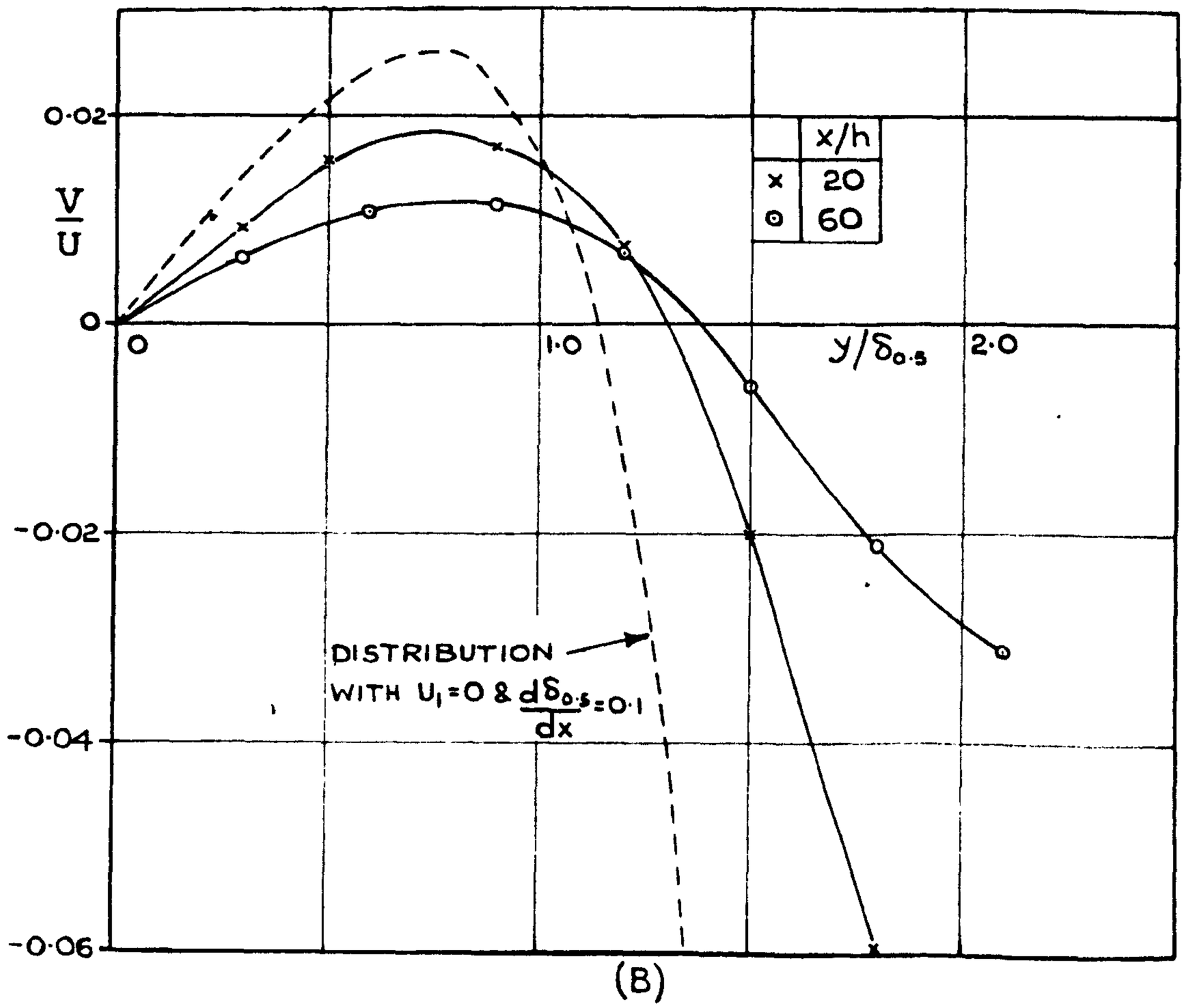

(B)

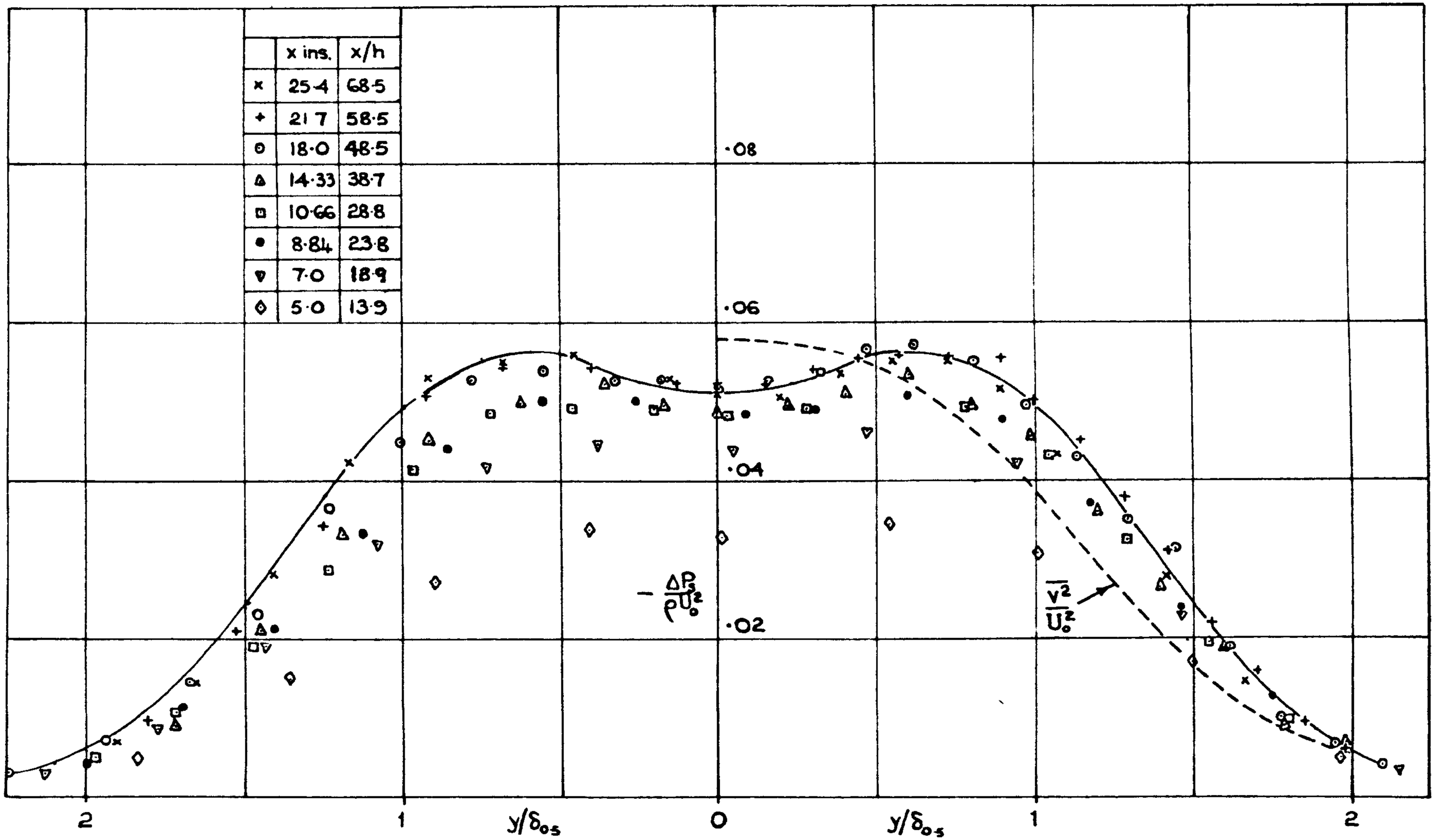

STATIC PRESSURE PROFILES IN A PLANE JET WITH $U_1/U_J = 0.162$

FIGURE 48 .

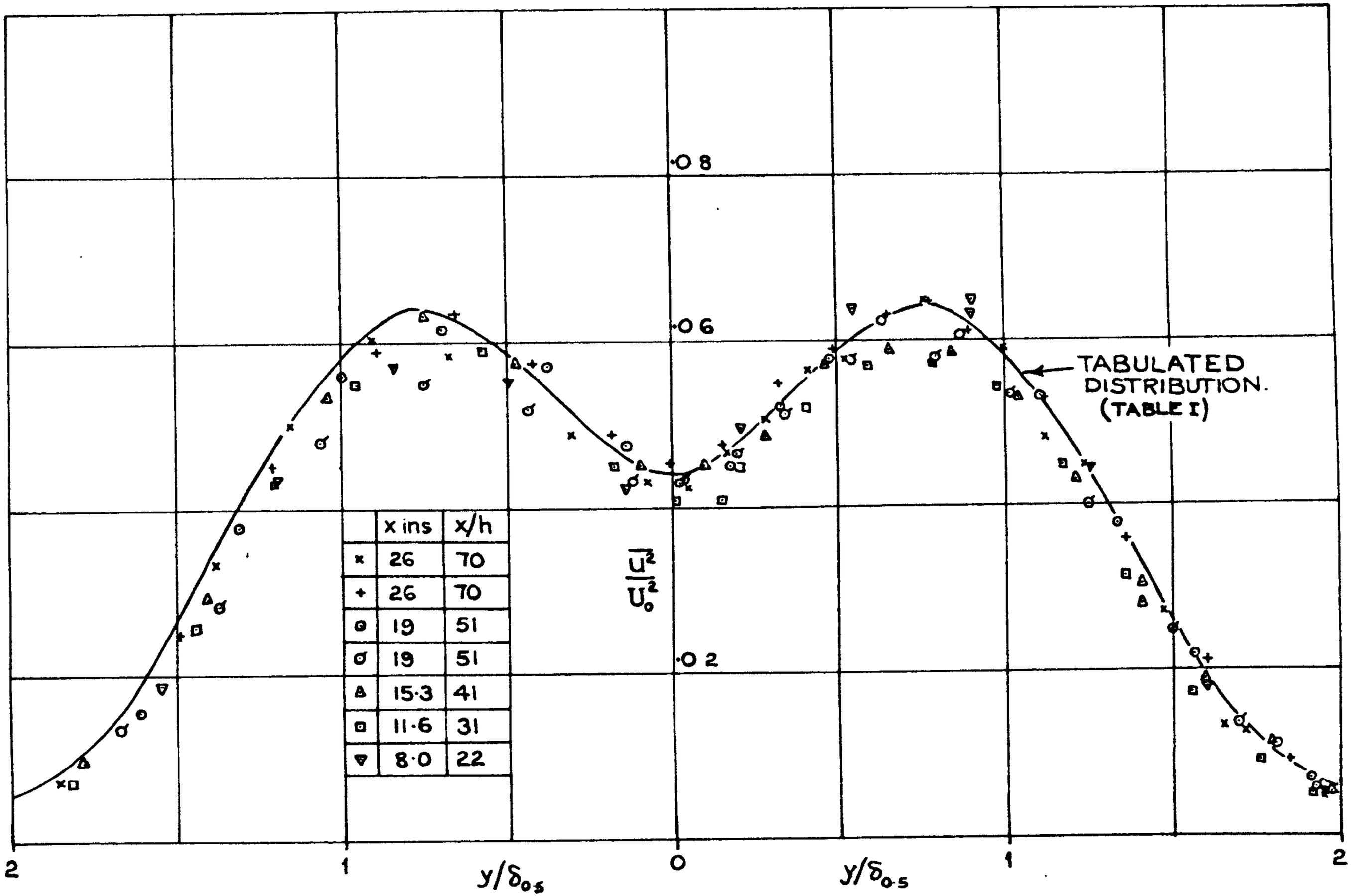

	x ins	x/h
×	26	70
+	26	70
⊙	19	51
σ	19	51
△	15·3	41
□	11·6	31
▽	8·0	22

$\overline{u^2}$ PROFILES IN A PLANE JET WITH $U_1/U_j = 0.162$
(MEASURED WITH A 0·0001" DIA. Pt. WIRE)
FIG. 49

FIG. 50

STATIC PRESSURE ON THE CENTRE LINE OF A PLANE JET.
$U_1/U_J = 0{\cdot}162$

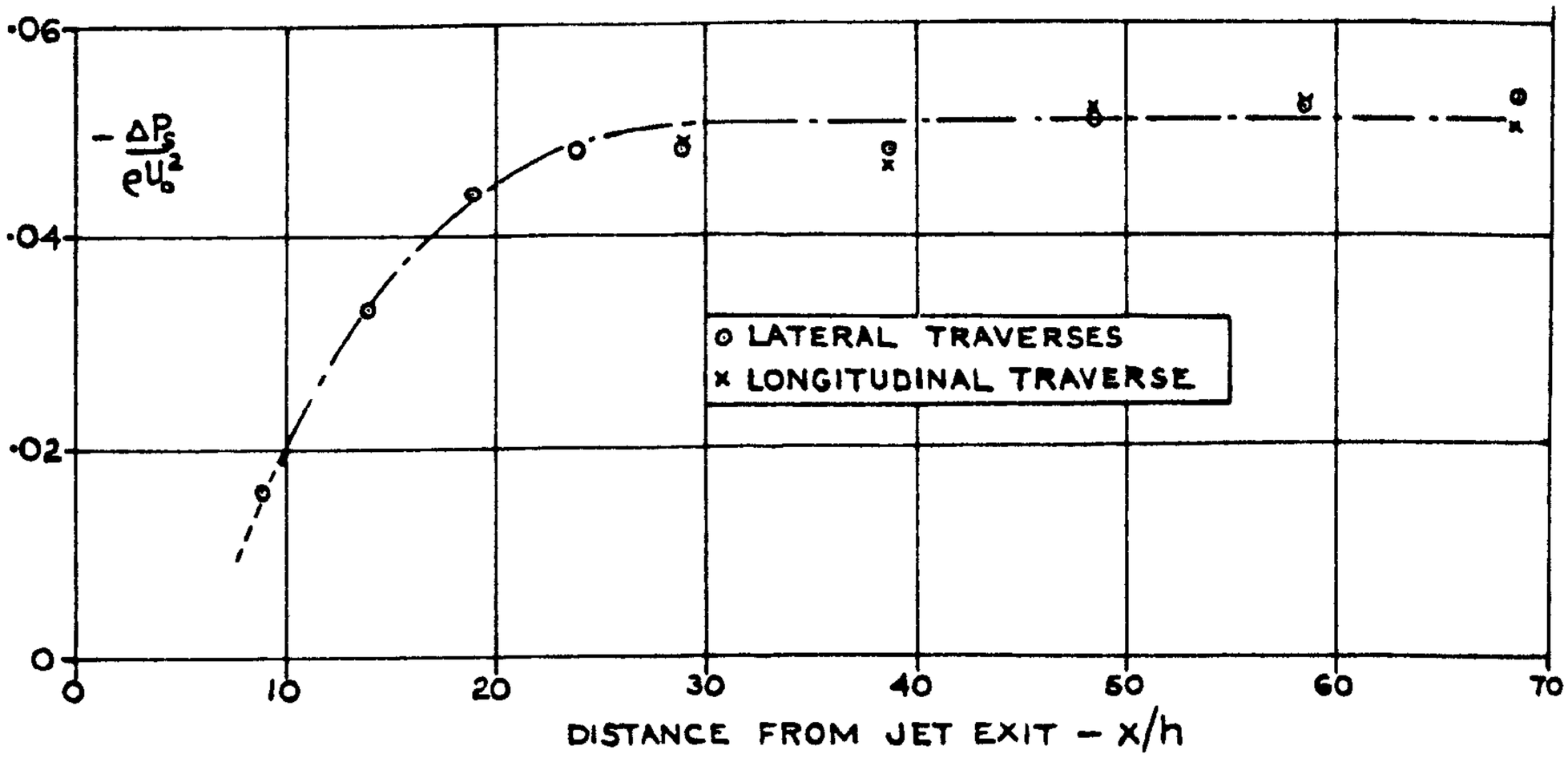

FIG. 51

$\overline{U^2}$ ON THE CENTRE LINE OF A PLANE JET
$U_1/U_J = 0{\cdot}162$

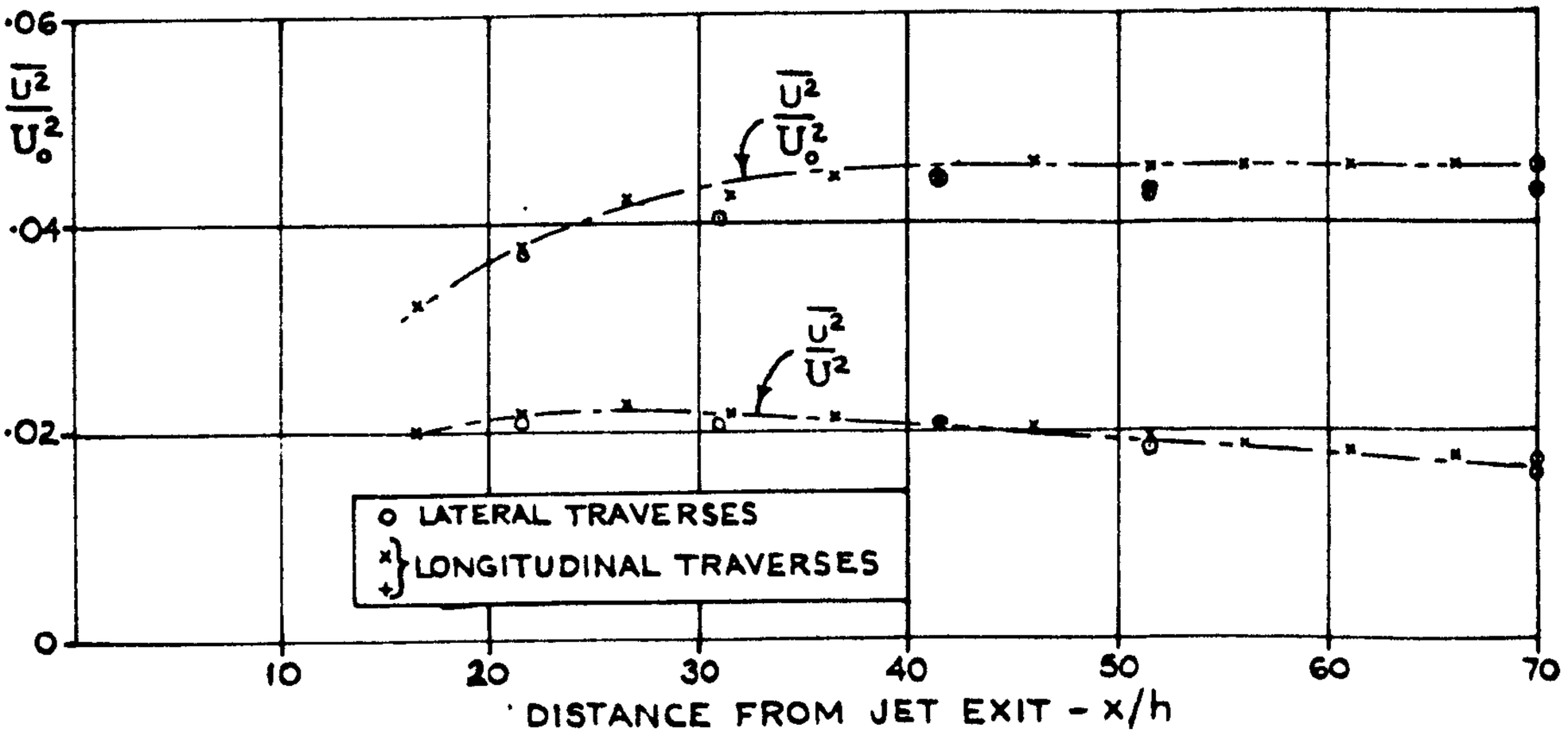

FIG. 52

INTERMITTENCY MEASUREMENTS FOR A SINUSOIDAL BOUNDARY.

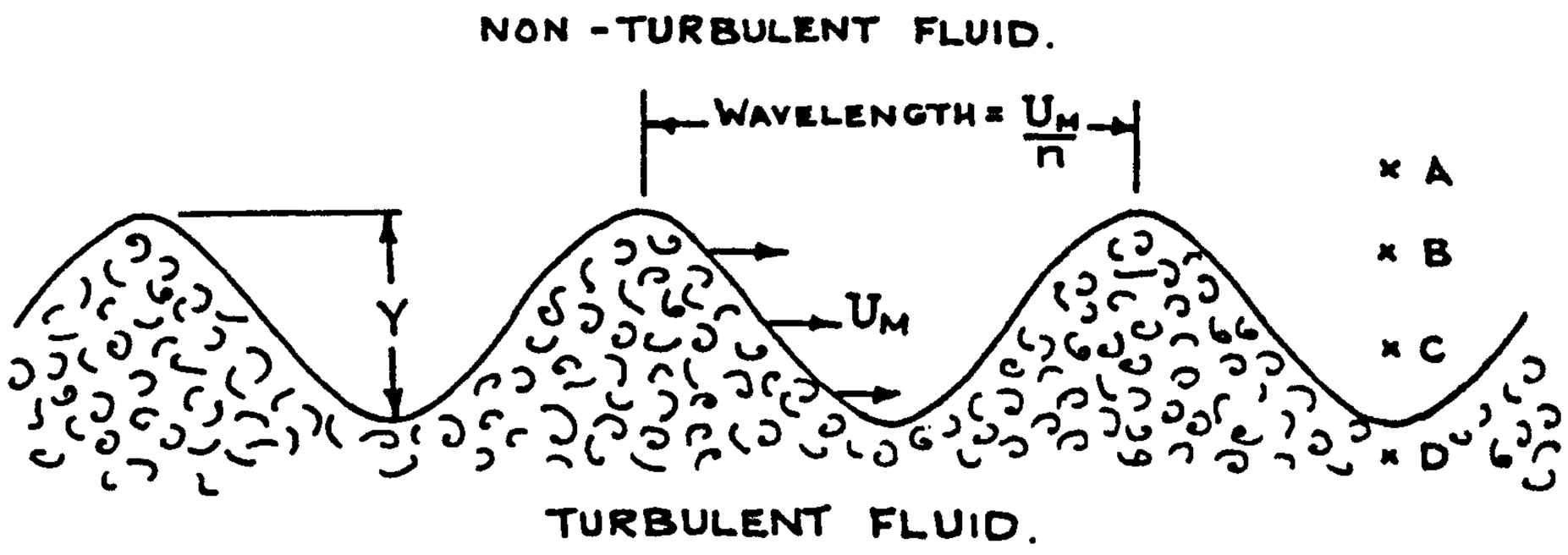

(A) SCHEMATIC REPRESENTATION OF INTERMITTENT REGION.

HOT WIRE POSITION	INTERMITTENCY METER OUTPUTS.
A	—DATUM —
B	—DATUM —
C	—DATUM —
D	—DATUM—

(B) SIGNALS FROM INTERMITTENCY METER

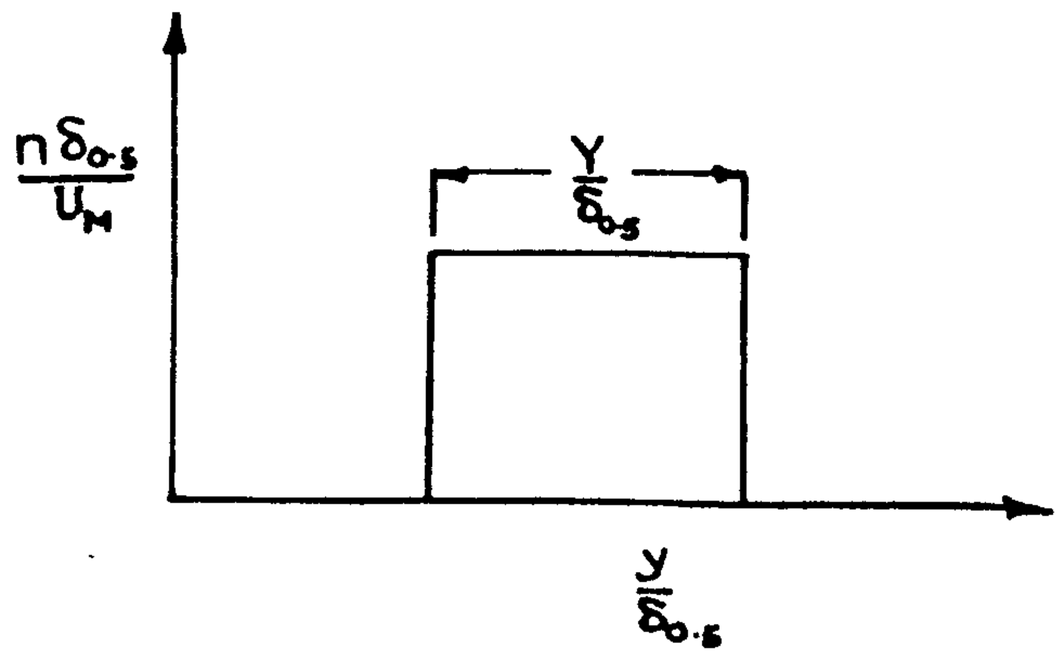

(C) FREQUENCY MEASUREMENTS IN INTERMITTENT REGION.

FIGURE 53

THE INTERMITTENCY FACTOR IN A PLANE JET.
$U_1/U_J = 0.162$

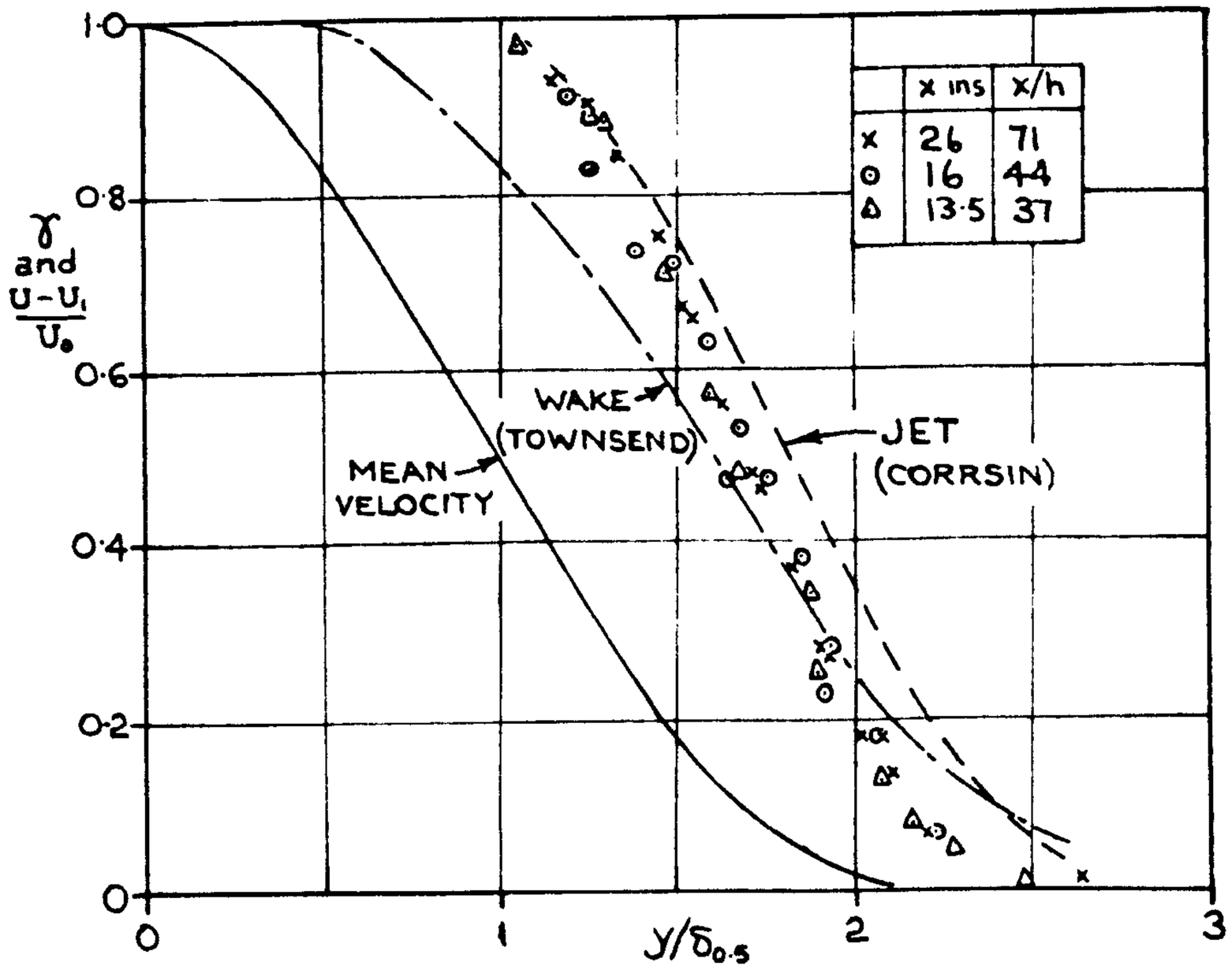

FIGURE 54.

FREQUENCY OF EDDIES RESPONSIBLE FOR INTERMITTENCY.
$U_1/U_J = 0.162$

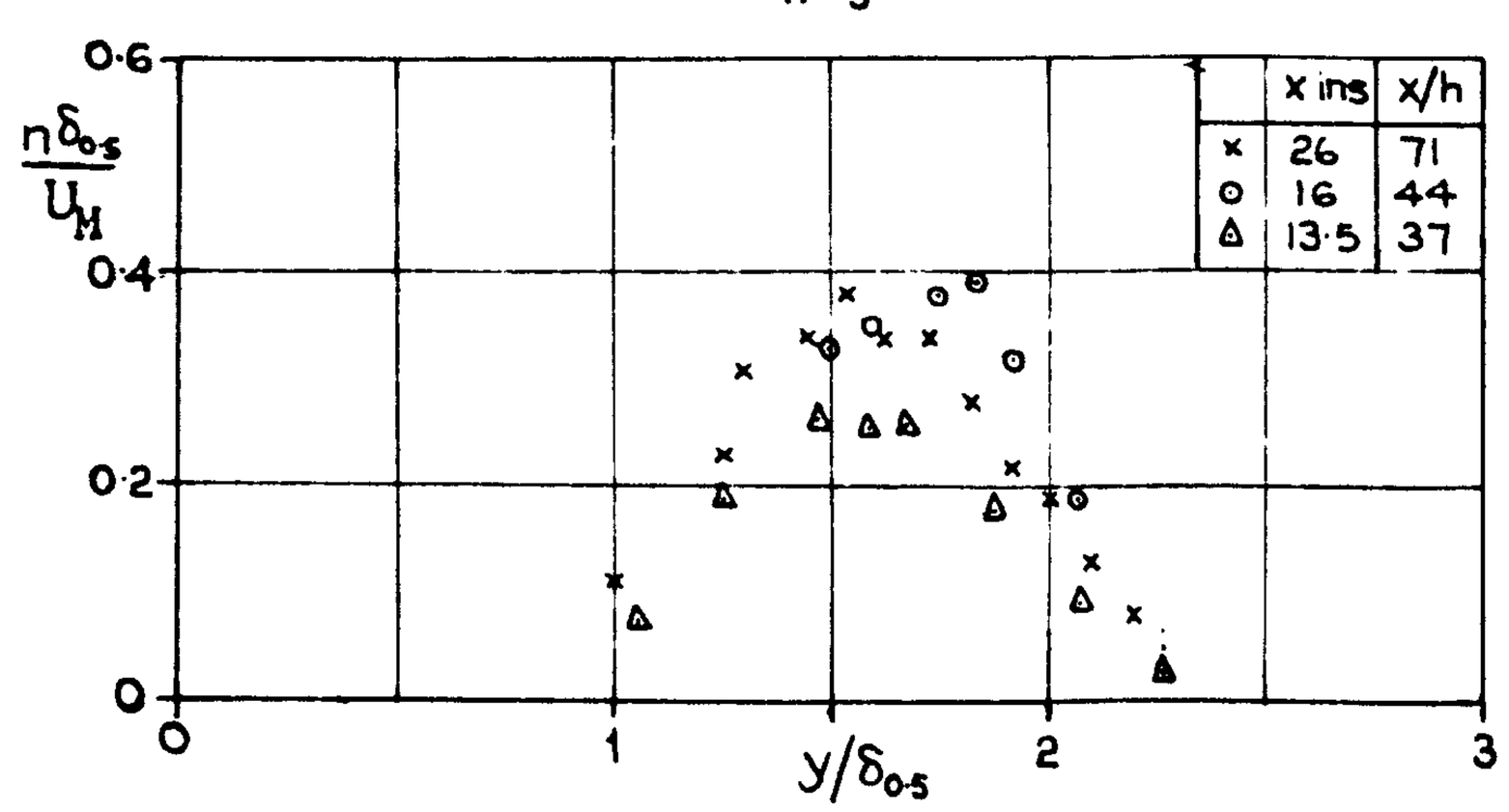

FIGURE 55
THE TURBULENT SHEAR STRESS PROFILE.

$U_1/U_J = 0.162$

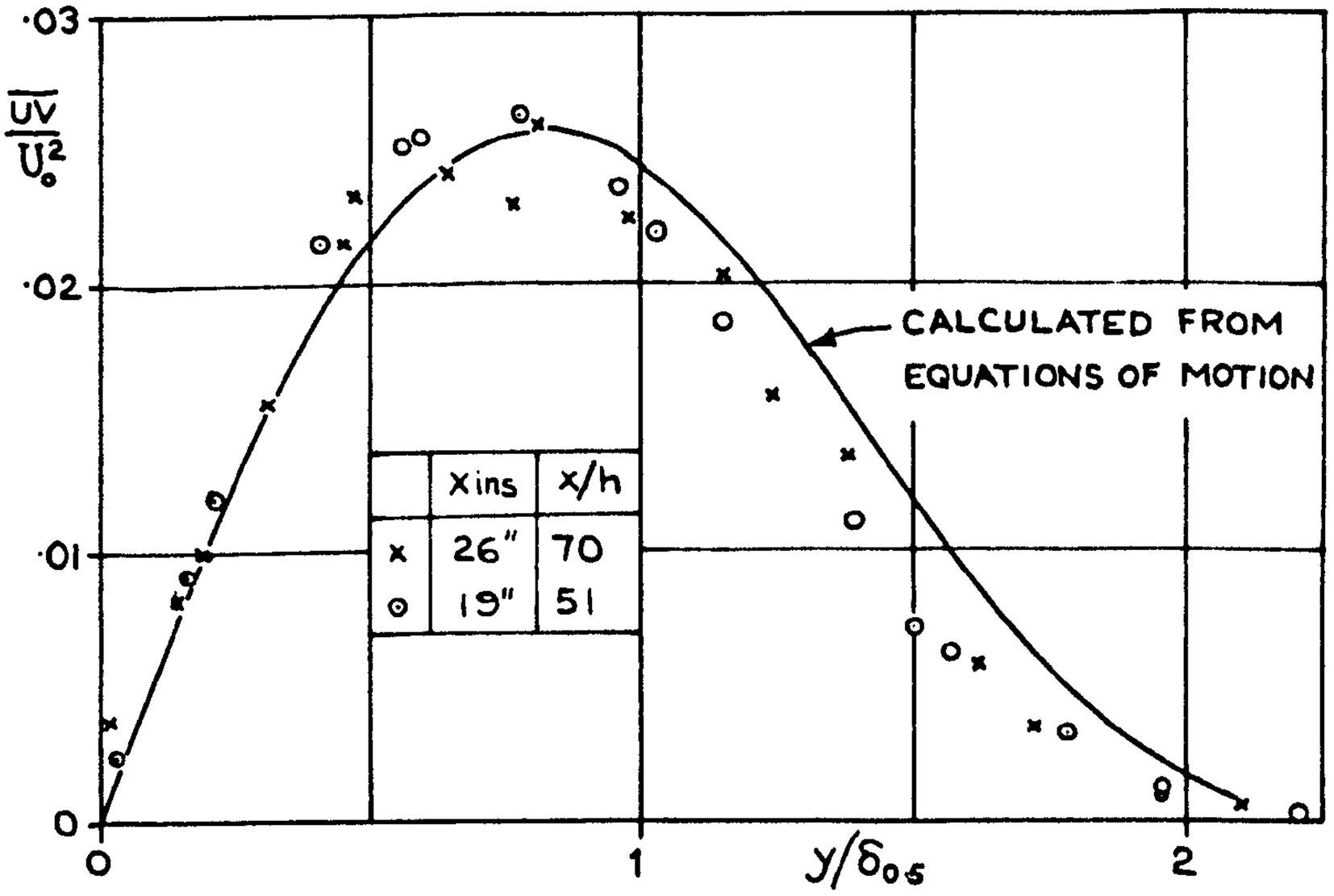

FIGURE 56
THE $\overline{V^2}$ AND $\overline{W^2}$ PROFILES
$U_1/U_J = 0.162$

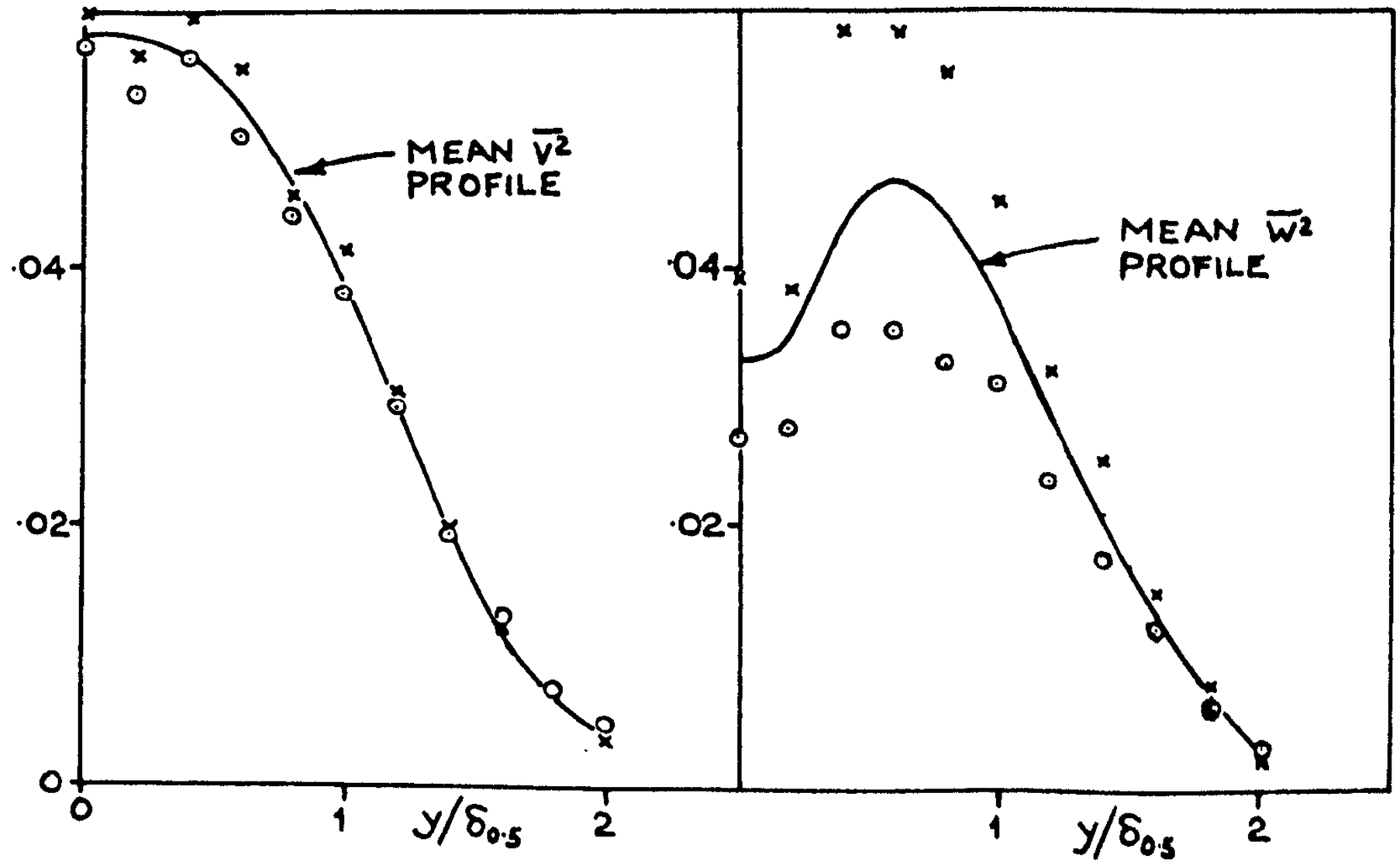

FIGURE 57

TURBULENT INTENSITY DISTRIBUTIONS ACROSS A PLANE JET

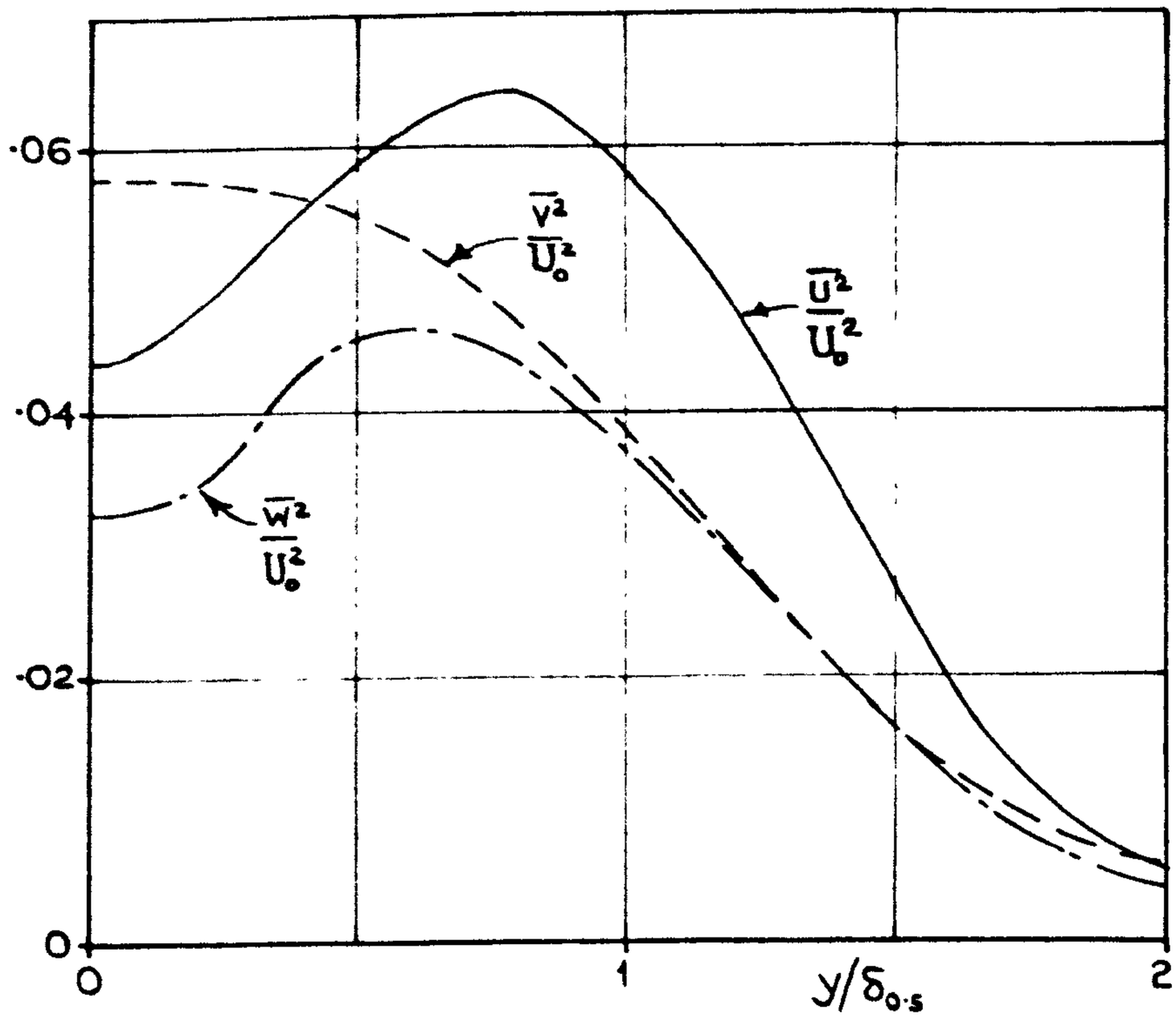

FIGURE 58.

TURBULENT ENERGY DISTRIBUTION ACROSS A PLANE JET.

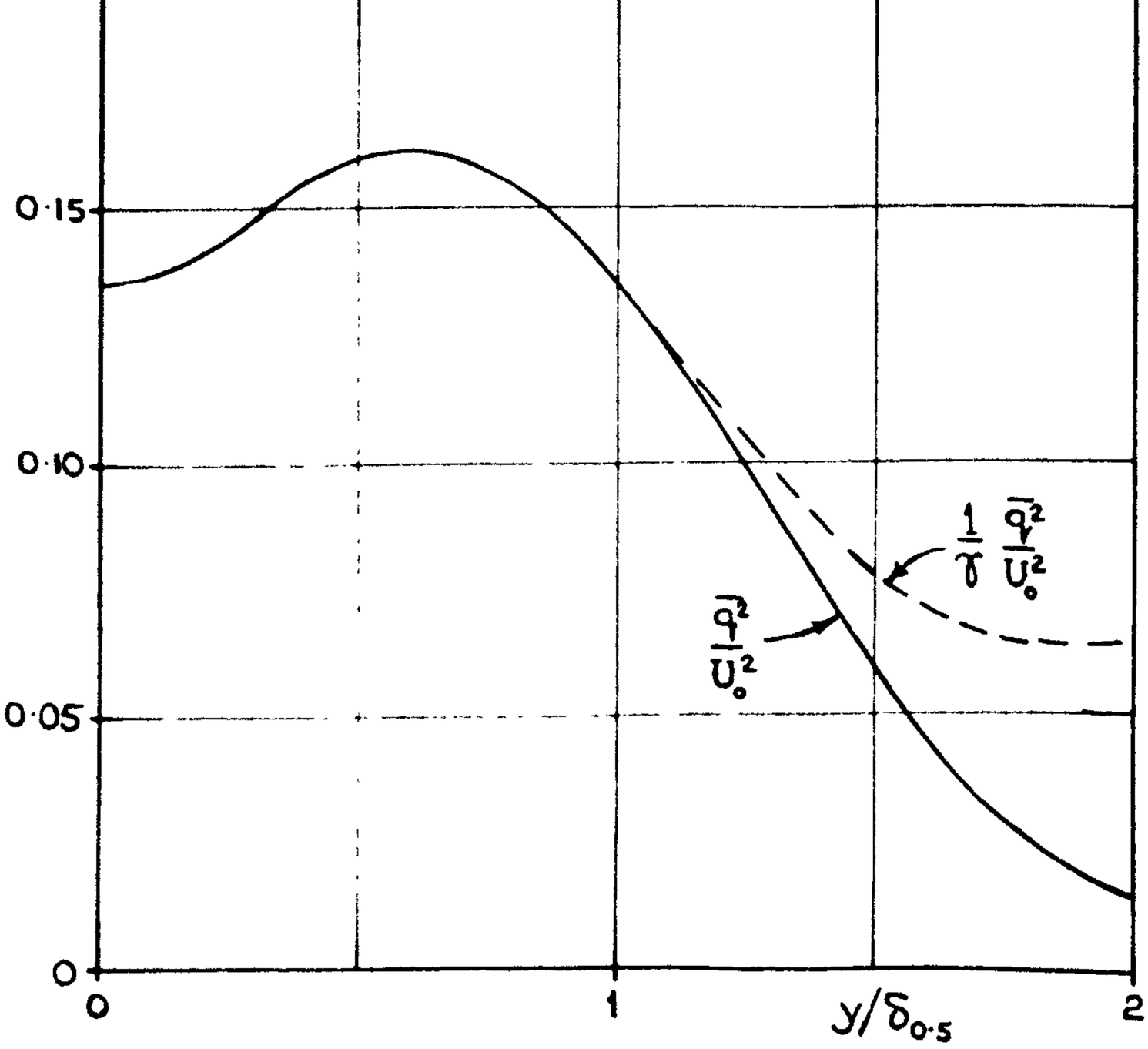

FIGURE 59.

RATIO OF TURBULENT INTENSITIES ACROSS A PLANE JET.

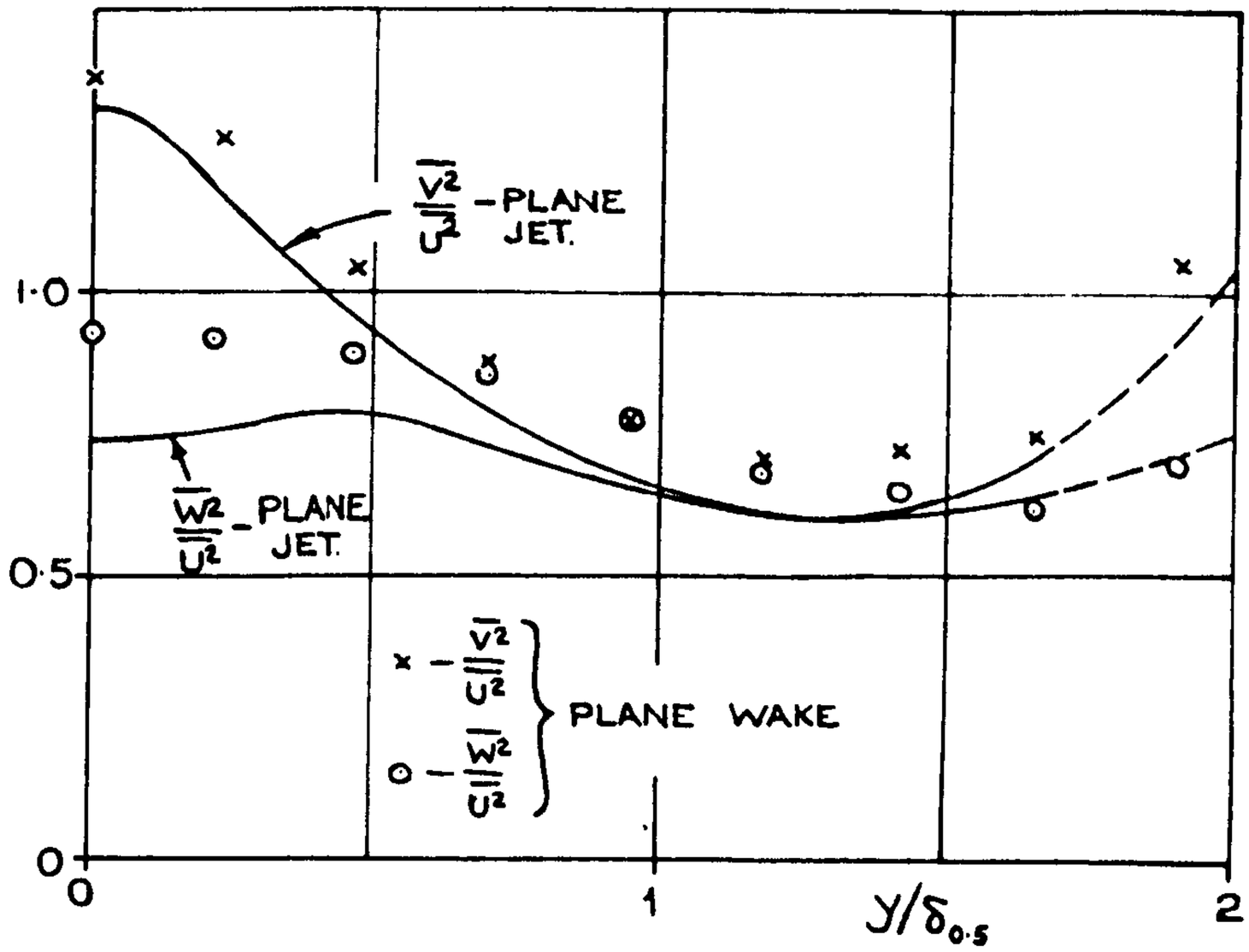

FIGURE 60

$\frac{\overline{UV}}{\overline{U^2}}$ PROFILE IN A PLANE JET

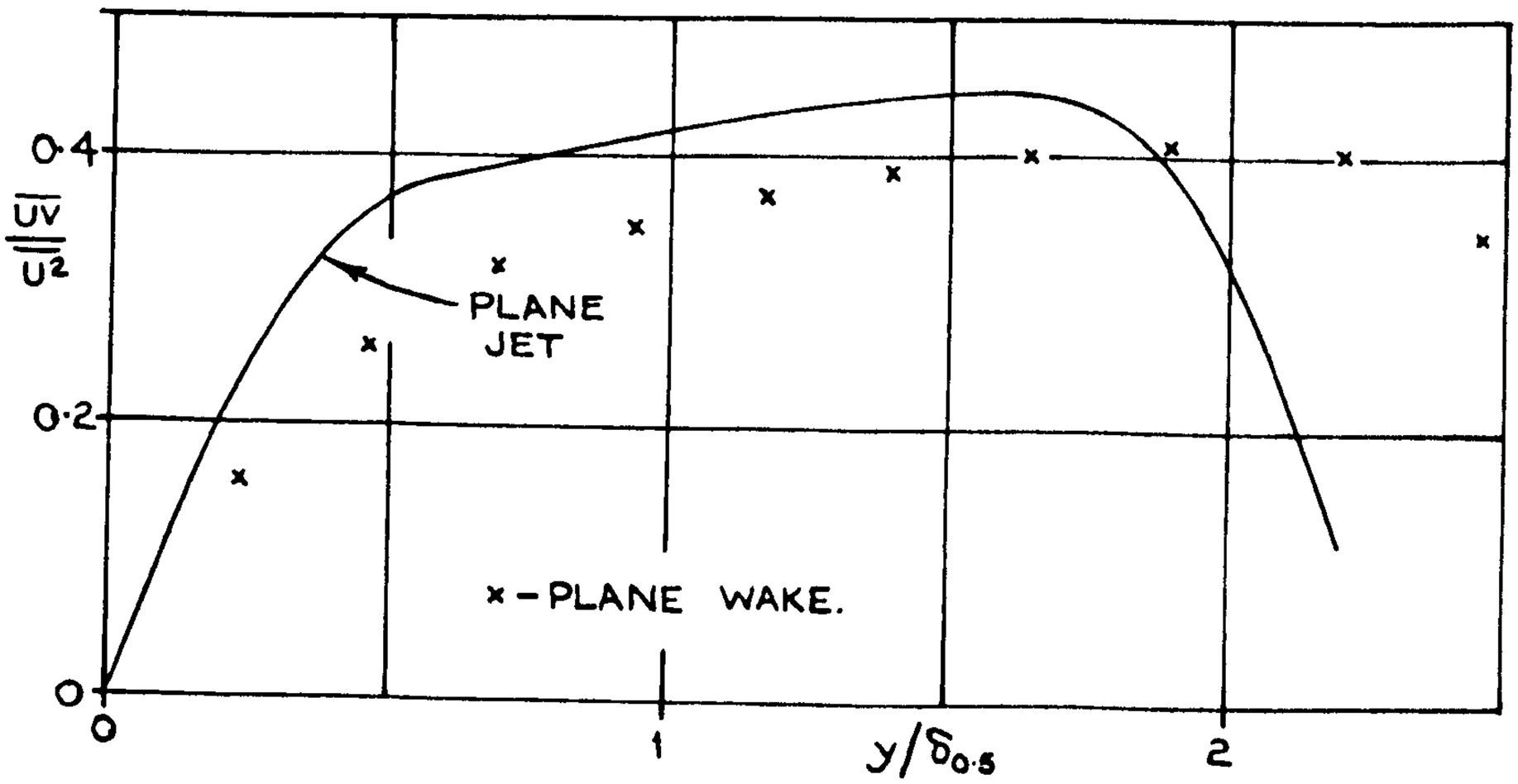

FIGURE 61

SHEAR STRESS CORRELATION COEFFICIENT IN A PLANE JET

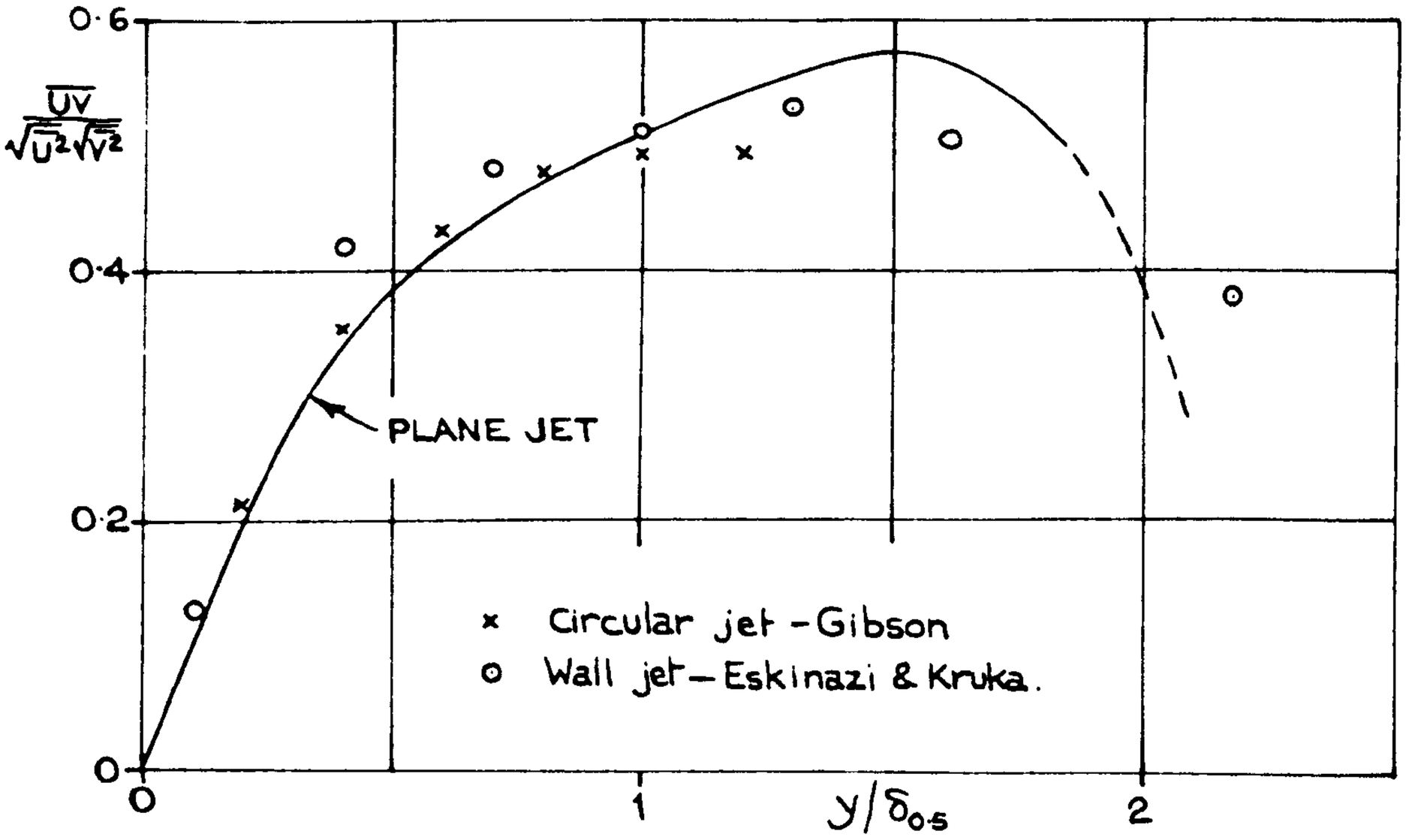

FIGURE 62

MICRO-SCALE OF TURBULENCE ACROSS A PLANE JET.

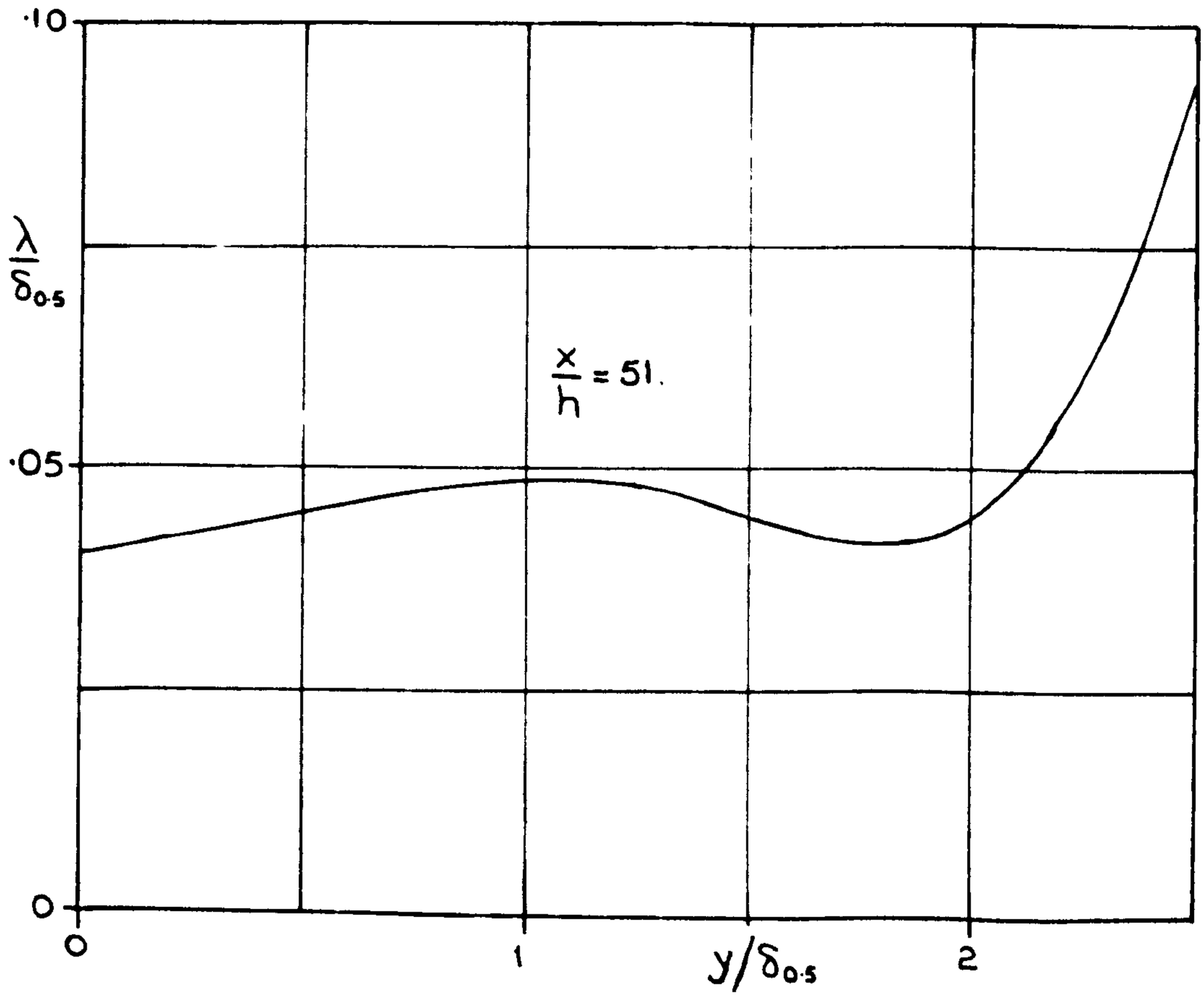

FIGURE 63

THE TURBULENT ENERGY BALANCE IN A PLANE JET.

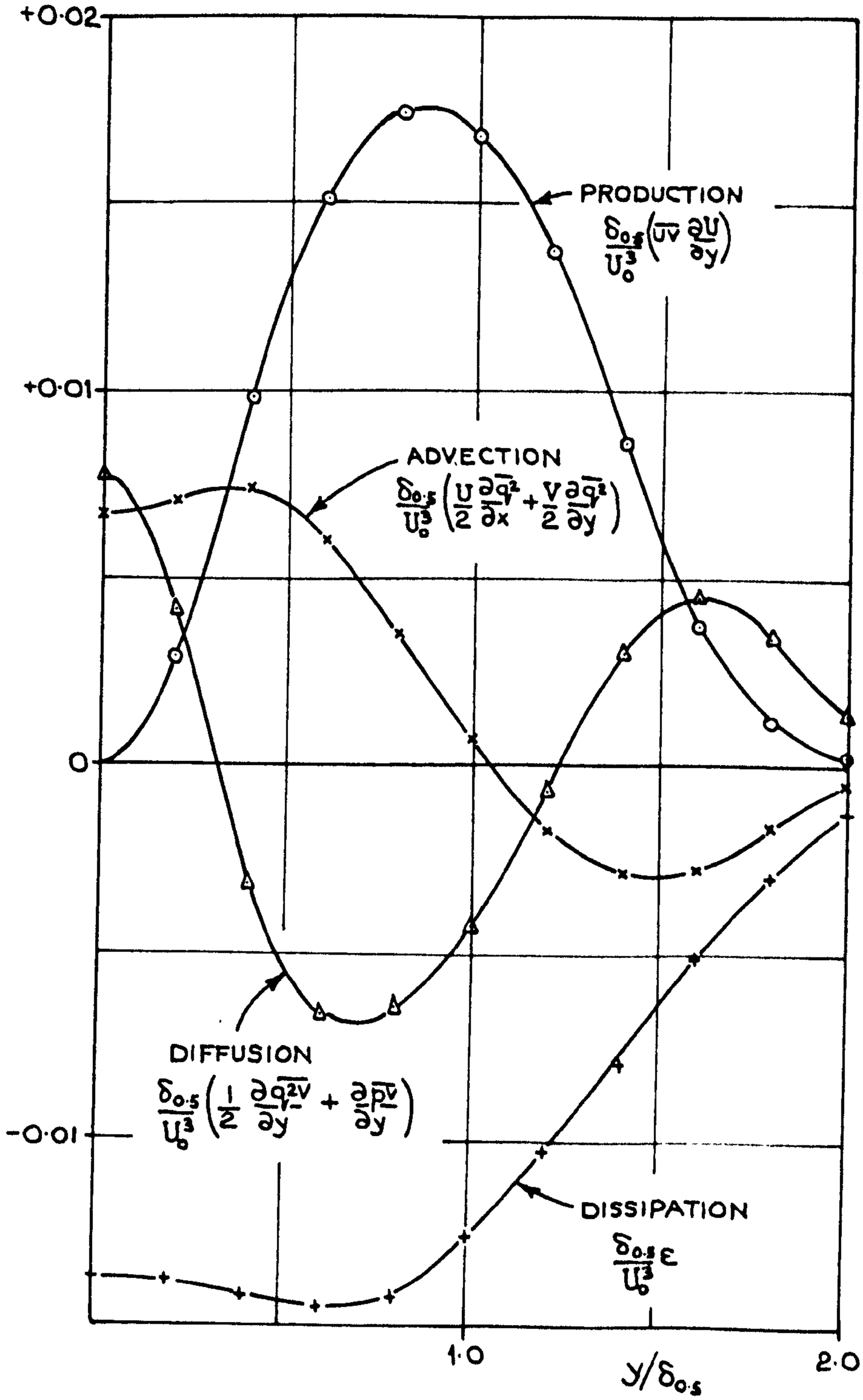

FIGURE 64

VARIATION OF TRANSVERSE CORRELATION COEFFICIENT WITH CUT-OFF FREQUENCY.
$U_1/U_J = 0.162$

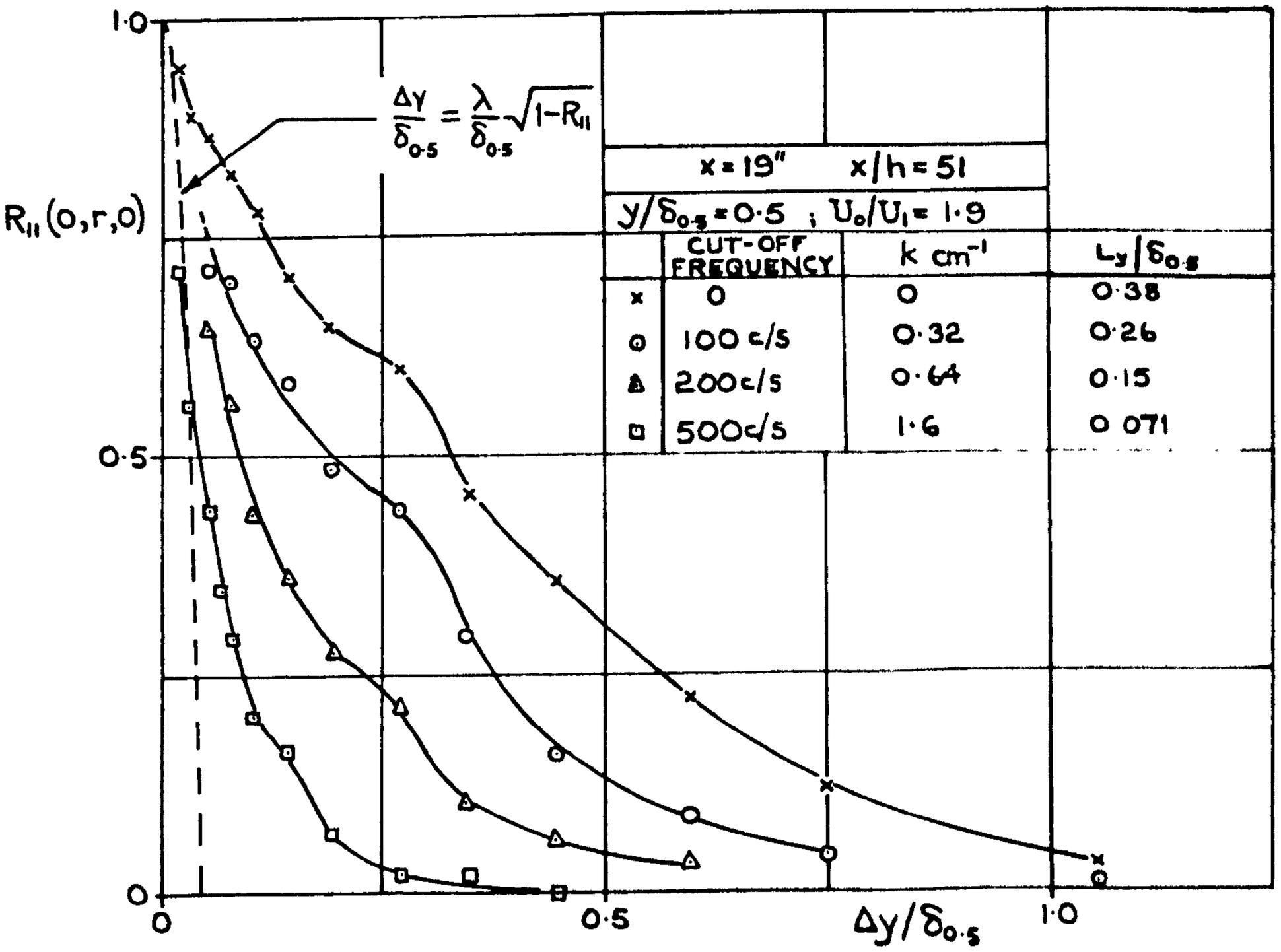

FIGURE 65.
SHEAR STRESS AND $\overline{u^2}$ SPECTRA.
$U_1/U_J = 0.162$

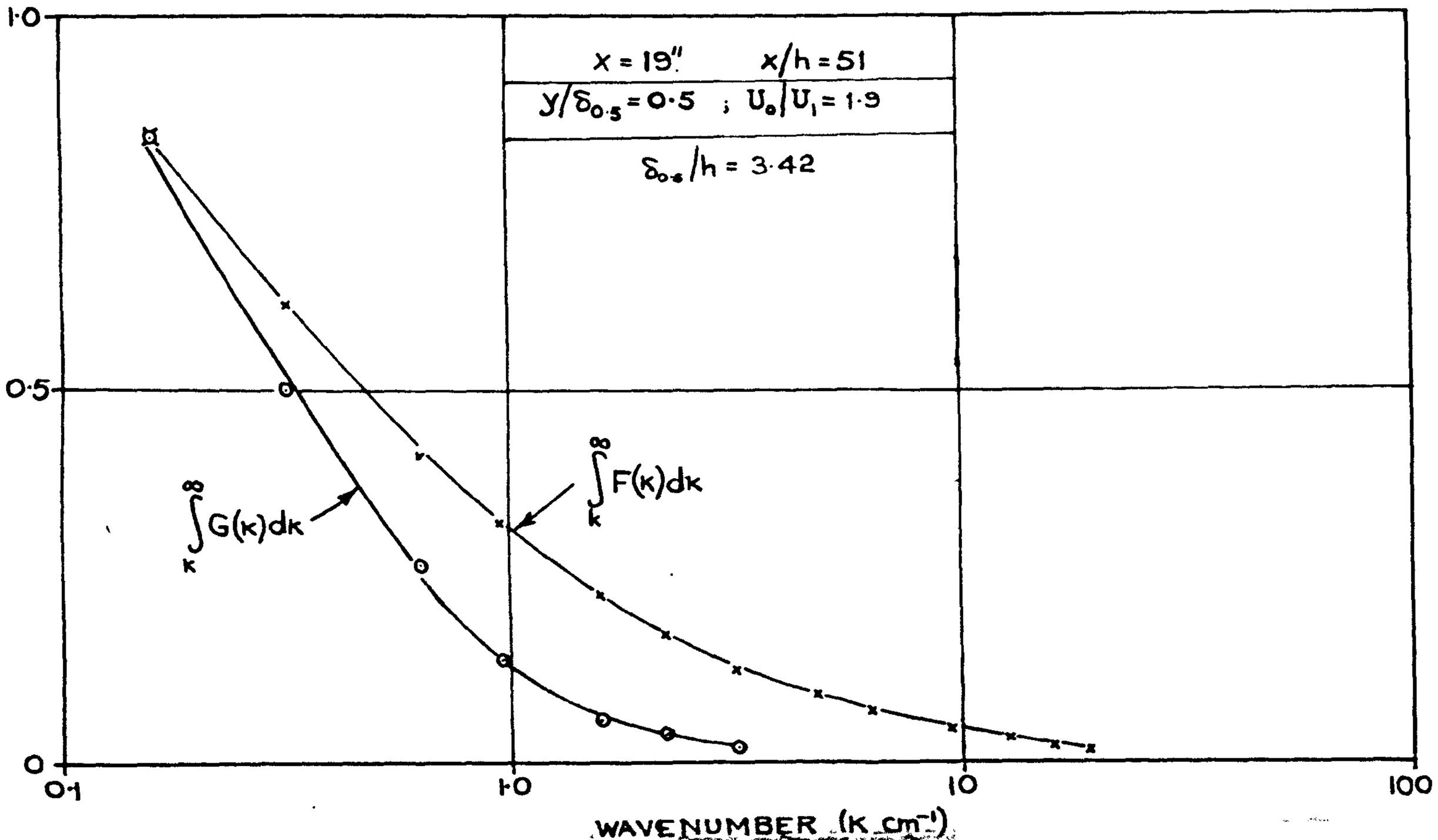

FIGURE 66.
$\overline{u^2}$ AND DISSIPATION SPECTRA.
$U_1/U_J = 0.162$

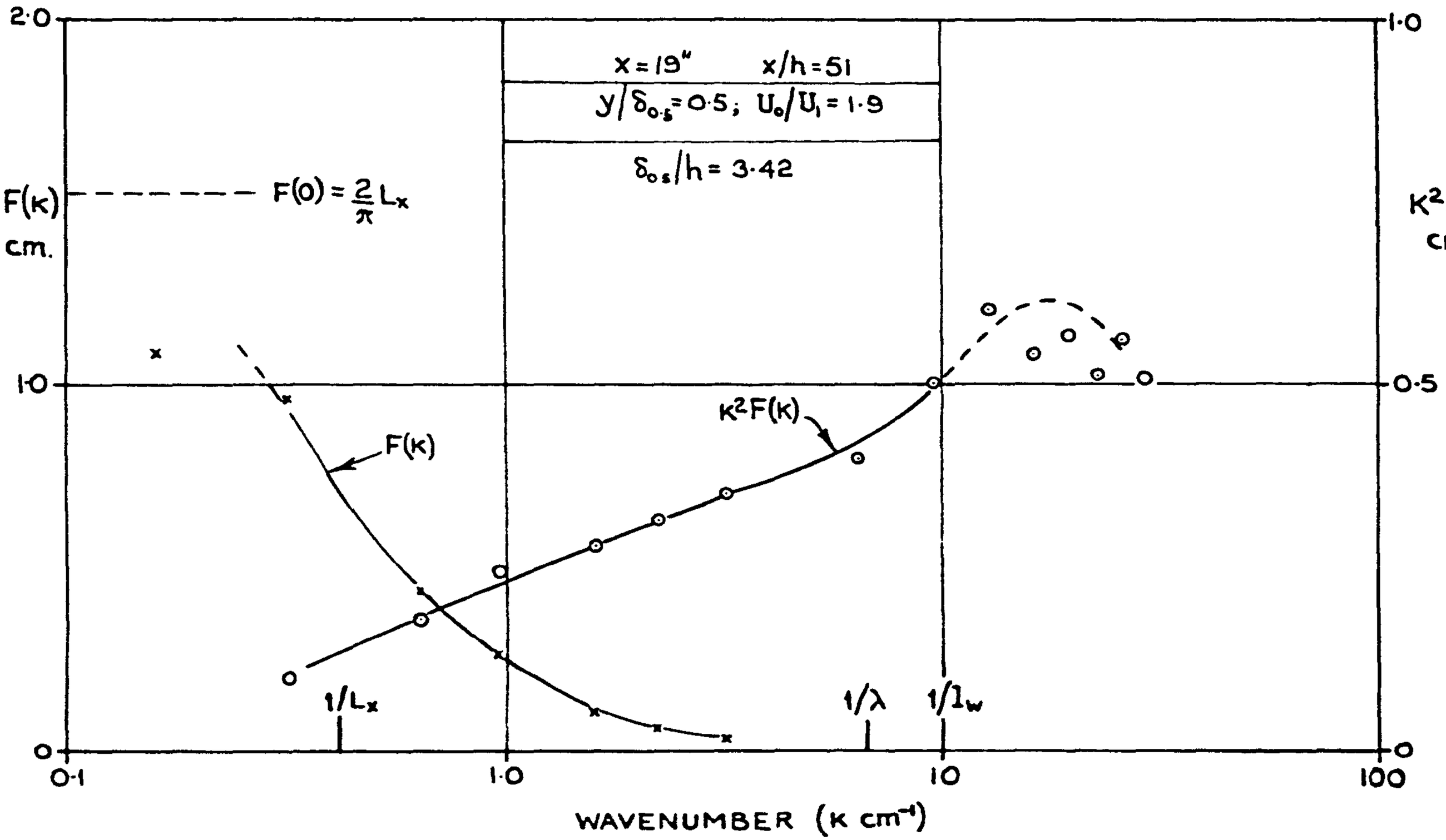

FIGURE 67

$\overline{U^2}$ SPECTRUM

$U_1/U_J = 0.162$

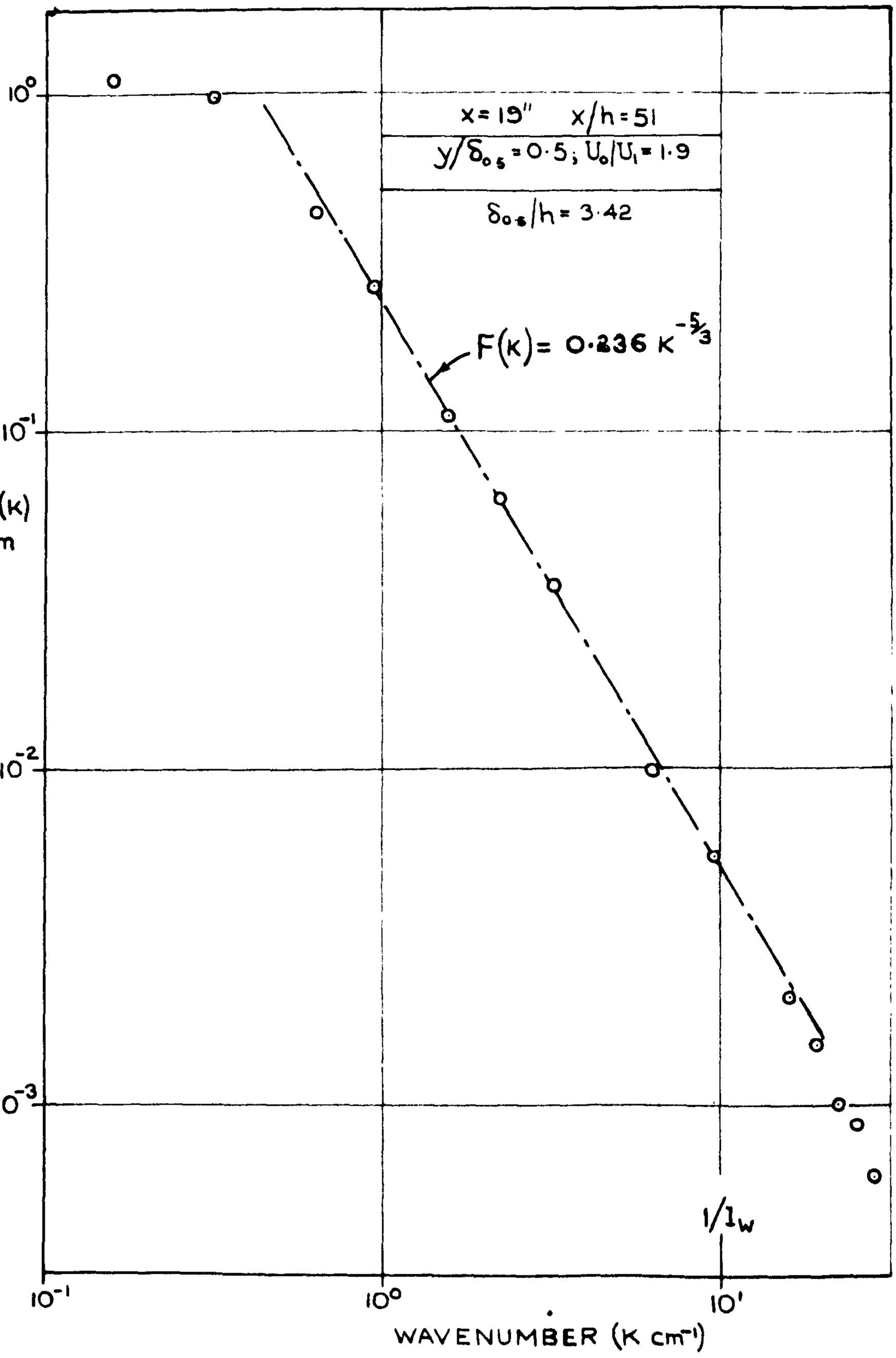

FIGURE 68

THE $\overline{u^2}$ DISTRIBUTION IN THE IRROTATIONAL REGION OF THE FLOW

$U_1/U_j = 0.162$

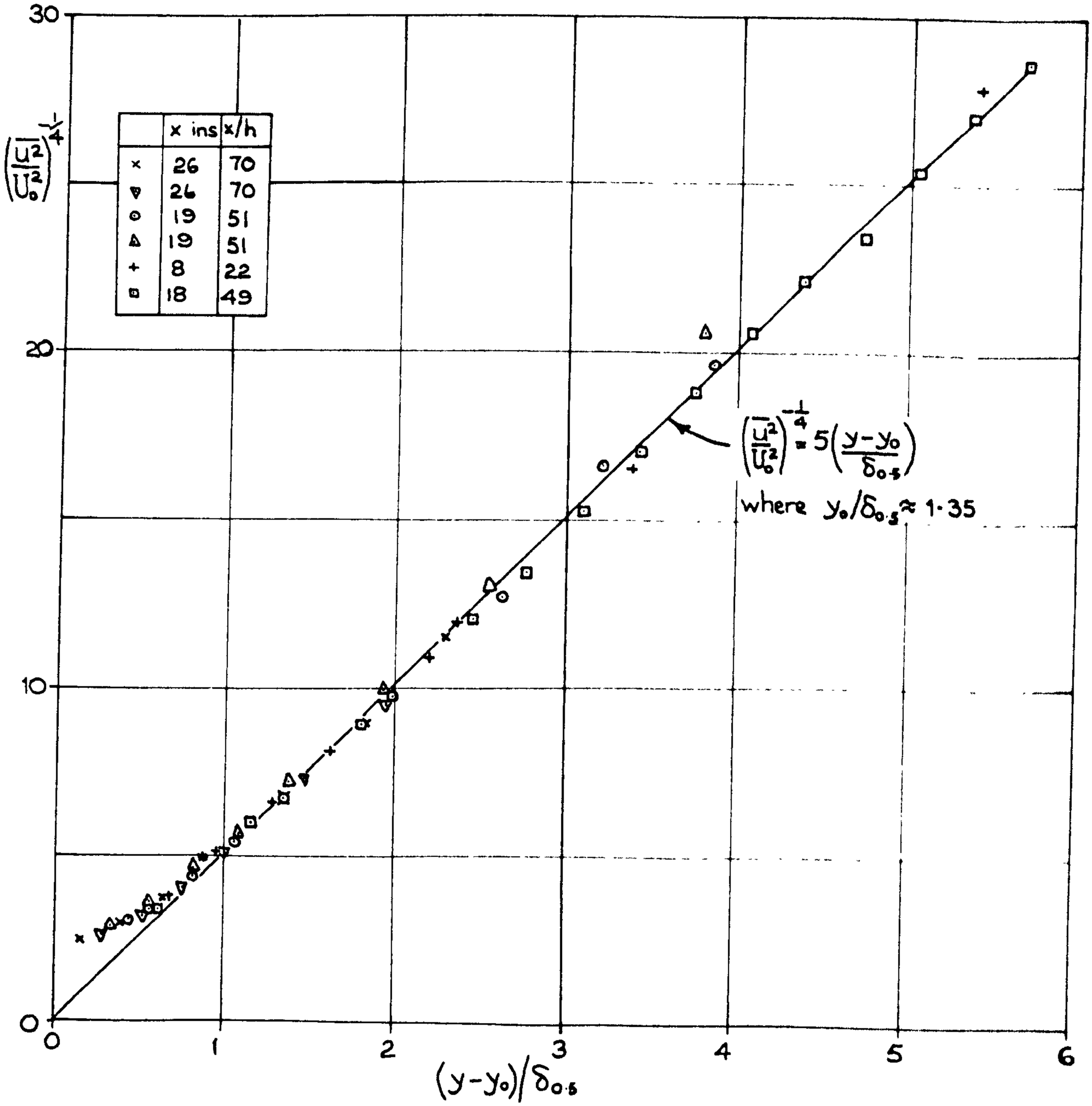

FIGURE 69.

EDDY VISCOSITY DISTRIBUTION ACROSS A PLANE JET.

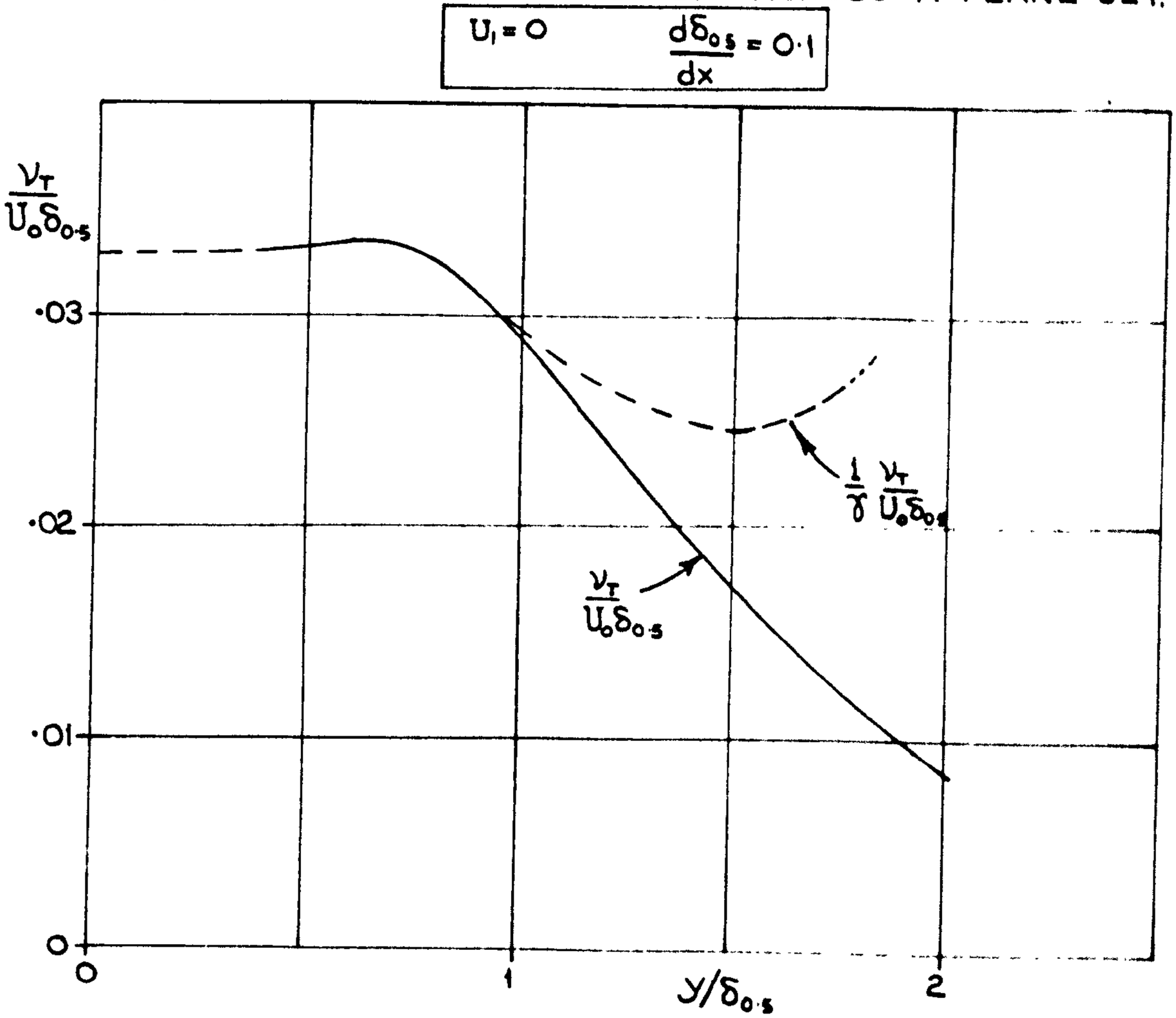

FIGURE 70

MIXING LENGTH DISTRIBUTION ACROSS A PLANE JET.

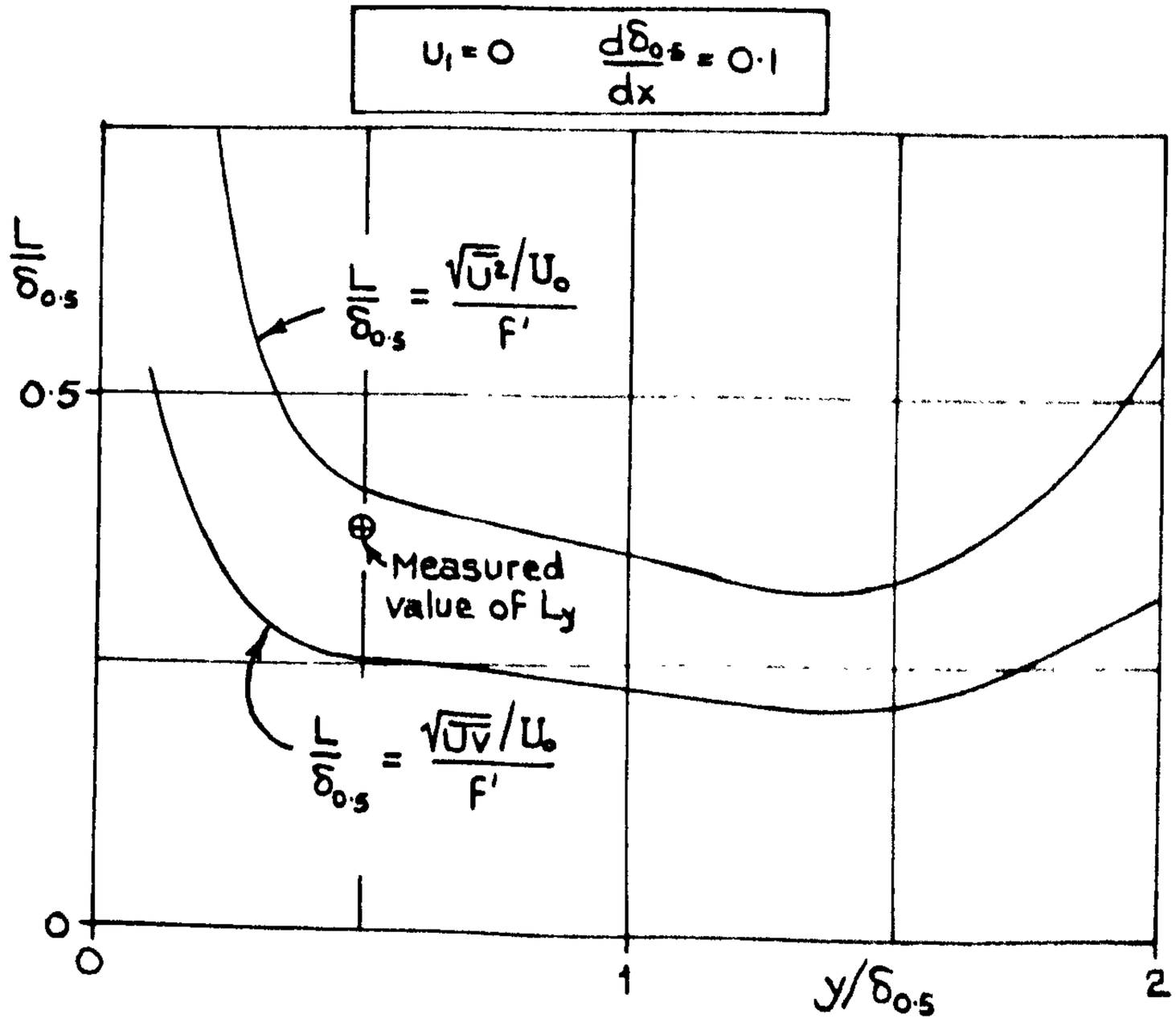

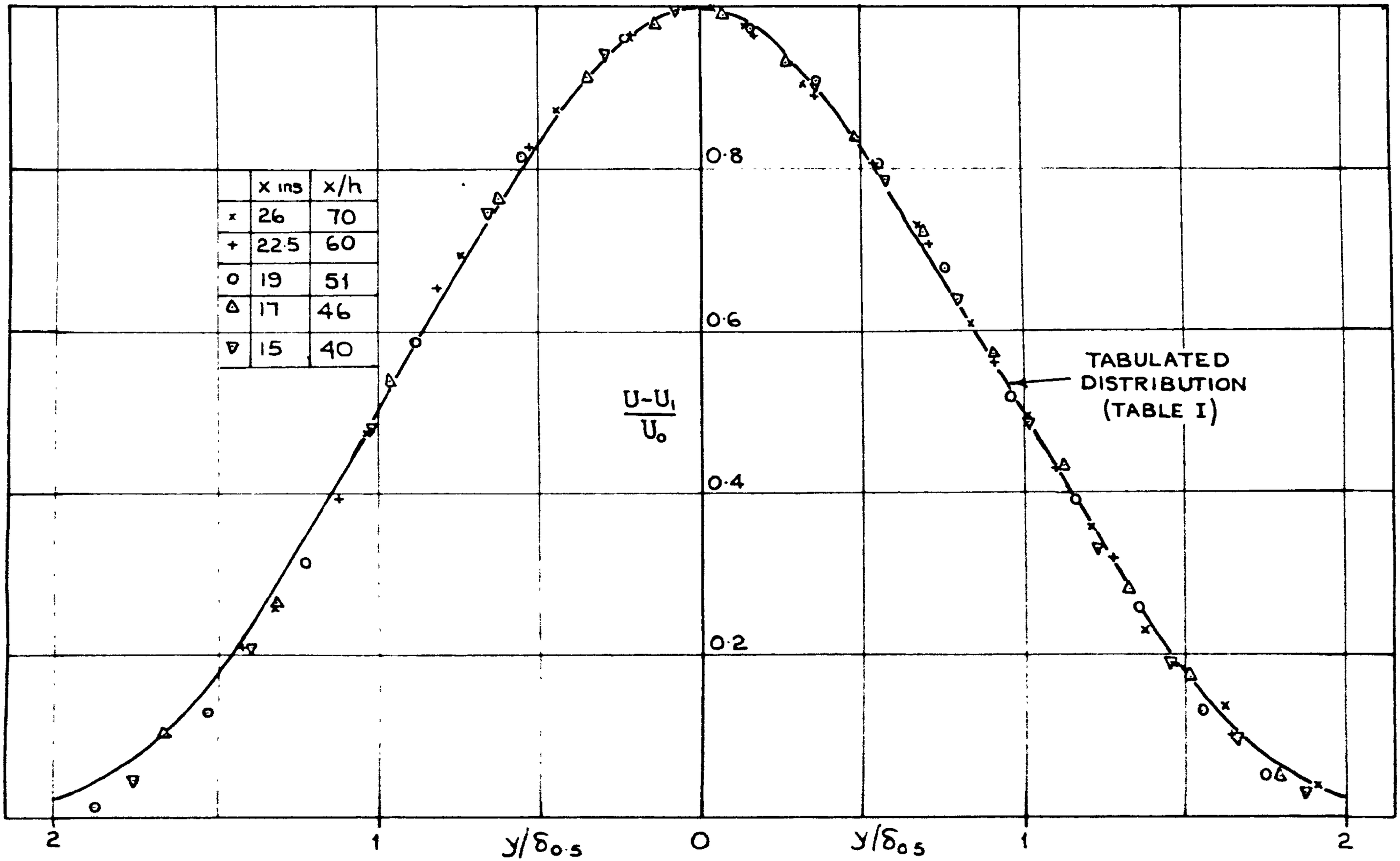

MEAN VELOCITY PROFILES IN A PLANE JET WITH $U_1/U_j = 0.58$
(MEASURED WITH A PITOT AND A STATIC TUBE)
FIGURE 71

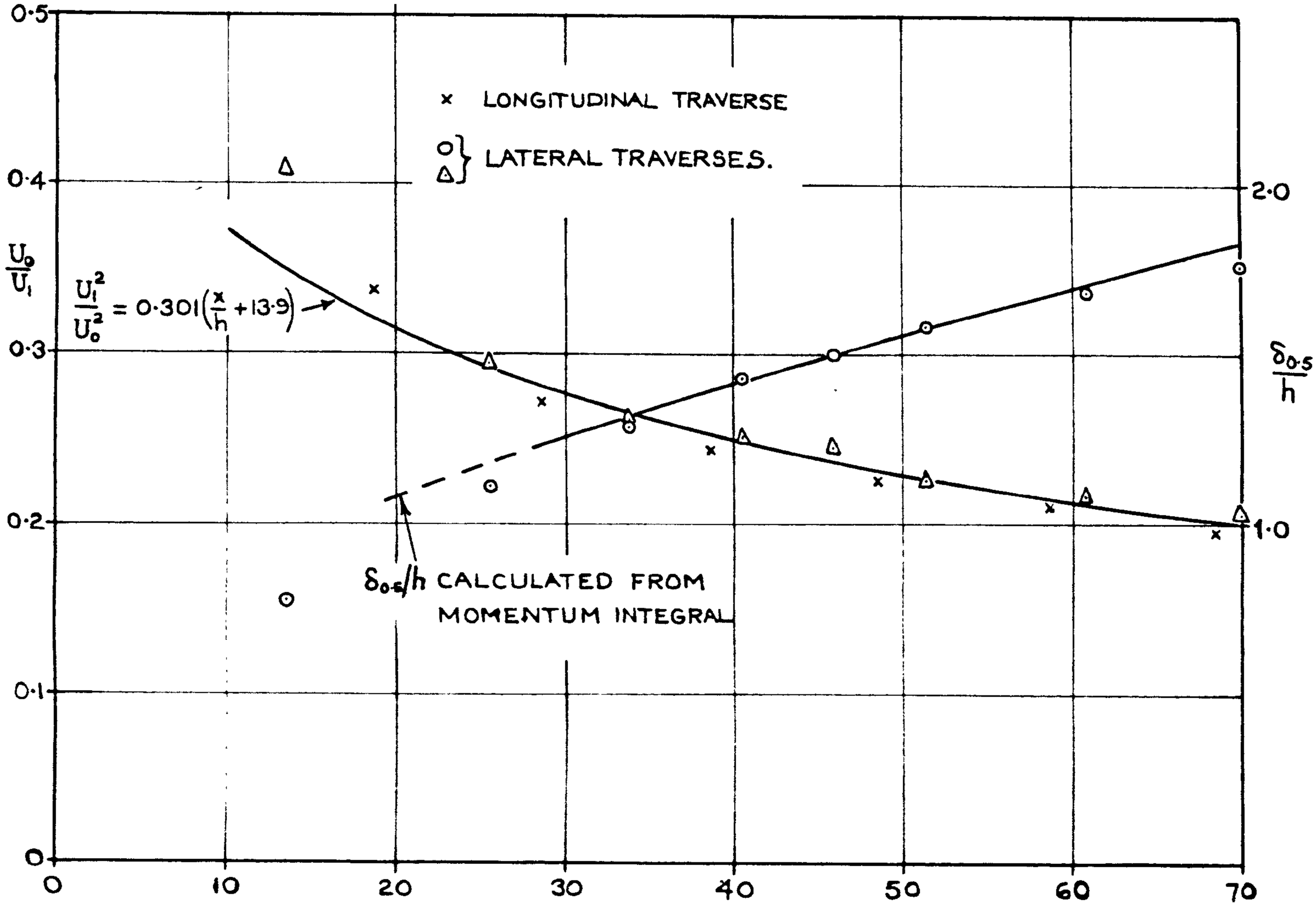

VARIATION OF JET WIDTH AND CENTRE-LINE VELOCITY IN A PLANE JET.

$U_1/U_j = 0.58$

FIGURE 72.

FIGURE 73

LATERAL MEAN VELOCITY PROFILES IN A PLANE JET.
$U_1/U_J = 0.58$

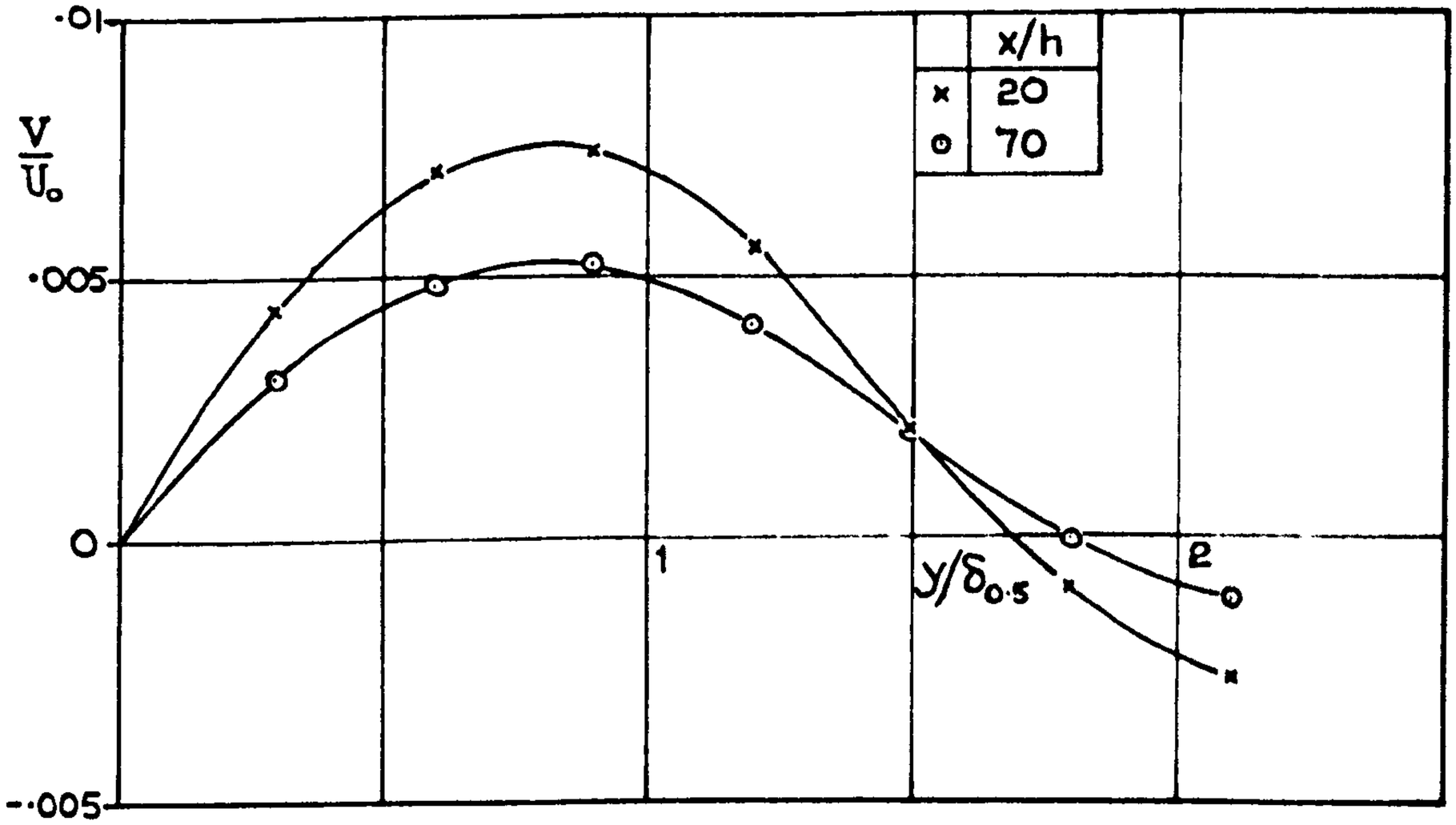

FIGURE 74

$\overline{U^2}$ AND STATIC PRESSURE ON THE CENTRE-LINE OF A PLANE JET - $U_1/U_J = 0.58$

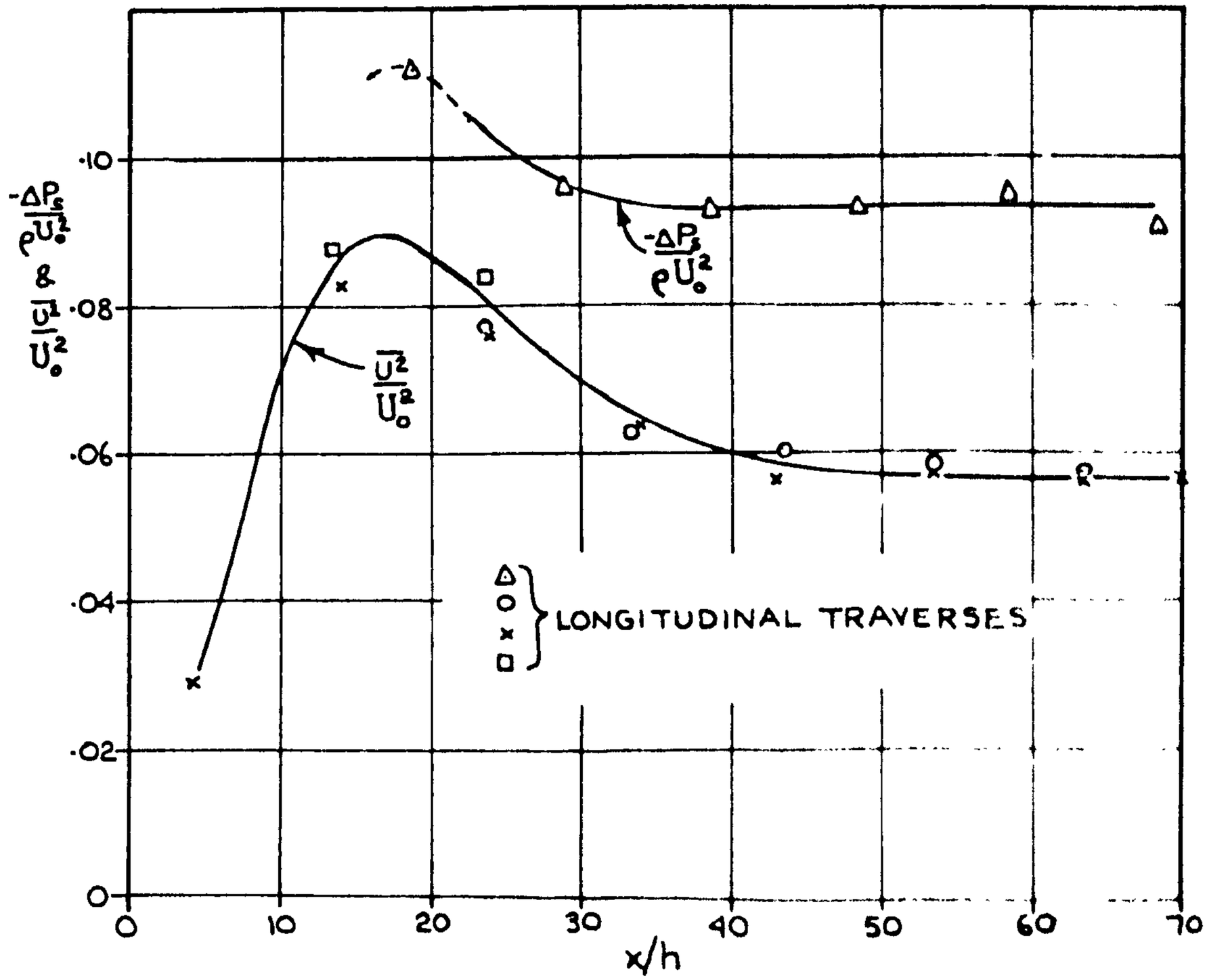

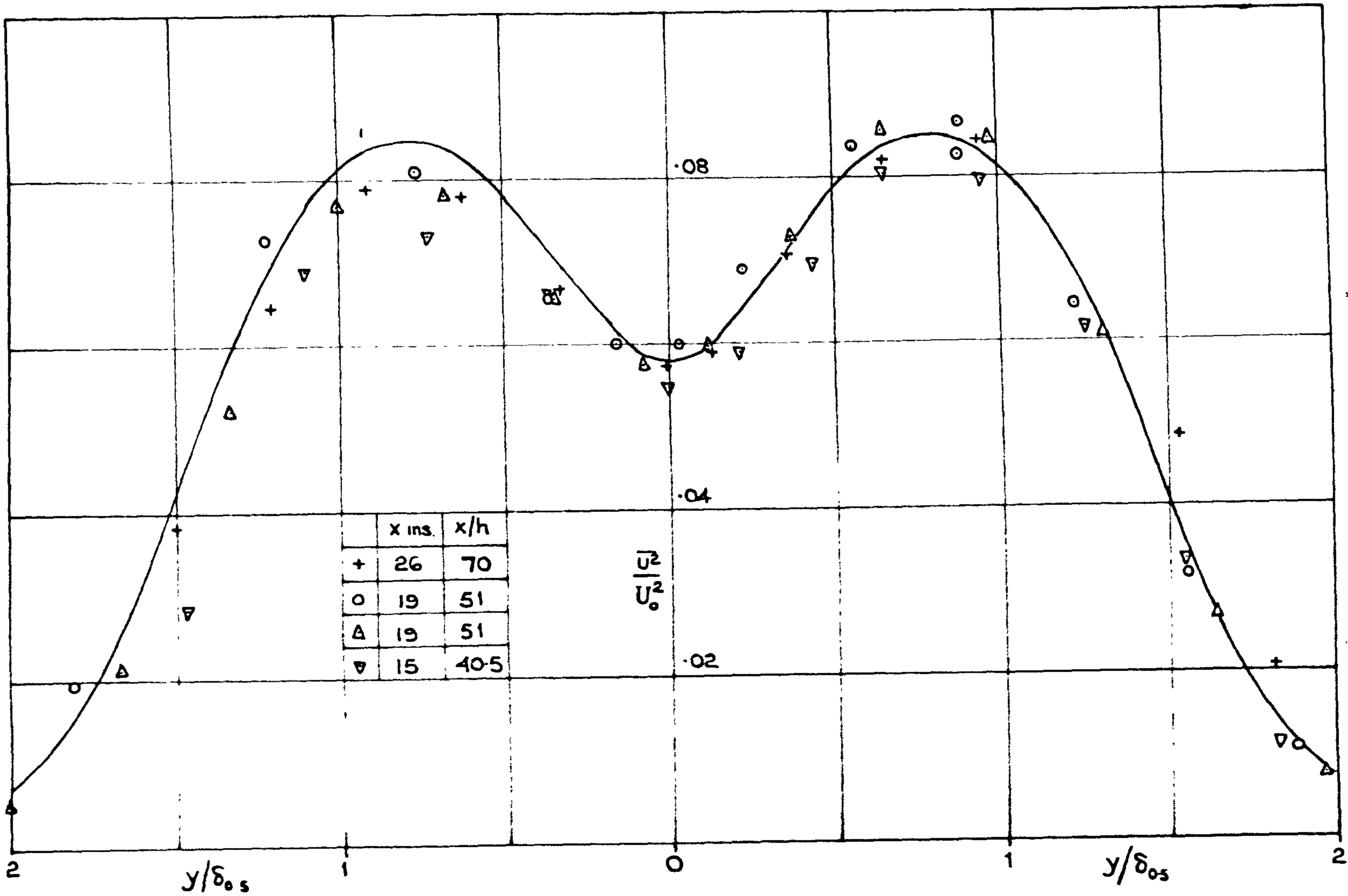

	x ins.	x/h
+	26	70
o	19	51
Δ	19	51
∇	15	40·5

$\overline{u^2}$ PROFILES IN A PLANE JET WITH $U_1/U_j = 0.58$

(MEASURED WITH A 0·0001" DIA Pt. WIRE)

FIGURE 75 .

FIGURE 76

THE TURBULENT SHEAR STRESS PROFILE.

$U_1/U_J = 0.58$

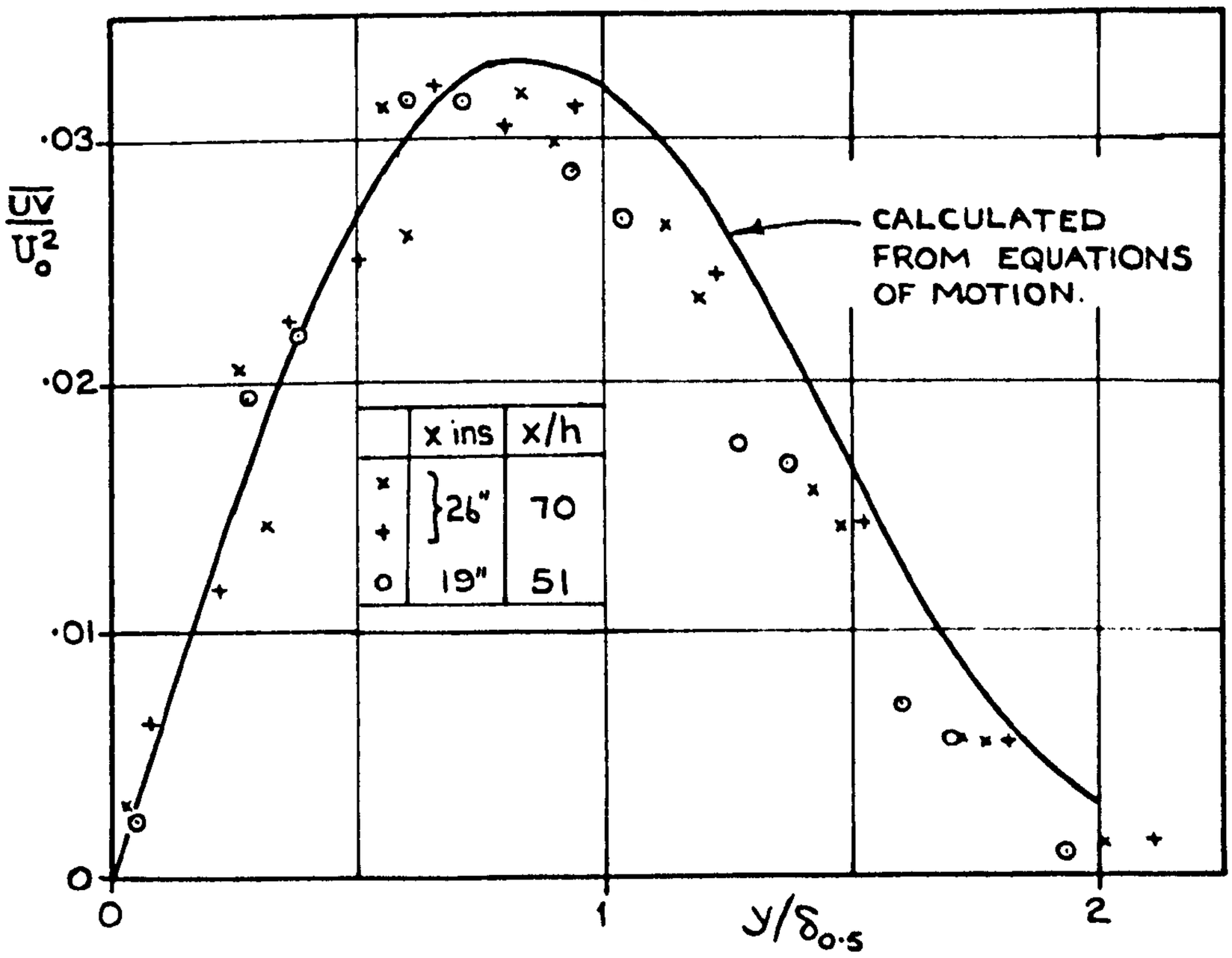

FIGURE 77.

TURBULENT INTENSITY PROFILES IN A PLANE JET. $U_1/U_J = 0.58$

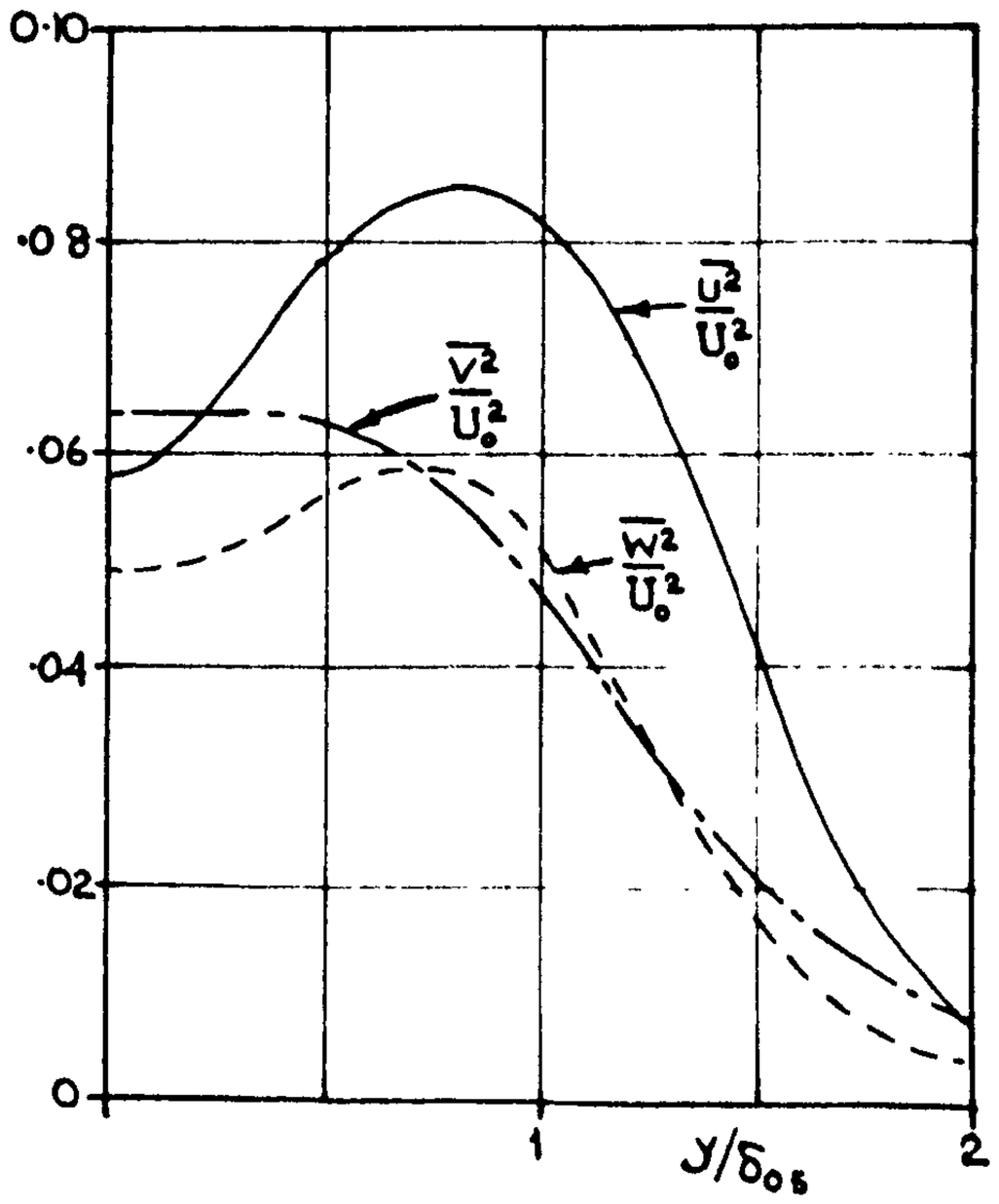

FIGURE 78 .

THE INTERMITTENCY FACTOR IN A PLANE JET.

$U_1/U_J = 0.58$

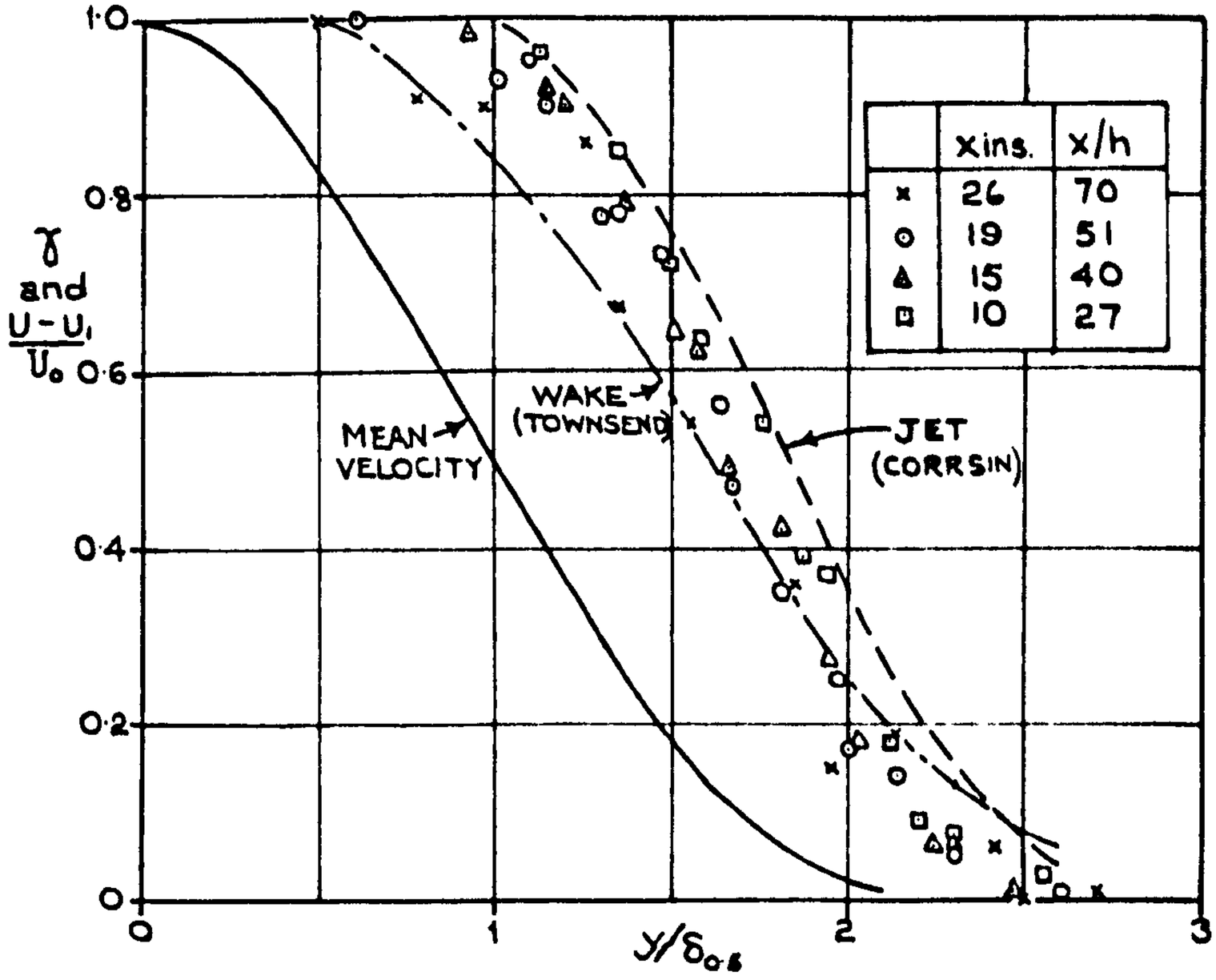

FIGURE 79

FREQUENCY OF EDDIES RESPONSIBLE FOR INTERMITTENCY

$U_1/U_J = 0.58$

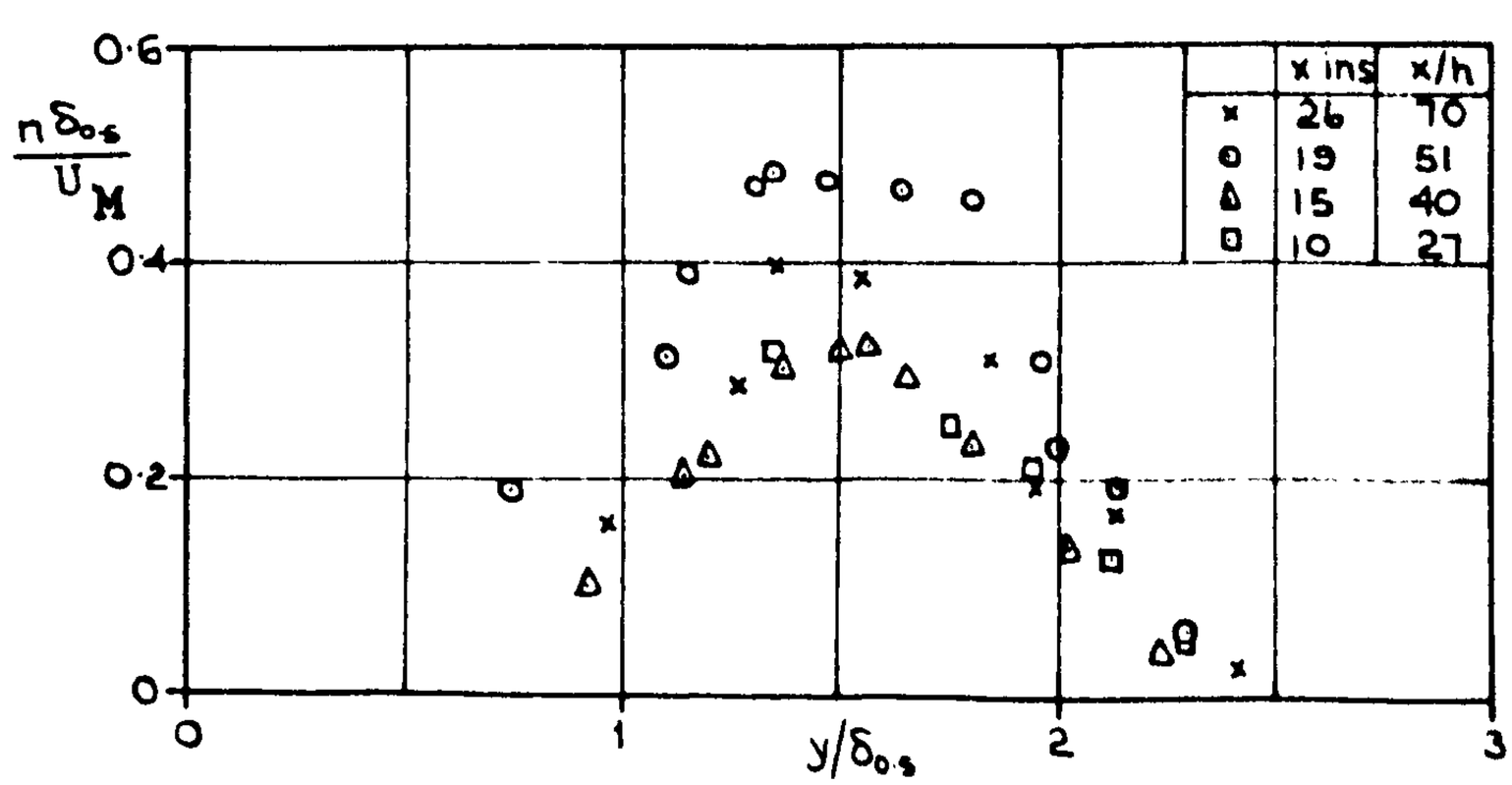

FIGURE 80

THE TURBULENT ENERGY BALANCE IN A PLANE JET.

$U_1/U_J = 0.58$

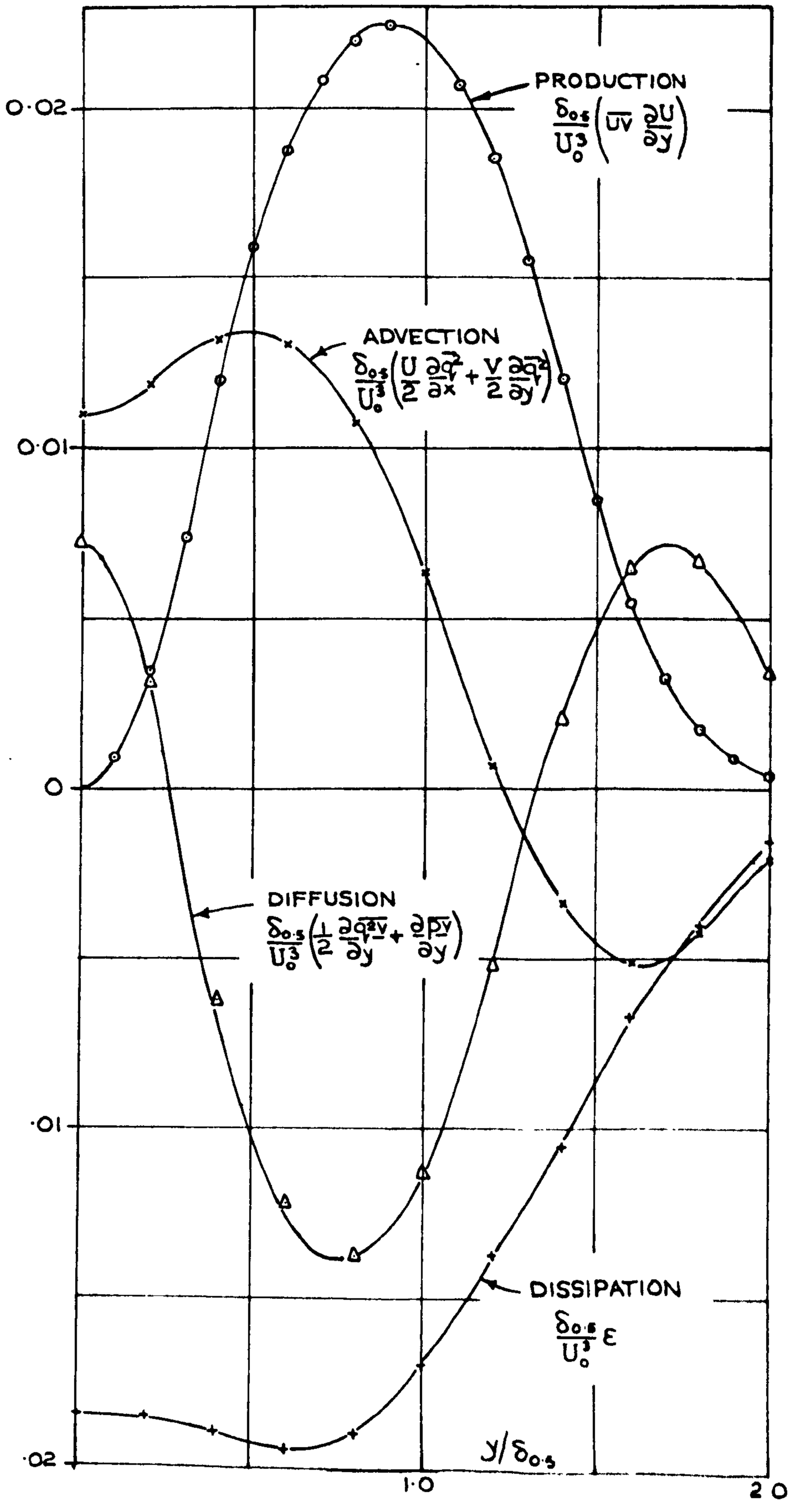

FIGURE 81

A COMPARISON BETWEEN THEORETICAL AND EXPERIMENTAL RESULTS FOR THE DEVELOPMENT OF A PLANE JET. $0 \leq \frac{(x-x_0)}{J/\rho U_1^2} \leq 10$

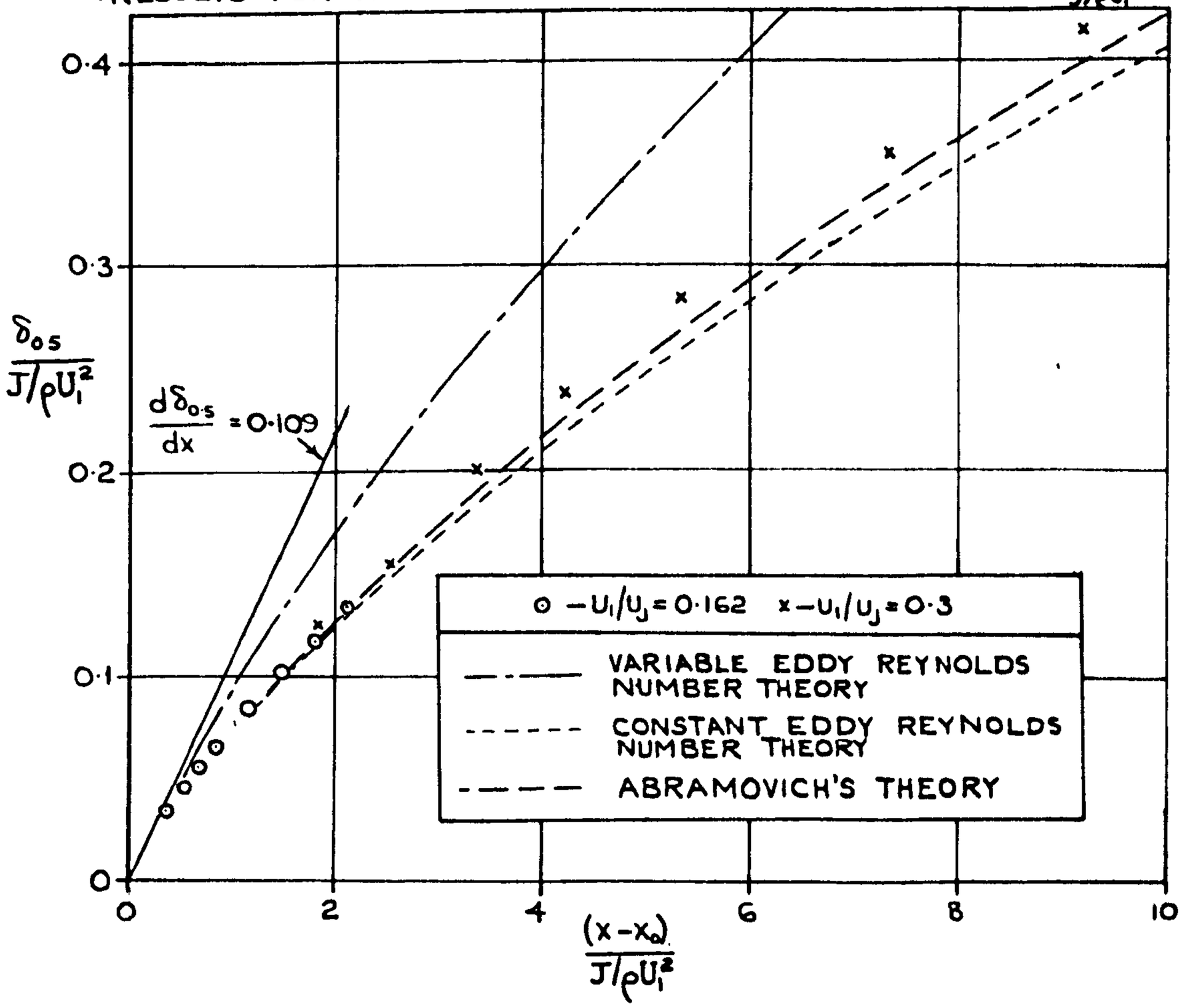

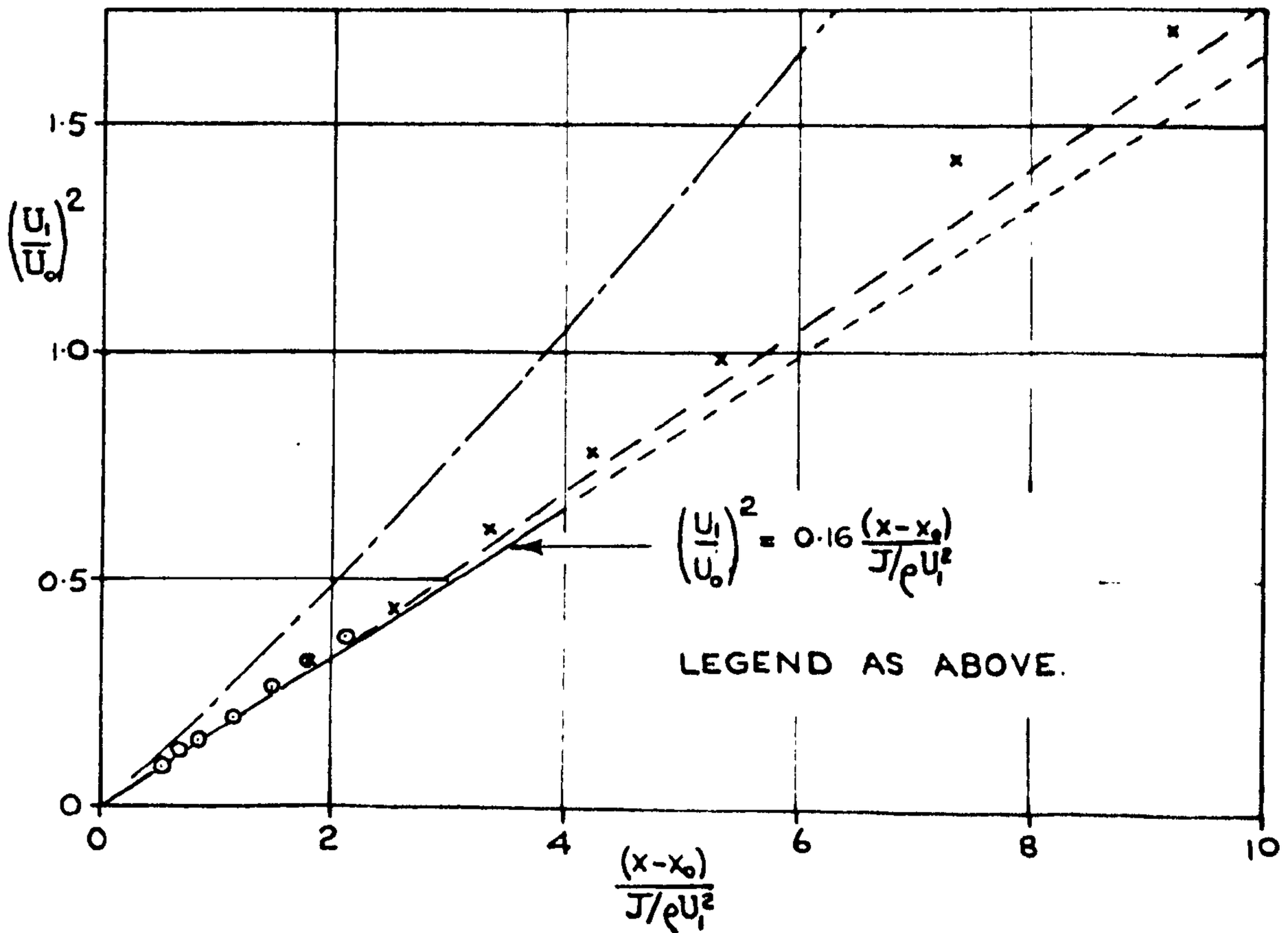

FIGURE 82

A COMPARISON BETWEEN THEORETICAL AND EXPERIMENTAL RESULTS FOR THE DEVELOPMENT OF A PLANE JET. $0 \leq \frac{(x-x_0)}{J/\rho U_1^2} \leq 100$

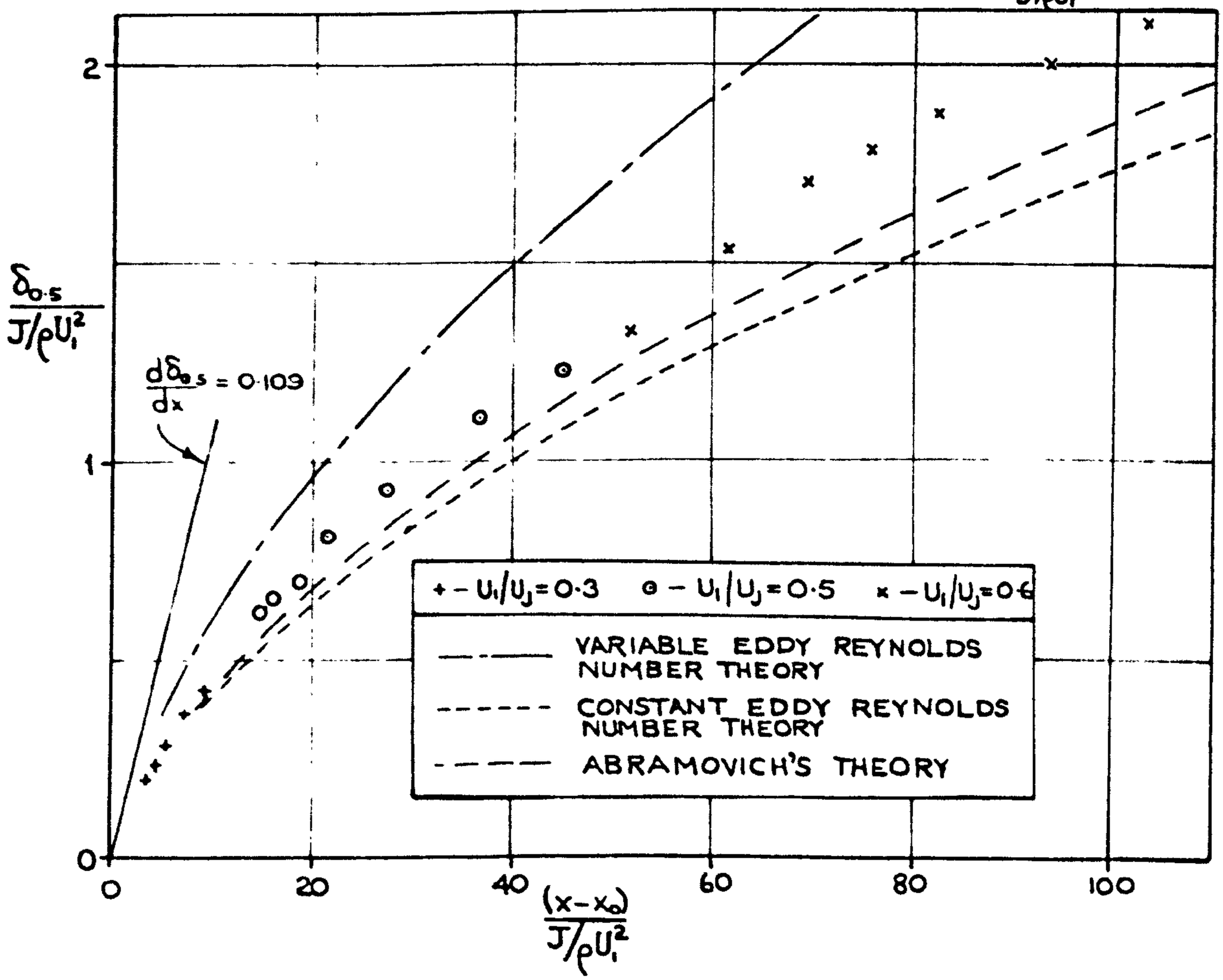

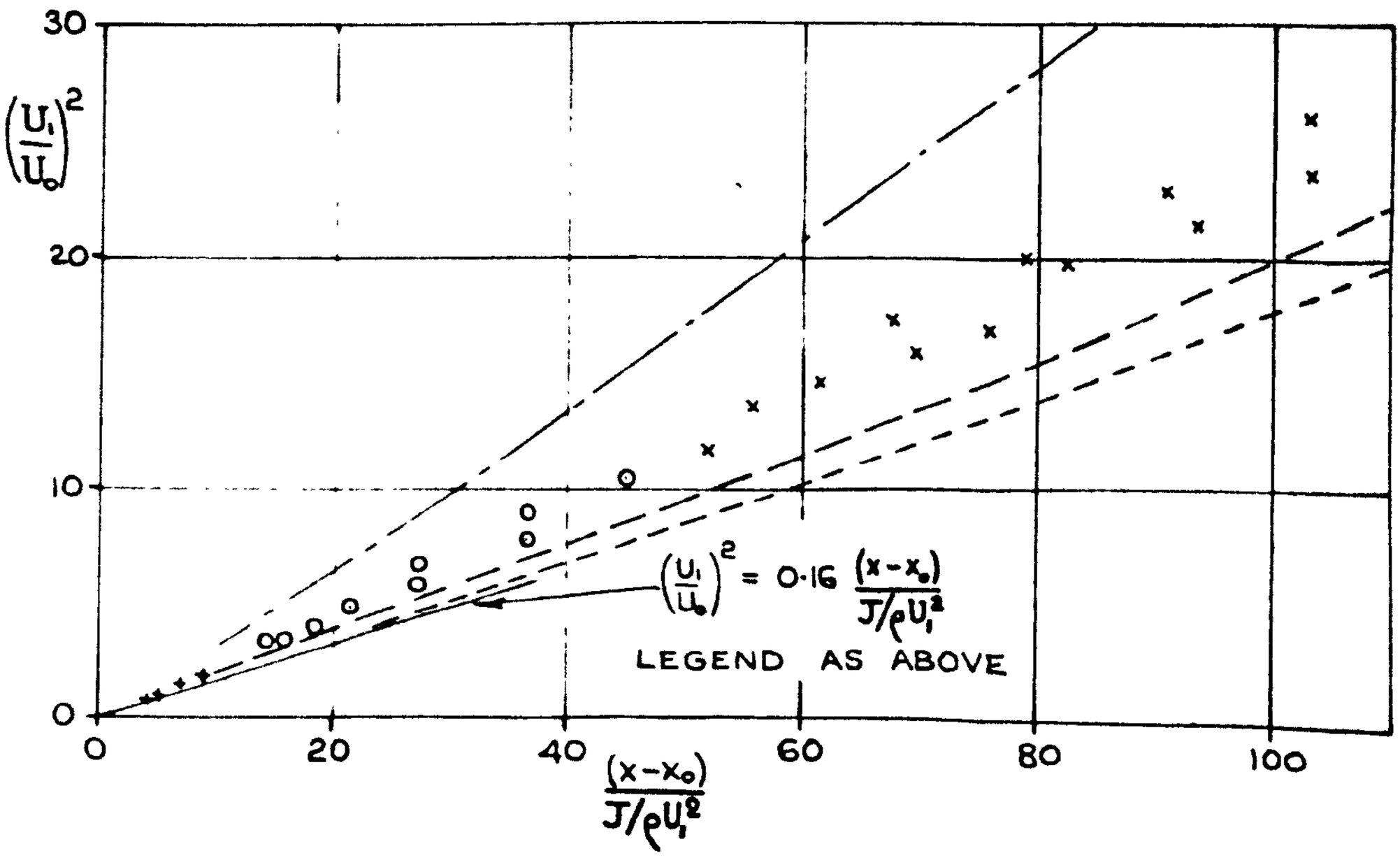

FIG. 83

DESIGN OF AEROFOIL NOSE.

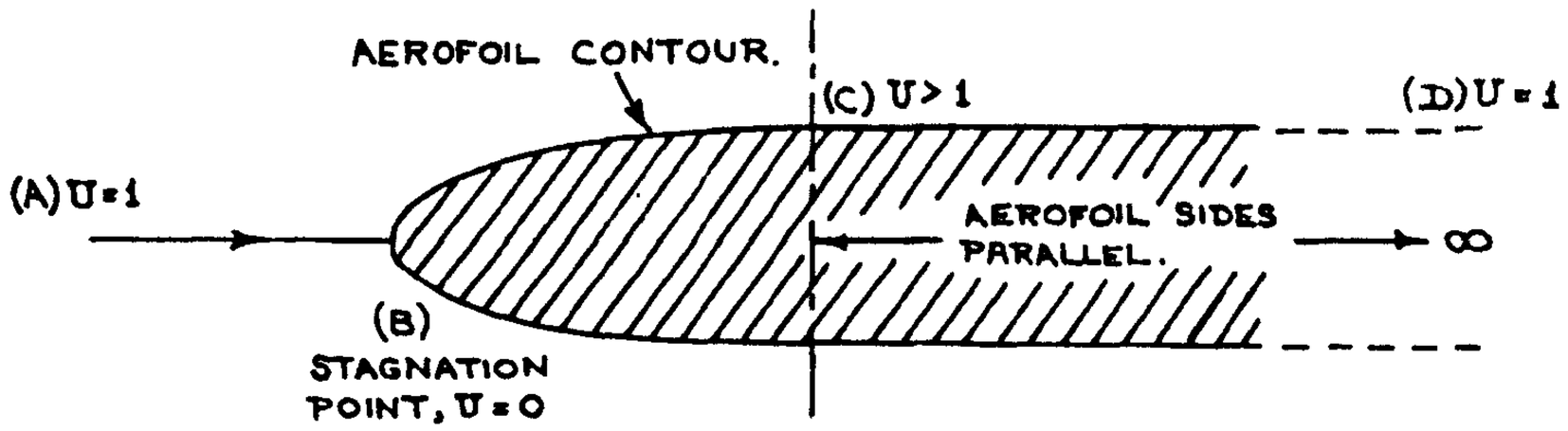

(A) THE PHYSICAL PLANE.

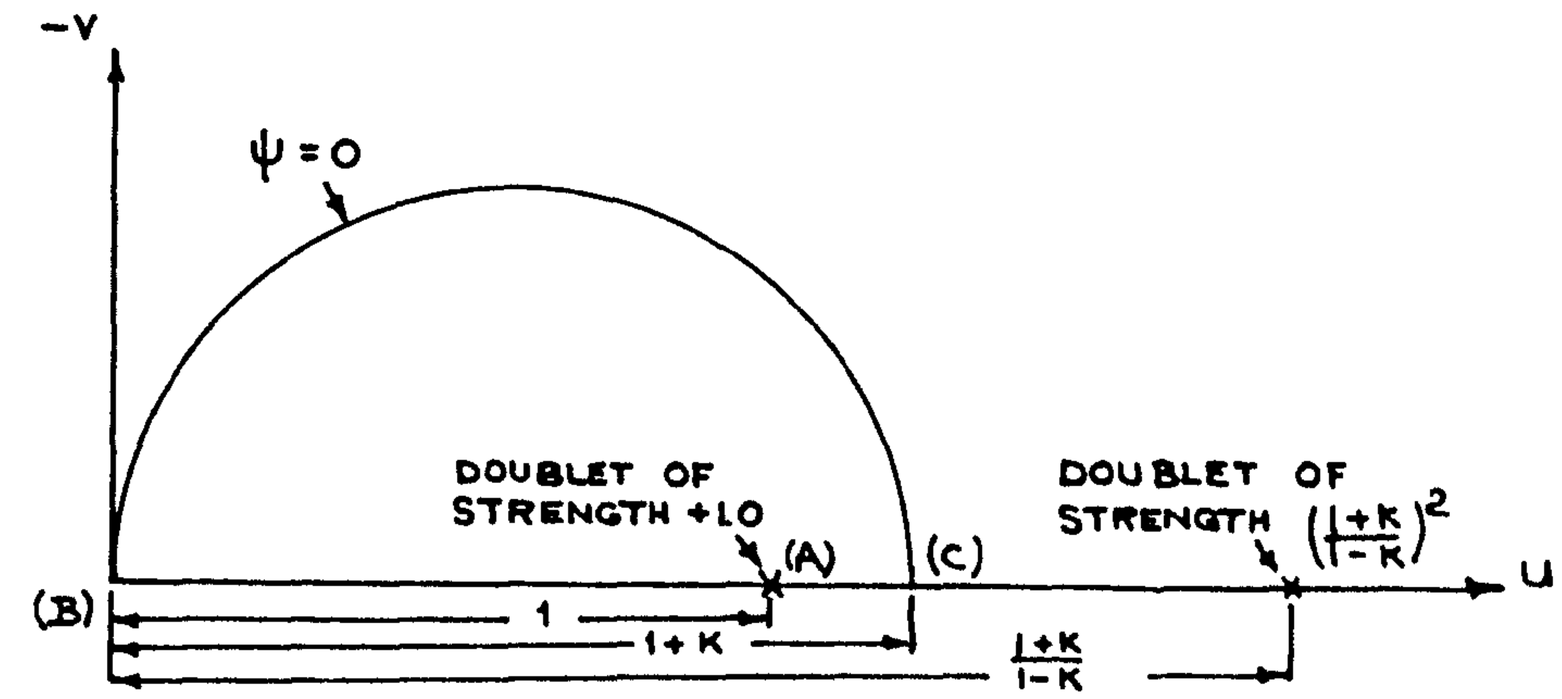

(B) THE HODOGRAPH, PLANE.

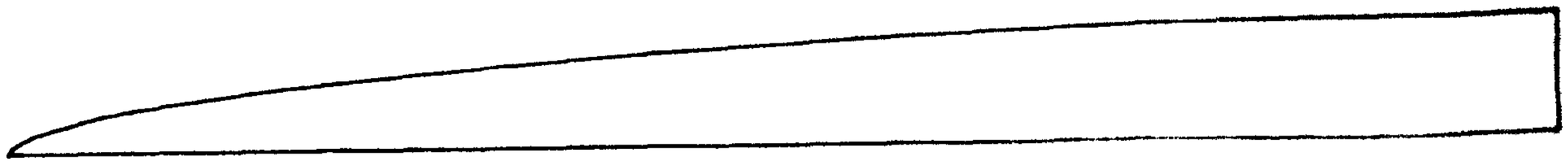

(C) NOSE CONTOUR TAKING K = 0·05.